

Univerzita Karlova

1. lékařská fakulta

Studijní program: Biochemie a patobiochemie



UNIVERZITA KARLOVA
1. lékařská fakulta

Mgr. Nikola Capková

Studium bilirubinu a jeho oxidačních produktů

Study of bilirubin and its oxidation products

Disertační práce

Vedoucí závěrečné práce/Školitel: RNDr. Aleš Dvořák, PhD.

Praha, 2023

Prohlášení:

Prohlašuji, že jsem závěrečnou práci zpracovala samostatně a že jsem řádně uvedla a citovala všechny použité prameny a literaturu. Současně prohlašuji, že práce nebyla využita k získání jiného nebo stejného titulu.

Souhlasím s trvalým uložením elektronické verze mé práce v databázi systému meziuniverzitního projektu Theses.cz za účelem soustavné kontroly podobnosti kvalifikačních prací.

V Praze, 30.3.2023

Nikola Capková

Identifikační záznam:

CAPKOVÁ, Nikola. Studium bilirubinu a jeho oxidačních produktů. [Study of bilirubin and its oxidation products]. Praha, 2023. 128 stran, 4 přílohy. Disertační práce. Univerzita Karlova v Praze, 1. lékařská fakulta, Ústav lékařské biochemie a laboratorní diagnostiky 1. LF UK a VFN v Praze. Vedoucí závěrečné práce: RNDr. Aleš Dvořák, PhD.

Acknowledgements

I would like to thank to my supervisor RNDr. Aleš Dvořák, PhD. mostly for his expert advice and perfect guidance, never-ending support and infinite amount of patience.

Many thanks belong to Prof. MUDr. Libor Vitek, Ph.D., MBA, for his introduction into an interesting field of bilirubin and great support. As well, I would like to also thank to my colleagues and friends from the Hepatology lab who were always supportive and helpful.

Very significant acknowledgement belongs to my partner and his support and understanding during the difficult times of my studies. Without his help and patience, I would not be able to finish my postgraduate study.

ABSTRAKT

Fototerapie (PT) modrozeleným světlem (420-490 nm) se řadí mezi standardní léčbu těžké novorozenecké žloutenky, která brání toxickému působení bilirubinu (BR) u kojenců. Vystavením se modrozelenému světlu je BR přeměněn na polárnější fotoizomer (PI) lumirubin (LR) a další oxidační produkty (mono-, di-, tripyrroly), které lze snadněji vyloučit z těla močí a/nebo žlučí. Ačkoli je PT považována za bezpečnou, je doprovázena zvýšeným rizikem různých patofyziologických stavů (zánětlivých procesů, alergií, cukrovky i některých typů rakoviny), zejména u novorozenců s extrémně nízkou porodní hmotností. Účelem této práce bylo pochopení mechanismu vylučování BR v různých tkáních i buněčných liniích a zkoumání bioaktivních vlastností BR i jeho hlavního fotooxidačního produktu LR.

Nejprve jsme se zaměřili na detekci BR v žluči a stolici hyperbilirubinemických potkanů Gunn. Současně jsme testovali antioxidační a prooxidační účinky nekonjugovaného BR u lidských hepatoblastomových (HepG2), proximálních tubulárních (HK2), neuroblastomových (SH-SY5Y) a myších endotelových (H5V) buněk, jejich vystavením postupně se zvyšujícím koncentracím BR. Pro porovnání účinků BR a LR na markery metabolismu a oxidačního stresu byly biologické aktivity zkoumány *in vitro* na buňkách lidského hepatoblastomu (HepG2), fibroblastu (MRC5) a myších makrofázích (RAW 264.7). Zaměřili jsme se také na proliferaci, morfologii, expresi specifických genů i proteinů a diferenciaci neurálních kmenových buněk (NSC).

Naše experimenty potvrdily, že souvislost mezi regulací transintestinálního vylučování cholesterolu a plazmatickými koncentracemi nekonjugovaného BR u potkanů Gunn není přítomna. U všech studovaných buněčných linií jsme zjistili, že nízké koncentrace BR vedly k antioxidačním účinkům, zatímco vyšší koncentrace k prooxidačním nebo cytotoxickým účinkům, čím se potvrzuje, že každý typ buněk má jiný práh pro BR. Při porovnání s LR, jsme sledovali výrazně nižší toxicitu a zachování antioxidační kapacity v séru. LR také potlačil aktivitu vedoucí k produkci mitochondriálního superoxidu, avšak byl méně účinný v prevenci lipoperoxidace. Naše data také potvrdily vliv BR a LR na časnou fázi diferenciaci NCS a schopnost LR ovlivňovat polaritu a identitu NSC během časného vývoje lidského neuronu, což může mít klinický význam, protože buněčná polarita hraje významnou roli během vývoje CNS.

Klíčová slova: Metabolismus hemu, bilirubin, fotooxidační produkty, novorozenecká žloutenka

ABSTRACT

Phototherapy (PT) with blue-green light (420-490 nm) is the standard treatment for severe neonatal jaundice to prevent infants from toxic bilirubin (BR). Upon blue-green light exposure, BR is converted to more polar photoisomer (PI) lumirubin (LR) and the other oxidation products (mono-, di-, tripyrrols) which can be more easily disposed of the body via urine and/or bile. Although generally considered to be safe, PT is accompanied by an increased risk of various pathophysiological conditions (inflammatory processes, allergies, diabetes, and some types of cancer), in extremely low-birth-weight newborns. Thus, to account for these consequences, our study aimed to understand the mechanism of BR secretion in different tissues and cell lines and investigate the bioactive properties of BR and its main photooxidation product LR.

At first, we focused on the detection of BR in the bile and feces of hyperbilirubinemic Gunn rats. Simultaneously, we tested the antioxidant and pro-oxidant effects of unconjugated BR in human hepatoblastoma (HepG2), proximal tubular (HK2), neuroblastoma (SH-SY5Y), and murine endothelial (H5V) cells by exposing them to progressively increasing concentrations of BR. To compare the BR and LR effects on metabolic and oxidative stress markers, the biological activities were investigated in vitro on human hepatoblastoma (HepG2), fibroblast (MRC5), and murine macrophage (RAW 264.7) cells. We also focused on proliferation, morphology, expression of specific genes and proteins, and differentiation of neural stem cells (NSC).

Our experiments confirmed no link between the regulation of transintestinal cholesterol excretion and plasma concentrations of unconjugated BR in Gunn rats. We observed in all studied cell lines, that low concentrations of BR exhibit antioxidant effects, whereas higher concentrations exhibit a prooxidant or cytotoxic effect, confirming that each cell type has a different threshold for BR. When compared to LR, significantly lower toxicity and maintenance of antioxidant capacity in serum were observed. LR also suppressed the activity leading to mitochondrial superoxide production but was less effective in preventing lipoperoxidation. Our data also confirmed the effect of BR and LR on the early phase of NCS differentiation and the ability of LR to influence the polarity and identity of NSCs during early human neuronal development, which may have clinical relevance since cell polarity has an important role during CNS development.

Key words: Haem metabolism, bilirubin, photo-oxidation products, neonatal jaundice

Table of Contents

ABSTRAKT	5
ABSTRACT	6
1 INTRODUCTION	8
1.1 Heme catabolism	8
1.2 Bilirubin metabolism	9
1.2.1 Bilirubin structure	10
1.2.2 Transport and excretion of bilirubin	12
1.3 Biological properties of bilirubin	15
1.3.1 Positive effects of bilirubin	15
1.3.2 Toxicity of bilirubin	17
1.3.3 Hyperbilirubinemia	17
1.3.4 Neonatal jaundice	19
1.5 Phototherapy	20
1.5.1 Bilirubin photoisomers	22
1.5.2 Bilirubin oxidation products	24
2 AIMS	29
3 METHODS	30
4 RESULTS	31
5 DISCUSSION	32
6 SUMMARY	42
8 LIST OF ABBREVIATIONS	67
9 ANNEXES	69
Annex 1	70
Annex 2	78
Annex 3	95
Annex 4	113

1 INTRODUCTION

1.1 Heme catabolism

Heme is an important iron-containing cyclic tetrapyrrolic molecule expressed ubiquitously in organisms which serves as a prosthetic group for a variety of hemoproteins including hemoglobin, myoglobin, cytochrome P-450, catalase, peroxidase, tryptophan pyrrolase, cytochrome b5, and mitochondrial cytochromes which are implicated in multiple cellular functions including oxygen transport, energy generation, defence against increased oxidative stress or cell signalling (Vitek & Ostrow, 2009) (Jayanti et al., 2020) (B. Wu et al., 2019). Due to 65-75 % of the iron pool in the human body being derived from heme, this molecule also acts as a major storage of bioavailable iron (Korolnek & Hamza, 2014) (Schultz et al., 2010). After its release from red blood cells, heme is bound to hemopexin or haptoglobin and recycled or transported back to the splenic sinusoids in reticuloendothelial system where its degradation process occurs (Schultz et al., 2010).

The mammalian heme degradation pathway (*Fig. 1*) consists of two enzymatic steps, which are mediated by heme oxygenase (HMOX) and biliverdin reductase (BLVR) (Maines, 2005). HMOX is the enzyme classified as oxidoreductase crucial for the first step of the heme degradation. HMOX system consists of HMOX and NADPH–cytochrome P450 reductase with the protective effect of cells against heme-induced oxidative stimuli (B. Wu et al., 2019). The process of heme degradation is initiated when HMOX catalyses the opening of the heme ring at α -carbon bridge to yield equimolar quantities of non-toxic polar biliverdin (BV) with tetrapyrrole structure, carbon monoxide (CO) and free iron with the consumption of three molecules of oxygen (O_2) and the reducing equivalent of NADPH (Otterbein & Choi, 2000). After this cleavage, BV is directly converted by reduction of the middle -CH= bridge into non-polar unconjugated BR mainly by the cytosolic enzyme BVR with a unique feature which increases the production of bilirubin and thus enhancing defence against oxidative stress (Tenhunen et al., 1972) (Salim et al., 2001).

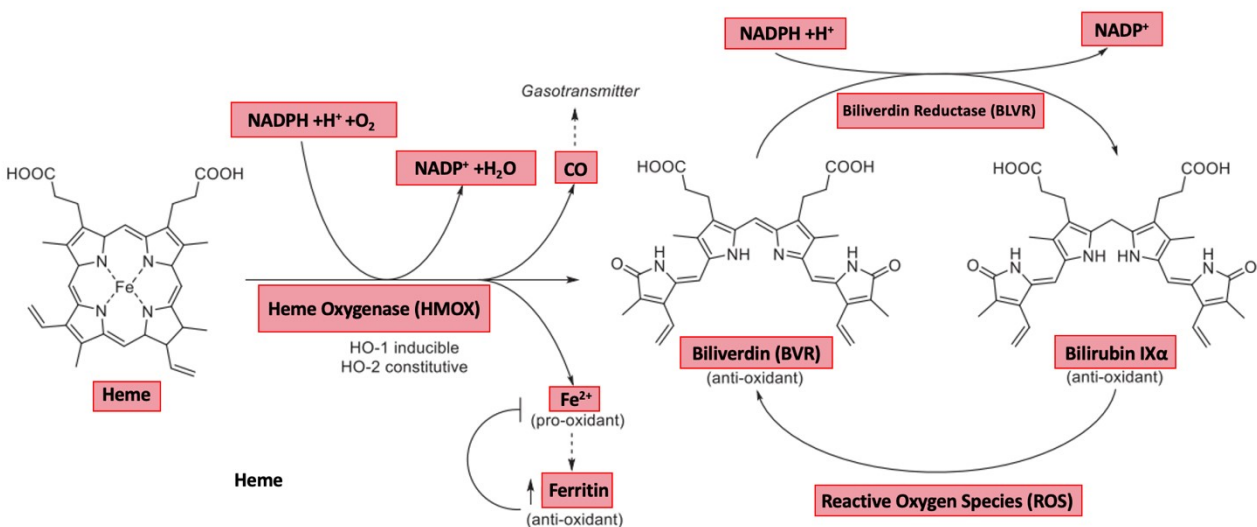


Fig.1. Heme degradation pathway. Conversion of heme molecule generates an equimolar amount of CO, ferrous ion (Fe^{2+}), and biliverdin which is subsequently reduced by biliverdin reductase to non-polar unconjugated bilirubin IX α – 4Z, 15Z. Modified from (Nocentini et al., 2022).

The presence of unconjugated BR produced entirely from the degradation of heme and heme proteins is 4.4 ± 0.7 mg/kg (Berk et al., 1974) accounting for an average of 300 – 375 mg of daily *de novo* unconjugated BR production (Salehi et al., 2014). Of this amount, 75% to 80% of unconjugated BR derives from hemoglobin released during destruction of senescent red blood cells in the reticuloendothelial system (Salehi et al., 2014). The remaining 25% of unconjugated BR synthesis is derived from non-hemoglobin heme proteins in the liver, from accelerated destruction in the spleen of immature or defectively formed red cells, and the bone marrow from heme formed in excess of globin (Vitek & Ostrow, 2009).

1.2 Bilirubin metabolism

Unconjugated BR was discovered in 1847 by Dr. Virchow. Its chemical tetrapyrrolic structure was defined by Fischer and Orth in 1937 (Tschesche, 1938) and in 1942 its successful synthesis was reported (Fisher H. & Plieninger H., 1942).

1.2.1 Bilirubin structure

The natural bilirubin in humans is the unconjugated BR IX α 4Z,15Z molecule and its other isoforms include III α and XIII α isomers formed by a nonenzymatic process so called molecular scrambling, in which unconjugated BR IX α is split into two halves which then randomly reassemble (**Fig. 2**) (Vitek & Ostrow, 2009).

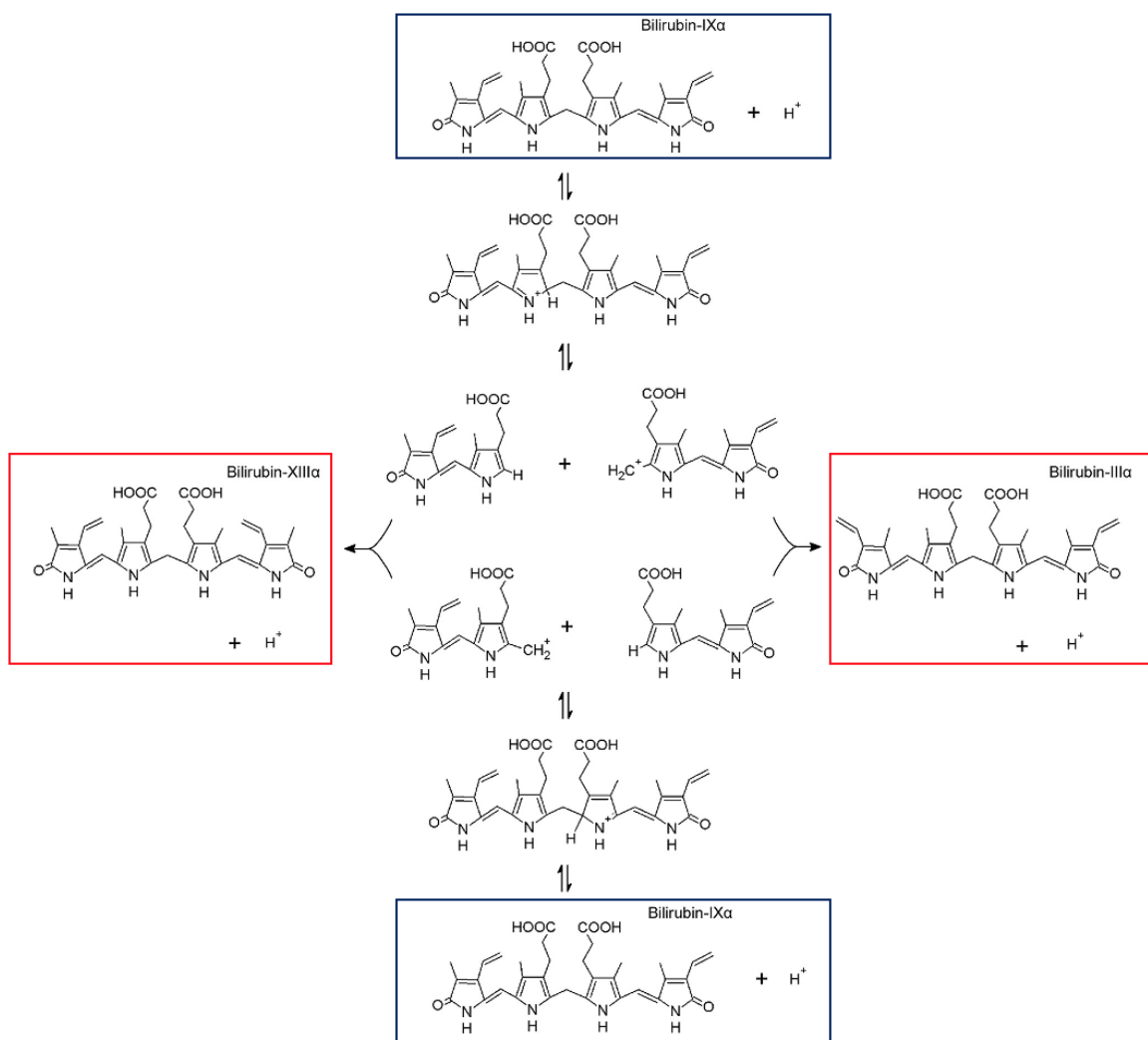


Fig.2. Formation of bilirubin IX α , the dominant bilirubin molecule in the circulation, and its constitutional isomers III α and XIII α formed by dipyrrole exchange reaction. Modified from (Itoh et al., 2017).

The structure of unconjugated BR IX α 4Z,15Z molecule is nearly symmetrical and composed of two planar dipyrrole units (rings A-B and C-D) joined to each other by a central methylene group (-CH₂-). In each dipyrrolic half, the two monopyrroles are linked by an unsaturated (double-bonded) methene group (-CH=) and lie in the same plane. Each outer pyrrole rings (A & D) have a polar lactam (-CO-NH-) group, while each central pyrrole ring (B & C) carries a carboxyethyl sidechain (-CH₂-CH₂-COOH), which can ionize by loss of the terminal proton. The remaining sites on the pyrrole rings are occupied by ethyl (-CH₃) and vinyl (-CH=CH₂) substituents; these are asymmetrically arranged in the A and D rings, giving to unconjugated BR optical activity (**Fig. 3**) (Vitek & Ostrow, 2009).

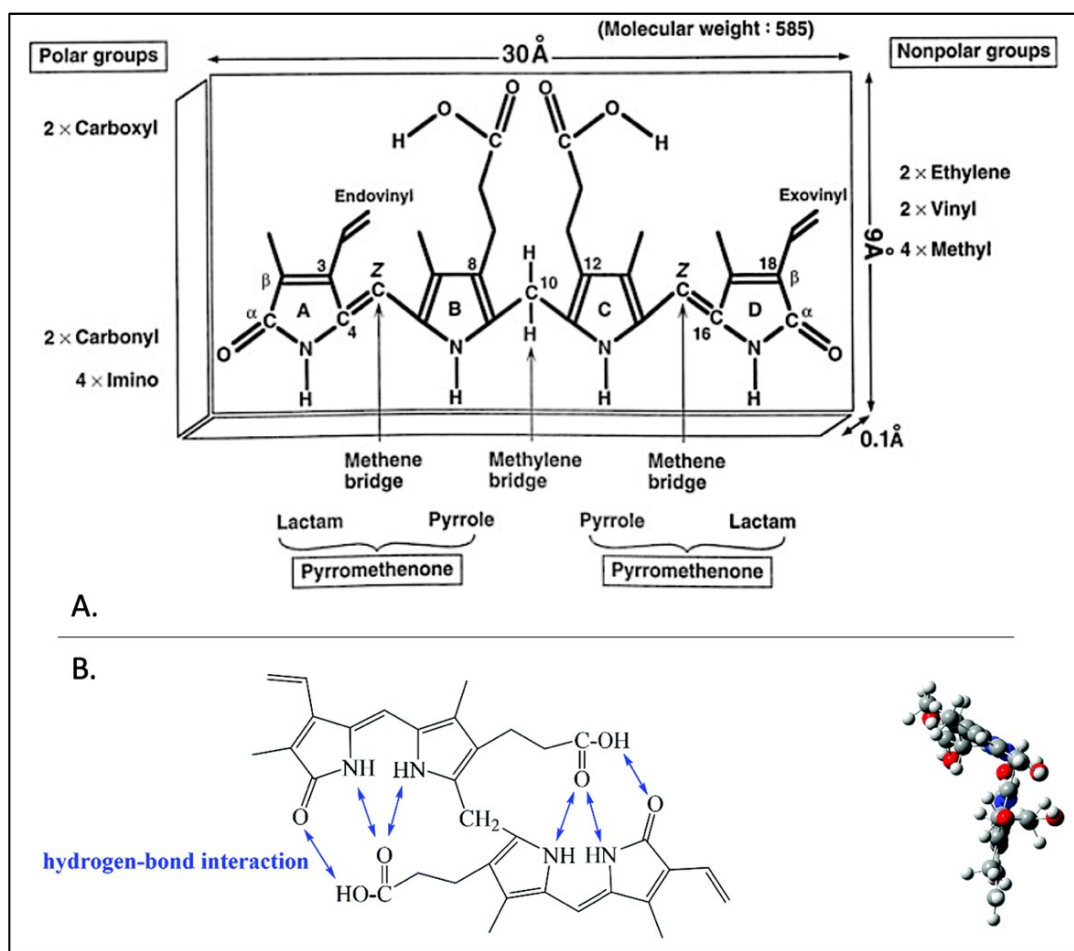


Fig. 3. Bilirubin-IX α molecule and its nomenclature (A) with visualization of an internal hydrogen bonds in its molecular configuration (B). Modified from (Itoh et al., 2017) (Kou & Wang, 2022).

Due to an internal hydrogen bonding of its polar groups hidden from interaction with water molecules (**Fig. 3B**), unconjugated BR appears to have very low solubility in aqueous media - ranging from 7 to 100 nM (the solubility threshold in plasma is 70 nM) at a pH of 7.4 and temperature of 37°C (Gazzin et al., 2017) (Levitt & Levitt, 2014). Transport of non-polar unconjugated BR in the plasma is provided mainly (90%) by bounding to human serum albumin (HSA) and secondary (10%) to the apolipoprotein D found primarily in the high density (HDL) (Jacobsen, 1969) (Suzuki et al., 1988) (Goessling & Zucker, 2000) or by high-affinity bilirubin transporter α 1-fetoprotein in the fetus and early neonates (Aoyagi et al., 1979). Only < 0.1% of the concentration of unconjugated BR in plasma is not bound to any carrier molecule and is termed as „free unconjugated bilirubin“ (Bf) which represent a fraction with the ability to diffuse into tissues leading to cytotoxicity (Calligaris et al., 2007).

1.2.2 Transport and excretion of bilirubin

HSA with the primary high-affinity site binds one mol of unconjugated BR dianion through ionic bonds of its $-\text{COO}^-$ groups with the terminal $-\text{NH}^+$ groups of two lysine residues in an otherwise hydrophobic pocket (Gazzin et al., 2017). Binding with albumin keeps BR dissolved in the circulation and prevents excessive amounts of Bf from passing through membranes when accumulating in cells with the exertion of cytotoxic effects (Lauff et al., 1983). Unbound unconjugated BR and its albumin enter the hepatocyte complex predominantly via passive diffusion across the porous sinusoidal endothelium to reach the basolateral membrane of the hepatocytes (Cui et al., 2001) (Briz et al., 2006). The conjugation of unconjugated BR in hepatocytes occurs when one or both $-\text{COOH}$ groups are modified by covalent attachment of 1- 2 molecules of glucuronic acid by the action of the UDP- glucuronosyl transferase 1A1 isoform (UGT1A1), resulting information of conjugated bilirubin (**Fig. 4**) (Gazzin et al., 2017). Substantial fraction of bilirubin conjugates might be transported by the multidrug resistance-associated protein MRP3 at the sinusoidal membrane into the blood, from where is subsequently reuptaken by sinusoidal membrane-bound organic anion transporting polypeptides (OATP) 1B1 and 1B3 of downstream hepatocyte to prevent oversaturation of canalicular excretion mechanism in periportal hepatocytes (Sticova, 2013a). The activity of UGT1A1 is under hormonal control enhancing progesterone and inhibiting testosterone activity (Muraca & Fevery, 1984). In the following step,

the excretion of conjugated BR into bile through the bile canaliculi is mediated by an ATP-dependent transporter identified as the multidrug resistance-associated protein MRP2/cMOAT and, to a lesser extent, also by ATP-binding cassette (ABC) efflux transporter ABCG2 (Sticova, 2013a). The absence of functionally active MRP2 prevents the secretion of conjugated BR into the bile and redirects this conjugate into sinusoidal blood (Gartung & Matern, 1997). Due to differences in the expression of the transporters OATP1B1/3 at the sinusoidal face which increases from the portal to the centrilobular space intralobular transport system (the sinusoidal liver-to-blood loop) is formed with the possible protecting function of the periportal hepatocytes from the excessive bilirubin and xenobiotics accumulation (Gazzin et al., 2017) (Sticova, 2013b).

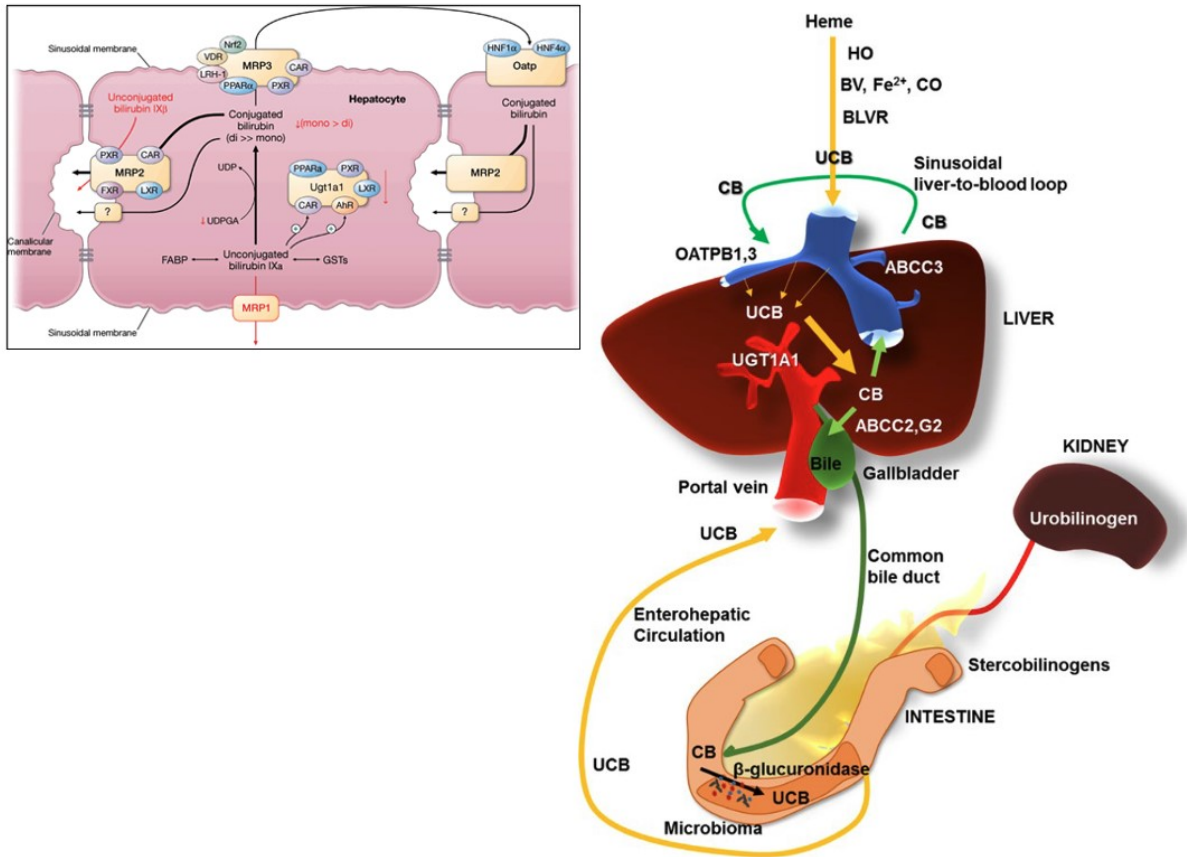


Fig. 4. Intracellular and extracellular metabolism of bilirubin. Modified from (Gazzin et al., 2017) and (Stevenson DK et al., 2012).

The vast majority of conjugated BR absorbed in the small intestine is deconjugated to unconjugated BR by the action of β-glucuronidases and reduced by the coliform bacteria to

urobilinogen and stercobilinogen (**Fig. 5**). However, a part is excreted as unconjugated BR (Vítek et al., 2000) (Morelli, 2008) (Gritz & Bhandari, 2015). Most of the urobilinogen undergoes oxidation and feces excretion. Only a tiny fraction is filtered by the kidney and excreted in the urine due to enterohepatic / enterosystemic circulation. Under certain conditions, a small amount of unconjugated BR can also undergo these reabsorption processes. However, the reabsorption of a small amount of unconjugated BR occurs in the colon when delivered by portal circulation back to the liver (Vítek et al., 2000) (Tiribelli & Ostrow, 2005).

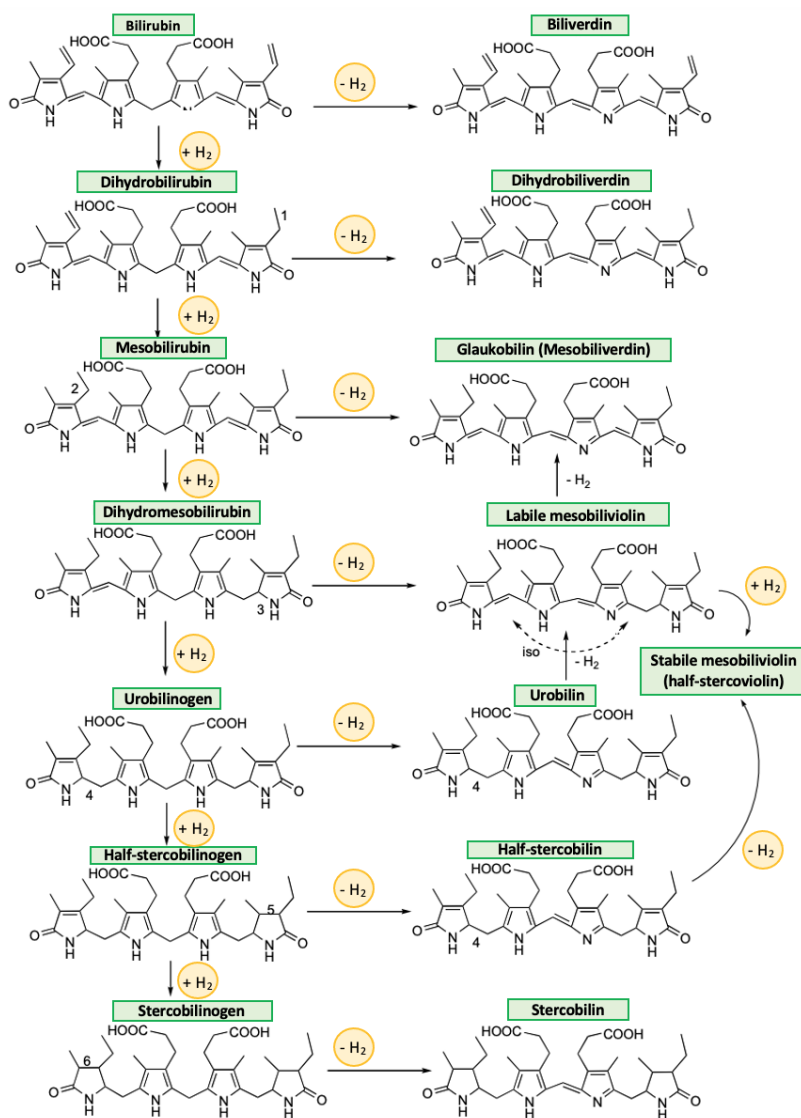


Fig. 5. Reduction of UCB by intestinal microflora showing the chemical structure of its formed products. Modified from (Vitek & Ostrow, 2009).

1.3 Biological properties of bilirubin

Our understanding of bilirubin, originally considered only as a waste substance associated with liver disease, has rapidly changed during the recent fifty years of active in vivo and in vitro research. BR is now regarded as a molecule with many intricate biological functions from cell signalling (behaving almost like a “real” hormonal substance), and modulation of metabolism, to immune regulation, affecting biological activities with apparent clinical and even therapeutic consequences. These may indicate the lower incidence of civilization diseases such as diabetes, obesity, cardiovascular diseases, arterial hypertension, metabolic syndrome, certain cancers, and autoimmune or neurodegenerative diseases observed in individuals with chronic mild unconjugated hyperbilirubinemia. Meanwhile, high concentrations of bilirubin are associated with the opposite effect when becomes toxic (Vítek & Tiribelli, 2021) .

1.3.1 Positive effects of bilirubin

As early as the 1950s, research shows the protection effects of BR against lipid oxidation such as vitamin A or linoleic acid (Pranty et al., 2022) but intensive research of its antioxidant effects began later on in 1987 with a ground-breaking study of Roland Stocker found the ability of BR to inhibit fatty acid oxidation (Stocker, Yamamoto, et al., 1987a). In the research of Wu *et al.* was confirmed and demonstrated 20 times more effective antioxidant effect of BR than a vitamin E analogue Trolox (T.-W. Wu et al., 1994). These antioxidant effects are mainly due to the presence of the tetrapyrrole C-10 methylene group which provides an electron to reactive oxygen species (ROS) and serves as a free radical scavenger. However, when compared with the other antioxidants, BR physiological concentrations in the human body are relatively low and not sufficient to provide such intensive protection that has been observed in many clinical and experimental studies in relation to BR (Jansen & Daiber, 2012), (Gazzin et al., 2016), (DiNicolantonio et al., 2018).

A possible explanation is the existence of the so-called called biliverdin-bilirubin redox cycle (**Fig. 1.**) when BR is oxidized by ROS (hydrogen peroxide, lipid peroxide, or peroxy radicals) back to BV and later on enzymatically regenerated back to BR (Greenberg, 2002),

(Sedlak et al., 2009). In addition, BR enhances its antioxidant effect by inhibition of the common isoforms of the NADPH-oxidase enzyme which represent the superoxide-releasing complexes in the cells (Lanone et al., 2005), prevent peroxidation of proteins (Stocker & Ames, 1987), phospholipids (Sedlak et al., 2009), or LDL protein (T.-W. Wu et al., 1994) and reduce protein carbonylation. BR also reduces oxidative liver damage induced by the accumulation of bile acids during cholestasis (Muchova et al., 2011) and counteracts the harmful effects of pro-oxidants including bile acids *in vitro* and *in vivo* (Zelenka et al., 2012). The association between BR concentration and total serum antioxidant capacity is affecting the development of coronary heart disease (Schwertner et al., 1994) specifically, in middle-aged individuals with Gilbert's syndrome, when the incidence of coronary heart disease was 2% compared to the general population in the same age group, where this risk was up to 12% (Sedlak & Snyder, 2004). Another function of BR as an antioxidant is present in human vascular endothelial cells (Ziberna et al., 2016), and at low concentrations protects neuronal cells from oxidative stress (Doré et al., 1999).

Moderately elevated concentrations of BR are considered to be protective and directly associated with reduced atherosclerotic plaque formation in carotid arteries, which decreases the risk of stroke (Ishizaka et al., 2001) and reduction of developing atherosclerosis in the general population (Novotný & Vitek, 2003). On contrary, the concentration of BR below 7 $\mu\text{mol/L}$ increased risk of developing systemic diseases associated with higher oxidative stress (Wagner et al., 2015), including systemic lupus erythematosus (Vitek et al., 2010), multiple sclerosis (Peng et al., 2011), asthma (Horsfall et al., 2014), diabetes (Abbasi et al., 2015), hypertension (L. Wang & Bautista, 2015), and obesity (DiNicolantonio et al., 2018) or certain forms of cancer such as colon cancer (Temme et al., 2001).

Other important data were brought in experimental and clinical studies focused on the anti-inflammatory effects of BR with the first consistent evidence seen almost 80 years ago in patients with rheumatoid arthritis, who experienced a surprising alleviation of symptoms as a result of the development of liver disease due to increased BR concentrations (Sidel & Abrams, 1934) (Hench, 1938). Later on, in 2010, a large epidemiological study demonstrated a direct association between a reduced risk of developing rheumatoid arthritis and higher total serum BR concentrations (Fischman, 2010). When comparing the patients with ulcerative colitis or primary sclerosing

cholangitis and hyperbilirubinemia when a higher concentration of BR was observed milder colitis occurred (Papatheodoridis et al., 1998). Likewise with Gilbert's syndrome when BR is naturally increased, individuals have a reduced predisposition for the development of inflammatory bowel disease (Crohn's disease) (Leníček et al., 2014) (Jangi et al., 2013).

1.3.2 Toxicity of bilirubin

Excessively elevated concentrations of BR are toxic due to the binding capacity of albumin being exceeded and Bf permeates the plasma membrane into the intracellular space which has the ability to interfere with the respiratory chain by inhibiting mitochondrial enzymes (Diamond, 1970) (Mancuso, 2017) resulting in the release and accumulation of cytochrome c into the cytosol, decrease in mitochondrial membrane potential with disruption of lipid or protein membrane structure and finally to the induction of apoptosis (Rodrigues, Solá, & Brites, 2002a). Bf has many other negative effects on the cell including inhibition of protein kinases like cAMP, cGMP, or Ca²⁺ dependent kinase affecting cellular phosphorylation (Hansen et al., 1996), inhibition of DNA synthesis (Yamada et al., 1977), or neuronal proteins (Gurba & Zand, 1974). High concentrations of BR lead to the inhibition of ion exchange and water transport in renal cells (Dennery et al., 2001). Due to its affinity for membrane phospholipids, BR inhibits also tyrosine uptake (Amato et al., 1994) and in the auditory nerve may disrupt neuroexcitation signals (Dennery et al., 2001). When focused on *in vivo* experiments, the toxicity of BR in the central nervous system (CNS) was observed in the brainstem, cerebral cortex, hippocampus, basal ganglia, and Purkinje cells (Ahdab-Barmada & Moossy, 1984) (Ahlfors & Shapiro, 2001) (Watchko, 2006) (Ye et al., 2019). Observations of high concentrations of BR *in vitro* reveal toxicity in astrocytes (Deliktaş et al., 2019), neurons (Grojean et al., 2000), and organotypic brain sections (Dani et al., 2019).

1.3.3 Hyperbilirubinemia

Physiological total serum bilirubin concentration varies within the range of 0.2- 1 mg/dL (3.4-17.1 $\mu\text{mol/L}$) (Gazzin et al., 2017). Elevated concentrations above 17 $\mu\text{mol/L}$ so called hyperbilirubinemia are related to impaired BR metabolism (Strassburg, 2010). Once bilirubin levels in the circulation rise above its physiological concentrations, icteric discoloration of sclera,

mucosal surfaces and skin is observed. Much more severe hyperbilirubinemias (usually above 340 $\mu\text{mol/L}$) could be accompanied with deleterious bilirubin effects, among them bilirubin-induced neurological dysfunction and kernicterus being the worst and most dangerous complications (Watchko & Tiribelli, 2013).

Hyperbilirubinemias can be classified into conjugated (postmicrosomal), unconjugated (premicrosomal), and mixed hyperbilirubinemias (van Dijk et al., 2015). **Conjugated** hyperbilirubinemias are caused mainly by extrahepatic cholestasis (biliary obstruction), intrahepatic cholestasis (viral and alcoholic hepatitis, steatohepatitis, intrahepatic cholestasis of pregnancy, posttransplant conditions, etc.), when compared with **mixed** hyperbilirubinemias caused by hepatocellular damage (toxic, infectious, immunological, systemic damage, neoplasms, etc.) (Krige, 2001) (Stratta et al., 1989) (Brumbaugh & Mack, 2012) (Mendenhall et al., 1984). **Unconjugated** hyperbilirubinemias are caused mainly by following pathophysiological mechanisms: BR overproduction (intra/extravascular hemolysis, erythrocyte phagocytosis during extravasation, defective haemoglobin synthesis, impaired uptake of BR by the hepatocyte (during the administration of drugs such as certain antibiotics, etc.) and by impaired bilirubin conjugation due to UGT1A1 activity such as in Gilbert syndrome, Crigler-Najjar syndrome type I and II or due to its inhibition by specific drugs such as antibiotics, antiviral atazanavir or irinotecan (Robinson et al., 1962) (Kenwright & Levi, 1974) (Bosma, 2003) (Muchová et al., 2004) (Dhawan et al., 2005) (Strassburg, 2010).

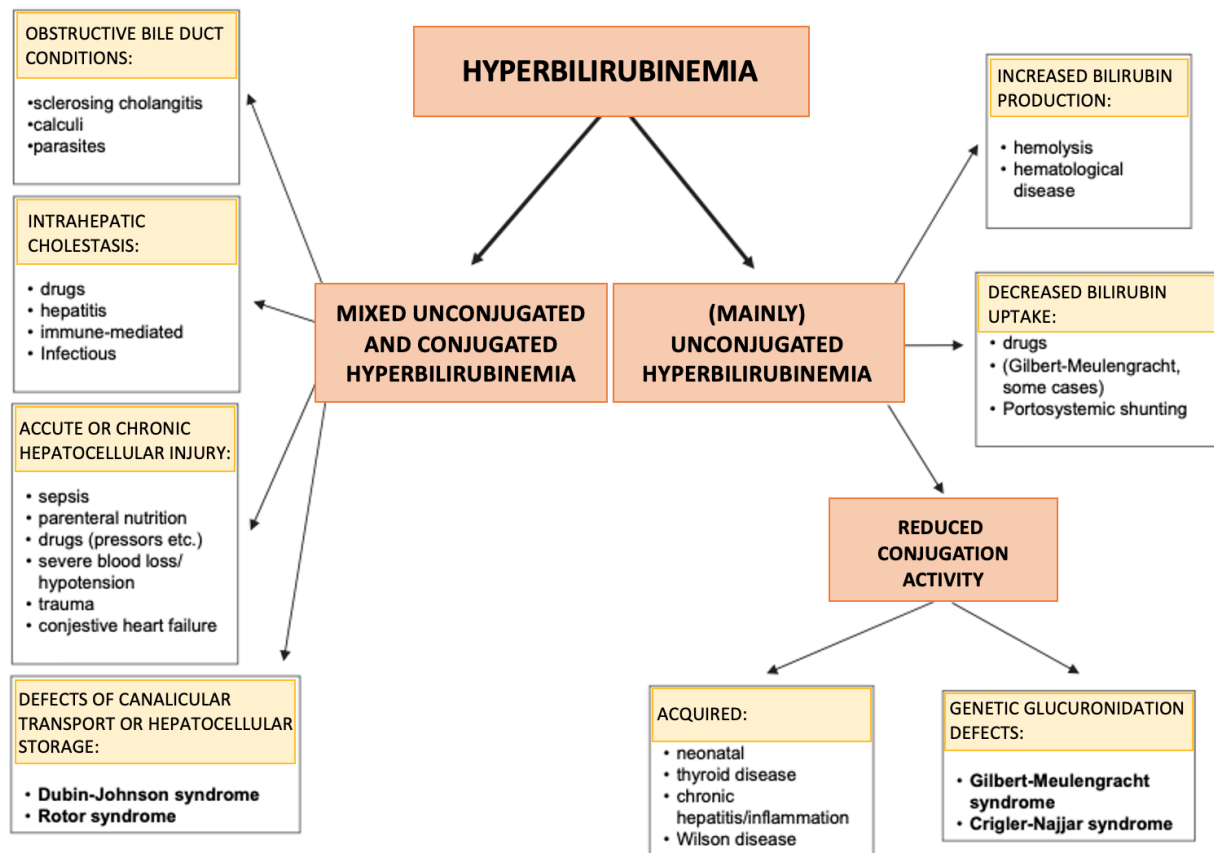


Fig. 6. Differential diagnostic approach to hyperbilirubinemia. Modified from (Strassburg, 2010).

1.3.4 Neonatal jaundice

Neonatal jaundice, one of the most common clinical conditions in the newborn period, is defined as the elevation of a total serum bilirubin concentration above 85 $\mu\text{mol/L}$ (Stevenson DK et al., 2012). Nearly 60% of term and 80% of preterm infants develop jaundice in the first week of life, and 10% of breastfed infants remain jaundiced until 1 month of age (Olusanya et al., 2014) (Battersby et al., 2017). Neonatal jaundice has multifactorial pathogenesis due to an imbalance between the production and excretion of bilirubin after birth (Hakan et al., 2015). The most important factors involved in its manifestation include immaturity of the blood-brain barrier, which is, therefore, more permeable to Bf, and immaturity of hepatic transporters and glucuronosylation

mechanisms, where the body is unable to rapidly adapt to BR overproduction shortly after birth (Shapiro et al., 2006).

Mild to moderate neonatal jaundice is associated with protection from the development of various oxidative stress-mediated diseases and resolves spontaneously within a few days after birth. However, other risk factors such as low birth weight, ABO and rhesus blood group incompatibility, glucose-6-phosphate dehydrogenase (G6PD) deficiency, neonatal immaturity, sepsis, or breastfeeding are all prerequisites for the manifestation of severe neonatal hyperbilirubinemia with bilirubin concentrations above 342 $\mu\text{mol/L}$ which could lead to accumulation of bilirubin in the basal ganglia and brainstem nuclei, resulting in acute or chronic bilirubin neurotoxicity and the risk of subsequent kernicterus which may result in acute bilirubin encephalopathy with clinical significance (MacDonald, 1995) (Dennery et al., 2001) (Watchko, 2003) (Ostrow et al., 2004) (Shapiro et al., 2006).

Many therapeutic approaches have been attempted in the past for the treatment of severe neonatal jaundice. To reduce the toxic effects of BR is still commonly used as the golden standard phototherapy (PT) with blue-green light (450-510 nm) in which BR is converted into more polar photoisomers that can be easily disposed of the body (McDonagh et al., 2009).

1.5 Phototherapy

During the neonatal period and 5–10% of them require treatment by phototherapy with visible light for which the range of wavelengths between 450 and 510 nm is the most effective (Bhutani & Johnson-Hamerman, 2015).

PT for unconjugated hyperbilirubinemia was discovered in 1958 by the team of Cremer et al. (Cremer et al., 1958) and later on in 1968 the first studies focused on the evaluation of the efficacy and safety were performed by the Lucey and co-workers (Lucey et al., 1968). The principle of this therapy has been based on the photoconversion of bilirubin to its more polar structural photo-isomers and photo-oxidative products easily excreted from the body by urine and/or bile (**Fig. 7.**) (McDonagh, 2001). Considering the fact that bilirubin concentrations in neonates can change within hours, it is quite difficult to determine the appropriate phototherapeutic

treatment and its recommendations are constantly being updated (Porter & Dennis, 2002) (Hansen et al., 2020). The guidelines for clinics that use the definitions for quality of evidence and balance of benefits and harms established by the AAP Steering Committee on Quality Improvement Management when PT used for infants at age 25 - 48 hours with bilirubin levels above 256 $\mu\text{mol/L}$, infants at age 49 - 72 hours with levels 308 $\mu\text{mol/L}$, and infants older than 72 hours with bilirubin levels above 342 $\mu\text{mol/L}$ (Porter & Dennis, 2002) (Kemper et al., 2022).

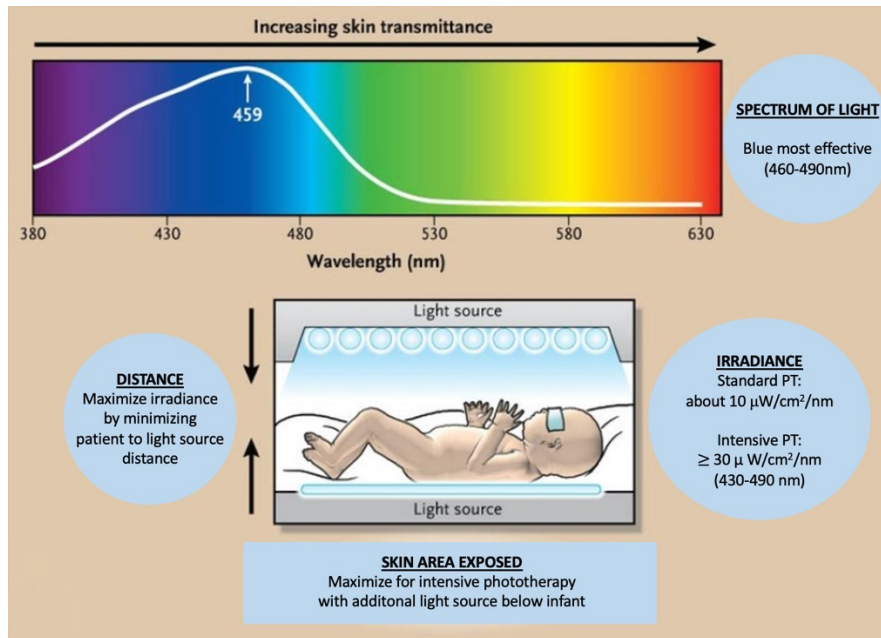


Fig. 7. The principle of phototherapeutic treatment. Modified from (Maisels & McDonagh, 2008).

Even though PT is worldwide used as the golden standard, is accompanied with side effects such as development of a bronze baby syndrome, water loss, impairment of thermoregulation, damage to unprotected eyes, and/or hypocalcaemia (Stevenson DK et al., 2012) (Khan et al., 2016). Surprisingly, recent studies suggest that PT might also be associated with an increased risk of ileus (Raghavan et al., 2005), allergic diseases (Wei et al., 2015), type 1 diabetes (McNamee et al., 2012), cancer (Wickremasinghe et al., 2016) (Cnattingius et al., 1995), and even mortality (Arnold et al., 2014; Morris et al., 2008) especially in extremely low birthweight (ELBW) neonates. The principle of the whole process is to reduce serum bilirubin concentrations and thus

the toxic effects by transformation of unconjugated BR into easily excreted photoproducts (McDonagh et al., 2009).

1.5.1 Bilirubin photoisomers

During the therapeutic approach, BR is transformed by the action of blue or blue-green light (within the wavelength range 450 - 510 nm, close to the absorption maximum of BR) into its structural BR photoisomers (PI) (Maisels & McDonagh, 2008). Exact structures of PI were established by McDonagh et al. and Onishi et al. (McDonagh et al. 1982) (McDonagh & Assisi, 1972) (Onishi et al., 1984) (McDonagh et al., 2009b). Configurational isomerization of BR leads to the fast and reversible formation of ZE- and EZ-bilirubin when compared to structural isomerization that leads to an irreversible change of BR into the most important PI E- and Z-lumirubin (*Fig. 8.*) (Onishi et al., 1984).

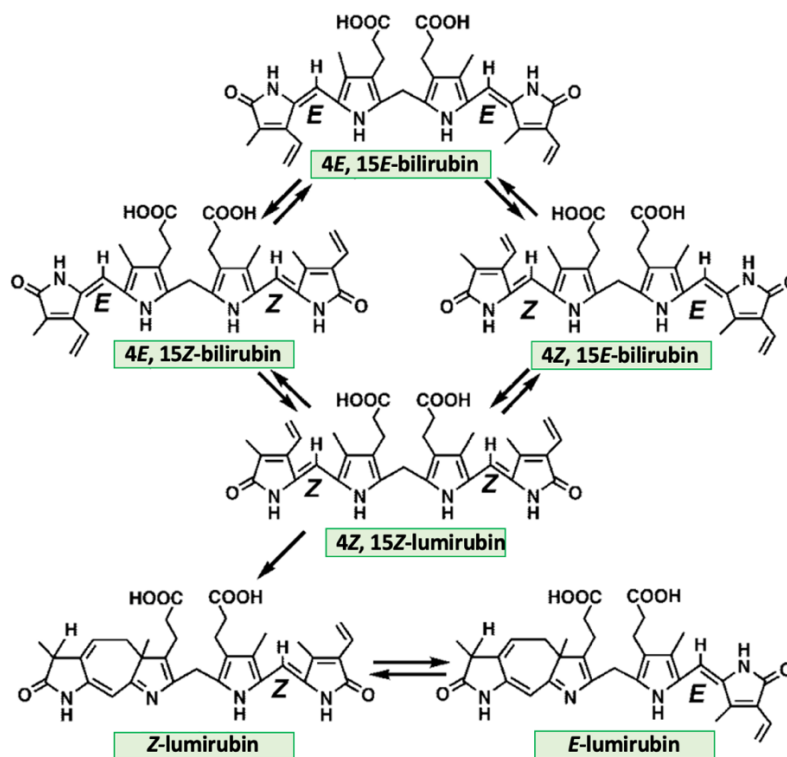


Fig. 8. Linear 2-dimensional representations of the chemical structures of bilirubin IX and its major PI lumirubin with photochemical interconversion pathways. Modified from (McDonagh et al., 2009).

Bilirubin PI could be detected by HPLC and LCMS/MS in bile, serum, and urine but none of these methods has been used in clinical practice. In 1982, McDonagh and co-workers focused on the LR determination, but this method has limited resolution of the separated PI (McDonagh, Palma, Trull, et al., 1982). Later on, another method based on the correction of the HPLC chromatogram peak areas according to the different relative molar absorption coefficients of bilirubin PI was established, but this method was not tested on the clinical samples (Itoh et al., 1999). Latest research from Jašprová and co-workers established a sensitive LC-MS/MS method for simultaneous determination of LR in HSA spiked with BR when exposed to continuous PT and in the serum of neonates that undergoes PT to understand the kinetics of bilirubin PI. Surprisingly, very low concentrations of LR $6.4 \pm 2.9 \mu\text{mol/L}$ were observed in the serum of neonates, despite a dramatic decrease in unconjugated BR concentrations. When compared to the spiked HSA, LR was produced at a 24% yield from unconjugated BR, giving LR concentrations of $75 \mu\text{mol/L}$ and the sum of the LR with unconjugated BR molar concentrations accounted only for 43% of the initial unconjugated BR concentration. After 6h of irradiation LR concentrations decreased to only $3 \mu\text{mol/L}$ and the mass balance changed dramatically (Jašprová et al., 2020). The possible main factors accounting for the low concentration of LR in clinical samples are certainly the increased excretion of LR and bilirubin photoproducts via the urine and bile (McDonagh, 1985) and the efficient degradation to the secondary photoproducts (most likely tri-, di-, and monopyrroles) (Jašprová et al., 2020). However, no quantitative data focused on the efficiency of LR photoproduction, distribution among different biological compartments, or even its transfer across the blood-brain barrier exist. Difficulties in establishing such an analytical methods are most importantly related to the low stability of bile pigments and their photodegradation products, resulting in both preanalytical as well as analytical problems.

Another studies from Jašprová and co-workers (Jasprova et al., 2016) (Jašprová et al., 2018) focused on *in vitro* effects of bilirubin photo-oxidative products on cell viability using three CNC models (SH-SY5Y a human neuroblastoma line, U-87 a human glioblastoma line, and HMC3 a human microglial line) did not result to any negative effect on the cell viability even when a high concentration of LR ($25 \mu\text{mol/L}$) was used. A similar observation was explored when performed *in vivo* studies using organotypic rat hippocampal slices, which is more representative of the complex physiologic multicellular environment. Moreover, these findings are consistent with the

early studies of Silberberg and co-workers who did not detect any toxic effects of photo-irradiated bilirubin on myelinating cerebellum cultures (Silberberg et al., 1970). Surprisingly, when Jašprová and co-workers focused on the effect of LR on the expression of pro-inflammatory genes (TNF- α , IL-1 β , IL-6, and cyclooxygenase-2 (COX-2)), increasing expression of all studied pro-inflammatory genes was observed. LR, although not affecting the viability of neuronal cells (Falcão et al., 2006), can produce pro-inflammatory cytokines (Jašprová et al., 2018a). Collectively, all viability studies demonstrated that short-term exposure to LR did not lead to cell damage or apoptosis.

1.5.2 Bilirubin oxidation products

Photochemical reactions of bilirubin occurring during light exposure lead to the formation of more polar bilirubin oxidative metabolites (Jašprová et al., 2018). Although these photodegradation products are generally regarded as being benign (Stevenson DK et al., 2012), potential biological effects have never been properly investigated. These metabolites are divided into tripyrrolic, dipyrrolic, and monopyrrolic degradation products.

The first group of BR oxidation products are tripyrrolic biopyrrins firstly discovered and studied by Yamaguchi and co-workers in 1994 as diazo-negative pigments. They identified by mass spectroscopy (MS) and nuclear magnetic resonance (NMR) the structure of two metabolites 1,14,15,17-tetrahydro-2,7,13-trimethyl-1,14-dioxo-3vinyl-16H-tripyrin-8,12-dipropionic acid (biopyrrin a) and 1,14,15,17-tetrahydro-3,7,13-trimethyl-1,14-dioxo-2-vinyl-16H-tripyrin-8,12-dipropionic acid (biopyrrin b) (**Fig. 9.**) from the urine of healthy people using anti-bilirubin monoclonal antibody 24G7 (Yamaguchi et al., 1994).

Biopyrrins were observed in higher concentrations in the urine of the patients who underwent laparotomy (Yamaguchi et al., 1994), after acute myocardial infarction (KUNII et al., 2009) and in the urine of mice exposed to social stress (Miyashita et al., 2006). The higher levels of biopyrrins were also found in patients with schizophrenia (Yasukawa et al., 2007) and during pregnancy were related to the smoking of mothers (Matsuzaki et al., 2014). Biopyrrins levels were studied by Vitek and co-workers in subjects with Gilbert syndrome (GS) who demonstrated that

mild hyperbilirubinemia protecting from oxidative stress is associated with decreased urinary biopyrrin excretion (Vítek et al., 2007). Moreover, tripyrrols were also confirmed as markers of increased oxidative stress in rats subjected to endotoxin treatment (Yamaguchi et al., 1995) (Yamaguchi et al., 1997) or fenofibrate treatment (Kobayashi et al., 2003), as well as in the hepatic ischemia-reperfusion model in the rat (Yamaguchi et al., 1996).

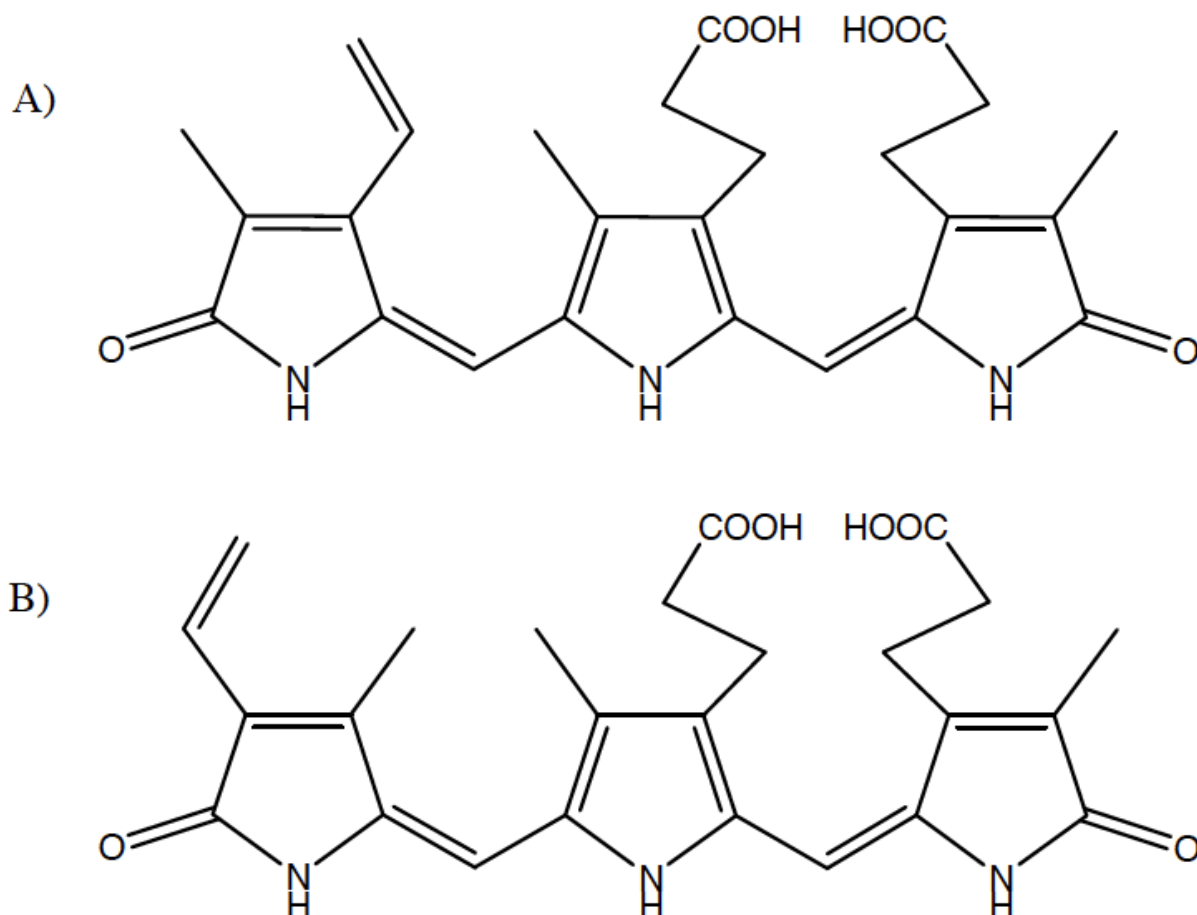


Fig. 9. Structure of biopyrrin a (A) and biopyrrin b (B). Modified from (Jašprová et al., 2018).

The second group of BR oxidation products are dipyrrolic propentdyopents, products of oxidative degradation of BR (**Fig. 10.**) firstly discovered by Stokvis and co-workers in 1870 by alkalization of icteral urine when its red coloration was observed and in 1934 by Bengold and co-workers (Dolphin, 1978). In 1957 was described a chromatographic and electrophoretic method to characterize propentdyopents by Heikel and co-workers (Heikel, 1958). Propentdyopents can be

possibly determined by Stokvis reaction spectrometrically at 525 nm (Ostrow et al., 1961), and the first discovery of their *in vitro* formation was reported in 1972 (Lightner & Quistad, 1972). Lightner and co-workers observed the production of these dipyrroles in the urine of newborn undergoing PT (Lightner et al., 1984) and the same results were demonstrated by Kunikata and co-workers when also oxidation of BR to propentdyopents during PT in neonates was observed (Kunikata et al., 2000). The latest research from Joerk and co-workers performed experiments when propentdyopents have been considered potential additional effectors in the development of arterial vasoconstriction and are present in the cerebrospinal fluid of patients with subarachnoid hemorrhage (SAH) (Joerk et al., 2019).

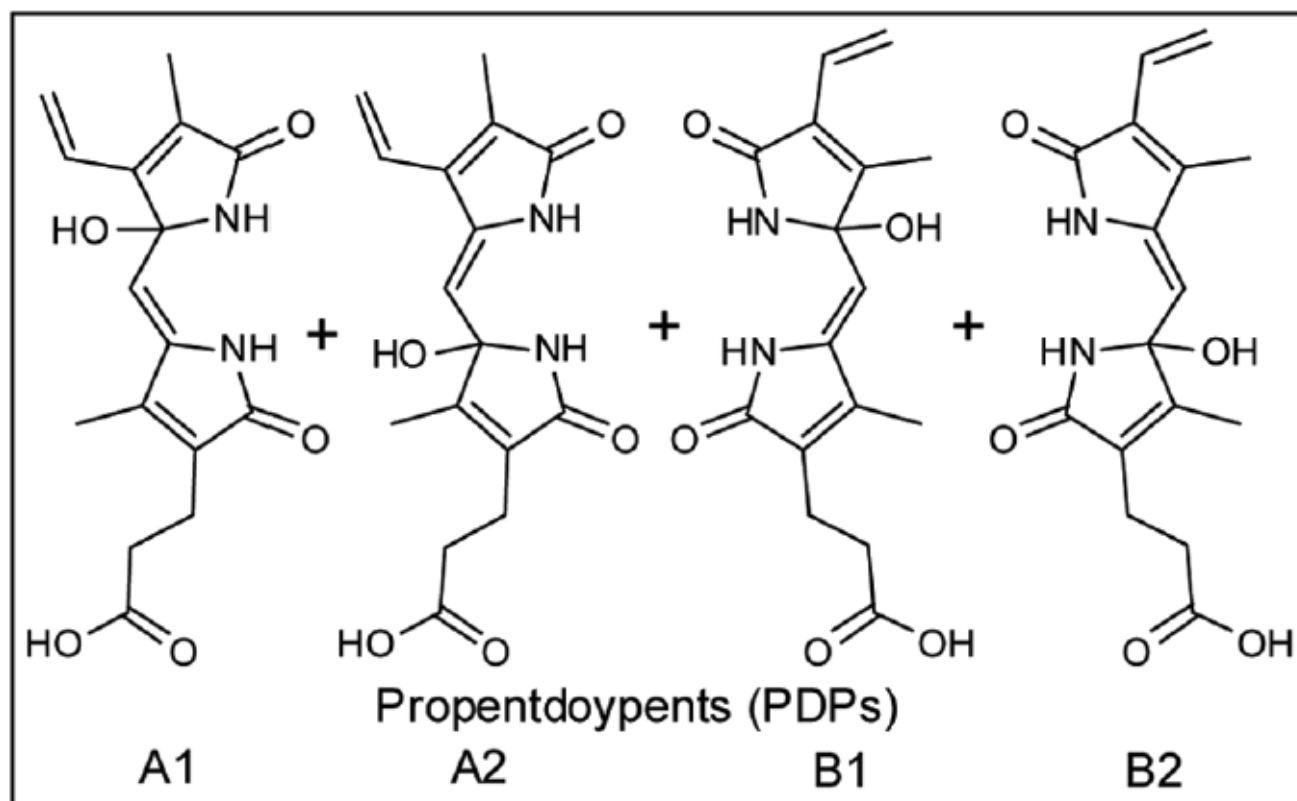


Fig. 10. Structure of propentdyopents. Modified from (Ritter et al., 2016).

The third group of BR oxidation products are mono-pyrrolic BOXes A-D (**Fig. 11**). BOX A, 2-(4-methyl-5-oxo-3-vinyl-1,5-dihydro-2H-pyrrol-2-ylidene)acetamide and BOX B, 2-(3-methyl-5-oxo-4-vinyl-1,5-dihydro-2H-pyrrol-2-ylidene)acetamide were identified as first in the

cerebrospinal fluid of patients after SAH with developed cerebral vasospasm (Kranc et al., 2000). Later in 2008 a significant production of BOXes, malondialdehyde, and superoxide dismutase, indicating a potent oxidizing environment was observed by Clark and co-workers in hematomas from the porcine model of intracerebral hemorrhage (ICH). To confirm the formation of bioactive molecules such as BOX-es by oxidation of UCB, Clark and co-workers synthesized in vitro BOX-es by oxidation of UCB at room temperature with a large excess of hydrogen peroxide. These results suggest potent oxidation processes in hematoma when the conversion of bilirubin to BOX-es is associated with a biochemical state that may cause or contribute to pathological sequelae after ICH (Clark et al., 2008).

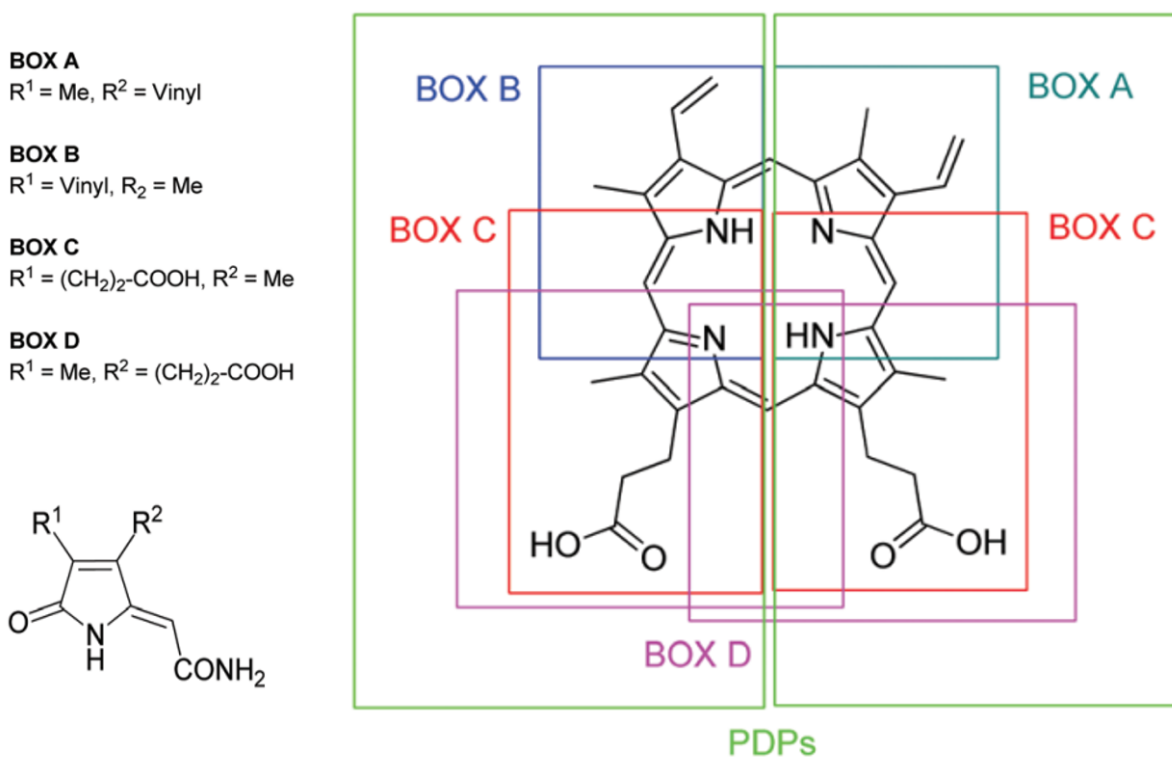


Fig. 11. The structure of bilirubin oxidation end products (BOX A-D) via intermediately formed di-pyrrolic propentdyopents (PDP) depicted in frames. Modified from (Schulze et al., 2019).

Total synthesis and characterization of BOX A and BOX B were performed by Seidel and co-workers *via* a five-step *de novo* synthesis (Seidel et al., 2014), and determination of these compounds in HSA was performed by LC-MS/MS one year later (Seidel et al., 2015). The total synthesis with NMR characterization of the BR oxidation end product BOX C (Z)-3-(5-(2-amino-2-oxoethylidene)-4-methyl-2-oxo-2,5-dihydro-1H-pyrrol-3-yl)propanoic acid and its isomeric form BOX D (Z)-3-(2-(2-amino-2-oxoethylidene)-4-methyl-5-oxo-2,5-dihydro-1H-pyrrol-3-yl)propanoic acid which might not be a direct product of oxidative degradation of BR but could derive from heme were performed by Schulze and co-workers (Schulze et al., 2019). Jašprová and co-workers demonstrated that BOX A and B are toxic *in vitro* only in very high, non-physiological concentrations contrasting to data published in SAH patients (Jašprová et al., 2018).

2 AIMS

The aim of this thesis was to study the biological properties of BR and its most common photoisomer LR. Specifically, our aims were:

- Isolation of LR for *in vitro* studies in cell lines.
- Determination of the BR excretion in different tissues and cell populations.
- Establishment of the intracellular unconjugated BR concentrations thresholds differentiating between anti- and pro-oxidant effects in different cell populations.
- Determination of the BR and LR stability and its effects on metabolic and oxidative stress markers in different cell populations.
- Determination of the effect of BR and LR on the proliferation, morphology, specific gene and protein expression, and differentiation of self-renewing neural stem cells (NSC) derived from human pluripotent stem cells (hPSC)
- Visualization of predicted morphological and genomic changes of NSC by 3D super-resolution microscopy.

3 METHODS

Following list represents the methods used in the submitted dissertation thesis by author. Detail description and other information about particular methods are listed in publications related to this thesis in section “Materials and Methods”.

- Cultivation of immortalized cell lines (HEPG2, SH-SY5Y, MRC5, RAW 264.7)
- Cultivation and differentiation of neurons (CoMo-NSC derived from ESI-017)
- Preparation and purification of BR and LR
- Stability and detection of BR and LR (LC-MS/MS)
- Detection of LR fragments (LC-MS/MS)
- Quantification of TNF α and FGF21 proteins (ELISA)
- Analysis of intracellular metabolites of the TCA Cycle (GC-MS)
- Viability/cytotoxicity measurement (MTT Assay)
- Determination of the glycolytic reserve (Oxygen Consumption Rate - OCR Seahorse)
- Cell cycle analyses (Flow cytometry)
- RNA isolation and Real-Time qPCR
- Western blot analyses
- DNA damage analyses (Comet Assay)
- Immunofluorescence and 3D Cell Imaging (fluorescent microscopy)
- Statistical analyses

4 RESULTS

The results of this thesis are presented in the form of four original manuscripts focused on BR and LR metabolism. Each publication is separately discussed in the context with current literature.

1 BLANKESTIJN, Maïke, Ivo P. VAN DE PEPPEL, Aleš DVOŘÁK, **Nikola CAPKOVÁ**, Libor VÍTEK, Johan W. JONKER & Henkjan J. VERKADE.

Induction of fecal cholesterol excretion is not effective for the treatment of hyperbilirubinemia in Gunn rats. 2021, *Pediatric Research* 89, 510–517.

2 BIANCO, Annalisa, Aleš DVOŘÁK, **Nikola CAPKOVÁ**, Camille GIRONDE, Claudio TIRIBELLI, Christophe FURGER, Libor VÍTEK, and Cristina BELLAROSA.

The extent of intracellular accumulation of bilirubin determines its anti- or pro-oxidant effect. 2021, *International Journal of Molecular Sciences* 21, no. 21: 8101.

3 DVOŘÁK, Aleš, Kateřina POSPÍŠILOVÁ, Kateřina ŽÍŽALOVÁ, **Nikola CAPKOVÁ**, Lucie MUCHOVÁ, Marek VECKA, Nikola VRZÁČKOVÁ, Jana KŘÍŽOVÁ, Jaroslav ZELENKA, Libor VÍTEK.

The effects of bilirubin and lumirubin on metabolic and oxidative stress markers. 2021, *Frontiers Pharmacology* 12, 567001.

4 **CAPKOVÁ, Nikola**, Veronika POSPÍŠILOVÁ, Veronika FEDOROVÁ, Jan RAŠKA, Kateřina POSPÍŠILOVÁ, Matteo DAL BEN, Aleš DVOŘÁK, Jitka VIKTOROVÁ, Dáša BOHAČIAKOVÁ, and Libor VÍTEK.

The effects of bilirubin and lumirubin on the differentiation of human pluripotent cell-derived neural stem cells. 2021, *Antioxidants* 10, no. 10: 1532.

5 DISCUSSION

The research of a presented thesis was focused on the understanding of the fecal cholesterol excretion related to the treatment of the hyperbilirubinemia in Gunn rats and to the biological properties of BR and its photo-oxidation products, which might have clinical relevance in phototherapy-treated hyperbilirubinemic neonates.

During the last decades, BR was determined as an important bioactive molecule, with substantial toxic effects when accumulated in high concentrations within the human body (Watchko & Tiribelli, 2013). However, mildly elevated systemic BR concentrations (such as in Gilbert syndrome) may protect against various oxidative stress-mediated and metabolic diseases including type 2 diabetes, cardiovascular diseases, or metabolic syndrome (Bosma et al., 1995) (Vítek, 2012). To understand the mechanism of BR excretion in different tissues and cells that can give us important data and information for possible therapeutic lowering of hyperbilirubinemia we tested the hypothesis that stimulation of fecal neutral sterol (FNS) excretion lowers total plasma bilirubin (TB) in hyperbilirubinemic Gunn rats *in vivo* in our paper “**Induction of fecal cholesterol excretion is not effective for the treatment of hyperbilirubinemia in Gunn rats**“. Gunn rats are a mutant strain of Wistar rats that due to the deficiency of UGT1A1 activity exhibit lifelong nonhemolytic unconjugated hyperbilirubinemia inherited as an autosomal recessive trait. These rats are used as only natural mutant model for the studies that could provide important information on BR toxicity and have helped in developing new therapeutic modalities for hyperbilirubinemia, including cell transplantation and gene therapies (Roy-Chowdhury et al., 2020). In Gunn rats, around 2 - 15% of intestinal unconjugated BR originates from biliary disposal, while 85 - 98% is derived from transintestinal unconjugated BR excretion, which is stimulated by enhancement of the fecal fatty acid excretion, which makes transintestinal bilirubin excretion the major route of unconjugated BR disposal in Gunn rats (Kotal et al., 1997) (Nishioka et al., 2003) (Cuperus et al., 2009). However, the underlying mechanism of these processes is not fully understood.

Since transintestinal excretion route is present for both cholesterol (TICE) and unconjugated BR (Kotal et al., 1997) (de Boer et al., 2018) (Hafkamp et al., 2006) we assumed that TICE - stimulated treatment could affect unconjugated BR excretion. Earlier studies showed

that plasma unconjugated BR decreased by administration of a high-fat diet (HFD) and/or the lipase inhibitor orlistat in Gunn rats (Nishioka et al., 2003) (Cuperus et al., 2011) and the increase in fecal fat excretion was correlated to the decrease in plasma unconjugated BR levels (Hafkamp et al., 2005) (Hafkamp et al., 2006). By use of radiolabelled BR, the decrease of unconjugated BR upon orlistat was observed due to an increase in transintestinal excretion (Hafkamp et al., 2006) and feeding HFD to mice enhanced TICE, resulting in increased fecal neutral sterol (FNS) excretion (van der Velde et al., 2008). Therefore, a possible increase in fecal unconjugated BR and subsequent decrease in plasma unconjugated BR levels upon higher intestinal fat concentrations could be the results of unconjugated BR “capturing” by fatty acids, meaning that the reabsorption of unconjugated BR is decreased upon its association with non-absorbed fat in the intestinal lumen (Nishioka et al., 2003) (Bulmer et al., 2013). However, our results showed that the transintestinal excretion pathways for cholesterol and for unconjugated BR are not quantitatively linked.

Since liver X receptor (LXR) and farnesoid X receptor (FXR) are involved in the regulation of the hepatic and intestinal cholesterol metabolism we inhibited intestinal cholesterol absorption by its inhibitor ezetimibe (EZE) and stimulated TICE via LXR and FXR. However, our observation resulted in the conclusion that neither stimulation of FNS excretion nor LXR or FXR stimulation exerts hypobilirubinemic effects in Gunn rats, however, fecal unconjugated BR excretion was increased. The fecal unconjugated BR excretion only accounts for an estimated ~ 50% of TB turnover (van der Veere et al., 1996) and we cannot definitively determine whether the increase was caused by increased transintestinal unconjugated BR secretion, decreased transintestinal unconjugated BR reabsorption, or decreased intraluminal (microbial) unconjugated BR degradation due to not proper quantitative estimation of unconjugated BR turnover. When compared to the Gunn rats treated with a FXR agonist obeticholic acid (OCA) with or without EZE, the lower biliary bile acid concentrations and a more hydrophilic profile since hydrophilic muricholic bile acids inhibit intestinal cholesterol absorption, and promote FNS excretion. These observations support another previous study when the underlying mechanism by which OCA increases FNS excretion in mice has been suggested to be mediated by a smaller and more hydrophilic bile acid pool (de Boer et al., 2017). Moreover, simultaneous treatment with OCA and EZE slightly increased net intestinal cholesterol excretion further than either treatment alone.

Therefore, most of the OCA effects are mediated through decreased cholesterol absorption in Gunn rats, a small part of the effects could be due to direct stimulation of TICE.

Interesting data were observed while Gunn rats treated with the liver X receptor agonist T0901317 (T09), resulting to increased bilirubin and severely increased triglycerides (TG) levels in plasma followed by optical yellow - coloured and turbid appearance. The possible effect should be explained by the data from another study when has been demonstrated that plasma TG levels > 12 mmol/L increase hemolysis, possibly due to increased membrane instability of erythrocytes (Dimeski et al., 2005) since BR is a degradation product of heme metabolism and the presence of increased hemolysis due to hypertriglyceridemia upon T09 treatment is supported by decreased plasma-free haptoglobin concentrations which is a marker for intravascular hemolysis (Shih et al., 2014). However, we did not have proper samples to perform another red blood cell analyses to determine whether hemolysis had been induced. Collectively, our data suggest that FNS excretion, LXR, or FXR activation do not result in a hypobilirubinemic effect in Gunn rats and the link between the regulation of transintestinal excretion of cholesterol and plasma unconjugated BR concentrations is not present.

In our second paper “**The extent of intracellular accumulation of bilirubin determines its anti- or pro-oxidant effect**“ we aimed to establish the intracellular unconjugated BR concentrations thresholds differentiating between anti- and pro-oxidant effects in vitro on the cells derived from the normal human kidney (HK2), murine endothelium (H5V), human hepatoblastoma (HepG2) and human neuroblastoma (SH-SY5Y) since intracellular unconjugated BR concentration was found to be cell-specific due to several factors including the extent of uptake, excretion, and metabolic transformation, with each of these steps differing in various organs. Our results showed that HepG2 cells have the lowest concentrations, while the SH-SY5Y are the most sensitive. As expected, the HepG2 cell line was less sensitive to unconjugated BR toxicity, even at the highest concentration. Conversely, the neuronal cells appeared the most sensitive since cytotoxicity started at the lowest unconjugated BR concentration while HK2 and H5V showed an intermediate behaviour.

Since cells developed multiple systems (such as enzymes with antioxidant actions including catalase and superoxide dismutase (SOD) which together convert superoxide to water) to protect against ROS, the principal endogenous intracellular antioxidant cytoprotective molecule is regarded as Glutathione (GSH). However, BR has been demonstrated to be a powerful antioxidant substance in *in vitro* studies (Gopinathan et al., 1994) (Farrera et al., 1994) (Marilena, 1997), suppressing oxidation more strongly than many other antioxidants, (Stocker, Yamamoto, et al., 1987b) (Stocker, Glazer, et al., 1987) (T.-W. Wu et al., 1991). *In vitro* studies focused on cells while depletion of GSH or bilirubin indicate that bilirubin is of comparable importance to GSH in cytoprotection (Barañano et al., 2002) (Gopinathan et al., 1994). Since bilirubin has the most potent superoxide and peroxide radical scavenger activities (Farrera et al., 1994) its potent physiological antioxidant action is further amplified by its oxidation to biliverdin and then recycle by BVR back to BR (Barañano et al., 2002). Doré and Snyder with co-workers reported the maximal neuroprotective effects of BR in hippocampal cultures when reached at nanomolar concentrations (10–50 nM), while at higher concentrations the prooxidant effects of BR were observed (Dore & Snyder, 1999) and almost similar effect was reported by Liu and co-workers in the primary cultures of oligodendrocytes (Liu et al., 2003). Latest research by Zelenka and co-workers present data focused on long-term, mildly elevated BR concentrations resulting to protection of mitochondria and the respiratory chain, with a concomitant decrease of ROS and pro-inflammatory cytokine production (Zelenka et al., 2016). These observations are consistent with another *in vitro* and *in vivo* study, demonstrating the anti-inflammatory effects of BR (Valaskova et al., 2019). However, the exact concentration thresholds between pro- and anti-oxidant effects of BR remain still unclear (Gazzin et al., 2012).

To test the pro-oxidant ability of unconjugated BR, we measured intracellular ROS induction by H₂O₂ when unconjugated BR did not result in any significant increase in intracellular ROS production in HepG2 cells even at higher concentration. On the contrary, in SH-SY5Y cells resulted in a threefold increase in intracellular ROS production and in H5V cells and HK2 cells doubled the intracellular ROS concentration. These data clearly indicates that each cell type has a different BR threshold switching between beneficial or toxic effects and expand the previous studies by Dore and co-workers with Liu and co-workers (Dore & Snyder, 1999) (Liu et al., 2003). Another experiment focused on the anti-oxidant effect of UCB revealed direct antioxidant activity

of lower concentrations of unconjugated BR in all four live cell lines. For HepG2 cells, the dose effect was measured at higher concentrations while for SH-SY5Y cells at the lowest concentrations, whereas in H5V and HK2 cells the antioxidant effect occurred at intermediate lower unconjugated BR concentration. No cytotoxic effect was observed on HepG2 and HK2 cells while it was present at low concentrations on SH-SY5Y and at very high concentrations on H5V cells. Since the cells use multiple systems to protect against ROS overproduction, we measured the total reduced GSH concentrations and SOD activity. While previously observed by Giraudi and co-workers that unconjugated BR modulated the GSH concentration in neuroblastoma cells through the induction of the System Xc-increasing cysteine uptake and intracellular GSH content (Giraudi et al., 2011) our results confirmed no effect of unconjugated BR on GSH concentration except in SH-SY5Y cells where the concentration increased upon a lower UCB treatment. In addition, the induction of SOD activity was observed in the H5V, HK2, and SH-SY5Y cells at its unconjugated BR pro-oxidant/cytotoxic concentrations while in HepG2 cell line was not affected.

While a mild elevation of BR concentration is associated with anti-oxidant effects, severe hyperbilirubinemia can cause a permanent neurological damage in neonates. Although, PT is worldwide used as the golden standard for the treatment of neonatal jaundice, the biological properties of BR photoisomers and their oxidation products have not properly been investigated. However, the still scarce data obtained until now suggests some biological activity of these products (Jašprová et al., 2018), there is still a lack of complex data and research focused on these molecules. The main reason should be the stability of these photo-sensitive molecules and the difficulty in the preparation processes of bilirubin PI in their pure forms.

In our paper “**The effects of bilirubin and lumirubin on metabolic and oxidative stress markers**“ we aimed to compare the effects of BR and LR, the major BR photo-oxidation product, on metabolic and oxidative stress markers. The biological activities of these pigments were investigated on human neuroblastoma SH-SY5Y cells, human hepatoblastoma HepG2 cells, fibroblast-like MRC5 cells from human lung tissue, and murine macrophage-like RAW 264.7 cells with a focus on mitochondrial respiration, substrate metabolism, ROS production, and the overall effects on cell viability. The stability of LR and BR in HSA and standard medium were tested before any experiments with the biological samples. The results showed relatively fast degradation

of LR in both relevant biological matrices and the remaining LR level after the experiment in medium and in HSA. In contrast, BR was stable during the entire experiment. Due to the remaining concentrations of LR from previous experiment, we focused on its stability under different oxygen conditions (normoxia 21% O₂ and hypoxia 1% O₂) when the presence of oxygen contributed to LR degradation beginning only early after the start of incubation. The rate of degradation during this time was much faster under normoxic conditions and these results suggest that the degradation of LR can be triggered by higher oxygen concentration.

When focused on the effect of LR and BR on cell viability, LR was found to be much less toxic and had no effect on the viability in all four cell lines even in the highest concentrations, while all the BR concentrations were negatively correlated with cell viability. Cytotoxicity of BR was compromised by the cellular glycolytic reserve, which indicates the capability of a cell to respond to an energetic demand as well as how close the glycolytic function is to the cell's theoretical maximum. The results showed that the most affected cell line was HepG2 (*Annex 3 – Fig. 6F*). Production of mitochondrial superoxide was measured for both lower and higher concentrations of BR and LR since the highest concentration was too apoptotic and cell debris interfered with the determination of mitochondrial superoxide. Only the higher concentrations of LR or BR caused a significant drop in superoxide production in HepG2 and SH-SY5Y cells while in MRC5 cells, even the lower concentrations were significantly efficient. Therefore, both LR and BR were almost equally capable of scavenging mitochondrial superoxide.

Since previous studies had demonstrated an inhibitory role of BR on mitochondrial respiration (Mustafa et al., 1969) (Noir et al., 1972), (Almeida & Rezende, 1981) (Rodrigues, Solá, & Brites, 2002) we focused on the effects of LR in comparison to BR on mitochondrial respiration in our cell lines incubated overnight with BR and LR. We observed no changes in respiration except for the higher concentrations of BR which decreased both basal as well as maximal respiration and indicated an overall depression of mitochondrial respiration. The ratio of maximal to basal respiration, corresponding to the respiratory capacity (Brand & Nicholls, 2011), differed for each cell line with no significant changes between the controls and treated cells. Under the serum – free conditions in HepG2 and SH-SY5Y cell lines no effect on the basal and maximal respiration was observed.

An important finding was observed for the LR effect on oxidative stress since BR is known to be one of the most potent endogenous antioxidants (Stocker, Yamamoto, et al., 1987). The antioxidant capacity (AOX) was tested in the different biological matrices in the following experiments. First, BR and LR capability to scavenge peroxy radicals in HSA with increasing concentrations was tested. Interestingly, LR had the same AOX as BR despite its degradation compared to vitamin E analog – Trolox in the same concentration. Since LR instability, the AOX of LR solutions with its spontaneous degradation was also tested and resulting in the decrease of AOX after 24 h approximately to 50% of the initial value. Moreover, substantial antioxidant effect of LR was observed in our cell models despite its marked degradation, suggesting a marked ROS - scavenging activity of LR degradation products. Nevertheless, in preventing lipoperoxidation, LR was much less efficient most likely due to its lower lipophilicity.

Since BR has impact on mitochondrial metabolism, we focused also on the possible effects of LR and BR on the production of intracellular metabolites of the TCA cycle well known for their ability to affect energy balance and to modulate multiple cellular functions as well being linked to oxidative phosphorylation (Martínez-Reyes & Chandel, 2020). Both BR/LR did not have any marked effect at lower concentrations in MRC5 and HepG2 cells; while in SH-SY5Y cells the concentrations significantly decreased in the presence of both compounds. A different response was observed with BR at higher concentration when most of the metabolites were significantly reduced in all cell lines; whereas virtually no effect was observed in cells exposed to LR (*Annex 3 – Fig. 10*). These data are consistent with the previous reports of the impact of BR on the mitochondrial metabolism and morphology demonstrated mostly in brain cells (Mustafa et al., 1969) (Almeida & Rezende, 1981) (Rodrigues, Solá, & Brites, 2002b) while no harmful effect present for LR. However, these effects on mitochondrial metabolism were beneficial in the other tissues such heart and liver (Mustafa et al., 1967) (Stumpf et al., 1985), same for the effect of BR on the mitochondrial function in adipocytes (Gordon et al., 2020). These data suggest the complex cell-specific and concentration-dependent effects of BR and its derivatives in specific conditions.

Additionally, we observed that BR behave as a pro-inflammatory molecule in the macrophage-like RAW264.7 cells, while only a mild and insignificant effect was observed for LR. This contrasts with a study performed by Jašprová and co-workers on different cell models of CNS

origin indicating substantial cell viability of BR/LR-induced pro-inflammatory effects (Jašprová et al., 2018). The possible explanation for this observation may be linked to the BR-induced TCA cycle dysregulation known to affect the inflammatory status, NO production, as well as post-translational acetylation (Williams & O'Neill, 2018), since both treatments lead to a decrease in NO availability. Since BR is known for its ability to scavenge NO by forming N-nitroso derivatives (Barone et al., 2009), the same might also be possible for LR. Moreover, BR inhibits inducible NO synthase to prevent cells from its production of large amount of NO (Zucker et al., 2015), while LR may also act in a similar manner.

Based on the recent observations by Jašprová and co-workers who demonstrated the striking upregulation of proinflammatory cytokines in organotypic rat hippocampal slices after short-term exposure to LR (Jašprová et al., 2018), we hypothesized that photoproducts of BR could possibly affect early human neurodevelopment. In our paper **“The effects of bilirubin and lumirubin on the differentiation of human pluripotent cell-derived neural stem cells”** we aimed to compare the effects of BR and LR on the proliferation, differentiation, morphology, and specific gene and protein expressions of self-renewing neural stem cells (NSC) derived from human pluripotent stem cells (hPSC) which has the ability to self-renew and terminally differentiate into neurons and glia, and thus they represent a biologically and developmentally relevant surrogate human model to study the influence of the potentially biologically active compounds on these processes. In the initial phase of our studies, we focused to assess the possible cytotoxic effects of both BR and its major photoisomer LR. We observed significant decrease in the viability/metabolic activity of the cells exposed to BR within the whole range of tested concentrations. Compared to LR, the effect was much lower, and only visible at the highest concentration indicating the much higher toxicity of BR on NSC, thus its cytotoxic effect on the CNS when severe neonatal hyperbilirubinemia occurs in neonates. Previous studies by Genc and co-workers shown that exposure to increasing concentrations of unconjugated BR is cytotoxic to rat oligodendrocytes and increase its apoptosis *in vitro* (Genc et al., 2003). Several additional studies have shown the cytotoxic and pro-apoptotic effects of BR on neuronal cultures (Rodrigues, Solá, & Brites, 2002b) (Silva et al., 2002) (Rodrigues, Solá, Silva, et al., 2002) (Kumral et al., 2005). Although under our study conditions no significant changes in DNA damage were

observed, while only a negligible modulation of the cell cycle of treated NSC exposed to BR was present.

To explore the possible effects on the protein expressions of the apoptotic or DNA damage-related markers we analysed NSC treated with both pigments. While BR exposure induced apoptotic and DNA damage markers, LR exposure in clinically relevant concentrations exerted protective effects against these changes. During the testing of toxicity, we noticed a significantly changed undifferentiated arrangement and acquired a different phenotype with increasing concentrations of LR. The neuroepithelium forming the neural tube represents the first polarized single-cell layer with a central lumen and cells displaying apicobasal polarity during the onset of neural differentiation (Wilson & Stice, 2006). These processes are mimicked under *in vitro* conditions by the radially organized neuroepithelial cells differentiated from hPSC so-called neural rosettes, a flower like structures, that represent the niche from which NSC are isolated (Wilson & Stice, 2006) (Banda et al., 2015) (Grabiec et al., 2016) (Fedorova et al., 2019). Such polarity ensures a different distribution of signalling molecules as well as of junction proteins (Miyamoto et al., 2015) (Banda et al., 2015) (Grabiec et al., 2016). When focused to Western blot analysis of transcription factors including those expressed upon differentiation of hPSC towards neuroectoderm and signalling pathway important for neural cell differentiation from NSC we observed interesting data in expressions of NSC-specific markers upon exposure to LR (**Annex 4 – Fig. 3**). These data strongly suggested that LR-treated self-renewing NSC acquire a significantly different morphology reminiscent of immature rosettes, with apically localized cell polarity proteins. Surprisingly, our study demonstrated for the first time that LR induces NSC to repolarize and that this induction is dose-dependent. Moreover, these repolarized NSC cultures, expressed higher amounts of phosphorylated ERK, important for the process of neurogenesis (possibly as a positive feedback mechanism), as well as showing an altered expression of NSC-specific. These data suggest that the potential to affect the identity and polarity of NCS during early human neural development by LR resulting to possible clinical relevance while aggressive PT used on preterm neonates is often accompanied by serious adverse effects (J. Wang et al., 2021) and the processes of neurogenesis and neurodevelopment are impaired in these neonates (Rice & Barone, 2000), which may even be exacerbated by BR photo-oxidation products generated during PT.

Lastly, we assessed the capacity of BR or LR to affect the terminal differentiation of NSC since previous studies by Brites and co-workers have shown that moderate to severe hyperbilirubinemia could induce neurological dysfunction and potentially impair brain myelination with long-term sequelae, particularly in preterm infants (Brites & Fernandes, 2015) and no possible effects of LR or other BR photo-oxidation products have been reported yet. We focused on the gene expression of selected differentiation-associated markers. The expression of NSC had gradually increased for glial markers as well as neuronal markers while there were no changes in the expression of the neural stem cells (*Annex 4 – Figure 4.*). However, we did not observe any significant changes in the expression after the treatment with BR and LR which is a notable observation since just a short-term exposure led to significant changes in these markers.

6 SUMMARY

Bilirubin has been for a long time considered only as a toxic waste product. But recent findings well documented this bioactive molecule as a powerful endogenous antioxidant with immunomodulatory, anti-inflammatory, antiproliferative and cell-signalling properties.

In the presented thesis, we investigated the kinetics and biological properties of BR compared to its photo-oxidation products, which might have clinical relevance in hyperbilirubinemic neonates treated by intensive phototherapy with blue-green light.

In Gunn rats, which represent the natural *in vivo* model for severe unconjugated hyperbilirubinemia, it is well known that only a tiny fraction of intestinal unconjugated BR originates from biliary disposal. At the same time, the biggest part is derived from transintestinal unconjugated BR excretion, which is stimulated by enhancing fecal fatty acid excretion, which makes transintestinal bilirubin excretion the major route of unconjugated BR disposal. Since transintestinal excretion also occurs for cholesterol, we hypothesized that increasing fecal cholesterol excretion and/or transintestinal excretion could also enhance fecal unconjugated BR disposal and subsequently lower plasma unconjugated BR concentrations. However, our data do not support the regulation of transintestinal excretion of cholesterol and bilirubin. Moreover, the FNS excretion, liver X receptor or farnesoid X receptor activation do not results in a hypobilirubinemic effect and has no potential for the therapy of unconjugated hyperbilirubinemia.

Unconjugated BR has the ability to diffuse into any cell while in mildly elevated concentrations is protective from various oxidative stress-mediated diseases. Hence, each cell has to maintain its intracellular concentration of unconjugated BR below the toxic threshold which is regulated by its intracellular metabolism. To understand these processes we performed an *in vitro* study using different human and murine cell lines exposed to increasing unconjugated BR concentration to find the thresholds differentiating between pro-oxidant and anti-oxidant effects while finding that a low concentration of unconjugated BR resulted in anti-oxidant effect while higher concentrations resulted to the pro-oxidant or cytotoxic effects in all studied cell lines. Our results expand and better substantiate that each cell type has a different bilirubin threshold

switching between the beneficial and toxic effects of bilirubin. Total unconjugated BR concentration treatment is an uncertain predictor of its biological effects because intracellular levels of unconjugated BR are modulated by its oxidation, conjugation, and export from the cells by membrane ABC transporters. The ability to measure real unconjugated BR concentration in the cells helps to better understand cytotoxicity induced by unconjugated BR as well as its protective effects.

While a mild elevation of BR concentration is associated with anti-oxidant effects, severe hyperbilirubinemia can cause permanent neurological damage in neonates. Although, the golden standard of the treatment of severe unconjugated hyperbilirubinemia, the biological properties of BR photo-oxidation products remain still unknown. Since intracellular metabolic impact of BR photoisomers has never been properly investigated, although our previous data suggest their biological importance we compared BR and its major photo-oxidation product LR on the metabolic and oxidative stress markers resulting in the data when LR was found to be much less toxic while still maintaining a similar anti-oxidant capacity in the serum as well as suppressing activity leading to the mitochondrial superoxide production. However, LR was less efficient in preventing lipoperoxidation due to its lower lipophilicity. Additionally, BR was found to behave as a pro-inflammatory molecule while only a mild and insignificant effect was observed for LR. Nevertheless, our data point to the biological effects of BR and its photo-oxidation products, which seem to have clinical relevance in phototherapy-treated hyperbilirubinemic neonates and adult patients.

Since aggressive PT used on preterm neonates is often accompanied by serious adverse effects and the processes of neurogenesis and/or neurodevelopment are impaired in these neonates we aimed to understand the possible impact of BR and LR on these processes using an *in vitro* model of neural stem cells. When compared to BR, LR exerted lower cytotoxicity on self-renewing neuronal stem cells. This dose-dependent effect was accompanied by mildly elevated proapoptotic markers for BR. Another interesting dose-dependent effect was observed for the morphology inducing cells to form highly polarized structures with lower expressions of some NSC-specific markers when treated by LR. Our data clearly indicate that BR and LR play a role in the earlier phases of differentiation, an influence which, however, was later lost and despite

visible changes in the morphology, at the level of the terminal differentiation, no major changes can be detected toward neuronal and glial cell types. However, LR has the potential to affect the polarity and identity of NSC during early human neural development. This observation may be of clinical importance since cellular polarity plays a significant role during the development of the CNS.

7 REFERENCES

- Abbasi, A., Deetman, P. E., Corpeleijn, E., Gansevoort, R. T., Gans, R. O. B., Hillege, H. L., van der Harst, P., Stolk, R. P., Navis, G., Alizadeh, B. Z., & Bakker, S. J. L. (2015). Bilirubin as a potential causal factor in type 2 diabetes risk: a mendelian randomization study. *Diabetes*, *64*(4), 1459–1469. <https://doi.org/10.2337/db14-0228>
- Ahdab-Barmada, M., & Moossy, J. (1984). The neuropathology of kernicterus in the premature neonate: diagnostic problems. *Journal of Neuropathology & Experimental Neurology*, *43*(1), 45–56. <https://doi.org/10.1097/00005072-198401000-00004>
- Ahlfors, C. E., & Shapiro, S. M. (2001). Auditory brainstem response and unbound bilirubin in jaundiced (jj) gunn rat pups. *Neonatology*, *80*(2), 158–162. <https://doi.org/10.1159/000047136>
- Almeida, M. A. S., & Rezende, L. (1981). The serum levels of unbound bilirubin that induce changes in some brain mitochondrial reactions in newborn guinea-pigs. *Experientia*, *37*(8), 807–809. <https://doi.org/10.1007/BF01985651>
- Amato, M. M., Kilguss, N. v., Gelardi, N. L., & Cashore, W. J. (1994). Dose-effect relationship of bilirubin on striatal synaptosomes in rats. *Neonatology*, *66*(5), 288–293. <https://doi.org/10.1159/000244119>
- Aoyagi, Y., Ikenaka, T., & Ichida, F. (1979). alpha-fetoprotein as a carrier protein in plasma and its bilirubin-binding ability. *Cancer Research*, *39*(9), 3571–3574.
- Arnold, C., Pedroza, C., & Tyson, J. E. (2014). Phototherapy in ELBW newborns: Does it work? Is it safe? The evidence from randomized clinical trials. *Seminars in Perinatology*, *38*(7), 452–464. <https://doi.org/10.1053/j.semperi.2014.08.008>
- Banda, E., McKinsey, A., Germain, N., Carter, J., Anderson, N. C., & Grabel, L. (2015). Cell polarity and neurogenesis in embryonic stem cell-derived neural rosettes. *Stem Cells and Development*, *24*(8), 1022–1033. <https://doi.org/10.1089/scd.2014.0415>
- Barañano, D. E., Rao, M., Ferris, C. D., & Snyder, S. H. (2002). Biliverdin reductase: A major physiologic cytoprotectant. *Proceedings of the National Academy of Sciences*, *99*(25), 16093–16098. <https://doi.org/10.1073/pnas.252626999>
- Barone, E., Trombino, S., Cassano, R., Sgambato, A., de Paola, B., Stasio, E. di, Picci, N., Preziosi, P., & Mancuso, C. (2009). Characterization of the S-denitrosylating activity of

- bilirubin. *Journal of Cellular and Molecular Medicine*, 13(8b), 2365–2375.
<https://doi.org/10.1111/j.1582-4934.2008.00680.x>
- Battersby, C., Michaelides, S., Upton, M., & Rennie, J. M. (2017). Term admissions to neonatal units in England: a role for transitional care? A retrospective cohort study. *BMJ Open*, 7(5), e016050. <https://doi.org/10.1136/bmjopen-2017-016050>
- Berk, P. D., Rodkey, F. L., Blaschke, T. F., Collison, H. A., & Waggoner, J. G. (1974). Comparison of plasma bilirubin turnover and carbon monoxide production in man. *The Journal of Laboratory and Clinical Medicine*, 83(1), 29–37.
- Bhutani, V. K., & Johnson-Hamerman, L. (2015). The clinical syndrome of bilirubin-induced neurologic dysfunction. *Seminars in Fetal and Neonatal Medicine*, 20(1), 6–13.
<https://doi.org/10.1016/j.siny.2014.12.008>
- Bosma, P. J. (2003). Inherited disorders of bilirubin metabolism. *Journal of Hepatology*, 38(1), 107–117. [https://doi.org/10.1016/S0168-8278\(02\)00359-8](https://doi.org/10.1016/S0168-8278(02)00359-8)
- Bosma, P. J., Chowdhury, J. R., Bakker, C., Gantla, S., de Boer, A., Oostra, B. A., Lindhout, D., Tytgat, G. N. J., Jansen, P. L. M., Elferink, R. P. J. O., & Chowdhury, N. R. (1995). The genetic basis of the reduced expression of bilirubin UDP-glucuronosyltransferase 1 in gilbert's syndrome. *New England Journal of Medicine*, 333(18), 1171–1175.
<https://doi.org/10.1056/NEJM199511023331802>
- Brand, M. D., & Nicholls, D. G. (2011). Assessing mitochondrial dysfunction in cells. *Biochemical Journal*, 435(2), 297–312. <https://doi.org/10.1042/BJ20110162>
- Brites, D., & Fernandes, A. (2015). Bilirubin-induced neural impairment: A special focus on myelination, age-related windows of susceptibility and associated co-morbidities. *Seminars in Fetal and Neonatal Medicine*, 20(1), 14–19. <https://doi.org/10.1016/j.siny.2014.12.002>
- Briz, O., Romero, M. R., Martinez-Becerra, P., Macias, R. I. R., Perez, M. J., Jimenez, F., Martin, F. G. S., & Marin, J. J. G. (2006). OATP8/1B3-mediated cotransport of bile acids and glutathione. *Journal of Biological Chemistry*, 281(41), 30326–30335.
<https://doi.org/10.1074/jbc.M602048200>
- Brumbaugh, D., & Mack, C. (2012). Conjugated hyperbilirubinemia in children. *Pediatrics in Review*, 33(7), 291–302. <https://doi.org/10.1542/pir.33-7-291>

- Bulmer, A. C., Verkade, H. J., & Wagner, K.-H. (2013). Bilirubin and beyond: A review of lipid status in Gilbert's syndrome and its relevance to cardiovascular disease protection. *Progress in Lipid Research*, 52(2), 193–205. <https://doi.org/10.1016/j.plipres.2012.11.001>
- Calligaris, S. D., Bellarosa, C., Giraudi, P., Wennberg, R. P., Ostrow, J. D., & Tiribelli, C. (2007). Cytotoxicity is predicted by unbound and not total bilirubin concentration. *Pediatric Research*, 62(5), 576–580. <https://doi.org/10.1203/PDR.0b013e3181568c94>
- Clark, J. F., Loftspring, M., Wurster, W. L., Beiler, S., Beiler, C., Wagner, K. R., & Pyne-Geithman, G. J. (2008). Bilirubin oxidation products, oxidative stress, and intracerebral hemorrhage. *Cerebral Hemorrhage*, 7–12. https://doi.org/10.1007/978-3-211-09469-3_2
- Cnattingius, S., Zack, M., Ekblom, A., Gunnarskog, J., Linet, M., & Adami, H. O. (1995). Prenatal and neonatal risk factors for childhood myeloid leukemia. *Cancer Epidemiology, Biomarkers & Prevention : A Publication of the American Association for Cancer Research, Cosponsored by the American Society of Preventive Oncology*, 4(5), 441–445.
- Cremer, R. J., Perryman, P. W., & Richards, D. H. (1958). Influence of light on the hyperbilirubinemia of infants. *The Lancet*, 271(7030), 1094–1097. [https://doi.org/10.1016/S0140-6736\(58\)91849-X](https://doi.org/10.1016/S0140-6736(58)91849-X)
- Cui, Y., König, J., Leier, I., Buchholz, U., & Keppler, D. (2001). Hepatic uptake of bilirubin and its conjugates by the human organic anion transporter SLC21A6. *Journal of Biological Chemistry*, 276(13), 9626–9630. <https://doi.org/10.1074/jbc.M004968200>
- Cuperus, F. J. C., Hafkamp, A. M., Havinga, R., Vitek, L., Zelenka, J., Tiribelli, C., Ostrow, J. D., & Verkade, H. J. (2009). Effective treatment of unconjugated hyperbilirubinemia with oral bile salts in Gunn rats. *Gastroenterology*, 136(2), 673–682.e1. <https://doi.org/10.1053/j.gastro.2008.10.082>
- Cuperus, F. J. C., Iemhoff, A. A., & Verkade, H. J. (2011). Combined treatment strategies for unconjugated hyperbilirubinemia in Gunn rats. *Pediatric Research*, 70(6), 560–565. <https://doi.org/10.1203/PDR.0b013e31823240bc>
- Dani, C., Pratesi, S., Ilari, A., Lana, D., Giovannini, M. G., Nosi, D., Buonvicino, D., Landucci, E., Bani, D., Mannaioni, G., & Gerace, E. (2019). Neurotoxicity of unconjugated bilirubin in mature and immature rat organotypic hippocampal slice cultures. *Neonatology*, 115(3), 217–225. <https://doi.org/10.1159/000494101>
- David Dolphin. (1978). *The Porphyrins*. Academic Press.

- de Boer, J. F., Kuipers, F., & Groen, A. K. (2018). Cholesterol transport revisited: A new turbo mechanism to drive cholesterol excretion. *Trends in Endocrinology & Metabolism*, *29*(2), 123–133. <https://doi.org/10.1016/j.tem.2017.11.006>
- de Boer, J. F., Schonewille, M., Boesjes, M., Wolters, H., Bloks, V. W., Bos, T., van Dijk, T. H., Jurdzinski, A., Boverhof, R., Wolters, J. C., Kuivenhoven, J. A., van Deursen, J. M., Oude Elferink, R. P. J., Moschetta, A., Kremoser, C., Verkade, H. J., Kuipers, F., & Groen, A. K. (2017). Intestinal farnesoid x receptor controls transintestinal cholesterol excretion in mice. *Gastroenterology*, *152*(5), 1126-1138.e6. <https://doi.org/10.1053/j.gastro.2016.12.037>
- Deliktaş, M., Ergin, H., Demiray, A., Akça, H., Özdemir, Ö. M. A., & Özdemir, M. B. (2019). Caffeine prevents bilirubin-induced cytotoxicity in cultured newborn rat astrocytes. *The Journal of Maternal-Fetal & Neonatal Medicine*, *32*(11), 1813–1819. <https://doi.org/10.1080/14767058.2017.1419175>
- Dennery, P. A., Seidman, D. S., & Stevenson, D. K. (2001). Neonatal hyperbilirubinemia. *New England Journal of Medicine*, *344*(8), 581–590. <https://doi.org/10.1056/NEJM200102223440807>
- Dhawan, A., Taylor, R. M., Cheeseman, P., de Silva, P., Katsiyiannakis, L., & Mieli-Vergani, G. (2005). Wilson’s disease in children: 37-year experience and revised King’s score for liver transplantation. *Liver Transplantation*, *11*(4), 441–448. <https://doi.org/10.1002/lt.20352>
- Diamond, I. F. (1970). Studies on the neurotoxicity of bilirubin and the distribution of its derivatives. *Birth Defects Original Article Series*, *6*(2), 124–127.
- Dimeski, G., Mollee, P., & Carter, A. (2005). Increased lipid concentration is associated with increased hemolysis. *Clinical Chemistry*, *51*(12), 2425–2425. <https://doi.org/10.1373/clinchem.2005.058644>
- DiNicolantonio, J. J., McCarty, M. F., & O’Keefe, J. H. (2018). Antioxidant bilirubin works in multiple ways to reduce risk for obesity and its health complications. *Open Heart*, *5*(2), e000914. <https://doi.org/10.1136/openhrt-2018-000914>
- Dore, S., & Snyder, S. H. (1999). Neuroprotective action of bilirubin against oxidative stress in primary hippocampal cultures. *Annals of the New York Academy of Sciences*, *890*(1 NEUROPROTECTI), 167–172. <https://doi.org/10.1111/j.1749-6632.1999.tb07991.x>
- Doré, S., Takahashi, M., Ferris, C. D., Hester, L. D., Guastella, D., & Snyder, S. H. (1999). Bilirubin, formed by activation of heme oxygenase-2, protects neurons against oxidative

- stress injury. *Proceedings of the National Academy of Sciences*, 96(5), 2445–2450.
<https://doi.org/10.1073/pnas.96.5.2445>
- Falcão, A. S., Fernandes, A., Brito, M. A., Silva, R. F. M., & Brites, D. (2006). Bilirubin-induced immunostimulant effects and toxicity vary with neural cell type and maturation state. *Acta Neuropathologica*, 112(1), 95–105. <https://doi.org/10.1007/s00401-006-0078-4>
- Farrera, J.-A., Jaumà, A., Ribó, J. M., Asunción Peiré, M., Parellada, P. P., Roques-Choua, S., Bienvenue, E., & Seta, P. (1994). The antioxidant role of bile pigments evaluated by chemical tests. *Bioorganic & Medicinal Chemistry*, 2(3), 181–185.
[https://doi.org/10.1016/S0968-0896\(00\)82013-1](https://doi.org/10.1016/S0968-0896(00)82013-1)
- Fedorova, V., Vanova, T., Elrefae, L., Pospisil, J., Petrasova, M., Kolajova, V., Hudacova, Z., Baniariova, J., Barak, M., Peskova, L., Barta, T., Kaucka, M., Killinger, M., Vecera, J., Bernatik, O., Cajanek, L., Hribkova, H., & Bohaciakova, D. (2019). Differentiation of neural rosettes from human pluripotent stem cells in vitro is sequentially regulated on a molecular level and accomplished by the mechanism reminiscent of secondary neurulation. *Stem Cell Research*, 40, 101563. <https://doi.org/10.1016/j.scr.2019.101563>
- Fischman, D. (2010). Bilirubin as a protective factor for rheumatoid arthritis: An NHANES study of 2003 - 2006 data. *Journal of Clinical Medicine Research*.
<https://doi.org/10.4021/jocmr444w>
- Fisher H., & Plieninger H. (1942). Synthese des biliverdins (uteroverdins) und bilirubins, der biliverdine iiii und iiii sowie der vinylneoxanthosäure. *Hoppe-Seyler's Zeitschrift Für Physiologische Chemie*, 274, 231–260.
- Gartung, C., & Matern, S. (1997). Molecular regulation of sinusoidal liver bile acid transporters during cholestasis. *The Yale Journal of Biology and Medicine*, 70(4), 355–363.
- Gazzin, S., Masutti, F., Vitek, L., & Tiribelli, C. (2017). The molecular basis of jaundice: An old symptom revisited. *Liver International*, 37(8), 1094–1102. <https://doi.org/10.1111/liv.13351>
- Gazzin, S., Strazielle, N., Tiribelli, C., & Ghersi-Egea, J.-F. (2012). Transport and metabolism at blood–brain interfaces and in neural cells: Relevance to bilirubin-induced encephalopathy. *Frontiers in Pharmacology*, 3. <https://doi.org/10.3389/fphar.2012.00089>
- Gazzin, S., Vitek, L., Watchko, J., Shapiro, S. M., & Tiribelli, C. (2016). A novel perspective on the biology of bilirubin in health and disease. *Trends in Molecular Medicine*, 22(9), 758–768. <https://doi.org/10.1016/j.molmed.2016.07.004>

- Genc, S., Genc, K., Kumral, A., Baskin, H., & Ozkan, H. (2003). Bilirubin is cytotoxic to rat oligodendrocytes in vitro. *Brain Research*, *985*(2), 135–141. [https://doi.org/10.1016/S0006-8993\(03\)03037-3](https://doi.org/10.1016/S0006-8993(03)03037-3)
- Giraudi, P. J., Bellarosa, C., Coda-Zabetta, C. D., Peruzzo, P., & Tiribelli, C. (2011). Functional induction of the cystine-glutamate exchanger system xc- activity in SH-SY5Y cells by unconjugated bilirubin. *PLoS ONE*, *6*(12), e29078. <https://doi.org/10.1371/journal.pone.0029078>
- Goessling, W., & Zucker, S. D. (2000). Role of apolipoprotein D in the transport of bilirubin in plasma. *American Journal of Physiology-Gastrointestinal and Liver Physiology*, *279*(2), G356–G365. <https://doi.org/10.1152/ajpgi.2000.279.2.G356>
- Gopinathan, V., Miller, N. J., Milner, A. D., & Rice-Evans, C. A. (1994). Bilirubin and ascorbate antioxidant activity in neonatal plasma. *FEBS Letters*, *349*(2), 197–200. [https://doi.org/10.1016/0014-5793\(94\)00666-0](https://doi.org/10.1016/0014-5793(94)00666-0)
- Gordon, D. M., Neifer, K. L., Hamoud, A.-R. A., Hawk, C. F., Nestor-Kalinoski, A. L., Miruzzi, S. A., Morran, M. P., Adeosun, S. O., Sarver, J. G., Erhardt, P. W., McCullumsmith, R. E., Stec, D. E., & Hinds, T. D. (2020). Bilirubin remodels murine white adipose tissue by reshaping mitochondrial activity and the coregulator profile of peroxisome proliferator-activated receptor α . *Journal of Biological Chemistry*, *295*(29), 9804–9822. <https://doi.org/10.1074/jbc.RA120.013700>
- Grabiec, M., Hříbková, H., Vařecha, M., Střítecká, D., Hampl, A., Dvořák, P., & Sun, Y.-M. (2016). Stage-specific roles of FGF2 signaling in human neural development. *Stem Cell Research*, *17*(2), 330–341. <https://doi.org/10.1016/j.scr.2016.08.012>
- Greenberg, D. A. (2002). The jaundice of the cell. *Proceedings of the National Academy of Sciences*, *99*(25), 15837–15839. <https://doi.org/10.1073/pnas.012685199>
- Gritz, E. C., & Bhandari, V. (2015). The human neonatal gut microbiome: A brief review. *Frontiers in Pediatrics*, *3*. <https://doi.org/10.3389/fped.2015.00017>
- Grojean, S., Koziel, V., Vert, P., & Daval, J.-L. (2000). Bilirubin induces apoptosis via activation of NMDA receptors in developing rat brain neurons. *Experimental Neurology*, *166*(2), 334–341. <https://doi.org/10.1006/exnr.2000.7518>

- Gurba, P. E., & Zand, R. (1974). Bilirubin binding to myelin basic protein, histones and its inhibition in vitro of cerebellar protein synthesis. *Biochemical and Biophysical Research Communications*, 58(4), 1142–1147. [https://doi.org/10.1016/S0006-291X\(74\)80262-7](https://doi.org/10.1016/S0006-291X(74)80262-7)
- Hafkamp, A. M., Havinga, R., Ostrow, J. D., Tiribelli, C., Pascolo, L., Sinaasappel, M., & Verkade, H. J. (2006). Novel kinetic insights into treatment of unconjugated hyperbilirubinemia: Phototherapy and orlistat treatment in Gunn rats. *Pediatric Research*, 59(4 Part 1), 506–512. <https://doi.org/10.1203/01.pdr.0000203180.79636.98>
- Hafkamp, A. M., Havinga, R., Sinaasappel, M., & Verkade, H. J. (2005). Effective oral treatment of unconjugated hyperbilirubinemia in Gunn rats. *Hepatology*, 41(3), 526–534. <https://doi.org/10.1002/hep.20589>
- Hakan, N., Zenciroglu, A., Aydin, M., Okumus, N., Dursun, A., & Dilli, D. (2015). Exchange transfusion for neonatal hyperbilirubinemia: An 8-year single center experience at a tertiary neonatal intensive care unit in Turkey. *The Journal of Maternal-Fetal & Neonatal Medicine*, 28(13), 1537–1541. <https://doi.org/10.3109/14767058.2014.960832>
- Hansen, T. W. R., Maisels, M. J., Ebbesen, F., Vreman, H. J., Stevenson, D. K., Wong, R. J., & Bhutani, V. K. (2020). Sixty years of phototherapy for neonatal jaundice – from serendipitous observation to standardized treatment and rescue for millions. *Journal of Perinatology*, 40(2), 180–193. <https://doi.org/10.1038/s41372-019-0439-1>
- Hansen, T. W. R., Mathiesen, S. B. W., & Walaas, S. I. (1996). Bilirubin has widespread inhibitory effects on protein phosphorylation. *Pediatric Research*, 39(6), 1072–1077. <https://doi.org/10.1203/00006450-199606000-00023>
- HEIKEL, T. (1958). A paper electrophoretic and paper chromatographic study of pentdyopent. *Scandinavian Journal of Clinical and Laboratory Investigation*, 10(2), 191–192.
- Hench, P. S. (1938). Effect of jaundice on rheumatoid arthritis. *BMJ*, 2(4050), 394–398. <https://doi.org/10.1136/bmj.2.4050.394>
- Horsfall, L. J., Hardy, R., Wong, A., Kuh, D., & Swallow, D. M. (2014). Genetic variation underlying common hereditary hyperbilirubinaemia (Gilbert’s syndrome) and respiratory health in the 1946 British birth cohort. *Journal of Hepatology*, 61(6), 1344–1351. <https://doi.org/10.1016/j.jhep.2014.07.028>

- Ishizaka, N., Ishizaka, Y., Takahashi, E., Yamakado, M., & Hashimoto, H. (2001). High serum bilirubin level is inversely associated with the presence of carotid plaque. *Stroke*, *32*(2), 580–583. <https://doi.org/10.1161/01.STR.32.2.580-b>
- Itoh, S., Isobe, K., & Onishi, S. (1999). Accurate and sensitive high-performance liquid chromatographic method for geometrical and structural photoisomers of bilirubin IX α using the relative molar absorptivity values. *Journal of Chromatography A*, *848*(1–2), 169–177. [https://doi.org/10.1016/S0021-9673\(99\)00469-0](https://doi.org/10.1016/S0021-9673(99)00469-0)
- Itoh, S., Okada, H., Kuboi, T., & Kusaka, T. (2017). Phototherapy for neonatal hyperbilirubinemia. *Pediatrics International*, *59*(9), 959–966. <https://doi.org/10.1111/ped.13332>
- Jacobsen, J. (1969). Binding of bilirubin to human serum albumin - determination of the dissociation constants. *FEBS Letters*, *5*(2), 112–114. [https://doi.org/10.1016/0014-5793\(69\)80307-8](https://doi.org/10.1016/0014-5793(69)80307-8)
- Jangi, S., Otterbein, L., & Robson, S. (2013). The molecular basis for the immunomodulatory activities of unconjugated bilirubin. *The International Journal of Biochemistry & Cell Biology*, *45*(12), 2843–2851. <https://doi.org/10.1016/j.biocel.2013.09.014>
- Jansen, T., & Daiber, A. (2012). Direct antioxidant properties of bilirubin and biliverdin. Is there a role for biliverdin reductase? *Frontiers in Pharmacology*, *3*. <https://doi.org/10.3389/fphar.2012.00030>
- Jašprová, J., Dal Ben, M., Hurný, D., Hwang, S., Žížalová, K., Kotek, J., Wong, R. J., Stevenson, D. K., Gazzin, S., Tiribelli, C., & Vitek, L. (2018a). Neuro-inflammatory effects of photodegradative products of bilirubin. *Scientific Reports*, *8*(1), 7444. <https://doi.org/10.1038/s41598-018-25684-2>
- Jašprová, J., Dal Ben, M., Hurný, D., Hwang, S., Žížalová, K., Kotek, J., Wong, R. J., Stevenson, D. K., Gazzin, S., Tiribelli, C., & Vitek, L. (2018b). Neuro-inflammatory effects of photodegradative products of bilirubin. *Scientific Reports*, *8*(1), 7444. <https://doi.org/10.1038/s41598-018-25684-2>
- Jasprova, J., Dal Ben, M., Vianello, E., Goncharova, I., Urbanova, M., Vyroubalova, K., Gazzin, S., Tiribelli, C., Sticha, M., Cerna, M., & Vitek, L. (2016). The Biological Effects of Bilirubin Photoisomers. *PLOS ONE*, *11*(2), e0148126. <https://doi.org/10.1371/journal.pone.0148126>

- Jašprová, J., Dvořák, A., Vecka, M., Leníček, M., Lacina, O., Valášková, P., Zapadlo, M., Plavka, R., Klán, P., & Vítek, L. (2020). A novel accurate LC-MS/MS method for quantitative determination of Z-lumirubin. *Scientific Reports*, *10*(1), 4411. <https://doi.org/10.1038/s41598-020-61280-z>
- Jayanti, S., Vítek, L., Tiribelli, C., & Gazzin, S. (2020). The role of bilirubin and the other “yellow players” in neurodegenerative diseases. *Antioxidants*, *9*(9), 900. <https://doi.org/10.3390/antiox9090900>
- Joerk, A., Ritter, M., Langguth, N., Seidel, R. A., Freitag, D., Herrmann, K.-H., Schaeffgen, A., Ritter, M., Günther, M., Sommer, C., Braemer, D., Walter, J., Ewald, C., Kalff, R., Reichenbach, J. R., Westerhausen, M., Pohnert, G., Witte, O. W., & Holthoff, K. (2019). Propentdyopents as heme degradation intermediates constrict mouse cerebral arterioles and are present in the cerebrospinal fluid of patients with subarachnoid hemorrhage. *Circulation Research*, *124*(12). <https://doi.org/10.1161/CIRCRESAHA.118.314160>
- Kemper, A. R., Newman, T. B., Slaughter, J. L., Maisels, M. J., Watchko, J. F., Downs, S. M., Grout, R. W., Bundy, D. G., Stark, A. R., Bogen, D. L., Holmes, A. V., Feldman-Winter, L. B., Bhutani, V. K., Brown, S. R., Maradiaga Panayotti, G. M., Okechukwu, K., Rappo, P. D., & Russell, T. L. (2022). Clinical practice guideline revision: Management of hyperbilirubinemia in the newborn infant 35 or more weeks of gestation. *Pediatrics*, *150*(3). <https://doi.org/10.1542/peds.2022-058859>
- Kenwright, S., & Levi, A. J. (1974). Sites of competition in the selective hepatic uptake of rifamycin-SV, flavaspidic acid, bilirubin, and bromsulphthalein. *Gut*, *15*(3), 220–226. <https://doi.org/10.1136/gut.15.3.220>
- Khan, M., Malik, K. A., & Bai, R. (2016). Hypocalcemia in jaundiced neonates receiving phototherapy. *Pakistan Journal of Medical Sciences*, *32*(6). <https://doi.org/10.12669/pjms.326.10849>
- Kobayashi, A., Takahashi, T., Sugai, S., Miyakawa, Y., Iwatsuka, H., & Yamaguchi, T. (2003). urinary excretion of oxidative metabolites of bilirubin in fenofibrate-treated rats. *The Journal of Toxicological Sciences*, *28*(2), 71–75. <https://doi.org/10.2131/jts.28.71>
- Korolnek, T., & Hamza, I. (2014). Like iron in the blood of the people: the requirement for heme trafficking in iron metabolism. *Frontiers in Pharmacology*, *5*. <https://doi.org/10.3389/fphar.2014.00126>

- Kotal, P., van der Veere, C. N., Sinaasappel, M., Elferink, R. O., Vitek, L., Brodanová, M., Jansen, P. L. M., & Fevery, J. (1997). Intestinal excretion of unconjugated bilirubin in man and rats with inherited unconjugated hyperbilirubinemia. *Pediatric Research*, 42(2), 195–200. <https://doi.org/10.1203/00006450-199708000-00011>
- Kou, Z., & Wang, C. (2022). Preparation of highly crosslinked polyvinylpyrrolidone–polydivinylbenzene adsorbents based on reinitiation of suspended double bonds to achieve excellent blood compatibility and bilirubin removal. *Materials Advances*, 3(12), 4839–4850. <https://doi.org/10.1039/D2MA00018K>
- Kranc, K. R., Pyne, G. J., Tao, L., Claridge, T. D. W., Harris, D. A., Cadoux-Hudson, T. A. D., Turnbull, J. J., Schofield, C. J., & Clark, J. F. (2000). Oxidative degradation of bilirubin produces vasoactive compounds. *European Journal of Biochemistry*, 267(24), 7094–7101. <https://doi.org/10.1046/j.1432-1327.2000.01812.x>
- Krige, J. E. J. (2001). ABC of diseases of liver, pancreas, and biliary system: Liver abscesses and hydatid disease. *BMJ*, 322(7285), 537–540. <https://doi.org/10.1136/bmj.322.7285.537>
- Kumral, A., Genc, S., Genc, K., Duman, N., Tatli, M., Sakizli, M., & Özkan, H. (2005). Hyperbilirubinemic serum is cytotoxic and induces apoptosis in murine astrocytes. *Neonatology*, 87(2), 99–104. <https://doi.org/10.1159/000081969>
- Kunii, H., Ishikawa, K., Yamaguchi, T., Komatsu, N., Ichihara, T., & Maruyama, Y. (2009). Bilirubin and its oxidative metabolite biopyrrins in patients with acute myocardial infarction. *Fukushima Journal Of Medical Science*, 55(2), 39–51. <https://doi.org/10.5387/fms.55.39>
- Kunikata, T., Itoh, S., Ozaki, T., Kondo, M., Isobe, K., & Onishi, S. (2000). Formation of propentdyopents and biliverdin, oxidized metabolites of bilirubin, in infants receiving oxygen therapy. *Pediatrics International*, 42(4), 331–336. <https://doi.org/10.1046/j.1442-200x.2000.01246.x>
- Lanone, S., Bloc, S., Foresti, R., Almolki, A., Taillé, C., Callebort, J., Conti, M., Goven, D., Aubier, M., Dureuil, B., El-Benna, J., Mottierlini, R., & Boczkowski, J. (2005). Bilirubin decreases NOS2 expression via inhibition of NAD(P)H oxidase: implications for protection against endotoxic shock in rats. *The FASEB Journal*, 19(13), 1890–1892. <https://doi.org/10.1096/fj.04-2368fje>

- Lauff, J. J., Kasper, M. E., & Ambrose, R. T. (1983). Quantitative liquid-chromatographic estimation of bilirubin species in pathological serum. *Clinical Chemistry*, *29*(5), 800–805.
- Leníček, M., Ďuricová, D., Hradsky, O., Dušátková, P., Jirásková, A., Lukáš, M., Nachtigal, P., & Vítek, L. (2014). The relationship between serum bilirubin and crohn's disease. *Inflammatory Bowel Diseases*, *20*(3), 481–487. <https://doi.org/10.1097/01.MIB.0000440817.84251.98>
- Levitt, D., & Levitt, M. (2014). Quantitative assessment of the multiple processes responsible for bilirubin homeostasis in health and disease. *Clinical and Experimental Gastroenterology*, *307*. <https://doi.org/10.2147/CEG.S64283>
- Lightner, D. A., Linnane, W. P., & Ahlfors, C. E. (1984). Bilirubin photooxidation products in the urine of jaundiced neonates receiving phototherapy. *Pediatric Research*, *18*(8), 696–700. <https://doi.org/10.1203/00006450-198408000-00003>
- Lightner, D. A., & Quistad, G. B. (1972). Hematinic acid and propentdyopents from bilirubin photo-oxidation *in vitro*. *FEBS Letters*, *25*(1), 94–96. [https://doi.org/10.1016/0014-5793\(72\)80462-9](https://doi.org/10.1016/0014-5793(72)80462-9)
- Liu, Y., Zhu, B., Wang, X., Luo, L., Li, P., Paty, D. W., & Cynader, M. S. (2003). Bilirubin as a potent antioxidant suppresses experimental autoimmune encephalomyelitis: implications for the role of oxidative stress in the development of multiple sclerosis. *Journal of Neuroimmunology*, *139*(1–2), 27–35. [https://doi.org/10.1016/S0165-5728\(03\)00132-2](https://doi.org/10.1016/S0165-5728(03)00132-2)
- Lucey, J., Ferriero, M., & Hewitt, J. (1968). Prevention of hyperbilirubinemia of prematurity by phototherapy. *Pediatrics*, *41*(6), 1047–1054.
- MacDonald, M. G. (1995). Hidden risks: early discharge and bilirubin toxicity due to glucose 6-phosphate dehydrogenase deficiency. *Pediatrics*, *96*(4 Pt 1), 734–738.
- Maines, M. D. (2005). The heme oxygenase system: Update 2005. *Antioxidants & Redox Signaling*, *7*(11–12), 1761–1766. <https://doi.org/10.1089/ars.2005.7.1761>
- Maisels, M. J., & McDonagh, A. F. (2008). Phototherapy for neonatal jaundice. *New England Journal of Medicine*, *358*(9), 920–928. <https://doi.org/10.1056/NEJMct0708376>
- Mancuso, C. (2017). Bilirubin and brain: A pharmacological approach. *Neuropharmacology*, *118*, 113–123. <https://doi.org/10.1016/j.neuropharm.2017.03.013>

- Marilena, G. (1997). New physiological importance of two classic residual products: Carbon monoxide and bilirubin. *Biochemical and Molecular Medicine*, *61*(2), 136–142.
<https://doi.org/10.1006/bmme.1997.2610>
- Martínez-Reyes, I., & Chandel, N. S. (2020). Mitochondrial TCA cycle metabolites control physiology and disease. *Nature Communications*, *11*(1), 102.
<https://doi.org/10.1038/s41467-019-13668-3>
- Matsuzaki, M., Haruna, M., Ota, E., Murayama, R., Yamaguchi, T., Shioji, I., Sasaki, S., Yamaguchi, T., & Murashima, S. (2014). Effects of lifestyle factors on urinary oxidative stress and serum antioxidant markers in pregnant Japanese women: A cohort study. *BioScience Trends*, *8*(3), 176–184. <https://doi.org/10.5582/bst.2014.01014>
- McDonagh, A. F. (1985). Light effects on transport and excretion of bilirubin in newborns. *Annals of the New York Academy of Sciences*, *453*(1), 65–72.
<https://doi.org/10.1111/j.1749-6632.1985.tb11798.x>
- McDonagh, A. F. (2001). Turning green to gold. *Nature Structural Biology*, *8*(3), 198–200.
<https://doi.org/10.1038/84915>
- McDonagh, A. F., & Assisi, F. (1972). The ready isomerization of bilirubin IX- α in aqueous solution. *Biochemical Journal*, *129*(3), 797–800. <https://doi.org/10.1042/bj1290797>
- McDonagh, A. F., Palma, L. A., & Lightner, D. A. (1982). Phototherapy for neonatal jaundice. Stereospecific and regioselective photoisomerization of bilirubin bound to human serum albumin and NMR characterization of intramolecularly cyclized photoproducts. *Journal of the American Chemical Society*, *104*(24), 6867–6869. <https://doi.org/10.1021/ja00388a104>
- McDonagh, A. F., Palma, L. A., Trull, F. R., & Lightner, D. A. (1982). Phototherapy for neonatal jaundice. Configurational isomers of bilirubin. *Journal of the American Chemical Society*, *104*(24), 6865–6867. <https://doi.org/10.1021/ja00388a103>
- McDonagh, A. F., Vreman, H. J., Wong, R. J., & Stevenson, D. K. (2009a). Photoisomers: Obfuscating Factors in Clinical Peroxidase Measurements of Unbound Bilirubin? *Pediatrics*, *123*(1), 67–76. <https://doi.org/10.1542/peds.2008-0492>
- McDonagh, A. F., Vreman, H. J., Wong, R. J., & Stevenson, D. K. (2009b). Photoisomers: Obfuscating factors in clinical peroxidase measurements of unbound bilirubin? *Pediatrics*, *123*(1), 67–76. <https://doi.org/10.1542/peds.2008-0492>

- McNamee, M. B., Cardwell, C. R., & Patterson, C. C. (2012). Neonatal jaundice is associated with a small increase in the risk of childhood type 1 diabetes: a meta-analysis of observational studies. *Acta Diabetologica*, *49*(1), 83–87. <https://doi.org/10.1007/s00592-011-0326-5>
- Mendenhall, C. L., Anderson, S., Weesner, R. E., Goldberg, S. J., & Crolic, K. A. (1984). Protein-calorie malnutrition associated with alcoholic hepatitis. *The American Journal of Medicine*, *76*(2), 211–222. [https://doi.org/10.1016/0002-9343\(84\)90776-9](https://doi.org/10.1016/0002-9343(84)90776-9)
- Miyamoto, Y., Sakane, F., & Hashimoto, K. (2015). N-cadherin-based adherens junction regulates the maintenance, proliferation, and differentiation of neural progenitor cells during development. *Cell Adhesion & Migration*, *9*(3), 183–192. <https://doi.org/10.1080/19336918.2015.1005466>
- Miyashita, T., Yamaguchi, T., Motoyama, K., Unno, K., Nakano, Y., & Shimoi, K. (2006). Social stress increases biopyrrins, oxidative metabolites of bilirubin, in mouse urine. *Biochemical and Biophysical Research Communications*, *349*(2), 775–780. <https://doi.org/10.1016/j.bbrc.2006.08.098>
- Morelli, L. (2008). Postnatal development of intestinal microflora as influenced by infant nutrition. *The Journal of Nutrition*, *138*(9), 1791S-1795S. <https://doi.org/10.1093/jn/138.9.1791S>
- Morris, B. H., Oh, W., Tyson, J. E., Stevenson, D. K., Phelps, D. L., O’Shea, T. M., McDavid, G. E., Perritt, R. L., van Meurs, K. P., Vohr, B. R., Grisby, C., Yao, Q., Pedroza, C., Das, A., Poole, W. K., Carlo, W. A., Duara, S., Lupton, A. R., Salhab, W. A., ... Higgins, R. D. (2008). Aggressive vs. conservative phototherapy for infants with extremely low birth weight. *New England Journal of Medicine*, *359*(18), 1885–1896. <https://doi.org/10.1056/NEJMoa0803024>
- Muchová, L., Kráslová, I., Leníček, M., & Vitek, L. (2004). [Gilbert’s syndrome--myths and reality]. *Casopis Lekarů Ceských*, *143*(6), 375–380.
- Muchova, L., Vanova, K., Zelenka, J., Lenicek, M., Petr, T., Vejrazka, M., Sticova, E., Vreman, H. J., Wong, R. J., & Vitek, L. (2011). Bile acids decrease intracellular bilirubin levels in the cholestatic liver: implications for bile acid-mediated oxidative stress. *Journal of Cellular and Molecular Medicine*, *15*(5), 1156–1165. <https://doi.org/10.1111/j.1582-4934.2010.01098.x>

- Muraca, M., & Fevery, J. (1984). Influence of sex and sex steroids on bilirubin uridine diphosphate-glucuronosyltransferase activity of rat liver. *Gastroenterology*, *87*(2), 308–313.
- Mustafa, M. G., Cowger, M. L., & King, T. E. (1967). On the energy-dependent bilirubin-induced mitochondrial swelling. *Biochemical and Biophysical Research Communications*, *29*(5), 661–666. [https://doi.org/10.1016/0006-291X\(67\)90267-7](https://doi.org/10.1016/0006-291X(67)90267-7)
- Mustafa, M. G., Cowger, M. L., & King, T. E. (1969). Effects of bilirubin on mitochondrial reactions. *Journal of Biological Chemistry*, *244*(23), 6403–6414. [https://doi.org/10.1016/S0021-9258\(18\)63479-9](https://doi.org/10.1016/S0021-9258(18)63479-9)
- Nishioka, T., Hafkamp, A. M., Havinga, R., van Lierop, P. P. E., Velvis, H., & Verkade, H. J. (2003). Orlistat treatment increases fecal bilirubin excretion and decreases plasma bilirubin concentrations in hyperbilirubinemic Gunn rats. *The Journal of Pediatrics*, *143*(3), 327–334. [https://doi.org/10.1067/S0022-3476\(03\)00298-1](https://doi.org/10.1067/S0022-3476(03)00298-1)
- Nocentini, A., Bonardi, A., Pratesi, S., Gratteri, P., Dani, C., & Supuran, C. T. (2022). Pharmaceutical strategies for preventing toxicity and promoting antioxidant and anti-inflammatory actions of bilirubin. *Journal of Enzyme Inhibition and Medicinal Chemistry*, *37*(1), 487–501. <https://doi.org/10.1080/14756366.2021.2020773>
- Noir, B. A., Boveris, A., Pereira, A. M. G., & Stoppani, A. O. M. (1972). Bilirubin: A multi-site inhibitor of mitochondrial respiration. *FEBS Letters*, *27*(2), 270–274. [https://doi.org/10.1016/0014-5793\(72\)80638-0](https://doi.org/10.1016/0014-5793(72)80638-0)
- Novotný, L., & Vítek, L. (2003). Inverse relationship between serum bilirubin and atherosclerosis in men: A meta-analysis of published studies. *Experimental Biology and Medicine*, *228*(5), 568–571. <https://doi.org/10.1177/15353702-0322805-29>
- Olusanya, B. O., Ogunlesi, T. A., & Slusher, T. M. (2014). Why is kernicterus still a major cause of death and disability in low-income and middle-income countries? *Archives of Disease in Childhood*, *99*(12), 1117–1121. <https://doi.org/10.1136/archdischild-2013-305506>
- Onishi, S., Miura, I., Isobe, K., Itoh, S., Ogino, T., Yokoyama, T., & Yamakawa, T. (1984). Structure and thermal interconversion of cyclobilirubin IX α . *Biochemical Journal*, *218*(3), 667–676. <https://doi.org/10.1042/bj2180667>
- Ostrow, J. D., Hammaker, L., & Schmid, R. (1961). The preparation of crystalline bilirubin-C¹⁴*. *Journal of Clinical Investigation*, *40*(8 Pt 1-2), 1442–1452. <https://doi.org/10.1172/JCI104375>

- Ostrow, J. D., Pascolo, L., Brites, D., & Tiribelli, C. (2004). Molecular basis of bilirubin-induced neurotoxicity. *Trends in Molecular Medicine*, *10*(2), 65–70.
<https://doi.org/10.1016/j.molmed.2003.12.003>
- Otterbein, L. E., & Choi, A. M. K. (2000). Heme oxygenase: colors of defense against cellular stress. *American Journal of Physiology-Lung Cellular and Molecular Physiology*, *279*(6), L1029–L1037. <https://doi.org/10.1152/ajplung.2000.279.6.L1029>
- Papatheodoridis, G. v, Hamilton, M., Mistry, P. K., Davidson, B., Rolles, K., & Burroughs, A. K. (1998). Ulcerative colitis has an aggressive course after orthotopic liver transplantation for primary sclerosing cholangitis. *Gut*, *43*(5), 639–644. <https://doi.org/10.1136/gut.43.5.639>
- Peng, F., Deng, X., Yu, Y., Chen, X., Shen, L., Zhong, X., Qiu, W., Jiang, Y., Zhang, J., & Hu, X. (2011). Serum bilirubin concentrations and multiple sclerosis. *Journal of Clinical Neuroscience*, *18*(10), 1355–1359. <https://doi.org/10.1016/j.jocn.2011.02.023>
- Porter, M. L., & Dennis, B. L. (2002a). Hyperbilirubinemia in the term newborn. *American Family Physician*, *65*(4), 599–606.
- Pranty, A. I., Shumka, S., & Adjaye, J. (2022). Bilirubin-induced neurological damage: current and emerging iPSC-derived brain organoid models. *Cells*, *11*(17), 2647.
<https://doi.org/10.3390/cells11172647>
- Raghavan, K., Thomas, E., Patole, S., & Muller, R. (2005). Is phototherapy a risk factor for ileus in high-risk neonates? *The Journal of Maternal-Fetal & Neonatal Medicine*, *18*(2), 129–131. <https://doi.org/10.1080/14767050500233076>
- Rice, D., & Barone, S. (2000). Critical periods of vulnerability for the developing nervous system: evidence from humans and animal models. *Environmental Health Perspectives*, *108*(suppl 3), 511–533. <https://doi.org/10.1289/ehp.00108s3511>
- Ritter, M., Seidel, R. A., Bellstedt, P., Schneider, B., Bauer, M., Görls, H., & Pohnert, G. (2016). Isolation and identification of intermediates of the oxidative bilirubin degradation. *Organic Letters*, *18*(17), 4432–4435. <https://doi.org/10.1021/acs.orglett.6b02287>
- Robinson, S., Vanier, T., Desforges, J. F., & Schmid, R. (1962). Jaundice in thalassemia minor. *New England Journal of Medicine*, *267*(11), 523–529.
<https://doi.org/10.1056/NEJM196209132671101>

- Rodrigues, C. M. P., Solá, S., & Brites, D. (2002). Bilirubin induces apoptosis via the mitochondrial pathway in developing rat brain neurons. *Hepatology*, *35*(5), 1186–1195. <https://doi.org/10.1053/jhep.2002.32967>
- Rodrigues, C. M. P., Solá, S., Silva, R. F. M., & Brites, D. (2002). Aging confers different sensitivity to the neurotoxic properties of unconjugated bilirubin. *Pediatric Research*, *51*(1), 112–118. <https://doi.org/10.1203/00006450-200201000-00020>
- Roy-Chowdhury, N., Wang, X., & Roy-Chowdhury, J. (2020). Bile pigment metabolism and its disorders. In *Emery and Rimoin's Principles and Practice of Medical Genetics and Genomics* (pp. 507–553). Elsevier. <https://doi.org/10.1016/B978-0-12-812532-8.00019-7>
- Salehi, N., Moosavi-Movahedi, A. A., Fotouhi, L., Yousefinejad, S., Shourian, M., Hosseinzadeh, R., Sheibani, N., & Habibi-Rezaei, M. (2014). Heme degradation upon production of endogenous hydrogen peroxide via interaction of hemoglobin with sodium dodecyl sulfate. *Journal of Photochemistry and Photobiology B: Biology*, *133*, 11–17. <https://doi.org/10.1016/j.jphotobiol.2014.02.014>
- Salim, M., Brown-Kipphut, B. A., & Maines, M. D. (2001). Human biliverdin reductase is autophosphorylated, and phosphorylation is required for bilirubin formation. *Journal of Biological Chemistry*, *276*(14), 10929–10934. <https://doi.org/10.1074/jbc.M010753200>
- Schultz, I. J., Chen, C., Paw, B. H., & Hamza, I. (2010). Iron and Porphyrin trafficking in heme biogenesis. *Journal of Biological Chemistry*, *285*(35), 26753–26759. <https://doi.org/10.1074/jbc.R110.119503>
- Schulze, D., Traber, J., Ritter, M., Görls, H., Pohnert, G., & Westerhausen, M. (2019). Total syntheses of the bilirubin oxidation end product Z -BOX C and its isomeric form Z -BOX D. *Organic & Biomolecular Chemistry*, *17*(26), 6489–6496. <https://doi.org/10.1039/C9OB01117J>
- Schwertner, H. A., Jackson, W. G., & Tolan, G. (1994). Association of low serum concentration of bilirubin with increased risk of coronary artery disease. *Clinical Chemistry*, *40*(1), 18–23.
- Sedlak, T. W., Saleh, M., Higginson, D. S., Paul, B. D., Juluri, K. R., & Snyder, S. H. (2009). Bilirubin and glutathione have complementary antioxidant and cytoprotective roles. *Proceedings of the National Academy of Sciences*, *106*(13), 5171–5176. <https://doi.org/10.1073/pnas.0813132106>

- Sedlak, T. W., & Snyder, S. H. (2004). Bilirubin benefits: Cellular protection by a biliverdin reductase antioxidant cycle. *Pediatrics*, *113*(6), 1776–1782.
<https://doi.org/10.1542/peds.113.6.1776>
- Seidel, R. A., Kahnes, M., Bauer, M., & Pohnert, G. (2015). Simultaneous determination of the bilirubin oxidation end products Z-BOX A and Z-BOX B in human serum using liquid chromatography coupled to tandem mass spectrometry. *Journal of Chromatography B*, *974*, 83–89. <https://doi.org/10.1016/j.jchromb.2014.10.027>
- Seidel, R. A., Schowtka, B., Klopffleisch, M., Kühl, T., Weiland, A., Koch, A., Görls, H., Imhof, D., Pohnert, G., & Westerhausen, M. (2014). Total synthesis and characterization of the bilirubin oxidation product (Z)-2-(4-ethenyl-3-methyl-5-oxo-1,5-dihydro-2H-pyrrol-2-ylidene)ethanamide (Z-BOX B). *Tetrahedron Letters*, *55*(48), 6526–6529.
<https://doi.org/10.1016/j.tetlet.2014.09.108>
- Shapiro, S. M., Bhutani, V. K., & Johnson, L. (2006). Hyperbilirubinemia and Kernicterus. *Clinics in Perinatology*, *33*(2), 387–410. <https://doi.org/10.1016/j.clp.2006.03.010>
- Shih, A. W. Y., McFarlane, A., & Verhovsek, M. (2014). Haptoglobin testing in hemolysis: Measurement and interpretation. *American Journal of Hematology*, *89*(4), 443–447.
<https://doi.org/10.1002/ajh.23623>
- Sidel, N., & Abrams, M. I. (1934). Jaundice in arthritis: its analgesic action. *New England Journal of Medicine*, *210*(4), 181–182. <https://doi.org/10.1056/NEJM193401252100404>
- Silberberg, D. H., Johnson, L., Schutta, H., & Linda, R. (1970). Effects of photodegradation products of bilirubin on myelinating cerebellum cultures. *The Journal of Pediatrics*, *77*(4), 613–618. [https://doi.org/10.1016/S0022-3476\(70\)80202-5](https://doi.org/10.1016/S0022-3476(70)80202-5)
- Silva, R. F. M., Rodrigues, C. M. P., & Brites, D. (2002). Rat cultured neuronal and glial cells respond differently to toxicity of unconjugated bilirubin. *Pediatric Research*, *51*(4), 535–541. <https://doi.org/10.1203/00006450-200204000-00022>
- Stevenson DK, Maisels M, & Watchko JF. (2012). *Care of the Jaundiced Neonate*. The McGraw-Hill Companies, Inc.
- Sticova, E. (2013). New insights in bilirubin metabolism and their clinical implications. *World Journal of Gastroenterology*, *19*(38), 6398. <https://doi.org/10.3748/wjg.v19.i38.6398>

- Stocker, R., & Ames, B. N. (1987). Potential role of conjugated bilirubin and copper in the metabolism of lipid peroxides in bile. *Proceedings of the National Academy of Sciences*, 84(22), 8130–8134. <https://doi.org/10.1073/pnas.84.22.8130>
- Stocker, R., Glazer, A. N., & Ames, B. N. (1987). Antioxidant activity of albumin-bound bilirubin. *Proceedings of the National Academy of Sciences*, 84(16), 5918–5922. <https://doi.org/10.1073/pnas.84.16.5918>
- Stocker, R., Yamamoto, Y., McDonagh, A. F., Glazer, A. N., & Ames, B. N. (1987). Bilirubin is an antioxidant of possible physiological importance. *Science*, 235(4792), 1043–1046. <https://doi.org/10.1126/science.3029864>
- Strassburg, C. P. (2010). Hyperbilirubinemia syndromes (Gilbert-Meulengracht, Crigler-Najjar, Dubin-Johnson, and Rotor syndrome). *Best Practice & Research Clinical Gastroenterology*, 24(5), 555–571. <https://doi.org/10.1016/j.bpg.2010.07.007>
- Stratta, R. J., Wood, R. P., Langnas, A. N., Hollins, R. R., Bruder, K. J., Donovan, J. P., Burnett, D. A., Lieberman, R. P., Lund, G. B., & Pillen, T. J. (1989). Diagnosis and treatment of biliary tract complications after orthotopic liver transplantation. *Surgery*, 106(4), 675–683; discussion 683-4.
- Stumpf, D. A., Eguren, L. A., & Parks, J. K. (1985). Bilirubin increases mitochondrial inner membrane conductance. *Biochemical Medicine*, 34(2), 226–229. [https://doi.org/10.1016/0006-2944\(85\)90115-2](https://doi.org/10.1016/0006-2944(85)90115-2)
- Suzuki, N., Yamaguchi, T., & Nakajima, H. (1988). Role of high-density lipoprotein in transport of circulating bilirubin in rats. *The Journal of Biological Chemistry*, 263(11), 5037–5043.
- Temme, E. H. M., Zhang, J., Schouten, E. G., & Kesteloot, H. (2001). Serum bilirubin and 10-year mortality risk in a Belgian population. *Cancer Causes and Control*, 12(10), 887–894. <https://doi.org/10.1023/A:1013794407325>
- Tenhunen, R., Marver, H., Pinstone, N. R., Trager, W. F., Cooper, D. Y., & Schmid, R. (1972). Enzymic degradation of heme. Oxygenative cleavage requiring cytochrome P-450. *Biochemistry*, 11(9), 1716–1720. <https://doi.org/10.1021/bi00759a029>
- Tiribelli, C., & Ostrow, J. D. (2005). Intestinal flora and bilirubin. *Journal of Hepatology*, 42(2), 170–172. <https://doi.org/10.1016/j.jhep.2004.12.002>
- Tschesche, R. (1938). Die Chemie des Pyrrols. Von H. Fischer u. H. Orth. II. Band: Pyrrolfarbstoffe. 1. Hälfte: Porphyrine – Hämin – Bilirubin und ihre Abkömmlinge. 764

- Seiten. Akademische Verlagsgesellschaft m. b. H., Leipzig 1937. Preis geh. RM. 42, —, geb. RM. 44, —. *Angewandte Chemie*, 51(1), 27–27.
<https://doi.org/10.1002/ange.19380510110>
- Valaskova, P., Dvorak, A., Lenicek, M., Zizalova, K., Kutinova-Canova, N., Zelenka, J., Cahova, M., Vitek, L., & Muchova, L. (2019). Hyperbilirubinemia in Gunn rats is associated with decreased inflammatory response in LPS-mediated systemic inflammation. *International Journal of Molecular Sciences*, 20(9), 2306.
<https://doi.org/10.3390/ijms20092306>
- van der Veere, C. N., Schoemaker, B., Bakker, C., van der Meer, R., Jansen, P. L., & Elferink, R. P. (1996). Influence of dietary calcium phosphate on the disposition of bilirubin in rats with unconjugated hyperbilirubinemia. *Hepatology*, 24(3), 620–626.
<https://doi.org/10.1002/hep.510240326>
- van der Velde, A. E., Vrins, C. L. J., van den Oever, K., Seemann, I., Oude Elferink, R. P. J., van Eck, M., Kuipers, F., & Groen, A. K. (2008). Regulation of direct transintestinal cholesterol excretion in mice. *American Journal of Physiology-Gastrointestinal and Liver Physiology*, 295(1), G203–G208. <https://doi.org/10.1152/ajpgi.90231.2008>
- van Dijk, R., Beuers, U., & Bosma, P. J. (2015). Gene replacement therapy for genetic hepatocellular jaundice. *Clinical Reviews in Allergy & Immunology*, 48(2–3), 243–253.
<https://doi.org/10.1007/s12016-014-8454-7>
- Vitek, L. (2012). The role of bilirubin in diabetes, metabolic syndrome, and cardiovascular diseases. *Frontiers in Pharmacology*, 3. <https://doi.org/10.3389/fphar.2012.00055>
- Vitek, L., Kotal, P., Jirsa, M., Malina, J., Černá, M., Chmelař, D., & Fevery, J. (2000). Intestinal colonization leading to fecal urobilinoid excretion may play a role in the pathogenesis of neonatal jaundice. *Journal of Pediatric Gastroenterology and Nutrition*, 30(3), 294–298.
<https://doi.org/10.1097/00005176-200003000-00015>
- Vitek, L., Kráslová, I., Muchová, L., Novotný, L., & Yamaguchi, T. (2007). Urinary excretion of oxidative metabolites of bilirubin in subjects with Gilbert syndrome. *Journal of Gastroenterology and Hepatology*, 22(6), 841–845. <https://doi.org/10.1111/j.1440-1746.2006.04564.x>
- Vitek, L., Muchová, L., Jančová, E., Pešičková, S., Tegzová, D., Peterová, V., Pavelka, K., Tesař, V., & Schwertner, H. (2010). Association of systemic lupus erythematosus with low

- serum bilirubin levels. *Scandinavian Journal of Rheumatology*, 39(6), 480–484.
<https://doi.org/10.3109/03009741003742748>
- Vitek, L., & Ostrow, J. (2009). Bilirubin chemistry and metabolism; harmful and protective aspects. *Current Pharmaceutical Design*, 15(25), 2869–2883.
<https://doi.org/10.2174/138161209789058237>
- Vitek, L., & Tiribelli, C. (2021). Bilirubin: The yellow hormone? *Journal of Hepatology*, 75(6), 1485–1490. <https://doi.org/10.1016/j.jhep.2021.06.010>
- Wagner, K.-H., Wallner, M., Mölzer, C., Gazzin, S., Bulmer, A. C., Tiribelli, C., & Vitek, L. (2015). Looking to the horizon: the role of bilirubin in the development and prevention of age-related chronic diseases. *Clinical Science*, 129(1), 1–25.
<https://doi.org/10.1042/CS20140566>
- Wang, J., Guo, G., Li, A., Cai, W.-Q., & Wang, X. (2021). Challenges of phototherapy for neonatal hyperbilirubinemia (Review). *Experimental and Therapeutic Medicine*, 21(3), 231.
<https://doi.org/10.3892/etm.2021.9662>
- Wang, L., & Bautista, L. E. (2015). Serum bilirubin and the risk of hypertension. *International Journal of Epidemiology*, 44(1), 142–152. <https://doi.org/10.1093/ije/dyu242>
- Watchko, J. F. (2003). Jaundice in low birthweight infants: pathobiology and outcome. *Archives of Disease in Childhood - Fetal and Neonatal Edition*, 88(6), 455F – 458.
<https://doi.org/10.1136/fn.88.6.F455>
- Watchko, J. F. (2006). Neonatal hyperbilirubinemia — what are the risks? *New England Journal of Medicine*, 354(18), 1947–1949. <https://doi.org/10.1056/NEJMe068053>
- Watchko, J. F., & Tiribelli, C. (2013). Bilirubin-induced neurologic damage — mechanisms and management approaches. *New England Journal of Medicine*, 369(21), 2021–2030.
<https://doi.org/10.1056/NEJMra1308124>
- Wei, C.-C., Lin, C.-L., Shen, T.-C., & Kao, C.-H. (2015). Neonatal jaundice and risks of childhood allergic diseases: a population-based cohort study. *Pediatric Research*, 78(2), 223–230. <https://doi.org/10.1038/pr.2015.89>
- Wickremasinghe, A. C., Kuzniewicz, M. W., Grimes, B. A., McCulloch, C. E., & Newman, T. B. (2016). Neonatal phototherapy and infantile cancer. *Pediatrics*, 137(6).
<https://doi.org/10.1542/peds.2015-1353>

- Williams, N. C., & O'Neill, L. A. J. (2018). A Role for the Krebs cycle intermediate citrate in metabolic reprogramming in innate immunity and inflammation. *Frontiers in Immunology*, 9. <https://doi.org/10.3389/fimmu.2018.00141>
- Wilson, P. G., & Stice, S. S. (2006). Development and differentiation of neural rosettes derived from human embryonic stem cells. *Stem Cell Reviews*, 2(1), 67–77. <https://doi.org/10.1007/s12015-006-0011-1>
- Wu, B., Wu, Y., & Tang, W. (2019). Heme Catabolic pathway in inflammation and immune disorders. *Frontiers in Pharmacology*, 10. <https://doi.org/10.3389/fphar.2019.00825>
- Wu, T.-W., Carey, D., Wu, J., & Sugiyama, H. (1991). The cytoprotective effects of bilirubin and biliverdin on rat hepatocytes and human erythrocytes and the impact of albumin. *Biochemistry and Cell Biology*, 69(12), 828–834. <https://doi.org/10.1139/o91-123>
- Wu, T.-W., Fung, K.-P., & Yang, C.-C. (1994). Unconjugated bilirubin inhibits the oxidation of human low density lipoprotein better than trolox. *Life Sciences*, 54(25), PL477–PL481. [https://doi.org/10.1016/0024-3205\(94\)90140-6](https://doi.org/10.1016/0024-3205(94)90140-6)
- Yamada, N., Sawasaki, Y., & Nakajima, H. (1977). Impairment of DNA synthesis in Gunn rat cerebellum. *Brain Research*, 126(2), 295–307. [https://doi.org/10.1016/0006-8993\(77\)90727-2](https://doi.org/10.1016/0006-8993(77)90727-2)
- Yamaguchi, T., Hashizume, T., Tanaka, M., Nakayama, M., Sugimoto, A., Ikeda, S., Nakajima, H., & Horio, F. (1997). Bilirubin oxidation provoked by endotoxins treatment is suppressed by feeding ascorbic acid in a rat mutant unable to synthesize ascorbic acid. *European Journal of Biochemistry*, 245(2), 233–240. <https://doi.org/10.1111/j.1432-1033.1997.00233.x>
- Yamaguchi, T., Horio, F., Hashizume, T., Tanaka, M., Ikeda, S., Kakinuma, A., & Nakajima, H. (1995). Bilirubin is oxidized in rats treated with endotoxin and acts as a physiological antioxidant synergistically with ascorbic acid in vivo. *Biochemical and Biophysical Research Communications*, 214(1), 11–19. <https://doi.org/10.1006/bbrc.1995.2250>
- Yamaguchi, T., Shioji, I., Sugimoto, A., Komoda, Y., & Nakajima, H. (1994). Chemical structure of a new family of bile pigments from human urine. *The Journal of Biochemistry*, 116(2), 298–303. <https://doi.org/10.1093/oxfordjournals.jbchem.a124523>
- Yamaguchi, T., Terakado, M., Horio, F., Aoki, K., Tanaka, M., & Nakajima, H. (1996). Role of bilirubin as an antioxidant in an ischemia–reperfusion of rat liver and induction of heme

- oxygenase. *Biochemical and Biophysical Research Communications*, 223(1), 129–135.
<https://doi.org/10.1006/bbrc.1996.0857>
- Yasukawa, R., Miyaoka, T., Yasuda, H., Hayashida, M., Inagaki, T., & Horiguchi, J. (2007). Increased urinary excretion of biopyrrins, oxidative metabolites of bilirubin, in patients with schizophrenia. *Psychiatry Research*, 153(2), 203–207.
<https://doi.org/10.1016/j.psychres.2006.04.009>
- Ye, H., Xing, Y., Zhang, L., Zhang, J., Jiang, H., Ding, D., Shi, H., & Yin, S. (2019). Bilirubin-induced neurotoxic and ototoxic effects in rat cochlear and vestibular organotypic cultures. *NeuroToxicology*, 71, 75–86. <https://doi.org/10.1016/j.neuro.2018.12.004>
- Zelenka, J., Dvořák, A., Alán, L., Zadinová, M., Haluzík, M., & Vitek, L. (2016). Hyperbilirubinemia protects against aging-associated inflammation and metabolic deterioration. *Oxidative Medicine and Cellular Longevity*, 2016, 1–10.
<https://doi.org/10.1155/2016/6190609>
- Zelenka, J., Muchova, L., Zelenkova, M., Vanova, K., Vreman, H. J., Wong, R. J., & Vitek, L. (2012). Intracellular accumulation of bilirubin as a defense mechanism against increased oxidative stress. *Biochimie*, 94(8), 1821–1827. <https://doi.org/10.1016/j.biochi.2012.04.026>
- Zibera, L., Martelanc, M., Franko, M., & Passamonti, S. (2016). Bilirubin is an endogenous antioxidant in human vascular endothelial cells. *Scientific Reports*, 6(1), 29240.
<https://doi.org/10.1038/srep29240>
- Zucker, S. D., Vogel, M. E., Kindel, T. L., Smith, D. L. H., Idelman, G., Avissar, U., Kakarlapudi, G., & Masnovi, M. E. (2015). Bilirubin prevents acute DSS-induced colitis by inhibiting leukocyte infiltration and suppressing upregulation of inducible nitric oxide synthase. *American Journal of Physiology-Gastrointestinal and Liver Physiology*, 309(10), G841–G854. <https://doi.org/10.1152/ajpgi.00149.2014>

8 LIST OF ABBREVIATIONS

ABC	ATP-binding cassette
ABCG5/8	ATP-binding cassette (ABC) transporters G5 (ABCG5) and G8 (ABCG8)
AOX	anti-oxidant capacity
Bf	free unconjugated bilirubin
BR	bilirubin
BV	biliverdin
BVR	biliverdin reductase
Ca ²⁺	calcium ions
cAMP	cyclic adenosine monophosphate
CNS	central nervous system
CO	carbon monoxide
DNA	deoxyribonucleic acid
EZE	ezetimibe
Fe ²⁺	ferrous ion
FNS	fecal neutral sterol
FXR	farnesoid X receptor
G6PD	glucose-6-phosphate dehydrogenase
GSH	glutathione
H5V	hearth endothelial cells
HDL	high density lipoprotein
HepG2	hepatic cells
HFD	high fat diet
HK2	kidney tubular cells
HO	heme oxygenase
HPLC	high-performance liquid chromatography
hPSC	human pluripotent stem cells
HSA	human serum albumin
ICH	intracerebral hemorrhage
IL-1 β	interleukin 1 beta

IL-6	interleukin 6
iUCB	intracellular unconjugated bilirubin
LC-MS/MS	liquid chromatography – mass spectrometry
LDL	low density lipoprotein
LR	lumirubin
LXR	liver X receptor
MRC5	fibroblast-like cells
MRP	multidrug resistance-associated protein
MS	mass spectroscopy
NADPH	nicotinamide adenine dinucleotide phosphate
NMR	nuclear magnetic resonance
NO	nitric oxide
NPC1L1	Niemann-Pick C1-Like 1
NSC	neural stem cells
O	oxygen
OATP	organic anion transporting polypeptides
OCA	obeticholic acid
PI	photoisomer
PT	phototherapy
RAW 264.7	murine macrophage-like cells
ROS	reactive oxygen species
SAH	subarachnoid hemorrhage
SOD	superoxide dismutase
SY5Y	neuronal cells
T09	liver X receptor agonist T0901317 (T09)
TB	total bilirubin
TCA	tricarboxylic Acid Cycle
TG	triglycerides
TICE	Transintestinal cholesterol excretion
TNF- α	tumor necrosis factor alpha
UGT1A1	UDP- glucuronosyl transferase 1A1 isoform

9 ANNEXES

ANNEX 1.....str 70

BLANKESTIJN, Maïke, Ivo P. VAN DE PEPPEL, Aleš DVOŘÁK, Nikola CAPKOVÁ, Libor VÍTEK, Johan W. JONKER & Henkjan J. VERKADE.

Induction of fecal cholesterol excretion is not effective for the treatment of hyperbilirubinemia in Gunn rats.2021, Pediatric Research 89, 510–517.

ANNEX 2.....str 78

BIANCO, Annalisa, Aleš DVOŘÁK, Nikola CAPKOVÁ, Camille GIRONDE, Claudio TIRIBELLI, Christophe FURGER, Libor VITEK & Cristina BELLAROSA.

The extent of intracellular accumulation of bilirubin determines its anti- or pro-oxidant effect. 2021, International Journal of Molecular Sciences 21, no. 21: 8101.

ANNEX 3.....str 95

DVOŘÁK, Aleš, Kateřina POSPÍŠILOVÁ, Kateřina ŽÍŽALOVÁ, Nikola CAPKOVÁ, Lucie MUCHOVÁ, Marek VECKA, Nikola VRZÁČKOVÁ, Jana KŘÍŽOVÁ, Jaroslav ZELENKA & Libor VÍTEK.

The effects of bilirubin and lumirubin on metabolic and oxidative stress markers. 2021, Frontiers Pharmacology 12, 567001.

ANNEX 4.....str 113

CAPKOVÁ, Nikola, Veronika POSPÍŠILOVÁ, Veronika FEDOROVÁ, Jan RAŠKA, Kateřina POSPÍŠILOVÁ, Matteo DAL BEN, Aleš DVOŘÁK, Jitka VIKTOROVÁ, Dáša BOHAČIAKOVÁ & Libor VÍTEK.

The effects of bilirubin and lumirubin on the differentiation of human pluripotent cell-derived neural stem cells. 2021, Antioxidants 10, no. 10: 1532.



BASIC SCIENCE ARTICLE

Induction of fecal cholesterol excretion is not effective for the treatment of hyperbilirubinemia in Gunn rats

Maaïke Blankestijn¹, Ivo P. van de Peppel¹, Ales Dvorak², Nikola Capkova², Libor Vitek², Johan W. Jonker¹ and Henkjan J. Verkade¹

BACKGROUND: Unconjugated hyperbilirubinemia, a feature of neonatal jaundice or Crigler–Najjar syndrome, can lead to neurotoxicity and even death. We previously demonstrated that unconjugated bilirubin (UCB) can be eliminated via transintestinal excretion in Gunn rats, a model of unconjugated hyperbilirubinemia, and that this is stimulated by enhancing fecal fatty acid excretion. Since transintestinal excretion also occurs for cholesterol (TICE), we hypothesized that increasing fecal cholesterol excretion and/or TICE could also enhance fecal UCB disposal and subsequently lower plasma UCB concentrations.

METHODS: To determine whether increasing fecal cholesterol excretion could ameliorate unconjugated hyperbilirubinemia, we treated hyperbilirubinemic Gunn rats with ezetimibe (EZE), an intestinal cholesterol absorption inhibitor, and/or a liver X receptor (LXR) and farnesoid X receptor (FXR) agonist (T0901317 (T09) and obeticholic acid (OCA), respectively), known to stimulate TICE.

RESULTS: We found that EZE treatment alone or in combination with T09 or OCA increased fecal cholesterol disposal but did not lower plasma UCB levels.

CONCLUSIONS: These findings do not support a link between the regulation of transintestinal excretion of cholesterol and bilirubin. Furthermore, induction of fecal cholesterol excretion is not a potential therapy for unconjugated hyperbilirubinemia.

Pediatric Research (2021) 89:510–517; <https://doi.org/10.1038/s41390-020-0926-2>

IMPACT:

- Increasing fecal cholesterol excretion is not effective to treat unconjugated hyperbilirubinemia.
- This is the first time a potential relation between transintestinal excretion of cholesterol and unconjugated bilirubin is investigated.
- Transintestinal excretion of cholesterol and unconjugated bilirubin do not seem to be quantitatively linked.
- Unlike intestinal fatty acids, cholesterol cannot “capture” unconjugated bilirubin to increase its excretion.
- These results add to our understanding of ways to improve and factors regulating unconjugated bilirubin disposal in hyperbilirubinemic conditions.

INTRODUCTION

Unconjugated hyperbilirubinemia, such as present in neonatal jaundice or Crigler–Najjar syndrome, can lead to bilirubin-induced neurotoxicity, kernicterus, and even to death.¹ In the liver, hydrophobic unconjugated bilirubin (UCB) is conjugated by bilirubin UDP glucuronic acid (UGT1A1) to form the more water-soluble bilirubin monoglucuronoside and bilirubin diglucuronoside, facilitating excretion into the bile. UGT1A1 is not only present in the liver but also highly expressed in the human intestine and was found to contribute to conjugation of UCB.² Despite its hydrophobic character, UCB is still partially excreted into the bile during unconjugated hyperbilirubinemia.^{3,4} In Gunn rats, an animal model for Crigler–Najjar disease type 1, around 2–15% of intestinal UCB originates from biliary disposal, while 85–98% is derived from transintestinal UCB excretion.⁴ This makes transintestinal bilirubin excretion the major route of UCB disposal in Gunn rats.^{4–6}

Transintestinal excretion also occurs for cholesterol (TICE) and can be stimulated by activation of several nuclear receptors, including peroxisome proliferator-activated receptor delta, liver X receptor (LXR), and farnesoid X receptor (FXR).^{7–12} Both LXR and FXR are involved in regulating hepatic and intestinal cholesterol metabolism. The ATP-binding cassette sub-family (ABCG5/G8) heterodimer is expressed on the canalicular membrane of hepatocytes and the apical membrane of enterocytes and regulated by LXR and FXR, where it facilitates the efflux of sterols. The intestinal ABCG5/G8 transporter is at least partially responsible for TICE.^{8,13} The Niemann–Pick C1-like 1 (NPC1L1) protein regulates intestinal cholesterol absorption and inhibition of NPC1L1 by ezetimibe (EZE) induces fecal neutral sterol (FNS) output (cholesterol and its bacterial metabolites) in mice and rats.^{9,11,14} Van de Peppel et al. showed that, under physiological conditions in mice, cholesterol excreted via TICE is largely reabsorbed.¹⁵ Decreasing intestinal cholesterol (re)absorption,

¹Section of Molecular Metabolism and Nutrition, Department of Pediatrics, University of Groningen, University Medical Center Groningen, Hanzeplein 1, 9713 GZ Groningen, The Netherlands and ²Institute of Medical Biochemistry and Laboratory Diagnostics, Faculty General Hospital and First Faculty of Medicine, Charles University, Na Bojsi 3, 12108 Prague, Czech Republic

Correspondence: Henkjan J. Verkade (h.j.verkade@umcg.nl)

Received: 22 November 2019 Revised: 28 February 2020 Accepted: 1 April 2020

Published online: 1 May 2020

either directly via an inhibition of NPC1L1 or indirectly via reducing the bile acid pool, resulted in a profound increase in FNS output beyond biliary and dietary input.¹⁵ The underlying mechanism of transintestinal excretion of UCB and that of cholesterol are not fully understood.

Earlier studies showed that plasma UCB decreased by administration of a high-fat diet (HFD) and/or the lipase inhibitor orlistat in Gunn rats.^{5,16–18} The increase in fecal fat excretion was correlated to the decrease in plasma UCB levels.^{16,17} It was demonstrated in a kinetic study using radiolabeled bilirubin that the decrease in UCB upon orlistat was due to an increase in transintestinal excretion of UCB.¹⁶ In addition, feeding a HFD to mice enhanced TICE, resulting in increased FNS excretion.¹⁹ It has been hypothesized that the increase in fecal UCB and subsequent decrease in plasma UCB levels upon higher intestinal fat concentrations is the result of UCB "capturing" by fatty acids, meaning that the reabsorption of UCB is decreased upon its association with non-absorbed fat in the intestinal lumen.^{5,20} In the present study, we tested whether selectively increasing FNS excretion, a different class of lipid, also exerts hypobilirubinemic effects in Gunn rats, similar to what was found by increasing fecal fatty acid excretion. We applied three manipulations to enhance FNS excretion: (1) activation of LXR by T09, a synthetic LXR activator, (2) activation of FXR by obeticholic acid (OCA), and/or (3) inhibition of intestinal cholesterol absorption using EZE. These different approaches allowed further differentiation into what effects were mediated through merely enhancing intestinal cholesterol concentrations (inhibition of cholesterol absorption) and effects specific to stimulating TICE (FXR and LXR stimulation). Insight into novel ways to lower plasma UCB could provide new possibilities to treat patients with unconjugated hyperbilirubinemia.

METHODS

Animals

Gunn rats (Gunn-UGT1A1/BluHsdRrrc) were obtained from the Rat Resource & Research Center (Columbia, MO) and bred in our animal facility in the University Medical Center Groningen (Groningen, The Netherlands). Animals were individually housed in a temperature- and light-controlled facility (12-h dark/light rhythm) and had ad libitum access to laboratory chow (RM3, Special Diets Services, Essex, UK) and normal drinking water during the experiments. Animal experiments were performed with the approval of the local Ethics Committee for Animal Experiments of the University of Groningen. Experiments were performed in accordance with relevant guidelines and regulations, including laboratory and biosafety.

Materials

The synthetic LXR ligand T09 was obtained from Cayman Chemical (Ann Arbor, MI, USA). The semi-synthetic bile acid OCA (INT-747; 6 α -ethyl-chenodeoxycholic acid) is a potent and selective FXR agonist and was purchased from MedChem Express (South Brunswick, NJ, USA). The cholesterol absorption inhibitor EZE was obtained as Ezetrol (Merck Sharp & Dohme, Haarlem, The Netherlands). EZE and OCA were prepared for oral administration using the oral suspension solution "ORA-Plus" (Perrigo, Allegan, MI, USA).

Experimental design

LXR agonist T09. For studying the effects of administration of T09, male Gunn rats were first fed with normal chow, and 24-h fecal outputs were collected. Subsequently, the rats were randomly divided over four experimental groups ($n=7$ per group) and received either chow diet (control group) or chow diet supplemented with EZE (0.005% w/w), T09 (0.015% w/w), or a combination of these two compounds (T09+EZE) for 14 days.

Body weights (BWs) were measured two times per week. Feces were collected and food intake was measured during the last 24 h of treatment. At day 14, rats were anesthetized using isoflurane, and the bile duct was cannulated for 20 min. Bile flow was determined gravimetrically (1 g = 1 mL bile secretion). Subsequently, blood was collected via cardiac puncture, protected against light, and stored under argon at -80°C . The liver was harvested and snap-frozen in liquid nitrogen. The small intestine was flushed with ice-cold phosphate-buffered saline (PBS) containing a protease inhibitor (cOmplete, Roche, Mannheim, Germany), snap-frozen, and stored at -80°C . Rats were terminated via decapitation under isoflurane anesthesia.

FXR agonist OCA. Rats were randomly divided to receive vehicle (ORA-Plus suspension, control group, $n=4$), EZE ($n=3$), OCA ($n=4$) or OCA+EZE ($n=5$) by oral gavage for 14 days. EZE was administered at a dose of 5 mg/kg/day and OCA at 10 mg/kg/day. A maximal administration volume of 5 mL per kg was applied. Feces were collected, and food intake was measured during the last 24 h of treatment. At day 14, the bile duct was cannulated for 20 min under isoflurane anesthesia within 6 h after the last dose, followed by blood collection via cardiac puncture. The liver was harvested and snap-frozen in liquid nitrogen. The small intestine was flushed with ice-cold PBS containing a protease inhibitor (cOmplete, Roche, Mannheim, Germany), snap-frozen, and stored at -80°C . Rats were terminated by decapitation under isoflurane anesthesia.

Analytical methods

Dietary NS and FNS and bile acids. Feces were freeze-dried, followed by mechanical homogenization. FNS and dietary NS and bile acids were extracted from 50 mg of fecal or dietary samples by 2 h of heating (80°C) with a mixture of 1 M sodium hydroxide and methanol (1:3). Specific extraction of NS was performed by petroleum ether (2 times 2 mL) and derivatized with BSTFA-pyridine-TMCS mixture (5:5:0.1). Extraction of fecal bile acids was performed using Sep-Pak C-18 columns (Waters Corporation, Milford, MA, USA), and samples were methylated with methanol/acetyl chloride (20:1) and subsequently derivatized with BSTFA-pyridine-TMCS (5:5:0.1). Dietary NS and FNS and bile acids were then both analyzed by gas chromatography (GC) as described.²¹

Plasma total bilirubin (TB) and haptoglobin. Terminal blood samples were collected and kept in EDTA-coated collecting tubes (MiniCollect, Greiner Bio-One, Kremsmünster, Austria) on ice in the dark. After centrifugation, plasma was stored in light-protecting tubes (Eppendorf, Hamburg, Germany) under argon at -80°C upon analysis. Plasma TB and free haptoglobin were analyzed on a Roche/Hitachi Cobas 501 Analyzer (Hitachi, Tokyo, Japan) using, respectively, the Bilirubin Total Gen 3 Kit and Tina-quant Haptoglobin ver.2 Kit (Roche Diagnostics, Rotkreuz, Switzerland).

Bilirubin determination in feces and bile. Fecal samples were put into the pre-weighted centrifugation tubes; then internal standard [mesobilirubin (MBR)] was added (10 μL of 5 μM MBR per sample). Then samples were extracted with concomitant protein precipitation by 2 mL of basic methanol (0.3% butylated hydroxytoluene, 0.1% ascorbic acid, and 0.5% ammonium acetate). The mixture was vigorously shaken and vortexed, and the suspension was centrifuged (3000 \times g/5 min). One mL of supernatant was collected into micro-tubes, and the solution was centrifuged again (16,000 \times g/30 min) for elimination of impurities before analytical measurement.

Bile samples were prepared similarly. Five μL of bile was pipetted into micro-tubes and 10 μL of MBR was added (5 μM); the extraction was performed with 1 mL of basic methanol. Samples were vigorously shaken and vortexed and the mixture was centrifuged (16,000 \times g/30 min).

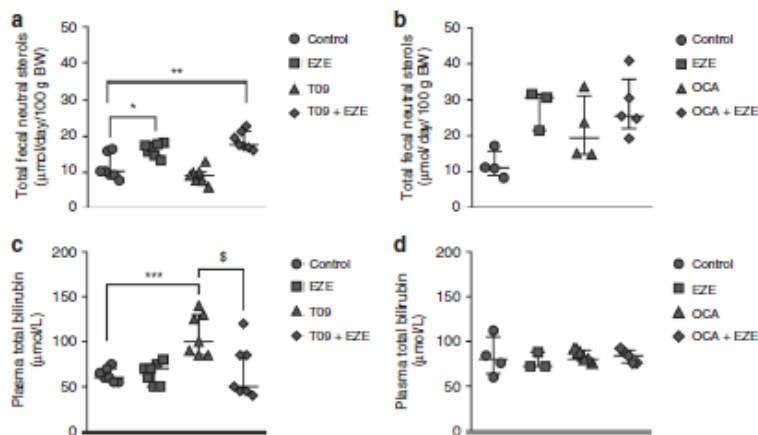


Fig. 1 The effect of stimulation of FNS on plasma levels of bilirubin in hyperbilirubinemic rats. Total FNS excretion after 2 weeks of a LXR or b FXR stimulation. Plasma TB after 2 weeks of c LXR or d FXR stimulation. a + c: n = 7; b + d, n = 3–5.

After final centrifugation steps, 100 µL of supernatant from bile as well as fecal samples was pipetted into glass vials with the inert insert (suitable for liquid chromatography tandem mass spectrometry (LC-MS) analysis), and 2 µL was directly injected to LC-MS apparatus.

LC-MS/MS analysis was performed using a high-performance liquid chromatography (Dionex Ultimate 3000, Dionex Softron GmbH, Germany) equipped with a Poroshell 120 EC-C18 column (2.1 µm, 3.0 × 100 mm; Agilent, CA, USA). For a gradient elution, the phase was prepared by mixing 1 mM of NH₄F (Honeywell, International Inc., Morris Plains, NJ, USA) in water and methanol (Biosolve Chimie SARL, France). The analytes were detected by mass spectrometer (TSQ Quantum Access Max with HESI-II probe, Thermo Fisher Scientific, Inc., USA) operating in a positive SRM mode: bilirubin [585.3 → 299.1 (20V); 585.3 → 271.2 (18V)]; MBR [589.3 → 301.1 (20V); 589.3 → 273.2 (44V)].

Samples remaining after extraction of feces were lyophilized overnight and freeze-dried tubes with dry matter were weighed by analytical scales. The empty tube weight (before analysis) was subtracted from the weight of the lyophilized tube.

Integrated areas of bilirubin were related to MBR areas, and ratios were normalized to dry weight of feces or volume of bile, respectively. The concentration was calculated according calibration curves measured in relevant matrices.

Hepatic and biliary lipids. Livers were crushed and homogenized in liquid nitrogen. A 15% liver homogenate was made with PBS to extract hepatic lipids using the Bligh and Dyer method.²² Hepatic triglycerides (TGs) and free and total cholesterol were measured using commercially available kits (Roche Diagnostics, Mannheim, Germany and DiaSys Diagnostic Systems, Holzheim, Germany, respectively). For analysis of biliary lipids, 15 µL of bile was used for extraction using the Bligh and Dyer method. Biliary cholesterol was derivatized using pyridine-acetic anhydride (1:1) for analysis by GC as previously described.²¹

Gene expression analysis. Isolation of total RNA from the liver and duodenum was performed using TRI-reagent (Sigma, St. Louis, MO, USA). RNA was quantified by NanoDrop (NanoDrop Technologies, Wilmington, DE, USA), and 1 µg RNA was used to create cDNA. Analysis of real-time quantitative polymerase chain reaction was performed on QuantStudio 7 Flex machine (Applied Biosystems, Thermo Fisher Scientific, Darmstadt, Germany). Gene

expression levels were normalized to *cyclophilin* for liver and *36b4* for intestine.

Plasma lipids. Plasma total cholesterol, triglycerides, and non-esterified fatty acids were spectrophotometrically analyzed using commercially available kits (Roche Diagnostics, Mannheim, Germany and DiaSys Diagnostic Systems, Holzheim, Germany).

Bile acid composition of bile and plasma. Biliary and plasma bile acid species were determined using LC-MS as described previously.¹⁵ Biliary hydrophobicity was calculated using Heuman values.²³ Total bile acid concentrations were calculated as the sum of the individual bile acid species. Total bile acid secretion was calculated using biliary bile acid concentrations multiplied by the bile flow and corrected for BW.

Statistics

For all statistical analyses, GraphPad Prism 6.0 (GraphPad Software, La Jolla, CA, USA) was used. Unless stated otherwise, graphs are presented as a scatter dot plot representing individual values with a median ± interquartile range. Statistical significance was tested by a non-parametric one-way analysis of variance (Kruskal-Wallis) test, followed by Mann-Whitney *U* tests to assess differences between the experimental groups. Differences before and after treatment were assessed using Wilcoxon signed-rank test. Statistical significance compared to control relative untreated groups is indicated as **p* < 0.05, ***p* < 0.01, and ****p* < 0.001. Statistical significance between the T09 and T09+EZE groups is indicated as §*p* < 0.05 and §§*p* < 0.01. Owing to low animal numbers, no statistical significance was determined for the OCA experiment.

RESULTS

The effect of EZE, LXR, and FXR activation on FNS excretion and plasma bilirubin in Gunn rats

To assess the effect of stimulated FNS excretion on plasma bilirubin levels in Gunn rats, we used three approaches previously shown to increase FNS excretion in mice: inhibition of cholesterol absorption using EZE^{9,10,14,15} and pharmacological activation of LXR and FXR using T09 and OCA, respectively.^{7,8,11,24,25} In line with murine studies, EZE treatment, either administered via the diet or via oral gavage, increased FNS excretion by about twofold to threefold (Fig. 1a, b). In contrast to studies in mice, T09

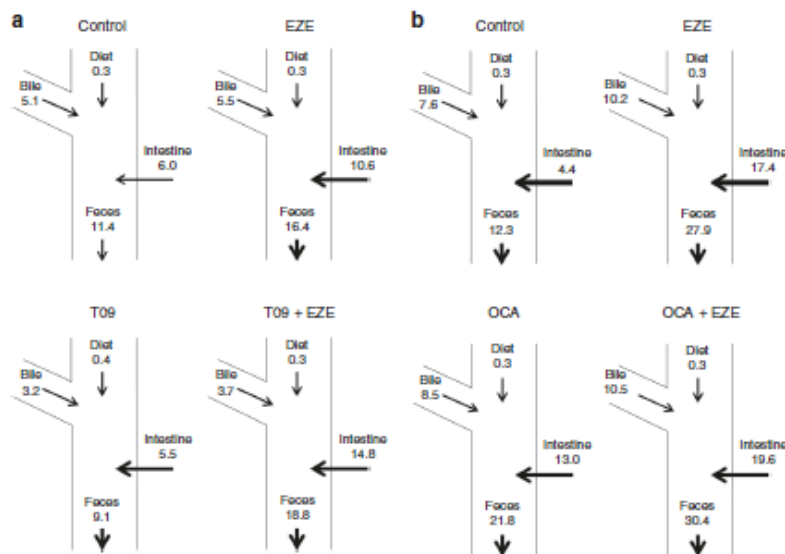


Fig. 2 Schematic representation of the calculated cholesterol fluxes. Net intestinal cholesterol balance was calculated by subtraction of mean dietary cholesterol intake and biliary cholesterol secretion from the FNS excretion for **a** LXR, $n = 7$, and **b** FXR activation, $n = 3-5$. Treatments in **a** were mixed in the diet, and treatments in **b** were administered through oral gavage. Numbers are represented as mean ($\mu\text{mol}/\text{day}/100\text{ g}$ body weight).

administration by itself did not stimulate FNS excretion in Gunn rats (Fig. 1a). Moreover, T09 even lowered FNS excretion compared to baseline, while FNS excretion remained unchanged in untreated controls (Supplementary Fig. S1A, B). Combined EZE and T09 treatment increased FNS excretion to a similar extent as EZE alone (Fig. 1a).^{9,26}

While OCA treatment showed a trend towards increased FNS, co-administration of OCA and EZE did not further increase FNS excretion as compared to EZE treatment alone (Fig. 1b). To assess whether the increase in FNS excretion affected hyperbilirubinaemia, we determined plasma TB levels. Since Gunn rats lack the conjugating activity of UGT1A1, plasma TB levels are equal to plasma UCB levels. Figure 1c shows that EZE did not lower plasma TB levels in Gunn rats. T09 increased plasma TB levels in Gunn rats, and this was partially prevented by co-administration of EZE (Fig. 1c). Treatment with T09 with or without EZE resulted in decreased free haptoglobin levels, an indication of increased intravascular hemolysis,²⁷ compared to control Gunn rats (Supplementary Fig. S2). Plasma TB levels were unaffected by administration of OCA, either alone or in combination with EZE (Fig. 1d). Taken together, these results demonstrate that plasma levels of bilirubin are not lowered by stimulation of FNS excretion in Gunn rats.

The effect of LXR and FXR activation on intestinal cholesterol fluxes in Gunn rats

The increase in FNS by EZE, T09, and OCA in previous studies has been explained by its effects on intestinal cholesterol fluxes.^{8,24,28} While T09 in our study did not affect total FNS excretion, this does not exclude the possibility of changes in intestinal cholesterol fluxes. To investigate this, we measured dietary cholesterol intake and biliary cholesterol secretion and subtracted these measurements from FNS excretion to obtain the net intestinal cholesterol balance (Fig. 2). In untreated Gunn rats, the intestinal cholesterol balance indicated a net cholesterol excretion into the intestine ($+6.0\mu\text{mol}/\text{day}/100\text{ g}$ BW) and was increased about twofold by

EZE treatment (Fig. 2a). These findings were similar in heterozygous Gunn rats indicating that the observed effects of EZE are independent of UGT1A1^{29,30} (Supplementary Fig. S3).

While T09 administration alone did not change the net intestinal cholesterol balance, the combination of T09 with EZE increased net intestinal cholesterol excretion into the intestine more than EZE alone (14.8 vs. 10.6 $\mu\text{mol}/\text{day}/100\text{ g}$ BW, Fig. 2a). This change was associated with a slight decrease in biliary cholesterol secretion, observed in both the T09-treated groups (Fig. 2a).

When EZE was administered through oral gavage instead of via the diet, net intestinal cholesterol excretion increased even further, to about 17.4 $\mu\text{mol}/\text{day}/100\text{ g}$ BW compared to 10.6 $\mu\text{mol}/\text{day}/100\text{ g}$ BW with dietary EZE (Fig. 2a, b). OCA alone increased net intestinal cholesterol excretion threefold. Previous reports indicated that OCA reduces cholesterol absorption in mice.²⁴ In our study, the addition of OCA to EZE treatment did not result in a major additive effect on the intestinal cholesterol balance compared to EZE alone (17.4 vs. 19.6 $\mu\text{mol}/\text{day}/100\text{ g}$ BW, Fig. 2b). Taken together, our results show that an increase in net intestinal cholesterol excretion does not result in lowering of plasma TB levels.

The effect of EZE, LXR, and FXR activation on biliary and fecal bilirubin secretion

Previous studies in rats have demonstrated that plasma UCB levels can be lowered through stimulation of fecal bilirubin excretion.^{5,16} We assessed whether EZE treatment or activation of LXR and FXR affected biliary and fecal UCB secretion rates. EZE resulted in a lower biliary UCB secretion rate both alone and combined with T09 (Fig. 3a). T09 by itself did not significantly alter biliary UCB secretion (Fig. 3a). Fecal UCB excretion rates were not altered by dietary administration of EZE; however, T09 alone or combined with EZE significantly increased fecal UCB excretion (Fig. 3b). No differences were observed in biliary and fecal UCB excretion after oral administration of EZE, OCA, or

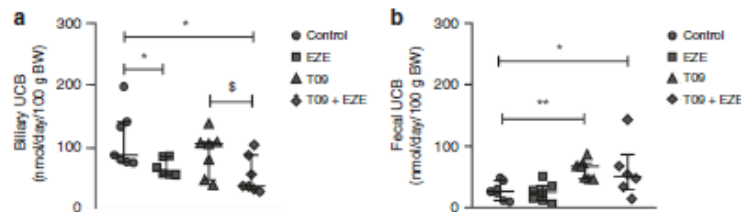


Fig. 3 The effect of T09 and EZE on UCB in bile and feces in Gunn rats. Secretion rates of UCB after administration of EZE, T09, or co-administration in **a** bile, $n = 6-7$, and **b** feces, $n = 7$.

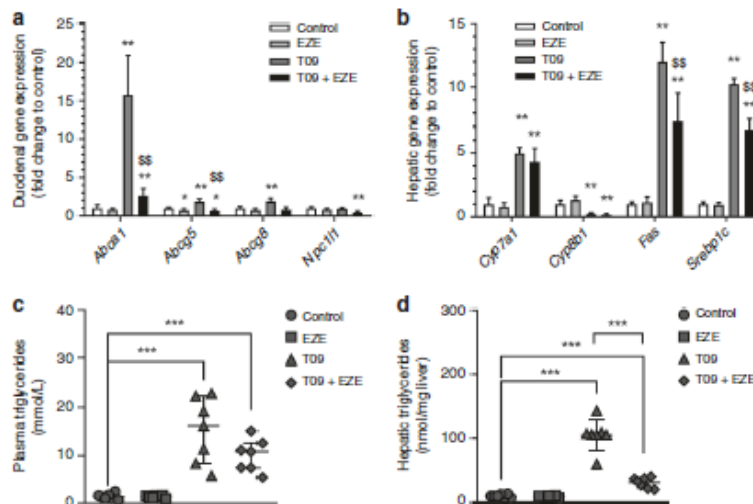


Fig. 4 The effect of T09 and EZE treatment on LXR target gene expression and triglyceride levels. Gene expression of target genes of LXR in the **a** duodenum and **b** liver, $n = 5$. **c** Triglyceride concentration in plasma after administration of EZE, T09, or combination treatment and **d** hepatic triglyceride content after administration of EZE, T09, or combination treatment, $n = 7$.

OCA+EZE (data not shown). These results show that, while T09 increased fecal UCB levels, this was not accompanied by a decrease in plasma UCB concentrations.

Validation of LXR activation by T09 in Gunn rats

In mice, the effect of LXR on FNS excretion are (at least partially) mediated via induction of ABCG5/8-mediated cholesterol efflux^{31,33,31}. Since we did not observe an increase in FNS excretion upon T09 treatment in Gunn rats (Fig. 1a), we wanted to exclude the possibility that LXR was not activated by T09 in our experiment. To determine the activation of LXR by T09, we analyzed duodenal mRNA expression of LXR target genes involved in cholesterol metabolism (Fig. 4a). In Gunn rats, T09 increased the expression of LXR target genes *Abcg5/8* and *Abca1* (Fig. 4a). *Npc1l1* gene expression was unchanged upon T09 treatment alone but lower, compared to untreated controls, when combined with EZE. Figure 4b depicts hepatic target genes of LXR involved in bile acid synthesis and lipogenesis. T09, with or without co-administration of EZE, increased the expression of cholesterol 7 α -hydroxylase (*Cyp7a1*), the rate-limiting enzyme in bile acid synthesis, while it decreased the expression of microsomal sterol 12 α hydroxylase (*Cyp8b1*), responsible for the synthesis of cholic acid (Fig. 4b). Administration of EZE alone did not affect the expression of these hepatic genes. The changes in gene expression levels of *Cyp7a1* and *Cyp8b1* by T09 were accompanied by a percentual decrease

of taurocholic acid (TCA) in the bile (Supplementary Fig. S4A). Treatment with T09 increased the hepatic mRNA expression of sterol-regulatory element-binding protein 1C (*Srebp-1c*) and fatty acid synthase (*Fas*), genes involved in lipogenesis. In line with an increase in lipogenesis, T09 highly increased both plasma and hepatic TG levels (Fig. 4c, d), similar to previous observations in mice,³² and were partly attenuated by EZE. Supplementary Fig. 5 shows that T09-induced increase in plasma TG is positively correlated to the increase in plasma TB in Gunn rats. Conversely, plasma and hepatic total cholesterol levels were lowered upon T09 treatment with or without EZE co-treatment (Supplementary Fig. S6A, B). Finally, T09 treatment also increased liver weight and bile flow (Supplementary Table S1). These data demonstrate that, while T09 did not affect FNS excretion in Gunn rats, it did induce other known LXR-mediated effects on lipid, cholesterol, and bile acid homeostasis without affecting plasma TB levels.

Validation of FXR activation by OCA in Gunn rats

In mice, OCA treatment activates intestinal and hepatic FXR, thereby reducing the hepatic expression of *Cyp7a1* and *Cyp8b1*, resulting in decreased bile acid synthesis and a subsequent reduction in size and hydrophobicity of the bile acid pool.¹¹ To determine whether OCA treatment resulted in similar effects in Gunn rats, we measured the expression of hepatic FXR target genes and the biliary bile acid concentration and composition.

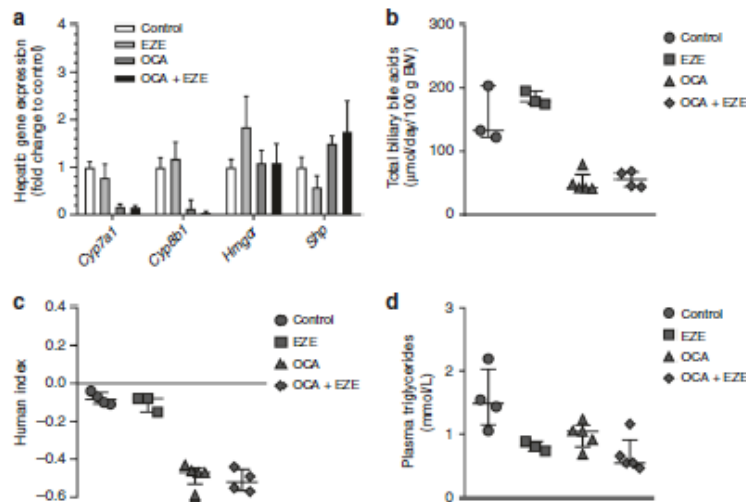


Fig. 5 The effect of OCA and EZE treatment on FXR target genes and bile acids in Gunn rats. **a** Hepatic gene expression of FXR target genes after administration of EZE, OCA, or co-administration. **b** Total biliary bile acid levels corrected for bile flow after FXR activation. **c** Hydrophobicity index of the bile. **d** Plasma triglyceride concentration after administration of EZE, OCA, or combination treatment, $n = 3-5$.

OCA treatment, either alone or with EZE, reduced hepatic *Cyp7a1* and *Cyp8b1* mRNA levels compared to untreated controls (Fig. 5a). EZE alone did not significantly alter *Cyp7a1* or *Cyp8b1* gene expression. OCA treatment decreased total biliary bile acid secretion by about 75%, either with or without co-administration of EZE (Fig. 5b). This was associated with a similar decrease in plasma and fecal bile acids (Supplementary Fig. S7). OCA reduced biliary hydrophobicity compared to controls, which was unaffected by EZE co-administration (Fig. 5c). The decrease in hydrophobicity resulted from a fractional decrease of TCA and increase of tauro- α - and tauro- β -muricholic acids (Supplementary Fig. S4B). In contrast to LXR agonist treatment, activation of FXR has been associated with a reduction of plasma TGs (reviewed in ref. 35). In Gunn rats, both EZE and OCA treatment, irrespective of EZE co-treatment, decreased plasma TG concentration compared to controls (Fig. 5d). Plasma and hepatic cholesterol levels were unaffected upon OCA and/or EZE treatment (Supplementary Fig. S6C, D). These results show that OCA treatment results in similar FXR-mediated effects on bile acid and cholesterol metabolism in Gunn rats compared to mice but did not affect plasma TB levels.

DISCUSSION

In this study, we tested the hypothesis that stimulation of FNS excretion lowers plasma TB in hyperbilirubinemic Gunn rats. To increase FNS excretion, we inhibited intestinal cholesterol absorption using EZE and stimulated TICE via LXR or FXR activation. We show that increasing FNS excretion by inhibition of intestinal cholesterol absorption did not lower plasma TB. We conclude that neither stimulation of FNS excretion nor LXR or FXR stimulation exert hypobilirubinemic effects in Gunn rats.

We previously demonstrated that increased fecal fat excretion, either via a HFD or orlistat, is associated with decreased plasma UCB in Gunn rats.^{5,17,18} Here we tested whether induction of fecal excretion of another lipid, cholesterol, could also exert hypobilirubinemic effects. In addition, a transintestinal excretion route is present for both UCB and cholesterol.^{4,15,16} Therefore, we hypothesized that treatments that stimulate TICE could potentially affect

transintestinal UCB excretion. Most of the induced FNS excretion in our present experiment originates from (non-reabsorbed) trans-intestinally excreted cholesterol. Our results provide two important new insights: (1) the transintestinal excretion pathways for cholesterol and for UCB are not quantitatively linked and (2) the intestinal "capture" hypothesis only relates to non-absorbed TGs/fatty acids and not to cholesterol.

While LXR activation did not lower plasma bilirubin levels in Gunn rats, fecal UCB excretion was increased (Fig. 3b). However, it should be realized that fecal UCB excretion only accounts for an estimated ~50% of TB turnover.³⁴ Since our analyses do not provide a quantitative estimation of UCB turnover (disposal and degradation, into urobilinoids and other compounds), we cannot definitively determine whether the increase in fecal UCB was due to (1) increased transintestinal UCB secretion, (2) decreased transintestinal UCB reabsorption, or (3) decreased intraluminal (microbial) UCB degradation. Based on biliary UCB secretion rates, however, it can be excluded that the T09-induced fecal UCB excretion is due to increased biliary excretion (Fig. 3a).

Despite clear activation of LXR by T09 in Gunn rats, as evidenced from upregulation of known target genes (e.g., *Abca1*, *Abcg5*, and *Abcg8*) and increased lipogenesis, we did not observe an effect on FNS excretion, in contrast to previous observations in mice.^{7,8} Intestinal ABCG5/8 stimulation has been implicated in the increase of TICE upon T09 treatment in mice.⁷ Van de Peppel et al. showed that, under physiological conditions, cholesterol excreted via TICE is largely reabsorbed by the intestine in an NPC1L1-dependent process.¹⁵ In mice, activation of LXR decreases *Npc1l1* expression, which could result in decreased cholesterol (re)absorption, thereby increasing FNS excretion independent of an effect on ABCG5/8.³⁵ In our study, *Npc1l1* gene expression in Gunn rats was unaffected upon T09 treatment, while *Abcg5/8* expression was increased. Potential differences between mice and rats in regulation of these transporters are illustrated by a study by Kawase et al., showing that a 2% cholesterol-enriched diet decreased intestinal mRNA and protein levels of NPC1L1 in mice, but not in rats, while increasing ABCG5/8 only in rats.³⁶ These observations suggest that the lack of an effect of T09 on FNS excretion in (Gunn) rats is potentially due to a species-specific

effect on intestinal *Npc1l1* expression and subsequent cholesterol (re)absorption. Interestingly, combined T09 and EZE treatment increased net intestinal cholesterol excretion more than EZE treatment alone (Fig. 2a), suggesting that T09 does increase TICE, but under the conditions of unaffected NPC1L1 function or expression, this is reabsorbed and does not contribute to FNS excretion.

The second approach to study whether higher FNS excretion could lower plasma bilirubin was by activating FXR using OCA. The underlying mechanism by which OCA increases FNS excretion in mice has been suggested to be mediated by a smaller and more hydrophilic bile acid pool.¹¹ Hydrophilic mucicholic bile acids inhibit intestinal cholesterol absorption, thereby promoting FNS excretion. In our current study, we showed that Gunn rats treated with OCA with or without EZE also had lower biliary bile acid concentrations and a more hydrophilic profile (Fig. 5b, c). While we did not measure intestinal cholesterol absorption directly, intestinal cholesterol balance data demonstrated net intestinal excretion upon OCA treatment (Fig. 2b). Co-administration of OCA with EZE slightly increased net intestinal cholesterol excretion further than either treatment alone, suggesting that, while most of the effects of OCA are also likely mediated through decreased cholesterol absorption in Gunn rats, a small part of the effects could be due to direct stimulation of TICE.

Surprisingly, administration of T09 led to an increase in plasma bilirubin, and this was partially prevented by EZE co-treatment. Our T09-treated Gunn rats displayed severely increased plasma TG levels, a well-known effect of LXR activation, resulting in an optical yellow-colored and turbid appearance. Therefore, hypertriglyceridemia could have potentially interfered with the plasma bilirubin measurements, resulting in higher values. However, it has also been demonstrated that plasma TG levels >12 mmol/L increase hemolysis, possibly due to increased membrane instability of erythrocytes.³⁷ Bilirubin is a degradation product of heme metabolism and can thus be further increased upon hemolysis in our T09-treated Gunn rats.³⁸ We observed a strong, positive correlation between plasma TG and bilirubin in Gunn rats treated with T09 with or without EZE (Supplementary Fig. S5). The presence of increased hemolysis due to hypertriglyceridemia upon T09 treatment is supported by decreased plasma-free haptoglobin concentrations, a marker for intravascular hemolysis,²⁷ in both T09-treated groups (Supplementary Fig. S2). However, decreased haptoglobin levels are not conclusive of hemolysis, and we did not have whole-blood samples to perform other red blood cell analyses to determine whether hemolysis indeed had been induced. Taken together, the present study demonstrates that neither induction of FNS excretion nor LXR or FXR activation results in a hypobilirubinemic effect in Gunn rats, in contrast to induction of fecal fat excretion.^{5,17} This shows that clinically relevant "capturing" of bilirubin can be realized only by fatty acids and not by cholesterol. These data also demonstrate that there is no quantitative link between TICE or FNS excretion and transintestinal UCB excretion. Therefore, increasing FNS excretion is not a potential target to treat unconjugated hyperbilirubinemia. Of further interest, we found that T09 did not increase FNS excretion in Gunn rats but did induce intestinal *Abcg5/8* expression without affecting *Npc1l1* expression. Based on this observation, we conclude that the increased expression of *Abcg5/8* per se upon T09 treatment is not critical for the induction of FNS excretion observed in mice but perhaps rather the reduced expression of *Npc1l1*.^{32,33} This underlines important species differences in (intestinal) lipid homeostasis, and caution is warranted in choosing what model to study.

ACKNOWLEDGEMENTS

The authors gratefully acknowledge the excellent technical contributions to this study by Rick Havinga, Renze Boverhof, Martijn Koehorst, and Anouk Bos. We thank

Folkert Kuipers for helpful discussions and advice. This study was funded by a grant from De Cock Haddes stichting. L.V. received a grant from the Czech Ministry of Health (RVO-VFN6416S).

AUTHOR CONTRIBUTIONS

M.B. designed and performed the experiments, analyzed and interpreted data, and wrote the manuscript. L.P.v.d.P. interpreted data and wrote the manuscript. A.D. and N.C. analyzed data and reviewed the manuscript. L.V. interpreted data and reviewed the manuscript. J.W.J. and H.J.V. designed the experiments, interpreted data, and wrote the manuscript.

ADDITIONAL INFORMATION

The online version of this article (<https://doi.org/10.1038/s41390-020-0926-2>) contains supplementary material, which is available to authorized users.

Competing interests: The authors declare no competing interests.

Publisher's note: Springer Nature remains neutral with regard to jurisdictional claims in published maps and institutional affiliations.





REFERENCES

- Ostrow, J. D., Pascolo, L., Brites, D. & Tinelli, C. Molecular basis of bilirubin-induced neurotoxicity. *Trends Mol. Med.* **10**, 65–70 (2004).
- McDonnell, W. M., Hitomi, E. & Askari, F. K. Identification of bilirubin UDP-GTs in the human alimentary tract in accordance with the gut as a putative metabolic organ. *Biochem. Pharmacol.* **51**, 483–488 (1996).
- Atas, I. M., Johnson, L. & Wolfson, S. Biliary excretion of injected conjugated and unconjugated bilirubin by normal and Gunn rats. *Am. J. Physiol.* **200**, 1091–1094 (1961).
- Kotil, P. et al. Intestinal excretion of unconjugated bilirubin in man and rats with inherited unconjugated hyperbilirubinemia. *Pediatr. Res.* **42**, 195–200 (1997).
- Nishioka, T. et al. Orlistat treatment increases fecal bilirubin excretion and decreases plasma bilirubin concentrations in hyperbilirubinemic Gunn rats. *J. Pediatr.* **143**, 327–334 (2003).
- Cuperus, F. J. C. et al. Effective treatment of unconjugated hyperbilirubinemia with oral bile salts in Gunn rats. *Gastroenterology* **136**, 673e1–682e1 (2009).
- Kruit, J. K. et al. Increased fecal neutral sterol loss upon liver X receptor activation is independent of biliary sterol secretion in mice. *Gastroenterology* **128**, 147–156 (2005).
- van der Veen, J. N. et al. Activation of the liver X receptor stimulates transintestinal excretion of plasma cholesterol. *J. Biol. Chem.* **284**, 19211–19219 (2009).
- Jalilu, L. et al. Transintestinal cholesterol transport is active in mice and humans and controls ezetimibe-induced fecal neutral sterol excretion. *Cell Metab.* **24**, 783–794 (2016).
- Vlins, C. L. J. et al. Peroxisome proliferator-activated receptor delta activation leads to increased transintestinal cholesterol efflux. *J. Lipid Res.* **50**, 2046–2054 (2009).
- de Boer, J. F. et al. Intestinal farnesoid X receptor controls transintestinal cholesterol excretion in mice. *Gastroenterology* **152**, 1126.e6–1138.e6 (2017).
- Grefhorst, A. et al. Pharmacological LXR activation induces presence of SR-B1 in liver membranes contributing to LXR-mediated induction of HDL-cholesterol. *Atherosclerosis* **222**, 382–389 (2012).
- de Boer, J. F., Kuipers, F. & Groen, A. K. Cholesterol transport revisited: a new turbo mechanism to drive cholesterol excretion. *Trends Endocrinol. Metab.* **29**, 123–133 (2018).
- Terunuma, S., Kumata, N. & Osada, K. Ezetimibe impairs uptake of dietary cholesterol oxidation products and reduces alterations in hepatic cholesterol metabolism and antioxidant function in rats. *Lipids* **48**, 587–595 (2013).
- van de Peppel, L. P. et al. Efficient reabsorption of transintestinally excreted cholesterol is a strong determinant for cholesterol disposal in mice. *J. Lipid Res.* **60**, 1562–1572 (2019).
- Hafkamp, A. M. et al. Novel kinetic insights into treatment of unconjugated hyperbilirubinemia: phototherapy and orlistat treatment in Gunn rats. *Pediatr. Res.* **59**, 506–512 (2006).
- Hafkamp, A. M., Havinga, R., Sinaasappel, M. & Verkade, H. J. Effective oral treatment of unconjugated hyperbilirubinemia in Gunn rats. *Hepatology* **41**, 526–534 (2005).
- Cuperus, F. J. C., Iemhoff, A. A. & Verkade, H. J. Combined treatment strategies for unconjugated hyperbilirubinemia in Gunn rats. *Pediatr. Res.* **70**, 560–565 (2011).
- van der Velde, A. E. et al. Regulation of direct transintestinal cholesterol excretion in mice. *Am. J. Physiol. Gastrointest. Liver Physiol.* **295**, G203–G208 (2008).

20. Bulmer, A. C., Verkade, H. J. & Wegner, K. H. Bilirubin and beyond: a review of lipid status in Gilbert's syndrome and its relevance to cardiovascular disease protection. *Prog. Lipid Res.* **52**, 193–205 (2013).
21. Ronda, O. A. H. O., van Dijk, T. H., Verkade, H. J. & Groen, A. K. Measurement of intestinal and peripheral cholesterol fluxes by a dual-tracer balance method. *Curr. Protoc. Mouse Biol.* **6**, 408–434 (2016).
22. Bligh, E. G. & Dyer, W. J. A rapid method of total lipid extraction and purification. *Can. J. Biochem. Physiol.* **37**, 911–917 (1959).
23. Heuman, D. M. Quantitative estimation of the hydrophilic-hydrophobic balance of mixed bile salt solutions. *J. Lipid Res.* **30**, 719–730 (1989).
24. Xu, Y. et al. Farnesoid X receptor activation increases reverse cholesterol transport by modulating bile acid composition and cholesterol absorption in mice. *Hepatology* **64**, 1072–1085 (2016).
25. Hambruch, E. et al. Synthetic farnesoid X receptor agonists induce high-density lipoprotein-mediated transhepatic cholesterol efflux in mice and monkeys and prevent atherosclerosis in cholesterol ester transfer protein transgenic low-density lipoprotein receptor. *J. Pharmacol. Exp. Ther.* **343**, 556–567 (2012).
26. Sugizaki, T. et al. The Niemann-Pick C1 Like 1 (NPC1L1) inhibitor ezetimibe improves metabolic disease via decreased liver X receptor (LXR) activity in liver of obese male mice. *Endocrinology* **155**, 2810–2819 (2014).
27. Shih, A. W. Y., McFarlane, A. & Vekhovsek, M. Haptoglobin testing in hemolysis: measurement and interpretation. *Am. J. Hematol.* **89**, 443–447 (2014).
28. Nakano, T. et al. Ezetimibe promotes brush border membrane-to-lumen cholesterol efflux in the small intestine. *PLoS ONE* **11**, e0152207 (2016).
29. Van Heek, M. et al. Comparison of the activity and disposition of the novel cholesterol absorption inhibitor, SCH58235, and its glucuronide, SCH60663. *Br. J. Pharmacol.* **129**, 1748–1754 (2000).
30. Ghosal, A. et al. Identification of human UDP-glucuronosyltransferase enzyme(s) responsible for the glucuronidation of ezetimibe (Zetia). *Drug Metab. Dispos.* **32**, 314–320 (2004).
31. Calpe-Berdiel, L. et al. Liver X receptor-mediated activation of reverse cholesterol transport from macrophages to feces in vivo requires ABCG5/G8. *J. Lipid Res.* **49**, 1904–1911 (2008).
32. Oosterveer, M. H., Gefforst, A., Groen, A. K. & Kuipers, F. The liver X receptor: control of cellular lipid homeostasis and beyond. *Prog. Lipid Res.* **49**, 343–352 (2010).
33. Jonker, J. W., Liddle, C. & Downes, M. FXR and PXR: potential therapeutic targets in cholestasis. *J. Steroid Biochem. Mol. Biol.* **130**, 147–158 (2012).
34. Van Der Veeke, C. N. et al. Influence of dietary calcium phosphate on the disposition of bilirubin in rats with unconjugated hyperbilirubinemia. *Hepatology* **24**, 620–626 (1996).
35. Duval, C. et al. Niemann-Pick C1 like 1 gene expression is down-regulated by LXR activators in the intestine. *Biochem. Biophys. Res. Commun.* **340**, 1259–1263 (2006).
36. Kawase, A., Anaki, Y., Ueda, Y., Nakazaki, S. & Iwakaki, M. Impact of a high-cholesterol diet on expression levels of Niemann-Pick C1-like 1 and intestinal transporters in rats and mice. *Eur. J. Drug Metab. Pharmacokinet.* **41**, 457–463 (2016).
37. Dimeski, G., Mollee, P. & Carter, A. Increased lipid concentration is associated with increased hemolysis. *Clin. Chem.* **51**, 2425 (2005).
38. London, I. M., West, R., Shemin, D. & Rittenberg, D. On the origin of bile pigment in normal man. *J. Biol. Chem.* **184**, 351–358 (1950).

Article

The Extent of Intracellular Accumulation of Bilirubin Determines Its Anti- or Pro-Oxidant Effect

Annalisa Bianco ^{1,2}, Aleš Dvořák ³ , Nikola Capková ³, Camille Gironde ⁴, Claudio Tiribelli ¹ , Christophe Furger ⁴, Libor Vitek ^{3,5}  and Cristina Bellarosa ^{1,*} 

¹ Italian Liver Foundation (FIF), Bldg Q—AREA Science Park Basovizza, SS14 Km 163,5, 34149 Trieste, Italy; annalisa.bianco@fegato.it (A.B.); ctliver@fegato.it (C.T.)

² Department of Life Sciences, University of Trieste, 34127 Trieste, Italy

³ Institute of Medical Biochemistry and Laboratory Diagnostics, Faculty General Hospital and 1st Faculty of Medicine, Charles University, 121 08 Prague 2, Czech Republic; aleshdvorak@gmail.com (A.D.); nikola.capkova@gmail.com (N.C.); vitek@cesnet.cz (L.V.)

⁴ AOP/MH2F Team, LAAS-CNRS, 7 avenue de l'Europe, 31400 Toulouse, France; cgironde@laas.fr (C.G.); cfurger@laas.fr (C.F.)

⁵ 4th Department of Internal Medicine, Faculty General Hospital and 1st Faculty of Medicine, Charles University, 121 08 Prague 2, Czech Republic

* Correspondence: cristina.bellarosa@fegato.it

Received: 24 September 2020; Accepted: 28 October 2020; Published: 30 October 2020



Abstract: Background: Severe hyperbilirubinemia can cause permanent neurological damage in particular in neonates, whereas mildly elevated serum bilirubin protects from various oxidative stress-mediated diseases. The present work aimed to establish the intracellular unconjugated bilirubin concentrations (iUCB) thresholds differentiating between anti- and pro-oxidant effects. Methods: Hepatic (HepG2), heart endothelial (H5V), kidney tubular (HK2) and neuronal (SH-SY5Y) cell lines were exposed to increasing concentration of bilirubin. iUCB, cytotoxicity, intracellular reactive oxygen species (ROS) concentrations, and antioxidant capacity (50% efficacy concentration (EC₅₀)) were determined. Results: Exposure of SH-SY5Y to UCB concentration > 3.6 μM (iUCB of 25 ng/mg) and >15 μM in H5V and HK2 cells (iUCB of 40 ng/mg) increased intracellular ROS production ($p < 0.05$). EC₅₀ of the antioxidant activity was 21 μM (iUCB between 5.4 and 21 ng/mg) in HepG2 cells, 0.68 μM (iUCB between 3.3 and 7.5 ng/mg) in SH-SY5Y cells, 2.4 μM (iUCB between 3 and 6.7 ng/mg) in HK2 cells, and 4 μM (iUCB between 4.7 and 7.5 ng/mg) in H5V cells. Conclusions: In all the cell lines studied, iUCB of around 7 ng/mg protein had antioxidant activities, while iUCB > 25 ng/mg protein resulted in a prooxidant and cytotoxic effects. UCB metabolism was found to be cell-specific resulting in different iUCB.

Keywords: bilirubin; ROS; antioxidant; redox state; bilirubin neurotoxicity

1. Introduction

Unconjugated bilirubin (UCB) is the final product of the heme catabolic pathway in the intravascular compartment. UCB is produced by the activity of heme oxygenase (HMOX), an enzyme that splits the tetrapyrrolic ring of heme into biliverdin, carbon monoxide, and ferrous iron. Subsequently, biliverdin is reduced by biliverdin reductase (BLVR) into UCB, which is transported in blood tightly bound to serum albumin before uptake by the hepatocyte. Only less than 0.1% of UCB is unbound to albumin (so-called free bilirubin, Bf). The Bf fraction determines the biological activities of bilirubin [1].

UCB can diffuse into any cell [2,3] and although being a potent antioxidant at low concentrations, it is toxic at high concentrations. Hence, all cells must maintain the intracellular concentration

of UCB below toxic thresholds. This is regulated by its intracellular metabolism (conjugation and oxidation) as well as export out of the cells. UCB interacts mainly with three families of detoxifying enzymes: cytochrome P-450-oxygenase (CYPs) [4,5], glutathione-S-transferases (GSTs) [6], and UDP-glucuronosyltransferases (UGTs) [7]. UCB export is another mechanism used by hepatic and non-hepatic cells to prevent their intracellular accumulation. The export proteins include ATP Binding Cassette Subfamily C Member 2 (ABCC2) involved in the hepatobiliary secretion of bilirubin conjugates, as well as another three ABC transporters that were demonstrated to transport of UCB: ATP Binding Cassette Subfamily B Member 1 (ABCB1 also called MDR1/PGP1) [8], ATP Binding Cassette Subfamily C Member 1 (ABCC1 also called MRP1) [9–12] and ATP Binding Cassette Subfamily C Member 3 (ABCC3 also called MRP3) [13]. Under physiological conditions, these efflux pumps are expressed in organs involved in the elimination of endo- and xeno-biotics, such as the liver and the kidney, and in epithelial tissues that protect the organs from the entry of xenobiotics, like the small intestine, testes, placenta, and blood–brain barrier (BBB) [14].

Hence, bilirubin behavior in a human body has two faces, similar to Janus Bifrons, a Roman god. Elevated serum/plasma UCB concentration, and in particular the Bf fraction, expose babies to the risk of neurotoxicity [15]. Conversely, mildly elevated systemic bilirubin concentrations such as in Gilbert syndrome (GS) [16] protect against various oxidative stress-mediated and metabolic diseases including cardiovascular diseases (CVD), type 2 diabetes, and/or metabolic syndrome [17].

Cells use multiple systems to protect against reactive oxygen species (ROS). Enzymes with antioxidant actions include catalase and superoxide dismutase that together convert superoxide to water. Glutathione (GSH) is regarded as the principal endogenous intracellular small molecule antioxidant cytoprotectant. Studies on cells depleted of GSH or bilirubin indicate that bilirubin is of comparable, or greater, importance to GSH in cytoprotection [18] since bilirubin is one of the most abundant endogenous antioxidants in mammalian tissues [19]. Among extensive series of antioxidants, bilirubin has the most potent superoxide and peroxide radical scavenger activities [20]. The potent physiologic antioxidant actions of bilirubin are further amplified by the oxidation of bilirubin to biliverdin and then recycled by biliverdin reductase back to bilirubin [18].

Nevertheless, it seems that each cell type and tissue may have a different bilirubin threshold switching between beneficial and toxic effects. Doré and Snyder [21] reported that its maximal neuroprotective effects in hippocampal cultures were reached at nanomolar concentrations (10–50 nM), while at higher concentrations the prooxidant effects of bilirubin became dominant. A similar dual effect was reported in the primary cultures of oligodendrocytes, showing protective effects at UCB concentration from 0.05 to 20 μ M and a diminished cytoprotective effects at 100 μ M [22].

However, the exact concentration thresholds between anti- and pro-oxidant effects of bilirubin remain undefined and need further investigation [23]. Thus, in the present work, we performed an *in vitro* study using different human and murine cell lines exposed to increasing concentrations of UCB, and correlated the intracellular unconjugated bilirubin concentrations with cytotoxic, antioxidant and prooxidant effects.

2. Results

2.1. UCB Cytotoxicity

The four cell lines were exposed to a dose-dependent UCB treatment for 24 h and cytotoxicity was assessed by the propidium iodide (PI) test (Figure 1).

UCB cytotoxicity showed three different levels of susceptibility among the cell lines. HepG2 cell line was less sensitive, while the neuronal cells appeared the most sensitive. HK2 and H5V showed an intermediate dose-dependent cytotoxicity behavior. The first significant increase in dead cells was detected at UCB concentrations of 3.6 μ M for SH-SY5Y, 7.5 μ M for HK2 and 15 μ M for H5V. No changes were observed in HepG2.

The metabolic activity measured by MTT was also substantially affected upon the same UCB exposure (Figure 2). In HepG2 cells, formazan generation was reduced by 30% upon exposure to increasing UCB concentrations, and similar data were obtained also in H5V and HK2 cells, while the SH-SY5Y cells were substantially more sensitive with reduction of formazan generation to 75% upon exposure to as low as 0.4 μM UCB concentrations.

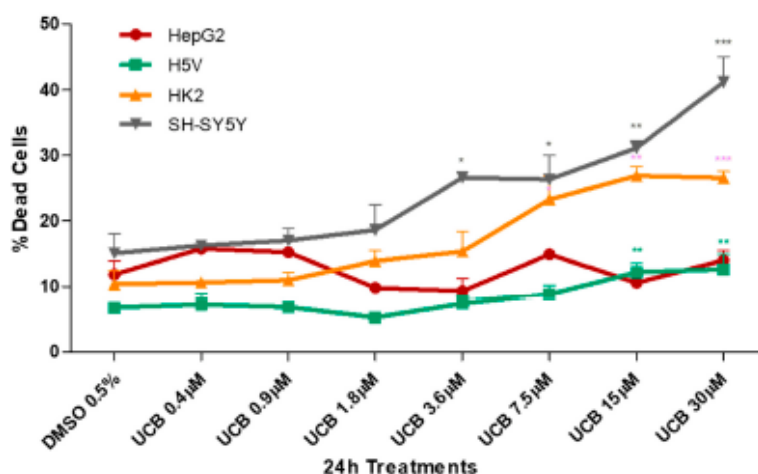


Figure 1. The effect of unconjugated bilirubin (UCB) treatment on cell viability. The cell lines were exposed to the increasing UCB concentration (from 0.4 to 30 μM in the presence of 30 μM BSA) or 0.5% DMSO for 24 h and then treated with propidium iodide (PI). The percentage of dead cells was calculated as the proportion of fluorescence intensity of dead cells to that of total cells. Data are expressed as mean \pm SD of at least four independent experiments. * $p < 0.05$, ** $p < 0.01$, *** $p < 0.001$.

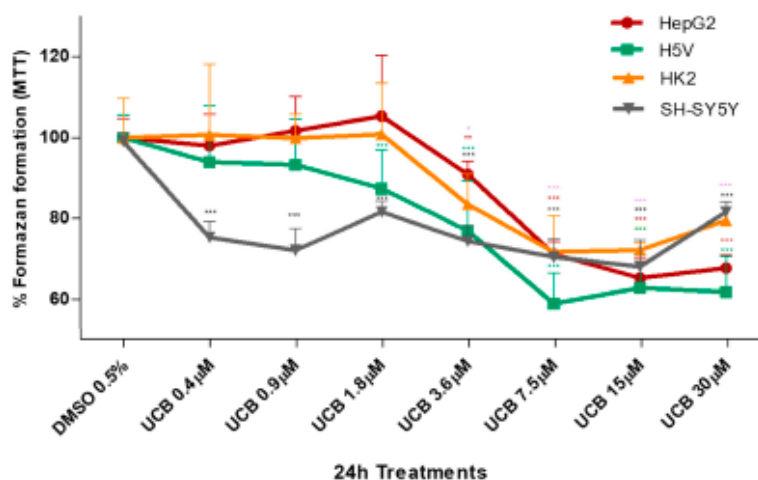


Figure 2. The effect of UCB on the metabolic activity of studied cells. The cell lines were exposed to the increasing UCB concentrations (from 0.4 to 30 μM in the presence of 30 μM BSA) or 0.5% DMSO for 24 h and then MTT test was performed. The capacity of control DMSO-treated cells to modify MTT into formazan was considered as 100%. Data are expressed as mean \pm SD of at least four independent experiments. * $p < 0.05$, ** $p < 0.01$, *** $p < 0.001$.

2.2. The Effect of UCB Exposure to Intracellular UCB Concentration

All four cell lines were exposed for 24 h to increasing UCB concentrations, and then the intracellular bilirubin concentrations were determined (Table 1).

Table 1. The effect of UCB exposure to intracellular UCB concentrations. The cell lines were exposed for 24 h to the increasing UCB concentrations (from 0.4 to 30 μ M in the presence of 30 μ M BSA) or 0.5% DMSO. Data are expressed as mean \pm SD of three independent experiments, UCB concentrations were recalculated per mg of protein. *p*-values represent comparison with control cells.

Treatment	HepG2		H5V		HK2		SH-SY5Y	
	Mean \pm SD (ng/mg)	<i>p</i> -Value (vs. Ctrl)	Mean \pm SD (ng/mg)	<i>p</i> -Value (vs. Ctrl)	Mean \pm SD (ng/mg)	<i>p</i> -Value (vs. Ctrl)	Mean \pm SD (ng/mg)	<i>p</i> -Value (vs. Ctrl)
Control	5.0 \pm 1.8		0.0 \pm 0.0		0.0 \pm 0.0		0.0 \pm 0.0	
UCB 0.4 μ M	4.1 \pm 1.5	0.735	0.0 \pm 0.0		1.8 \pm 0.2	0.014	3.34 \pm 1.06	0.503
UCB 0.9 μ M	5.1 \pm 2.0	0.984	1 \pm 1.09	0.546	3.5 \pm 0.4	0.013	7.5 \pm 2.0	0.309
UCB 1.8 μ M	2.4 \pm 0.7	0.311	3.4 \pm 3.51	0.415	3.0 \pm 0.6	0.037	13.0 \pm 3.0	0.163
UCB 3.6 μ M	2.0 \pm 0.5	0.245	4.7 \pm 0.6	0.018	6.7 \pm 0.1	0.000	25.5 \pm 5.4	0.043
UCB 7.5 μ M	4.6 \pm 2.3	0.900	7.5 \pm 1.6	0.042	13.4 \pm 0.9	0.004	29.5 \pm 6.3	0.043
UCB 15 μ M	5.4 \pm 0.7	0.874	42.4 \pm 4.5	0.011	40.1 \pm 9.5	0.052	79.1 \pm 8.4	0.011
UCB 30 μ M	21.3 \pm 2.4	0.033	122.3 \pm 2.8	0.001	123.8 \pm 11.5	0.009	303.3 \pm 11.2	0.001

The intracellular bilirubin concentrations differ substantially among the cell lines, with HepG2 cells being the most resistant (intracellular UCB concentration remained comparable to the control level until 15 μ M treatment). SH-SY5Y, HK2, and H5V cells showed a significant dose-dependent intracellular bilirubin content, though the extent differs among the three cell lines: SH-SY5Y was the most sensitive, having one order of magnitude higher intracellular concentrations compared to HepG2 cells (*p* = 0.0014).

2.3. The Effect of UCB Exposure on Intracellular ROS Production

To test the prooxidant ability of UCB, the intracellular ROS production was measured (Figure 3).

UCB did not result in any significant increase in intracellular ROS production in HepG2 cells at any time point despite a two fold ROS increase by H₂O₂ after 45 min (*p* \leq 0.05) and 90 min (*p* \leq 0.01) of treatment (Figure S1). On the contrary, in SH-SY5Y cells, UCB concentration higher than 3.6 μ M (corresponding to intracellular bilirubin concentration of 25 ng/mg) resulted in a threefold increase in intracellular ROS production. In H5V cells and HK2 cells, UCB treatments higher than 15 μ M (corresponding to intracellular bilirubin concentration of 40 ng/mg) doubled the intracellular ROS concentration.

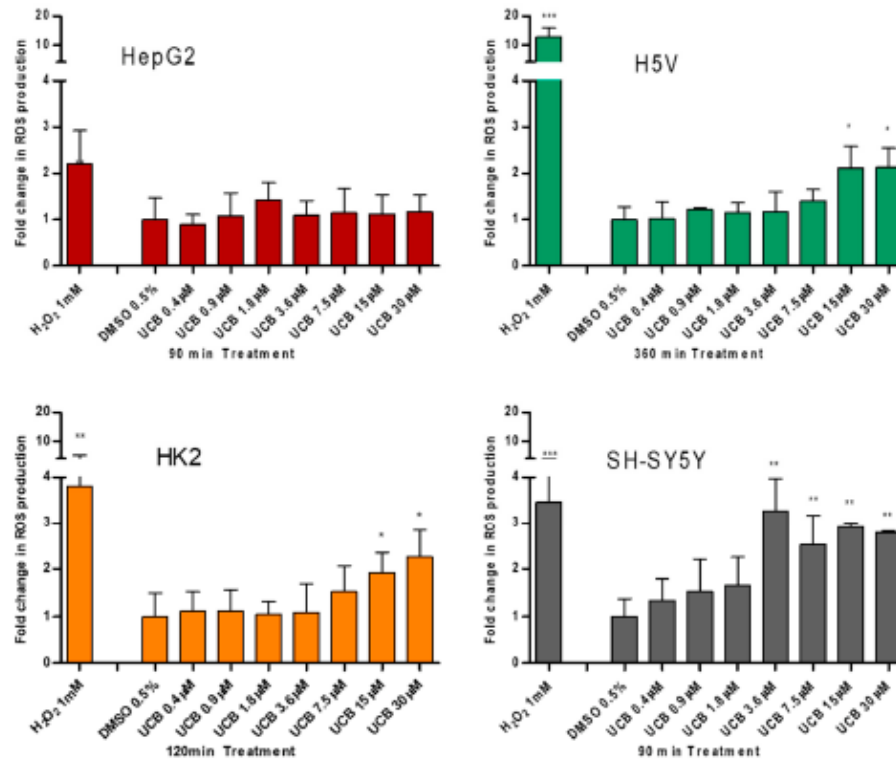


Figure 3. The effect of UCB treatment on intracellular reactive oxygen species (ROS) production. The cell lines were exposed to the increasing UCB concentration (from 0.4 to 30 μ M in the presence of 30 μ M BSA) or 0.5% DMSO for the time indicated on x-axis. The time of exposure to UCB was defined based on a time course performed in each cell line. The time with the highest increase in ROS production by UCB and 1 mM H₂O₂ (used as positive control) was selected for each cell line (90 min for HepG2 cells, 120 min for SH-SY5Y and HK2 cells, and 360 min for H5V cells). Fluorescence results reflecting ROS production were normalized to the total protein content and compared to DMSO-treated cells. Data are expressed as mean \pm SD of three independent experiments. * $p < 0.05$, ** $p < 0.01$, *** $p < 0.001$.

2.4. The Antioxidant Effect of UCB on Live Cells Measured by LUCS Technology AOP1

Having assessed the prooxidant capacity of bilirubin by evaluating intracellular ROS accumulation, we tested possible antioxidant effects of UCB using the Light-Up Cell System (LUCS) technology (Figure 4). LUCS assay measures the ability of a condition to neutralize free radicals produced at the intracellular level by a photo-induction process [24]. When applied on a dose–response mode, the assay allows the evaluation of the 50% efficacy concentration (EC₅₀) of the intracellular antioxidant effect of a compound [25].

A direct antioxidant activity of lower concentrations of UCB was detected in all the four cell lines but differ significantly among cell lines. In HepG2 cells, the dose–effect curve showed an EC₅₀ of antioxidant effect around 21.2 μ M (corresponding to an intracellular UCB concentration of 5.4 ng/mg of total protein). In SH-SY5Y cells, the antioxidant effect showed at 0.68 μ M (corresponding to an intracellular UCB concentration between 3.3 and 7.5 ng/mg), whereas in H5V and HK2 cells the antioxidant effect occurred at intermediate UCB concentration. EC₅₀ of antioxidant effect was at 4 μ M

and 2.4 μM , respectively, corresponding to an intracellular UCB concentration between 5 and 7 ng/mg in both cell lines.

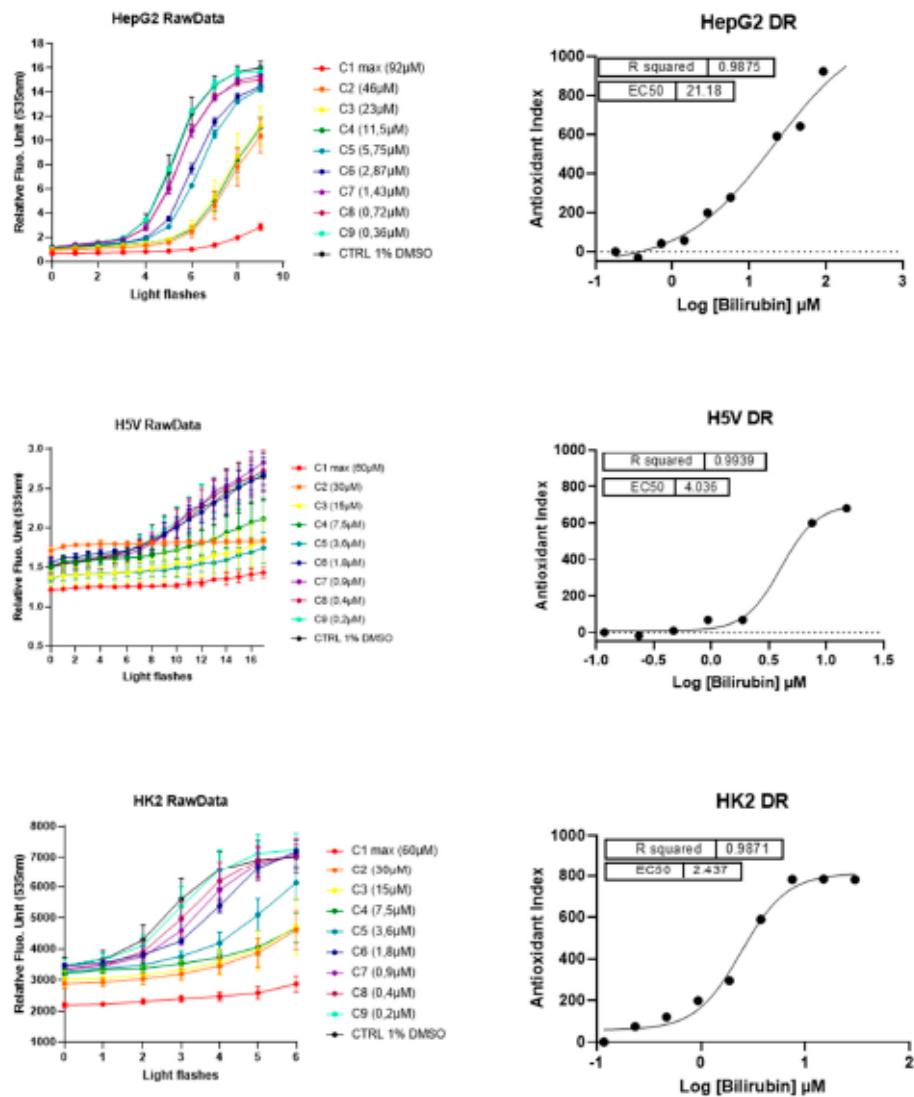


Figure 4. Cont.

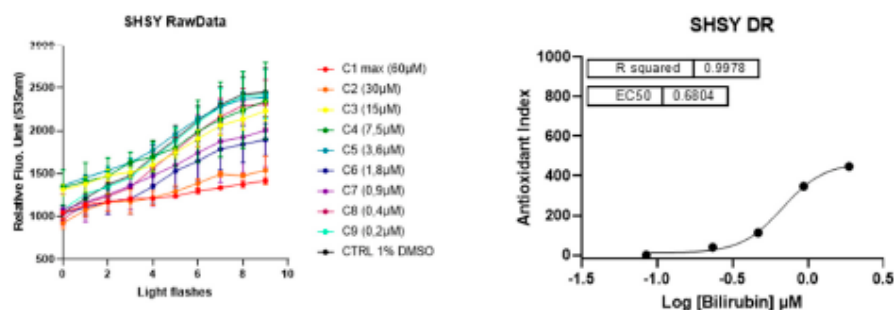


Figure 4. The antioxidant and cytotoxic effect of UCB. Each cell line was incubated for 24 h with indicated UCB concentrations and then treated with the fluorescent biosensor for 1 h. Left panel reports the kinetic profiles recorded for each cell line. Relative Fluorescence Units (RFU) were measured at *exc/em* 501/535 nm according to a recurrent 480 nm LED flash application (20 iterations). Antioxidant effect is measured as a delay (right shift) in fluorescence intensity increase in comparison to negative control profile. Fluorescence intensities higher than negative control at $t = 0$ (before light application) indicate prooxidant/cytotoxic effects (as describes in [25]). Error bars represent SD values from triplicates. Right panel reports dose–response curves obtained after integration of normalized kinetic data. R^2 's represent determination coefficients obtained by fitting data with a sigmoid regression analysis. Unexpected concentrations C4 (HepG2 cells) and C5 (H5V cells) were removed from the regression analysis. Each series of data corresponds to an experiment representative of at least three experiments.

LUCS is a dedicated approach to discriminate between prooxidant/cytotoxic and antioxidant effects [25]. Indeed, prooxidant/cytotoxic effect is revealed at the initial time course by a fluorescence intensity higher than control value [24]. No cytotoxic effect was seen on HepG2 and HK2 cells while it was present at low concentration on SH-SY5Y (treatment of 3.6 μM corresponding to an intracellular UCB concentration of 25 ng/mg) and at very high concentrations (treatment of 30 μM corresponding to an intracellular UCB concentration of 122 ng/mg) on H5V cells. Table 2 reports the intracellular UCB concentration (ng/mg protein) corresponding to the EC_{50} or cytotoxic effect in each cell line.

Table 2. The intracellular UCB concentrations corresponding to antioxidant (50% efficacy concentration (EC_{50})) or cytotoxic effects.

Cell Lines	Antioxidant EC_{50}		Cytotoxic Effect	
	UCB Treatment	Intracellular UCB Content (ng/mg Total Protein)	UCB Treatment	Intracellular UCB Content (ng/mg Total Protein)
HepG2	21.2 μM	between 5.4 and 21.3 ng/mg total protein		
H5V	4.04 μM	between 4.7 and 7.5 ng/mg total protein	>30 μM	>122.3 ng/mg
HK2	2.44 μM	between 3 and 6.7 ng/mg total protein		
SH-SY5Y	0.68 μM	between 3.3 and 7.5 ng/mg total protein	>3.6 μM	>25.5 ng/mg

2.5. The Effect of UCB on Total GSH and SOD Activity

Since the cells use multiple systems to protect against ROS overproduction, we measured total GSH concentrations (Figure 5) and SOD activity (Figure S2) in all the four cell lines exposed for 24 h to increasing UCB concentrations.

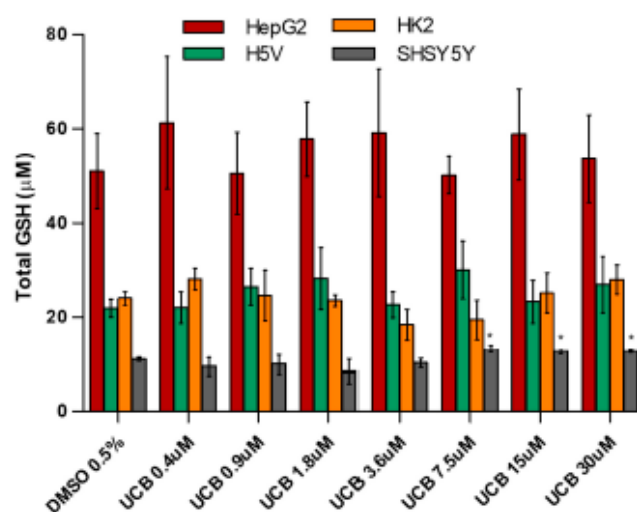


Figure 5. The effect of UCB exposure on intracellular glutathione (GSH) concentrations. The cell lines were exposed to increasing UCB concentrations (from 0.4 to 30 μM in the presence of 30 μM BSA) or 0.5% DMSO for 24 h and then total GSH concentration was measured. Data are expressed as mean \pm SD of three independent experiments. * $p < 0.05$.

The basal level of GSH was higher in HepG2 cells. GSH concentration was not affected by UCB treatment. The only exception was the SH-SY5Y cells, in which GSH concentrations increased upon a UCB treatment above 7.5 μM (corresponding to an intracellular bilirubin content of 30 ng/mg of total protein). SOD activity was not affected by UCB treatment in HepG2 cells, while its induction was observed in the other cell lines at UCB prooxidant/cytotoxic concentrations.

3. Discussion

Severe hyperbilirubinemia can cause permanent neurological damage in neonates [16], while a mild elevation of systemic bilirubin concentrations protects against some diseases such as CVD and diabetes thanks to its antioxidant and anti-inflammatory action [26]. To better understand the determinants of this Janus-like behavior of bilirubin, we performed a comparative study using four different cell lines coming from organs/tissues of different origins. HK2 and H5V derived from normal kidney and heart endothelium and were immortalized by viral transduction (see Methods). HepG2 and SH-SY5Y cells derived from hepatoblastoma and neuroblastoma, respectively. Although they are not normal cells, cancer cell lines are valuable surrogates for in vitro model systems that are widely used in basic and translational research [27] as they provide an unlimited source of biological material. The quantity of cells requested by the experimental plan developed in the present manuscript was not compatible with the yield of primary cell culture. Cells were exposed to the same UCB treatment, the intracellular UCB concentrations were measured and correlated with cytotoxic, antioxidant, and/or prooxidant effects. This approach allowed us to confirm that the intracellular UCB concentrations (and not the external UCB treatment) determine the antioxidant or prooxidant/cytotoxic effects and to define thresholds for antioxidant and cytotoxic effects in these cells.

Intracellular UCB concentration substantially differs among the four cell lines; HepG2 hepatic cells have the lowest concentrations, while the SH-SY5Y neuronal cells are the most sensitive (Table 1). Intracellular UCB concentration depends on several factors including the extent of uptake, excretion, and metabolic transformation, with each of these steps differing in various organs. The ability of HepG2 cells to maintain an intracellular UCB equilibrium in the presence of increasing extracellular UCB

treatment is not surprising since the hepatocyte has a flexible and robust system of bilirubin metabolism and detoxification via its conjugation with glucuronic acid by bilirubin UDP-glucuronosyltransferase (UGT1A1) [28–30]. In contrast, many cells of different origins do not possess UGT1A1 activity [7] and must either oxidize or export UCB to prevent its intracellular accumulation [14,23]. Hence, the vulnerability of the neurons may be due to lower activities of the mitochondrial enzymes that oxidize UCB as well as the decreased expression of MRP1, one of the bilirubin efflux pump limiting the intracellular accumulation of the pigment [10–12,31]. A different pattern of expression of efflux transporters and UCB metabolizing enzymes occurs also on H5V and HK2 cells [32] and can explain the difference of UCB accumulation between hepatic compared to those of non-hepatic origin.

UCB cytotoxicity showed three different levels of susceptibility among the cell lines (Figure 1). As expected, the hepatic HepG2 cell line was less sensitive to UCB toxicity, even at the highest UCB concentration tested (corresponding to an intracellular UCB concentration of 21 ng/mg of protein). Conversely, the neuronal cells appeared the most sensitive since cytotoxicity started at a UCB concentration of 3.6 μM corresponding to an intracellular UCB concentration of 25 ng/mg protein. HK2 and H5V showed an intermediate behavior, with UCB cytotoxicity starting from concentrations of 15 μM corresponding to an intracellular UCB concentration of around 40 ng/mg protein. Our results are consistent with previous data showing that different cells exhibited different susceptibilities to the cytotoxic effects of bilirubin; neuroblastoma was most susceptible while hepatocytes were the least vulnerable [33].

The effect of UCB on cell viability (Figure 1) and metabolic activity (Figure 2) varied substantially. The reduction in the metabolic activity occurred in HepG2 cells at UCB above 3.6 μM but was not associated with the cell toxicity. Similarly, in non-hepatic cell lines, the reduction in formazan formation occurred at UCB concentrations lower than cell mortality (i.e., on SH-SY5Y cells metabolic activity reduction occurred at 0.4 μM while mortality started from 3.6 μM). Most importantly, the percentage of dead cells detected by PI was dose-dependent while the reduction of formazan reached a plateau (25–30% of reduction) at least from UCB treatment of 7.5 μM in all cell lines. UCB has an anti-proliferative activity that prevents the cells from multiplying rapidly and maintains the same number of viable cells [34]. MTT test does not discriminate between cell viability and cell proliferation [35]. The plateau effect seen on MTT test in all cell lines points to the ability of UCB to stop the cell growth. Thanks to this comparative study, we demonstrated that, in case of UCB treatment, MTT test is not a reliable viability test but needs to be supported by a test measuring dead cells.

Among the molecular mechanisms contributing to UCB cytotoxicity, oxidative stress has emerged as a potential crucial event [36]. In various cellular systems, UCB causes ROS production, protein oxidation, and lipid peroxidation [37,38], leading to apoptosis [39]. On the protective side of mild hyperbilirubinemia, *in vivo* studies suggested that bilirubin significantly reduces the clinical signs of disease where oxidative stress is important, such as in autoimmune encephalomyelitis [22], coronary artery disease [40], renal tubular injury [41] or diabetic nephropathy [42]. Bilirubin has been demonstrated to be a powerful antioxidant substance in *in vitro* studies [19,20,43], suppressing oxidation more strongly than many other antioxidants, [44–46]. Bilirubin at low concentrations exerts its potent cytoprotective effects by bilirubin/biliverdin redox cycling. [18].

The exact concentration thresholds between anti- and prooxidant effects of bilirubin remained undefined [23]. Our results showed that, in spite of ROS induction by H_2O_2 , the highest UCB treatment dose not induce ROS production in the cell line of hepatic origin (HepG2 cells) while intracellular ROS increase starts in neuronal cell line (SH-SY5Y cells) from UCB concentrations of 3.6 μM , and from 15 μM in both aortic endothelial (H5V) and tubular kidney cells (HK2). On the other side, UCB antioxidant activity showed an EC_{50} of 21.8 μM in HepG2 cells, 0.95 μM in SH-SY5Y cells, 2.44 μM in HK2 cells, and 4 μM in H5V cells. Our results expand and better substantiate what was already published [21,22] showing that each cell type has a different bilirubin threshold switching between the beneficial and toxic effects of bilirubin. Total UCB concentration treatment is an uncertain predictor of its biological effects because intracellular levels of UCB are modulated by its oxidation, conjugation, and export from

the cells by membrane ABC transporters [11]. The ability to measure real UCB concentration in the cells much improve our understanding of UCB-induced cytotoxicity as well as its protective effects [3].

Considering the intracellular UCB concentration regardless of the UCB concentration treatment, we observed that all cell lines have a similar intracellular UCB threshold for antioxidant and prooxidant effects. Figure 6 summarizes all the results previously presented and demonstrates the proposed iUCB threshold. An intracellular UCB concentration around 7 ng/mg acts as an antioxidant, while an intracellular concentration higher than 25 ng/mg is associated with prooxidant and cytotoxic effects.

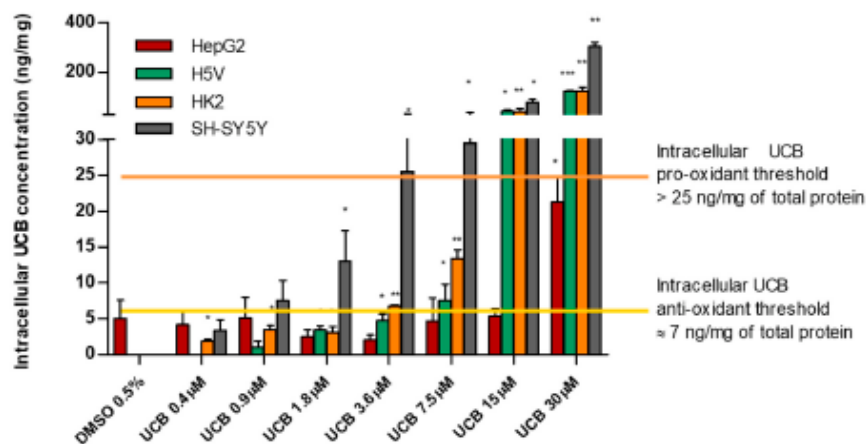


Figure 6. Intracellular UCB prooxidant and antioxidant thresholds. The cell lines were exposed for 24 h to the increasing UCB concentration (from 0.4 to 30 μ M in the presence of 30 μ M BSA) or 0.5% DMSO. Data are expressed as mean \pm SD of three independent experiments, UCB concentrations were recalculated per mg of protein. *p*-values represent comparison with control cells. * *p* < 0.05, ** *p* < 0.01, *** *p* < 0.001.

Finally, we showed that total GSH concentrations and SOD activity, other cellular systems to protect against ROS, do not contribute to the UCB antioxidant activity. Total GSH concentrations (Figure 5) are not influenced by UCB treatment, maintaining the same level of control cells upon UCB dose-dependent treatment. The only exception is on SH-SY5Y cells where GSH levels increased significantly upon a UCB treatment higher than 7.5 μ M (corresponding to an intracellular bilirubin content of 30 ng/mg of total protein). These results confirmed what was previously observed by our group when UCB modulated the GSH concentration in neuroblastoma cells through the induction of the System Xc- increasing cysteine uptake and intracellular GSH content [47]. In addition, SOD activity (Figure S2) increased in all cell lines in response to UCB's prooxidant effect [48].

4. Materials and Methods

4.1. Cell Cultures

SH-SY5Y human neuroblastoma cells (ATCC-CRL-2266) were maintained in EMEM/F12 1:1 supplemented with 15% fetal bovine serum (FBS), 1% penicillin/streptomycin solution (penicillin G (100 U/mL), streptomycin (100 mg/mL)), L-glutamine (2 mmol/L) (Euroclone S.p.A., Milano, Italy) and 1% non-essential amino acids (Sigma-Aldrich, St Louis, MO, USA).

HepG2 human hepatoblastoma cells were maintained in DMEM high glucose supplemented with 10% FBS, 1% penicillin/streptomycin solution (penicillin G (100 U/mL), streptomycin (100 mg/mL)), L-glutamine (2 mmol/L).

H5V, murine heart endothelial cells transformed by polyomavirus middle T antigen (kindly provided by Istituto Mario Negri, Milan, Italy), were grown in DMEM low glucose containing 10% (*v/v*) FBS, 1% penicillin/streptomycin solution (penicillin G (100 U/mL), streptomycin (100 mg/mL)), L-glutamine (2 mmol/L).

HK2, papillomavirus 16 transformed human proximal tubular epithelial cell line (kindly provided by Prof. R. Bulla, Department of Life Sciences, University of Trieste), was cultured in DMEM low glucose, Ham's F12 media (1:1) supplemented with decomplexed 5% (*v/v*) FBS, 1% penicillin/streptomycin solution (penicillin G (100 U/mL)), streptomycin (100 mg/mL), L-glutamine (2 mmol/L), bovine insulin (5 mg/mL), holo-transferrin (5 mg/mL), sodium selenite (5 ng/mL), hydrocortisone (5 ng/mL), EGF (10 ng/mL), T3 (5 pg/mL), and PGE (15 pg/mL).

When 80% of confluence was achieved, the cells were used in studies as described below.

4.2. Treatments

UCB (Sigma-Aldrich, St Louis, MO, USA) was purified as previously described [49], dissolved in DMSO (6 mM), and added to the cell medium (completed with FBS 10% and BSA in order to achieve a final BSA concentration of 30 μ M) to reach a range of final concentration from 0.4 to 30 μ M performing serial dilution. DMSO (0.5%) was used to treat control cells.

4.3. Quantification of Intracellular UCB Concentration

The cells at 80 % confluence were incubated with different UCB concentrations (from 0.4 to 30 μ M) for 24 h, or 0.5 % DMSO. After treatment time, the cells were collected by centrifugation and washed three times in PBS. The intracellular UCB level was quantified using an LC-MS/MS method as was described previously [50].

Briefly, the cells were mixed with internal standard (mesobilirubin), then lysed and deproteinated by 0.5% ammonium acetate in methanol. Finally, this suspension was sonicated and centrifuged. After the final centrifugation steps, 100 μ L of supernatant was pipetted into glass vials with the inert insert (suitable for liquid chromatography-tandem mass spectrometry (LC-MS) analysis), and 2 μ L was directly injected into the LC-MS apparatus. The LC-MS/MS analyses were performed using high-performance liquid chromatography (Dionex Ultimate 3000, Dionex Softron GmbH, Germany) equipped with a Poroshell 120 EC-C18 column (2.1 μ m, 3.0 \times 100 mm; Agilent, CA, USA). For a gradient elution, the phase was prepared by mixing 1 mM of NH₄F (Honeywell, International Inc., Morris Plains, NJ, USA) in water and methanol (40% \rightarrow 100%, 0–13 min) (Biosolve Chimie SARL, Dieuze, France) [50]. The analytes were detected by mass spectrometer (TSQ Quantum Access Max with a HESI-II probe, Thermo Fisher Scientific, Waltham, MA, USA) operating in a positive SRM mode: bilirubin [585.3 \rightarrow 299.1 (20 V); 585.3 \rightarrow 271.2 (18 V)]; MBR [589.3 \rightarrow 301.1 (20 V); 589.3 \rightarrow 273.2 (44 V)]. Protein concentration in the cell suspension was determined by DC Protein Assay (Bio-Rad Laboratories, Irvine, CA, USA) and results were expressed as nmol/mg of protein. All steps were performed at dim light.

4.4. Cytotoxicity Test (PI) and Metabolic Activity Test (MTT)

The tests were performed on cells cultured in black 96-well plates [51,52].

PI (Sigma-Aldrich, St Louis, MO, USA) was solubilized in PBS to a final concentration of 50 μ g/mL. After 60 min of incubation at 37 °C, the initial fluorescence intensity from the dead cells was measured using a multiplate reader (EnSpire 2300, PerkinElmer, Waltham, MA, USA). The excitation and the emission wavelengths were 530 and 620 nm, respectively. After the initial intensity was obtained, Triton X-100 at a final concentration of 0.6% was added to each well to permeabilize the cells and label all nuclei with PI. After 30 min of incubation on ice, fluorescence intensity was re-measured to obtain a value corresponding to the total cells. The percentage of dead cells was calculated as the proportion of fluorescence intensity of dead cells to that of total cells.

Metabolic activity was determined by assessing the reduction of 3(4,5-dimethyl thiazolyl-2)-2,5-diphenyl tetrazolium (MTT, Sigma-Aldrich, St Louis, MO, USA) to formazan by succinate dehydrogenase, a mitochondrial enzyme, as previously described. In brief, a stock solution of MTT was prepared in PBS (5 mg/mL). MTT solution was diluted to 0.5 mg/mL in the cell medium. The test was performed on the cells cultured in 96-well plates. Cells were incubated with the cell medium containing MTT for 1 h at 37 °C. At the end of the incubation period, the insoluble formazan crystals were dissolved in 100 µL of DMSO. Absorbance was determined at 562 nm using a multiplate reader (EnSpire 2300, PerkinElmer, Waltham, MA, USA). Results were expressed as the percentage of control cells not exposed to UCB, which were considered as being 100% viable. It is worth noting that MTT test is a quantitative colorimetric assay for detecting living, but not dead, mammalian cell survival and proliferation [53].

4.5. Determination of Intracellular ROS Production

Intracellular ROS concentrations were monitored by using the fluorescent dye 2',7'-dichlorodihydrofluorescein diacetate (H₂DCFDA, Invitrogen, Thermo Fisher Scientific, Waltham, MA, USA), which is a non-polar compound converted into a non-fluorescent polar derivative (H₂DCF) by cellular esterases after incorporation into cells. H₂DCF is membrane-impermeable and is oxidized rapidly to the highly fluorescent 2',7'-dichlorofluorescein (DCF) in the presence of intracellular ROS. Cells were seeded in 96-well black plates. At the end of UCB treatments, the cells were washed with PBS and were post-treated for 1 h with 10 µM H₂DCF-DA diluted in serum-free medium (free phenol red-DMEM high glucose 24.5 mM) (Sigma-Aldrich, St Louis, MO, USA). H₂O₂ treatment was used as a positive control. Cells were washed in PBS and then incubated in PBS solution to read a normal fluorescence (EnSpire 2300, PerkinElmer, Waltham, MA, USA) at an excitation and emission wavelengths of 505 and 525 nm, respectively. Time of exposure to UCB was defined by a time course performed in each cell line. The time with the highest peak of ROS increase, both by UCB and by H₂O₂ 1 mM (used as positive control), was chosen for each cell line (90 min for HepG2 cells, 120 min for SH-SY5Y and HK2 cells, and 360 min for H5V cells).

4.6. Anti Oxidant Power 1 (AOP1)

HepG2, SHSY5Y, H5V, and HK2 cells were seeded in 96-well plates and then incubated with UCB (9 concentrations obtained by serial log₂ dilutions) in the cell growth medium in the presence of FBS plus BSA to reach BSA final concentration of 30 µM. Cells were treated for 24 h at 37 °C in the presence of 5% CO₂. At least three independent experiments were performed each on triplicate wells. LUCS assay measures the ability of an antioxidant to neutralize oxidative stress and the effect is measured by a delay in the kinetic evolution of fluorescence emission according to Gironde et al. [25]. Briefly, after the 24-h incubation, the cells were treated with the fluorescent biosensor thiazole orange (4 µM, Sigma-Aldrich, St Louis, MO, USA) for 1 h and Relative Fluorescence Units (RFU) at 535 nm were recorded (Varioskan, Thermo Fisher Scientific, Waltham, MA, USA) after a recurrent (20 iterations) 480 nm LED application procedure (24 mJ/cm²) [25] of the whole 96-well plate. Kinetic profiles were recorded and dose–response curves were calculated. Prooxidant/cytotoxic effect is revealed at the initial time course by a fluorescence intensity higher than control value [24]. RFUs (Relative Fluorescence Units) presented in Figure 4 were plotted in a kinetics-like mode and analyzed by Prism8 software (GraphPad, San Diego, CA, USA) to generate dose–response curves. Results were normalized to control data and expressed as a Cellular Antioxidant Index (CAI) corresponding to the integration of all normalized data following the equation $CAI = 1000 - 1000 \cdot (AUC_x / AUC_{control})$ where $AUC_x = \int_0^{12} NFUFN_x$ and $AUC_{control} = \int_0^{12} NFUFN_{control}$ and $NFUFN_x = \text{flash number } x$. For dose–response experiments, CAI values were then used to calculate 50% efficacy concentration (EC₅₀) values from a mathematical non-linear regression model (sigmoid fit) following the equation: $Y = \text{Bottom} + (\text{Top} - \text{Bottom}) / (1 + 10^{(\log EC_{50} - X) \cdot \text{HillSlope}})$, where HillSlope = slope coefficient of the tangent at the inflection point. EC₅₀ and R² values were deduced from the regression model. Two AUCs whose

value was above AUC values obtained from higher concentrations were discarded from the fit model as regression sigmoid model should describe an increasing function.

4.7. GSH Determinations

Total GSH concentration was determined using a GSH Colorimetric Detection Kit (Invitrogen, Thermo Fisher Scientific, Waltham, MA, USA). The kit uses a colorimetric substrate that reacts with the free thiol group on GSH to produce a highly colored product. The cells were cultured in a 6-well plate at different concentrations according to the cell size. When a confluence of around 80% was reached, the cells were treated with different bilirubin concentrations. Afterward, the cells were washed with ice-cold PBS, suspended in ice-cold 5% aqueous 5-sulfosalicylic acid dehydrate, and sonicated to lyse cells. The dilution and assay were conducted as indicated by the kit instructions (the end-point method). Total GSH concentrations (μM) were obtained by interpolation on the standard curve. Results were normalized per 100,000 seeded cells.

4.8. SOD Activity

The superoxide dismutase activity was measured according to Ewing and Janero (1995) [54]. SOD activity was measured using an NBT/NADH/PMS system. The non-enzymatic phenazine methosulfate-nicotinamide adenine dinucleotide (PMS/NADH) system generates superoxide radicals that reduce nitro blue tetrazolium (NBT) into a purple-colored formazan. One SOD activity unit was defined as the amount of an enzyme required to cause 50% inhibition of the NBT photoreduction rate. Cell lysates were added to a reaction mixture containing 50 mM potassium phosphate, pH 7.0, 166 μM NADH, 43 μM NBT. The reaction was initiated with the addition of 50 μL freshly prepared PMS 0.75 μM . The absorbance (considered as an index of NBT reduction) was monitored at 560 nm over 5 min every 30 min using a multiplate reader (EnSpire 2300, PerkinElmer, Waltham, MA, USA) in the kinetic mode. The change in absorbance at 560 nm was plotted as a function of time. The slope obtained in the absence of SOD (the activity control) should be maximal and is taken as the 100% value; all other slopes generated with SOD standards or cell tissue extracts were compared to this slope. The % inhibition of the rate of increase in absorbance at 560 nm is calculated as follows: % Inhibition = $(\text{Slope of 1X SOD Buffer Control} - \text{Slope of Sample}) \times 100 / \text{Slope of 1XSOD Buffer Control}$.

IC50 values of the samples were determined by plotting percentage inhibition vs. the quantity (mg of total proteins) of the cell extract. The SOD activity was expressed in terms of units/mg of total protein considering that one SOD activity unit was defined as the amount of enzyme required to cause 50% inhibition of the NBT photoreduction rate. Protein concentration was determined by Bicinchoninic Acid Protein assay (Sigma-Aldrich, St Louis, MO, USA). Bovine SOD Cu,Zn-SOD (SOD1) (Sigma-Aldrich, St Louis, MO, USA) was used as an internal control to generate a standard curve of the SOD activity.

4.9. Statistical Analysis

All data are presented as mean \pm standard deviation. A statistically significant difference between two data sets was assessed by unpaired two-tailed Student's *t*-test using Prism5 software (GraphPad, San Diego, CA, USA). Statistical significance was determined at $p < 0.05$, unless otherwise indicated. Significance was graphically indicated as follows: * $p < 0.05$, ** $p < 0.01$, *** $p < 0.001$.

5. Conclusions

In all the cell lines studied, the intracellular UCB concentration of around 7 ng/mg protein had antioxidant activities, while its intracellular concentrations > 25 ng/mg protein resulted in prooxidant and cytotoxic effects. UCB metabolism was found to be cell-specific resulting in different UCB intracellular concentrations. Nevertheless, we could define the threshold of intracellular UCB concentration valid for various cell types that set the switch between the anti- and pro-oxidant effects of bilirubin.

Supplementary Materials: Supplementary materials can be found at <http://www.mdpi.com/1422-0067/21/21/8101/s1>.

Author Contributions: Conceptualization, A.B. and C.B.; data curation, C.B.; formal analysis, A.B., A.D., C.G., C.F. and C.B.; funding acquisition, C.T., C.F., L.V. and C.B.; investigation, A.B. and C.B.; methodology, C.F., L.V. and C.B.; project administration, C.T., C.F., L.V. and C.B.; resources, C.T., C.F., L.V. and C.B.; validation, A.B., A.D. and C.G.; writing—original draft, A.B. and C.B.; writing—review and editing, A.B., A.D., N.C., C.G., C.T., C.F., L.V. and C.B. All authors have read and agreed to the published version of the manuscript.

Funding: This research was funded by Beneficentia Stiftung, BANCA D'ITALIA, FIF internal grant, the Czech Ministry of Health, grants NV18-07-00342 and RVO-VFN64165/2020.

Acknowledgments: We thank Roberta Bulla who kindly provided HK2 cells.

Conflicts of Interest: The authors declare no conflict of interest.

Abbreviations

iUCB	Intracellular unconjugated bilirubin concentrations
UCB	Unconjugated bilirubin
EC50	Half maximal effective concentration
ROS	Reactive oxygen species
HMOX	Heme oxygenase
BLVR	Biliverdin reductase
Bf	Free bilirubin
CYPs	Cytochrome P-450-oxygenases
GSTs	Glutathione S-transferases
UGTs	UDP-Glucuronosyl-transferase
ABC	ATP Binding Cassette
ABCC1	ATP Binding Cassette Subfamily C Member 1
ABCC2	ATP Binding Cassette Subfamily C Member 2
ABCC3	ATP Binding Cassette Subfamily C Member 3
ABCB1	ATP Binding Cassette Subfamily B Member 1
MDR1	Multidrug resistance protein 1
MRP3	Multidrug resistance-associated Protein 3
PGP1	P-glycoprotein 1
BBB	Blood–brain barrier
GS	Gilbert syndrome
CVD	Cardiovascular diseases
PI	Propidium iodide
DMSO	Dimethyl sulfoxide
MTT	3(4,5-dimethylthiazolyl-2)-2,5 diphenyl tetrazolium
H2DCFDA	2',2'-dichlorodihydrofluorescein diacetate
DCF	2',7-dichlorofluorescein
H ₂ O ₂	Hydrogen peroxide
BSA	Bovine serum albumin
LUCs	Light-Up Cell System
AOP	Antioxidant power I
RFU	Relative fluorescence units
SOD	Superoxide dismutase
UGT1A1	UDP Glucuronosyltransferase family 1 member A1
GSH	Reduced glutathione
NBT	Nitro blue tetrazolium
NADH	β-Nicotinamide adenine dinucleotide reduced
PMS	Phenazine methosulfate
CuZnSOD	Copper- and zinc-containing superoxide dismutase
SOD1	Superoxide dismutase [Cu-Zn]

References

- Ahlfors, C.E.; Wennberg, R.P.; Ostrow, J.D.; Tiribelli, C. Unbound (free) bilirubin: Improving the paradigm for evaluating neonatal jaundice. *Clin. Chem.* **2009**, *55*, 1288–1299. [CrossRef] [PubMed]
- Zucker, S.D.; Goessling, W.; Hoppin, A.G. Unconjugated bilirubin exhibits spontaneous diffusion through model lipid bilayers and native hepatocyte membranes. *J. Biol. Chem.* **1999**, *274*, 10852–10862. [CrossRef] [PubMed]
- Zelenka, J.; Lenicek, M.; Muchová, L.; Jirsa, M.; Kudla, M.; Balaz, P.; Zadinová, M.; Ostrow, J.D.; Wong, R.J.; Vitek, L. Highly sensitive method for quantitative determination of bilirubin in biological fluids and tissues. *J. Chromatogr. B Analyt. Technol. Biomed. Life. Sci.* **2008**, *867*, 37–42. [CrossRef]
- Kapitulnik, J.; Gorzalez, F.J. Marked endogenous activation of the CYP1A1 and CYP1A2 genes in the congenitally jaundiced Gunn rat. *Mol. Pharmacol.* **1993**, *43*, 722–725.
- De Matteis, F.; Lord, G.A.; Kee Lim, C.; Pons, N. Bilirubin degradation by uncoupled cytochrome P450. Comparison with a chemical oxidation system and characterization of the products by high-performance liquid chromatography/electrospray ionization mass spectrometry. *Rapid Commun. Mass Spectrom.* **2006**, *20*, 1209–1217. [CrossRef]
- Coles, B.F.; Kadlubar, F.F. Human Alpha Class Glutathione S-Transferases: Genetic Polymorphism, Expression, and Susceptibility to Disease. In *Methods in Enzymology*; Sies, H., Packer, L., Eds.; Glutathione Transferases and Gamma-Glutamyl Transpeptidases; Academic Press: Cambridge, MA, USA, 2005; Volume 401, pp. 9–42.
- Nakamura, A.; Nakajima, M.; Yamanaka, H.; Fujiwara, R.; Yokoi, T. Expression of UGT1A and UGT2B mRNA in human normal tissues and various cell lines. *Drug Metab. Dispos. Biol. Fate Chem.* **2008**, *36*, 1461–1464. [CrossRef]
- Schinkel, A.H. The physiological function of drug-transporting P-glycoproteins. *Semin. Cancer Biol.* **1997**, *8*, 161–170. [CrossRef]
- Falcão, A.S.; Bellarosa, C.; Fernandes, A.; Brito, M.A.; Silva, R.F.M.; Tiribelli, C.; Brites, D. Role of multidrug resistance-associated protein 1 expression in the in vitro susceptibility of rat nerve cell to unconjugated bilirubin. *Neuroscience* **2007**, *144*, 878–888. [CrossRef]
- Corich, L.; Aranda, A.; Carrassa, L.; Bellarosa, C.; Ostrow, J.D.; Tiribelli, C. The cytotoxic effect of unconjugated bilirubin in human neuroblastoma SH-SY5Y cells is modulated by the expression level of MRP1 but not MDR1. *Biochem. J.* **2009**, *417*, 305–312. [CrossRef] [PubMed]
- Rigato, L.; Pascolo, L.; Ferretti, C.; Ostrow, J.D.; Tiribelli, C. The human multidrug-resistance-associated protein MRP1 mediates ATP-dependent transport of unconjugated bilirubin. *Biochem. J.* **2004**, *383*, 335–341. [CrossRef] [PubMed]
- Calligaris, S.; Cekic, D.; Roca-Burgos, L.; Gerin, F.; Mazzone, G.; Ostrow, J.D.; Tiribelli, C. Multidrug resistance associated protein 1 protects against bilirubin-induced cytotoxicity. *FEBS Lett.* **2006**, *580*, 1355–1359. [CrossRef] [PubMed]
- Scheffer, G.L.; Kool, M.; de Haas, M.; de Vree, J.M.L.; Pijnenborg, A.C.L.M.; Bosman, D.K.; Elferink, R.P.J.O.; van der Valk, P.; Borst, P.; Schepet, R.J. Tissue distribution and induction of human multidrug resistant protein 3. *Lab. Invest. J. Tech. Methods Pathol.* **2002**, *82*, 193–201. [CrossRef] [PubMed]
- Bellarosa, C.; Bortolussi, G.; Tiribelli, C. The role of ABC transporters in protecting cells from bilirubin toxicity. *Curr. Pharm. Des.* **2009**, *15*, 2884–2892. [CrossRef]
- Watchko, J.E.; Tiribelli, C. Bilirubin-induced neurologic damage. *N. Engl. J. Med.* **2014**, *370*, 979. [CrossRef] [PubMed]
- Bosma, P.J.; Chowdhury, J.R.; Bakker, C.; Gantla, S.; de Boer, A.; Oostra, B.A.; Lindhout, D.; Tytgat, G.N.; Jansen, P.L.; Oude Elferink, R.P. The genetic basis of the reduced expression of bilirubin UDP-glucuronosyltransferase 1 in Gilbert's syndrome. *N. Engl. J. Med.* **1995**, *333*, 1171–1175. [CrossRef]
- Vitek, L. The role of bilirubin in diabetes, metabolic syndrome, and cardiovascular diseases. *Front. Pharmacol.* **2012**, *3*, 55. [CrossRef] [PubMed]
- Baranano, D.E.; Rao, M.; Ferris, C.D.; Snyder, S.H. Biliverdin reductase: A major physiologic cytoprotectant. *Proc. Natl. Acad. Sci. USA* **2002**, *99*, 16093–16098. [CrossRef]
- Gopinathan, V.; Miller, N.J.; Milner, A.D.; Rice-Evans, C.A. Bilirubin and ascorbate antioxidant activity in neonatal plasma. *FEBS Lett.* **1994**, *349*, 197–200. [CrossRef]

20. Farrera, J.A.; Jaumà, A.; Ribó, J.M.; Peirè, M.A.; Parellada, P.P.; Roques-Choua, S.; Bienvenue, E.; Seta, P. The antioxidant role of bile pigments evaluated by chemical tests. *Bioorg. Med. Chem.* **1994**, *2*, 181–185. [\[CrossRef\]](#)
21. Dorè, S.; Snyder, S.H. Neuroprotective action of bilirubin against oxidative stress in primary hippocampal cultures. *Ann. N.Y. Acad. Sci.* **1999**, *890*, 167–172. [\[CrossRef\]](#)
22. Liu, Y.; Zhu, B.; Wang, X.; Luo, L.; Li, P.; Paty, D.W.; Cynader, M.S. Bilirubin as a potent antioxidant suppresses experimental autoimmune encephalomyelitis: Implications for the role of oxidative stress in the development of multiple sclerosis. *J. Neuroimmunol.* **2003**, *139*, 27–35. [\[CrossRef\]](#)
23. Gazzin, S.; Strazielle, N.; Tiribelli, C.; Ghersi-Egea, J.-F. Transport and Metabolism at Blood–Brain Interfaces and in Neural Cells: Relevance to Bilirubin-Induced Encephalopathy. *Front. Pharmacol.* **2012**, *3*. [\[CrossRef\]](#)
24. Derick, S.; Gironde, C.; Perio, P.; Keybier, K.; Nepveu, F.; Jauneau, A.; Furger, C. LUCS (Light-Up Cell System), a universal high throughput assay for homeostasis evaluation in live cells. *Sci. Rep.* **2017**, *7*, 18069. [\[CrossRef\]](#)
25. Gironde, C.; Rigal, M.; Dufour, C.; Furger, C. AOPI, a New Live Cell Assay for the Direct and Quantitative Measure of Intracellular Antioxidant Effects. *Antioxid. Basel Switz.* **2020**, *9*, 471. [\[CrossRef\]](#)
26. Vitek, L.; Bellarosa, C.; Tiribelli, C. Induction of Mild Hyperbilirubinemia: Hype or Real Therapeutic Opportunity? *Clin. Pharmacol. Ther.* **2018**. [\[CrossRef\]](#)
27. Mirabelli, P.; Coppola, L.; Salvatore, M. Cancer Cell Lines Are Useful Model Systems for Medical Research. *Cancers* **2019**, *11*, 1098. [\[CrossRef\]](#)
28. Keppeler, D. The roles of MRP2, MRP3, OATP1B1, and OATP1B3 in conjugated hyperbilirubinemia. *Drug Metab. Dispos. Biol. Fate Chem.* **2014**, *42*, 561–565. [\[CrossRef\]](#)
29. Iusuf, D.; van de Steeg, E.; Schinkel, A.H. Hepatocyte hopping of OATP1B substrates contributes to efficient hepatic detoxification. *Clin. Pharmacol. Ther.* **2012**, *92*, 559–562. [\[CrossRef\]](#)
30. Abu-Bakar, A.; Arthur, D.M.; Wikman, A.S.; Rahnasto, M.; Juvonen, R.O.; Vepsäläinen, J.; Raunio, H.; Ng, J.C.; Lang, M.A. Metabolism of bilirubin by human cytochrome P450 2A6. *Toxicol. Appl. Pharmacol.* **2012**, *261*, 50–58. [\[CrossRef\]](#)
31. Brites, D. Bilirubin injury to neurons and glial cells: New players, novel targets, and newer insights. *Semin. Perinatol.* **2011**, *35*, 114–120. [\[CrossRef\]](#)
32. Jenkinson, S.E.; Chung, G.W.; van Loon, E.; Bakar, N.S.; Dalzell, A.M.; Brown, C.D.A. The limitations of renal epithelial cell line HK-2 as a model of drug transporter expression and function in the proximal tubule. *Pflugers Arch.* **2012**, *464*, 601–611. [\[CrossRef\]](#) [\[PubMed\]](#)
33. Ngai, K.-C.; Yeung, C.-Y.; Leung, C.-S. Difference in susceptibilities of different cell lines to bilirubin damage. *J. Paediatr. Child Health* **2000**, *36*, 51–55. [\[CrossRef\]](#)
34. Ollinger, R.; Bilban, M.; Erat, A.; Froio, A.; McDaid, J.; Tyagi, S.; Cszmadia, E.; Graça-Souza, A.V.; Liloia, A.; Soares, M.P.; et al. Bilirubin: A natural inhibitor of vascular smooth muscle cell proliferation. *Circulation* **2005**, *112*, 1030–1039. [\[CrossRef\]](#)
35. Chan, G.K.Y.; Kleinheinz, T.L.; Peterson, D.; Moffat, J.G. A Simple High-Content Cell Cycle Assay Reveals Frequent Discrepancies between Cell Number and ATP and MTS Proliferation Assays. *PLoS ONE* **2013**, *8*, e63583. [\[CrossRef\]](#) [\[PubMed\]](#)
36. Tell, G.; Gustincich, S. Redox state, oxidative stress, and molecular mechanisms of protective and toxic effects of bilirubin on cells. *Curr. Pharm. Des.* **2009**, *15*, 2908–2914. [\[CrossRef\]](#)
37. Brito, M.A.; Lima, S.; Fernandes, A.; Falcão, A.S.; Silva, R.F.M.; Butterfield, D.A.; Brites, D. Bilirubin injury to neurons: Contribution of oxidative stress and rescue by glycoconjugated cholic acid. *Neurotoxicology* **2008**, *29*, 259–269. [\[CrossRef\]](#)
38. Kumar, S.; Guha, M.; Choubey, V.; Maity, P.; Srivastava, K.; Puri, S.K.; Bandyopadhyay, U. Bilirubin inhibits *Plasmodium falciparum* growth through the generation of reactive oxygen species. *Free Radic. Biol. Med.* **2008**, *44*, 602–613. [\[CrossRef\]](#)
39. Oakes, G.H.; Bend, J.R. Early steps in bilirubin-mediated apoptosis in murine hepatoma (Hepa 1c1c7) cells are characterized by aryl hydrocarbon receptor-independent oxidative stress and activation of the mitochondrial pathway. *J. Biochem. Mol. Toxicol.* **2005**, *19*, 244–255. [\[CrossRef\]](#)
40. Hopkins, P.N.; Wu, L.L.; Hunt, S.C.; James, B.C.; Vincent, G.M.; Williams, R.R. Higher Serum Bilirubin Is Associated With Decreased Risk for Early Familial Coronary Artery Disease. *Arterioscler. Thromb. Vasc. Biol.* **1996**, *16*, 250–255. [\[CrossRef\]](#) [\[PubMed\]](#)

41. Oh, S.W.; Lee, E.S.; Kim, S.; Na, K.Y.; Chae, D.W.; Kim, S.; Chin, H.J. Bilirubin attenuates the renal tubular injury by inhibition of oxidative stress and apoptosis. *BMC Nephrol.* **2013**, *14*, 105. [CrossRef] [PubMed]
42. Fujii, M.; Inoguchi, T.; Sasaki, S.; Maeda, Y.; Zheng, J.; Kobayashi, K.; Takayanagi, R. Bilirubin and biliverdin protect rodents against diabetic nephropathy by downregulating NAD(P)H oxidase. *Kidney Int.* **2010**, *78*, 905–919. [CrossRef] [PubMed]
43. Marilena, G. New physiological importance of two classic residual products: Carbon monoxide and bilirubin. *Biochem. Mol. Med.* **1997**, *61*, 136–142. [CrossRef]
44. Stocker, R.; Yamamoto, Y.; McDonagh, A.F.; Glazer, A.N.; Ames, B.N. Bilirubin is an antioxidant of possible physiological importance. *Science* **1987**, *235*, 1043–1046. [CrossRef]
45. Stocker, R.; Glazer, A.N.; Ames, B.N. Antioxidant activity of albumin-bound bilirubin. *Proc. Natl. Acad. Sci. USA* **1987**, *84*, 5918–5922. [CrossRef] [PubMed]
46. Wu, T.-W.; Carey, D.; Wu, J.; Sugiyama, H. The cytoprotective effects of bilirubin and biliverdin on rat hepatocytes and human erythrocytes and the impact of albumin. *Biochem. Cell Biol.* **1991**, *69*, 828–834. [CrossRef] [PubMed]
47. Giraudi, P.J.; Bellarosa, C.; Coda-Zabetta, C.D.; Peruzzo, P.; Tiribelli, C. Functional induction of the cystine-glutamate exchanger system Xc(-) activity in SH-SY5Y cells by unconjugated bilirubin. *PLoS ONE* **2011**, *6*, e29078. [CrossRef]
48. He, L.; He, T.; Farrar, S.; Ji, L.; Liu, T.; Ma, X. Antioxidants Maintain Cellular Redox Homeostasis by Elimination of Reactive Oxygen Species. *Cell. Physiol. Biochem.* **2017**, *44*, 532–553. [CrossRef]
49. McDonagh, A.F.; Assisi, F. The ready isomerization of bilirubin IX- in aqueous solution. *Biochem. J.* **1972**, *129*, 797–800. [CrossRef]
50. Jašprová, J.; Dvořák, A.; Vecka, M.; Leniček, M.; Lacina, O.; Valášková, P.; Zapadlo, M.; Plavka, R.; Klán, P.; Vitek, L. A novel accurate LC-MS/MS method for quantitative determination of Z-lumirubin. *Sci. Rep.* **2020**, *10*, 4411. [CrossRef]
51. Nieminen, A.-L.; Gores, G.J.; Bond, J.M.; Imberti, R.; Herman, B.; Lemasters, J.J. A novel cytotoxicity screening assay using a multiwell fluorescence scanner. *Toxicol. Appl. Pharmacol.* **1992**, *115*, 147–155. [CrossRef]
52. Dengler, W.A.; Schulte, J.; Berger, D.P.; Mertelsmann, R.; Fiebig, H.H. Development of a propidium iodide fluorescence assay for proliferation and cytotoxicity assays. *Anticancer Drugs* **1995**, *6*, 522–532. [CrossRef] [PubMed]
53. Mosmann, T. Rapid colorimetric assay for cellular growth and survival: Application to proliferation and cytotoxicity assays. *J. Immunol. Methods* **1983**, *65*, 55–63. [CrossRef]
54. Ewing, J.F.; Janero, D.R. Microplate superoxide dismutase assay employing a nonenzymatic superoxide generator. *Anal. Biochem.* **1995**, *232*, 243–248. [CrossRef]

Publisher's Note: MDPI stays neutral with regard to jurisdictional claims in published maps and institutional affiliations.



© 2020 by the authors. Licensee MDPI, Basel, Switzerland. This article is an open access article distributed under the terms and conditions of the Creative Commons Attribution (CC BY) license (<http://creativecommons.org/licenses/by/4.0/>).



The Effects of Bilirubin and Lumirubin on Metabolic and Oxidative Stress Markers

Aleš Dvořák¹, Kateřina Pospíšilová¹, Kateřina Žižalová¹, Nikola Capková¹, Lucie Muchová¹, Marek Vecka^{1,2}, Nikola Vrzáčková³, Jana Křížová⁴, Jaroslav Zelenka³ and Libor Vitek^{1,2*}

¹Institute of Medical Biochemistry and Laboratory Diagnostics, Faculty General Hospital and 1st Faculty of Medicine, Charles University, Prague, Czechia, ²4th Department of Internal Medicine, Faculty General Hospital and 1st Faculty of Medicine, Charles University, Prague, Czechia, ³Department of Biochemistry and Microbiology, University of Chemistry and Technology, Prague, Czechia, ⁴Department of Paediatrics and Inherited Metabolic Disorders, 1st Faculty of Medicine, Charles University, Prague, Czechia

OPEN ACCESS

Edited by:

Jaime Kapitulnik,
Hebrew University of Jerusalem, Israel

Reviewed by:

Stephan Krähenbühl,
University of Basel, Switzerland
Sabina Passamonti,
University of Trieste, Italy

*Correspondence:

Libor Vitek
vitek@cesnef.cz

Specialty section:

This article was submitted to
Drug Metabolism and Transport,
a section of the journal
Frontiers in Pharmacology

Received: 29 May 2020

Accepted: 05 January 2021

Published: 04 March 2021

Citation:

Dvořák A, Pospíšilová K, Žižalová K,
Capková N, Muchová L, Vecka M,
Vrzáčková N, Křížová J, Zelenka J and
Vitek L (2021) The Effects of Bilirubin
and Lumirubin on Metabolic and
Oxidative Stress Markers.
Front. Pharmacol. 12:567001.
doi: 10.3389/fphar.2021.567001

For severe unconjugated hyperbilirubinemia the gold standard treatment is phototherapy with blue-green light, producing more polar photo-oxidation products, believed to be non-toxic. The aim of the present study was to compare the effects of bilirubin (BR) and lumirubin (LR), the major BR photo-oxidation product, on metabolic and oxidative stress markers. The biological activities of these pigments were investigated on several human and murine cell lines, with the focus on mitochondrial respiration, substrate metabolism, reactive oxygen species production, and the overall effects on cell viability. Compared to BR, LR was found to be much less toxic, while still maintaining a similar antioxidant capacity in the serum as well as suppressing activity leading to mitochondrial superoxide production. Nevertheless, due to its lower lipophilicity, LR was less efficient in preventing lipoperoxidation. The cytotoxicity of BR was affected by the cellular glycolytic reserve, most compromised in human hepatoblastoma HepG2 cells. The observed effects were correlated with changes in the production of tricarboxylic acid cycle metabolites. Both BR and LR modulated expression of PPAR α downstream effectors involved in lipid and glucose metabolism. Proinflammatory effects of BR, evidenced by increased expression of TNF α upon exposure to bacterial lipopolysaccharide, were observed in murine macrophage-like RAW 264.7 cells. Collectively, these data point to the biological effects of BR and its photo-oxidation products, which might have clinical relevance in phototherapy-treated hyperbilirubinemic neonates and adult patients.

Keywords: antioxidant, bilirubin, cell respiration, lumirubin, intracellular metabolite

Abbreviations: AOX, antioxidant capacity; BSA, bovine serum albumin; BR, bilirubin; DMSO, dimethyl sulphoxide; HSA, human serum albumin; LR, lumirubin; PT, phototherapy

INTRODUCTION

Bilirubin (BR) (Figure 1A), the major product of the heme catabolic pathway in the intravascular compartment, has been identified as a molecule of unique biological significance. Whereas in the past BR was merely considered as waste and a potentially neurotoxic product of heme catabolism, experimental as well as clinical research over the recent decades has convincingly proven its important antioxidant, anti-inflammatory, and other positive biological effects (Wagner et al., 2015).

Thus, mild hyperbilirubinemia exhibits protective effects against various chronic diseases mediated by increased oxidative stress (Wagner et al., 2015). Long-term, mildly elevated BR concentrations protect mitochondria and the respiratory chain, with a concomitant decrease of reactive oxygen species (ROS) and pro-inflammatory cytokine production (Zelenka et al., 2016); these observations are consistent with our previous *in vitro* and *in vivo* data, further demonstrating the anti-inflammatory effects of BR (Valaskova et al., 2019). This data are also in line with recent observations on beneficial effects of BR on metabolic pathways implicated in pathogenesis of diabetes, metabolic syndrome and obesity (Stec et al., 2016; Hinds and Stec, 2019) proposing BR as a signaling molecule with “real” endocrine activities (Hinds and Stec, 2018; Vitek, 2020). These pathways include those activated by PPARA (Stec et al., 2016; Hinds and Stec, 2018; Hinds and Stec, 2019), although signaling pathways activated by other nuclear as well as cytoplasmic receptors are likely to contribute as well (Vitek, 2020).

On the other hand, BR virtually behaves as a yin/yang molecule, being beneficial when only mildly elevated, while harmful when overcoming a safe threshold (Wagner et al., 2015). In fact, due to its lipophilic nature BR binds to myelin-rich membranes, insulating neurons and consequently affecting their function (Watchko and Tiribelli, 2013). BR-induced changes in the CNS are multifactorial, with extensive impacts on the brain compartment, inflammatory status, morphology, and are followed by cognitive dysfunction (Dal Ben et al., 2017). In cultured rat neurons, BR causes DNA fragmentation (Grojean et al., 2000), decreases respiration, changes both membrane potential and permeability, releases cytochrome c from the mitochondria to cytosol, and initiates apoptosis via caspase 3 (Rodríguez et al., 2002). Similar effects, including suppression of respiration followed by mitochondrial swelling leading to apoptosis, were observed in other cell types as well (Mustafa et al., 1969; Noir et al., 1972; Almeida and Rezende, 1981).

To some extent, neonatal jaundice is believed to play a protective role against increased oxidative stress (Hegyi et al., 1994; Shekeeb et al., 2008; Hansen et al., 2018). However, a serum BR concentration above 340 $\mu\text{mol/L}$ is potentially dangerous for neonates with a high risk of BR neurotoxicity (Hyperbilirubinemia, 2004). The gold standard treatment for severe newborn jaundice is phototherapy (PT), which is generally considered a safe therapeutic method (AAP Subcommittee on Hyperbilirubinemia, 2004). During blue-green light PT (400–520 nm), BR is converted to photo-

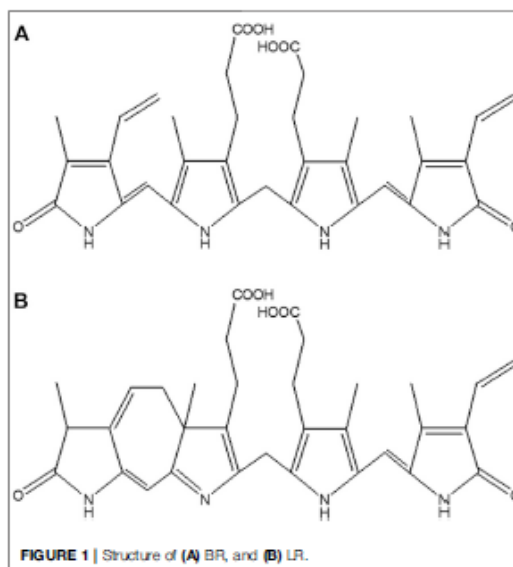


FIGURE 1 | Structure of (A) BR, and (B) LR.

oxidation products that can be more effectively excreted into the urine and/or bile (McDonagh and Palma, 1980; Onishi et al., 1981; Lightner et al., 1984; Maisels and McDonagh, 2008). These products include, among others, BR photoisomers *Z,E*-BR IXa, *E,Z*-BR IXa, *Z*-lumirubin (LR) (Figure 1B), as well as monopyrrolic (BOX A and BOX B), dipyrrolic (propentdyopents) and tripyrrolic (biopyrrolin A and biopyrrolin B) oxidation products (Jašprová et al., 2018). Surprisingly, the biological properties of BR photoisomers and oxidation products are only poorly understood, primarily because of the absence of commercial standards for BR photoisomers.

Nevertheless, the metabolism of BR photoisomers seems to have clinical importance. Although PT is an effective, non-invasive, and relatively safe therapeutic method, accompanying potential side effects of the treatment are known in clinical practice, including: hypocalcemia (Khan et al., 2016), dehydration (Xiong et al., 2011), ileus (Raghavan et al., 2005), type 1 diabetes (Mcnamee et al., 2012), allergies (Safar and Elsary, 2020), increased incidence of cancer at advanced age (Auger et al., 2019), and even increased mortality of extremely low birth-weight infants (Arnold et al., 2014).

Hence, the aim of the present study was to investigate the biological properties of LR, the most abundant BR photoisomer, in order to account for some of the clinical observations in PT-treated neonates. So far, the intracellular metabolic impact of BR photoisomers has never been properly investigated, although our previous data suggest their biological importance (Jašprová et al., 2016; Jašprová et al., 2018). Therefore, we had aimed to study the *in vitro* effects of BR and LR on redox homeostasis and energy substrate metabolism.

MATERIALS AND METHODS

Chemicals

All chemicals and cell culture reagents were obtained from Sigma-Aldrich (MO, United States) unless otherwise specified. Commercial BR was purified as previously described (McDonagh and Assisi, 1972) and diluted in DMSO or a stoichiometric concentration of bovine serum albumin (BSA) in PBS (Jašprová et al., 2018). BR stock solution (10 mmol/L in DMSO) was divided into aliquots and stored at -20°C to prevent degradation from repeated thawing. LR was isolated from the irradiated BR solution (BR was dissolved in a rabbit serum albumin solution) as previously described (Jašprova et al., 2020). For PPAR α activity experiments, BR was dissolved using serum/albumin-free conditions (see below). The LR was dissolved in PBS with the concentrations measured spectrophotometrically (TECAN Infinite M200, Switzerland). LR stock solution (1 mmol/L) was divided into aliquots and stored at -20°C .

Cell Cultures

Human neuroblastoma SH-SY5Y cells, hepatoblastoma HepG2 cells, murine macrophage-like RAW 264.7 cells, and fibroblast-like MRC5 cells from normal lung tissue were all purchased from the American Type Culture Collection (ATCC, VA, United States). HepG2, SH-SY5Y, and MRC5 were cultured in Minimum Essential Medium (MEM; Biosera, France) with 5 mmol/L glucose, and supplemented with both 2 mmol/L glutamine, 10% fetal bovine serum (FBS; Biosera), as well as with 1% non-essential amino acids (Biosera) in a normoxic CO_2 chamber at 37°C in a humidified atmosphere. RAW 264.7 cells were cultured in Dulbecco's Modified Eagle's Medium (DMEM with 4,500 mg/L glucose, L-glutamine, and sodium bicarbonate) with 10% FBS.

The medium was replaced 24–48 h prior, starting the experiments with fresh medium containing LR and BR in a final concentration of 5, 25, or 50 $\mu\text{mol/L}$ (control samples were treated by medium containing an adequate volume of LR/BR solvents; final concentration of DMSO = 0.5% v/v, concentration of BSA in FBS = 2.5 g/L (Soutar et al., 2019)). Thus, the respective concentrations of Bf (Bilirubin free, unbound, biologically active fraction of bilirubin) corresponded to non-toxic, borderline toxic and toxic concentrations, respectively (Roca et al., 2006; Zelenka et al., 2012). On the day of the experiment, the control cell culture reached a confluence of 80–90%.

GC-MS Analysis of Intracellular Metabolites of the Tricarboxylic Acid Cycle

The cell samples (pellets washed with PBS) with an internal standard (IS, oxalate) were extracted with water/methanol/chloroform (1:1:2, v/v/v) and centrifuged at $1,000 \times g$ for 10 min. The upper polar phase was transferred into a glass vial and lyophilized. The analytes were derivatized with pyridine/*N*,*O*-bis(trimethylsilyl)acetamide/chlorotrimethylsilane (8:4:2, v/v/v) at 65°C for 75 min. Derivatized samples were injected directly into a gas chromatograph - mass spectrometer (GC-MS, GC 6890N, MD 5973, Agilent Technologies, CA,

United States) (Dvorak et al., 2017). The analyte amount was normalized to the IS and the cell count and calculated as a % of the control.

High Resolution Respirometry

Cells pretreated for 24 h with BR/LR or their solvents were harvested and re-suspended in an adequate fresh medium (with BR/LR or their solvents) before measurement. The oxygen consumption of living cells was measured at 37°C using an Oxygraph-2k (Oroboros Instruments GmbH, Austria) in a 2 ml chamber in a MEM-based medium. The protein load reached roughly 3–15 mg/chamber, depending on the cell type. After air calibration and equilibration, the following inhibitors and uncoupler were used (SUIT-003 protocol): oligomycin (2.75 $\mu\text{mol/L}$), FCCP (6 $\mu\text{mol/L}$) (at least a 2-step titration), rotenone (0.2 $\mu\text{mol/L}$), and antimycin A (5 $\mu\text{mol/L}$). All respiratory parameters were analyzed in Datlab 7.4.0.4 software (Oroboros Instruments), and were expressed in pmol $\text{O}_2/\text{s}/\text{mg}$ protein (Smolkova et al., 2015).

The same procedure was used for experiments in serum-free medium. As recently reported, BR may affect PPAR α expression and modify cell respiration and lipid metabolism (Gordon et al., 2020), but unsaturated fatty acids or their derivatives from FBS may compete with BR in active site (ligand-binding pocket) of specific nuclear receptors (Stec et al., 2016). Hence, in specific experiments FBS in medium was replaced by fatty acid free-BSA (to avoid the BR precipitation) 24 h before experiments. BSA was dissolved in PBS (43 g/L) and BSA solution was added to the FBS-free medium to a final concentration of BSA = 4.3 g/L (10% v/v).

ATP Production

ATP amount was measured in cells exposed to a medium with glucose (normal phenotype) or galactose containing 25 $\mu\text{mol/L}$ BR. Galactose in medium was selected to mimic starving leading to increase in the cell respiration, since decrease of ATP production by glycolysis must be compensated by increased oxidative phosphorylation.

The CellTiter-Glo Luminescent Cell Viability Assay (Promega Corporation, WI, United States) was used to determine ATP amount in the HepG2, MRC5 and SHSY5Y cells after BR treatment in substrate-specific conditions (galactose/glucose). For determination, MEM culture medium was replaced by DMEM-based medium 24 h before experiment (components were made to order and prepared by Institute of Molecular Genetics of the Czech Academy of Sciences). Experimental medium contained DMEM, 10% FBS, 1% Penicillin-Streptomycin, glutamine (2 mmol/L), glucose (5 mmol/L) or galactose (5 mmol/L), NaHCO_3 (1.5 g/L) and BR (25 $\mu\text{mol/L}$) or respective solvent. To perform the assay, CellTiter-Glo reagent was prepared by reconstituting the lyophilized CellTiter-Glo substrate in the CellTiter-Glo buffer according to manufacturer's instructions. Before the measurement the cells were washed with 100 μL of fresh medium to avoid artificial ATP detection from disrupted cells. Equivalent amount of the reagent was added to each sample and the signal was measured by a luminometer (Synergy/HT Microplate Reader, Biotek Instruments, Inc., VT, United States) at 22°C within 0, 5 and

10 min. The ATP concentration was normalized to the protein concentration measured immediately after luminometric analysis. The 96-well plate was divided in half and first part was used for luminometric method, whereas the second for the protein determination (treatment, seeding and time management were comparable). The wells were washed by PBS, and the lysis buffer (Buffer LYSIS LR, Biotechrabbit GmbH, Germany) was added, then the plate was vigorously shaken for 30 min on ice and the lysates were measured by Nanodrop (DS-11+ Spectrophotometer, DeNOVIX Inc., DE, United States) at 280 nm.

Determination of Mitochondrial Superoxide Production

Superoxide production in live cells was detected using MitoSOX dye (Life Technologies, CA, United States). The cell suspension was stained for 15 min in a complete medium, then the sample was centrifuged ($250 \times G$, 5 min); then the medium was removed and the pellet re-suspended in PBS. Fluorescence of the stained cells was measured by a flow cytometer (Mindray, BriCyte E6, China) every minute (0–15 min; 10,000 events/minute), and the change in proportion of superoxide-producing cells upon various treatments was monitored. The slope of fluorescence change, reflecting the production of superoxide in real time, was calculated. Rotenone (10 μM) was used as a positive control of the increased superoxide production in the treated cells (Zelenka et al., 2016).

MTT Viability Test

The viability of cells exposed for 24 and 48 h to LR and BR was measured using the MTT test as previously described (Jašprová et al., 2018).

Determination of Lipoperoxidation

The degree of lipoperoxidation was determined by a modified method, as previously described (Vreman et al., 1998). In brief, rat brain tissue (stored at -80°C until analysis) was diced, diluted 1:9 (w/w) in a phosphate buffer and sonicated. Next, 20 μl of this suspension was added to carbon monoxide (CO)-free vials together with 1 μl of LR or BR (with a final concentration range of 1–50 μM). The LR was dissolved in PBS or BSA, and the BR was dissolved in DMSO or BSA; while the pure solvents served as control samples. The Fenton reaction was initiated by a ferrous salt-ascorbate system injected across the airtight cap. Samples were incubated for 30 min at 37°C , and then the reaction was stopped by 10 μl of 60% (w/v) sulfosalicylic acid, then the samples were incubated for 30 min on ice. CO released into the vial headspace was quantified by gas chromatography (GC-RGD Peak Performer 1, Peak Laboratories, CA, United States), and reflected the lipoperoxidation rate.

Determination of Serum Peroxyl Radical Scavenging Capacity

The serum peroxyl radical scavenging capacity (AOX, antioxidant capacity) was determined using a fluorimetric method, as the

relative proportion of chain breaking antioxidant consumption present in the serum compared to that of Trolox (a reference and calibration antioxidant compound) (McDonagh and Assisi, 1972). The samples (human serum of healthy volunteer mixed with BR or LR; then LR, BR and Trolox dissolved in HSA, and also degraded LR dissolved in PBS measured after 6 and 24 h after dissolution) were measured using a 96-well plate. Forty μl of dipyrindamol (dissolved in DMSO and diluted to 2.5 $\mu\text{mol/l}$ in PBS), 40 μl of sample (2.5, 5, 25 and 50 $\mu\text{mol/L}$ BR/LR) and 20 μl of 2,2'-azobis(2-methylpropionamide) dihydrochloride (100 mmol/L) were added into the reaction well and fluorescence (Ex. 415 nm, Em. 480 nm) was measured immediately. Total time of analysis was 2 h, fluorescence was measured every 2 min (plate was shaken periodically before each scan). For all samples, the time to fluorescence quenching was evaluated and was compared to respective control samples.

Determination of the Glycolytic Reserve

The glycolytic reserve of the cells (SH-SY5Y, HepG2, and MRC5) was measured using a Seahorse XF24 Analyzer (Agilent Technologies), with a combination of two standard Agilent protocols (the Mito Stress and Glycolysis Stress tests). The combination of both protocols made it possible to check if the cells were respiring normally.

To improve cell adherence, the plate was coated with poly-L-lysine (100 μl of 0.01% solution per well). One day before the experiment, the cells were seeded by adding 100 μl of suspension (at density of 500,000 cells/mL for HepG2 cells, and 750,000 cells/mL for MRC-5 and SH-SY5Y). The plate with cells was left overnight in a humidified incubator supplemented with 5% CO_2 at 37°C .

Assay medium preparation: D5030 DMEM assay medium was diluted in sterile water according to the manufacturer's instructions, the pH was adjusted to 7.4 with NaOH, and then the solution was made to make the accurate volume. Then, the DMEM solution (99 ml) was mixed with 1 ml of L-glutamine (water stock solution, 200 mmol/L). The assay medium was heated to 37°C and the pH was checked. This medium was used for preparation of the stressor compounds. Stock solutions were prepared as 10x concentrated (glucose 50 mmol/L, oligomycin 20 $\mu\text{mol/L}$, FCCP 5 $\mu\text{mol/L}$, rotenone 20 $\mu\text{mol/L}$, antimycin A 10 $\mu\text{mol/L}$, 2-deoxyglucose 0.5 mol/L).

On the day of the experiment, the cell culture medium in a 24-well plate was removed and changed for 100 μl of the assay medium. The plate was placed in a humidified, temperature-controlled (37°C) incubator without CO_2 atmosphere for 45–60 min for degassing, while the sensor cartridge was hydrated by loading of the stressor mix into every port A-D (A: 50 μl of glucose, B: 55 μl of oligomycin, C: 61 μl of FCCP, and D: 67 μl of 2-deoxyglucose, rotenone, and antimycin A).

The glycolytic capacity and reserve were evaluated as the difference of the extracellular acidification rate (ECAR) under conditions in the presence of oligomycin and glucose.

Determination of Nitric Oxide Production

Production of nitric oxide (NO) was measured in the media by determination of nitrite concentration using the Griess reagent.

Cells seeded in 96 wells were cultured in colorless medium and mixed with LR or BR (5 or 25 $\mu\text{mol/L}$), with or without lipopolysaccharide (LPS; 1 $\mu\text{g/ml}$), 24 h before measurement. Eighty μL of medium from each well were mixed with 80 μL of Griess solution (0.04 g/ml), and absorbance at 540 nm was measured by an iMark Microplate Reader.

Quantitative Real-Time PCR

Total RNA was extracted using a GenUP Total RNA Kit (BiotechRabbit, Germany), and complementary DNA (cDNA) was synthesized with a High Capacity cDNA Reverse Transcription Kit (Applied Biosystems, CA, United States). Amplification of the target genes was performed on a ViiA 7 instrument (Applied Biosystems) in 10- μL reaction volumes, containing 4.5 μL of 10-fold diluted cDNA template from a completed reverse transcription reaction, TaqMan™ Fast Advanced Master Mix (Applied Biosystems) and TaqMan™ Gene Expression Assay (Mm00443260_g1 TNF α ; Mm01545399_m1 HPRT, Hs00947536_m1 PPAR α , Hs99999909_m1 human HPRT, Hs00354519_m1 CD36, Hs00173927_m1 FGF21, Hs00912671_m1 CPT1A, Hs01037712_m1 PDK4, Hs01101123_g1 ANGPTL4, Hs01005622_m1 FASN; Applied Biosystems). The temperature profile was: 2' 50°C, 92°C 10' 40x (1" 95°C, 20" 60°C). The relative quantification was made by the 2- $\Delta\Delta\text{Ct}$ method with HPRT as a housekeeping gene.

For TNF α mRNA expression the murine macrophage-like RAW 264.7 cells were seeded in 6-well plates and incubated for 24 h with 5 and 25 $\mu\text{mol/L}$ BR or LR. To assess the effect of LPS on TNF α expression, the cells were incubated for the last hour with 50 ng/ml of LPS. Then the cells were washed with PBS and collected in a lysis buffer (Buffer LYSIS LR, BiotechRabbit GmbH, Germany).

For PPAR α and its downstream effector gene mRNA expressions (FASN, CPT1A, FGF21, PDK4, ANGPTL4 and CD36, (Rakshandehroo et al., 2010)), the HepG2 cells were seeded in 12-well plates. The medium was replaced by the fresh serum-free medium for 24 h, then BR, LR or solvent was added. After 0.5, 1, 2, 4, 6 and 24 h, the cells were washed with PBS and collected as described above. To maintain serum and albumin-free conditions in these experiments, BR was dissolved in 0.1 M NaOH, neutralized by 0.1 M H₃PO₄ and buffered by PBS (0.01 M, pH 8.0, added in large excess). Final concentration of BR stock solution was 480 μM . LR was dissolved directly by PBS used for final step of BR solution preparation. Final concentration of BR/LR in medium was 25 μM .

TNF α and FGF21 Protein Quantification

Concentrations of TNF α were measured in culture media (50 μL) removed from the murine cells RAW 264.7, incubated for 24 h with or without BR or LR (5 and 25 $\mu\text{mol/L}$), using a specific TNF α Mouse ELISA Kit (Thermo Fisher Scientific) according to the manufacturer's instructions. For TNF α expression with LPS, 50 ng/ml of LPS were added into the medium 4 h before the end of a 24 h incubation.

Concentration of fibroblast growth factor (FGF) 21 was measured in culture media (50 μL) removed from the HepG2, incubated for 48 h in serum-free media with or without BR or LR

15 $\mu\text{mol/L}$), using a specific Quantikine ELISA Human FGF-21 Immunoassay kit (R&D Systems, United Kingdom) according to the manufacturer's instructions. TNF α and FGF21 concentrations were measured in triplicates from individual wells on a microplate reader (TECAN Infinite M200). The concentrations were expressed in pg/mL. Due to increased toxicity of BR on HepG2 cells cultured in serum-free media, BR was used in concentration of 15 $\mu\text{mol/L}$ and the concentrations of FGF21 in media were related to g of the cell lysate protein.

Stability of LR and BR

The culture medium as well as the human serum of a healthy volunteer were mixed with LR and BR to a final concentration of 10 $\mu\text{mol/L}$. Both solutions (medium and serum) were incubated for 6 h in a CO₂ incubator (humidified atmosphere, 37°C, 5% CO₂). Spiked medium or serum (10 μL) were collected every h (0–6 h) and then immediately frozen at –80°C until the pre-analytical extraction. With the use of other solvents, the same procedure was performed for the evaluation of LR stability. The culture medium was used for hypoxic treatment as well (samples were collected in both normoxic and hypoxic conditions simultaneously). A special hypoxic box (OxyCycler GT4181CN, BioSpherix, NY, United States) within the CO₂ incubator was used for the experiments. The atmosphere was controlled by OxyCycler software, with the low oxygen volume compensated for by nitrogen. Gases certified for tissue culture experiments were used (Air Products, Czech Republic).

LC-MS/MS Analysis of LR and BR

Ten μL of liquid samples were spiked with 10 μL of IS (mesobilirubin, $c = 5 \mu\text{mol/L}$) (Frontier Scientific, UT, United States). The extraction was performed with 1 ml of basic methanol. The samples were vigorously shaken and vortexed, and then the mixture was centrifuged (16,000 \times G, 30 min). Next, 100 μL of supernatant were pipetted into glass vials with an inert insert (suitable for LC-MS analysis), and 3 μL were directly injected into the LC-MS/MS.

LC-MS/MS analysis was performed using an HPLC (Dionex Ultimate 3000, Dionex Softron GmbH, Germany) equipped with a Poroshell 120 EC-C18 column (2.1 μm , 3.0 \times 100 mm; Agilent Technologies). For the gradient elution, the phase was prepared by mixing 1 mmol/L of NH₄F (Honeywell, International Inc., Morris Plains, NJ, United States) in water and methanol (Biosolve Chimie SARL, France). The analytes were detected by MS (TSQ Quantum Access Max with HESI-II probe, ThermoFisher Scientific, CA, United States) operated in a positive SRM mode (Jašprová et al., 2020).

Detection of LR Oxidation Fragments

Samples of LR fragments (decay products) were obtained by the spontaneous degradation of LR dissolved in PBS (humidified atmosphere, 37°C, 5% CO₂, overnight incubation). The fragments were determined by direct injection of deproteinated samples into the MS.

The MS was set to scan parent ions in the 100–1,050 m/z range, with a 1 s scanning period. The initial tuning of the heated

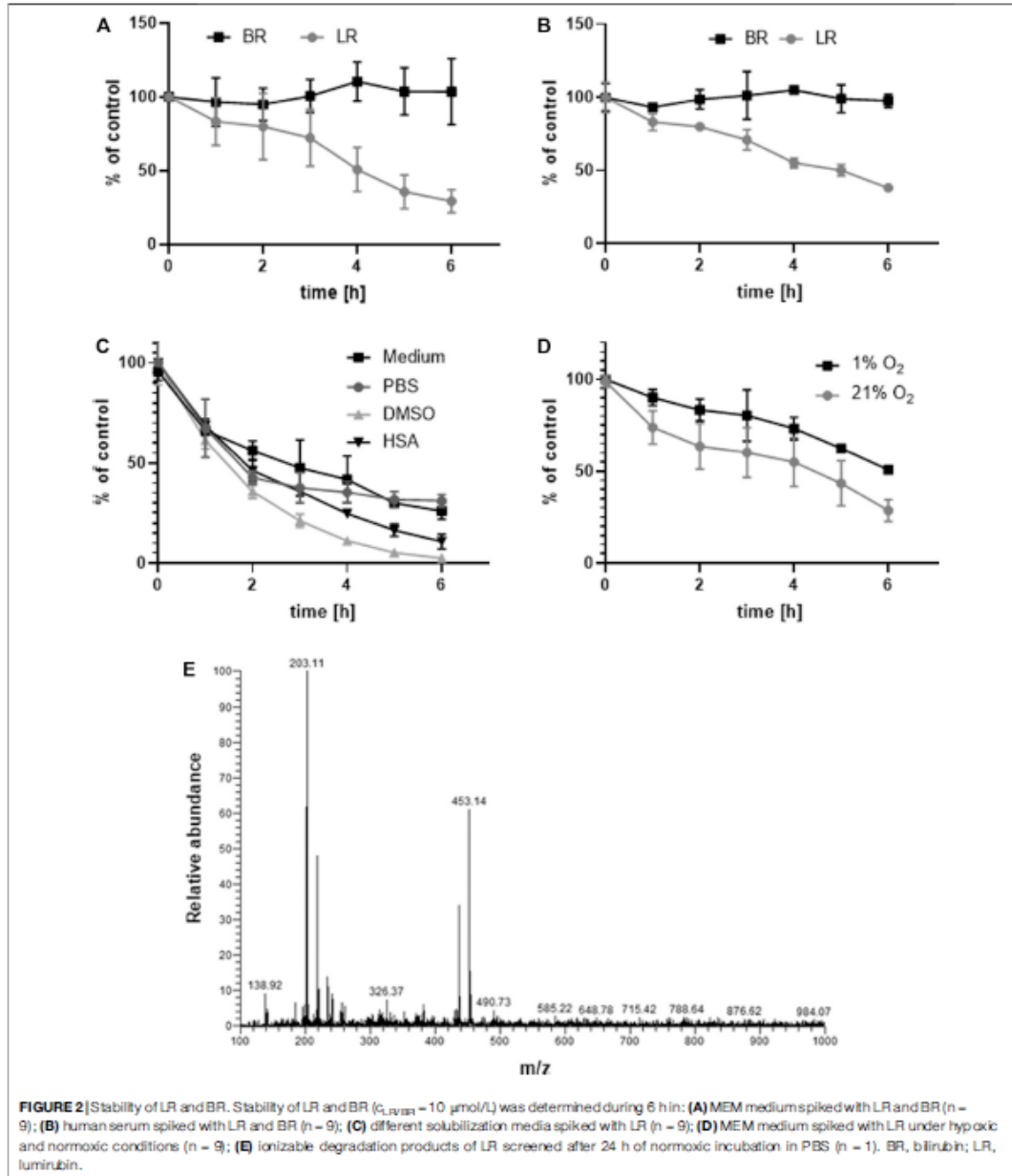


FIGURE 2 | Stability of LR and BR. Stability of LR and BR ($c_{LR/BR} = 10 \mu\text{mol/L}$) was determined during 6 h in: **(A)** MEM medium spiked with LR and BR ($n = 9$); **(B)** human serum spiked with LR and BR ($n = 9$); **(C)** different solubilization media spiked with LR ($n = 9$); **(D)** MEM medium spiked with LR under hypoxic and normoxic conditions ($n = 9$); **(E)** ionizable degradation products of LR screened after 24 h of normoxic incubation in PBS ($n = 1$). BR, bilirubin; LR, luminubin.

HESI-II probe was performed according to a previously published paper of LR analysis (Jašprová et al., 2020). Further tuning of MS/MS transitions, derived from the most intensive parent ions, was performed by the combined infusion of the analytes (10 mg/L in

the mobile phase, 20 $\mu\text{L}/\text{min}$) and the mobile phase (400 $\mu\text{L}/\text{min}$); the collision gas (Ar) pressure was set to 0.2 Pa.

Mono-, di-, and tri-pyrroles similarity was identified according to the described structures of known compounds

(e.g., monopyrrolic BOXes, propentdyopents, and biopyrins). Fragmentation of tetrapyrroles as well as their ionization in MS were taken into account for in molecular weight estimations (assuming the charge number = 1).

Statistical Analyses

The data are expressed as the mean \pm SD. Depending on data normality, differences among variables were evaluated by the one-way ANOVA, Mann-Whitney Rank Sum test and Student unpaired *t*-test. Differences were considered statistically significant at $p < 0.05$. Statistical analyses were performed using Prism 8.0.1 software (GraphPad, CA, United States).

RESULTS

Stability of LR and BR

The stability of LR and BR in the relevant biological matrices were tested before any experiments with the biological samples. LR and BR concentrations were measured in samples of a standard medium (Figure 2A) and human serum (Figure 2B) spiked with LR and BR during 6-h incubation at 37°C in a CO₂ atmosphere. The relatively fast degradation of LR was observed in both matrices. The half-life of LR was approximately 4 h; the remaining LR level after the 6 h-experiment was 29.3% and 38.2% in medium and serum, respectively. In contrast, BR was stable during the entire experiment. The half-life of LR was similar when using other solubilizing media (the rate of degradation in DMSO and PBS was comparable to that in MEM medium, even though the degradation curves were not identical; Figure 2C).

LR stability was also tested under different oxygen conditions (normoxia 21% O₂ and hypoxia 1% O₂) (Figure 2D). The presence of oxygen contributed to LR degradation beginning only 2 h after the start of incubation. The rate of degradation during the first 2 h was much faster under normoxic conditions (LR reduction: 8% per h in hypoxia, 17.5% per h in normoxia). After an additional 2–6 h, the same trend and rate of LR degradation was observed (LR reduction: 10% per h in hypoxia, 10.5% per h in normoxia) (Figure 2D). These results suggest that higher oxygen concentration can trigger LR degradation.

After 24 h of normoxic incubation of LR, degradation LR products were monitored with LC-MS/MS using a TIC scan between *m/z* 100–1,050. Two dominant (with *m/z* 203.1 and 453.1) and one less intensive (*m/z* 326.4) ions were observed in a MS scan of the PBS solution extract (Figure 2E). These are highly likely to be derived from mono-, di- and tripyrrolic structures (Lightner and Quistad, 1972; Yamaguchi et al., 1994; Seidel et al., 2014).

The Effect of LR and BR on Cell Viability

The effect of LR and BR on cell viability (SH-SY5Y neuroblastoma, HepG2 hepatoblastoma, and MRC5 lung fibroblasts cells) was measured by MTT test after 24 and 48 h-treatments with different concentrations of LR and BR. Whereas LR had no effect on the viability of any tested cells, BR

concentrations negatively correlated with cell viability of all cell lines (Figure 3). A significant time- and concentration-dependent decreases in cell viability were observed after incubation with BR ($p < 0.001$ for almost all of the BR concentrations used, Figure 3); with HepG2 cells being the most sensitive to BR, most likely due to having the lowest glycolytic reserve (see below).

Antioxidant Capacity of LR and BR

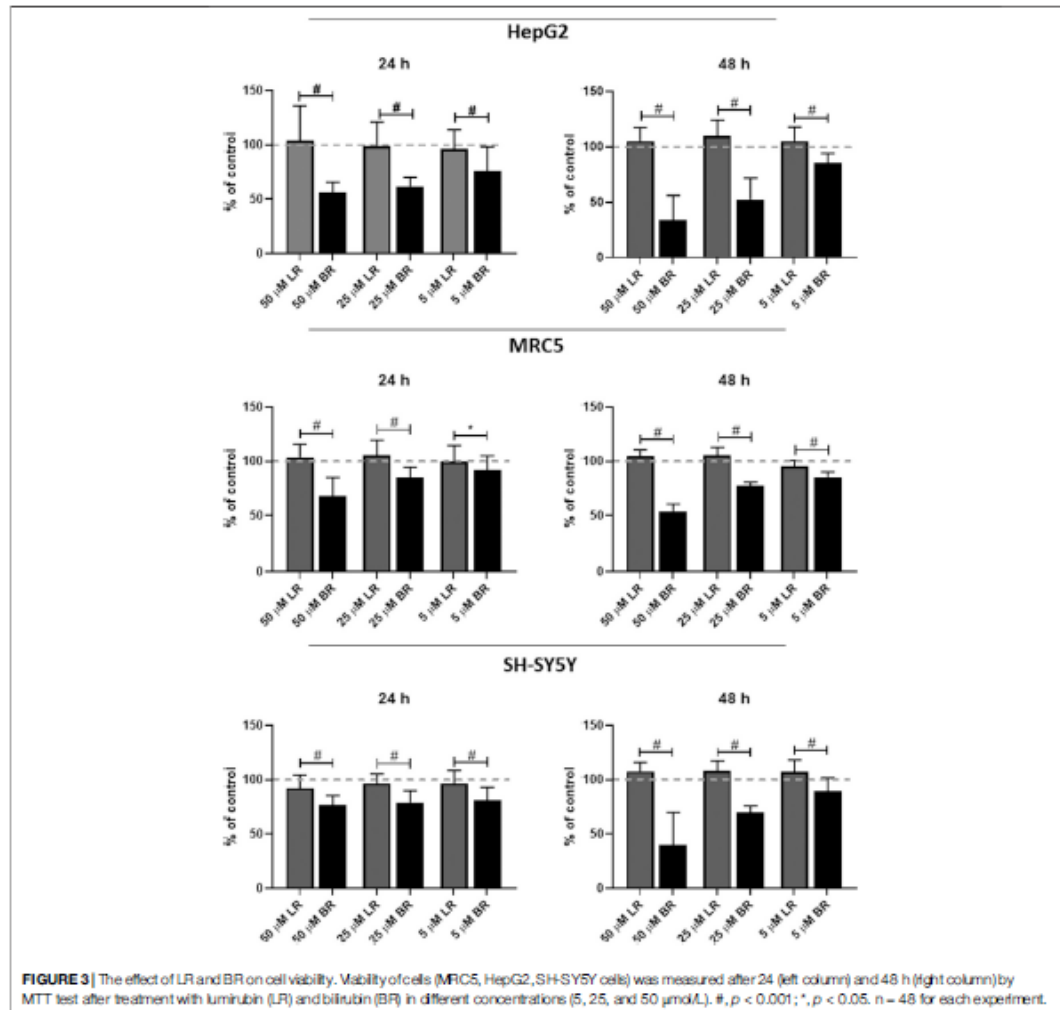
In the next step, the AOX of LR and BR was tested in different biological matrices. First, we tested the capability of BR and LR to scavenge peroxy radicals in human serum. BR and LR were added to the serum in increasing concentrations (2.5, 5, 25, and 50 $\mu\text{mol/L}$), which correlated well with the AOX of spiked serum (Figure 4A). Interestingly, LR had the same AOX as BR (Figure 4B) despite its degradation (Figure 4C). This observation was subsequently confirmed in the solution of human serum albumin (HSA) where both tetrapyrroles were compared to Trolox. The AOX of this vitamin E analogue was half that of BR and LR in the same concentration (5 $\mu\text{mol/L}$), respectively (Figure 4B). Because of the instability of LR (Figure 2C), the AOX of LR solutions with its spontaneous degradation was also tested. The AOX of LR solution decreased after 6 h to approximately 80% of the initial value (Figure 4C, $p < 0.05$), although the drop in LR concentrations reached 30% (Figure 2C). Even more interestingly, the decrease of AOX after 24 h reached approximately 50% of the initial value ($p < 0.001$, the data similar to that of Trolox from Figure 4B); although virtually no LR could be detected in the system (data not shown). This observation was suggestive of the antioxidant activity of the LR degradation products detected in our studies (Figure 2E).

Finally, the rate of lipoperoxidation (LPX) was measured in lipid-rich tissue (rat brain tissue). BR and LR were added to the matrix under different conditions. In the first set of experiments, LR was dissolved in PBS and BR in DMSO (Figure 4D); while in the other experiments, both tetrapyrroles were dissolved in BSA (Figure 4E). Surprisingly, a higher AOX of both compounds were observed in non-albumin solutions (Figures 4D,E). Compared to BR, LR was much less efficient in protecting lipid-rich cell homogenates from peroxidation, although still exerting a biologically relevant AOX (Figures 4D,E).

The Effect of LR and BR on Superoxide Production

Production of mitochondrial superoxide was measured using a mitochondrial specific fluorescent probe MitoSOX, with two concentrations of LR and BR (5 and 25 $\mu\text{mol/L}$). Higher concentrations of BR (50 $\mu\text{mol/L}$) were too apoptotic, and cell debris interfered with determination of mitochondrial superoxide.

After overnight pretreatment, both LR and BR were almost equally capable of the scavenging of mitochondrial superoxide in a concentration-dependent manner (Figure 5). In HepG2 and



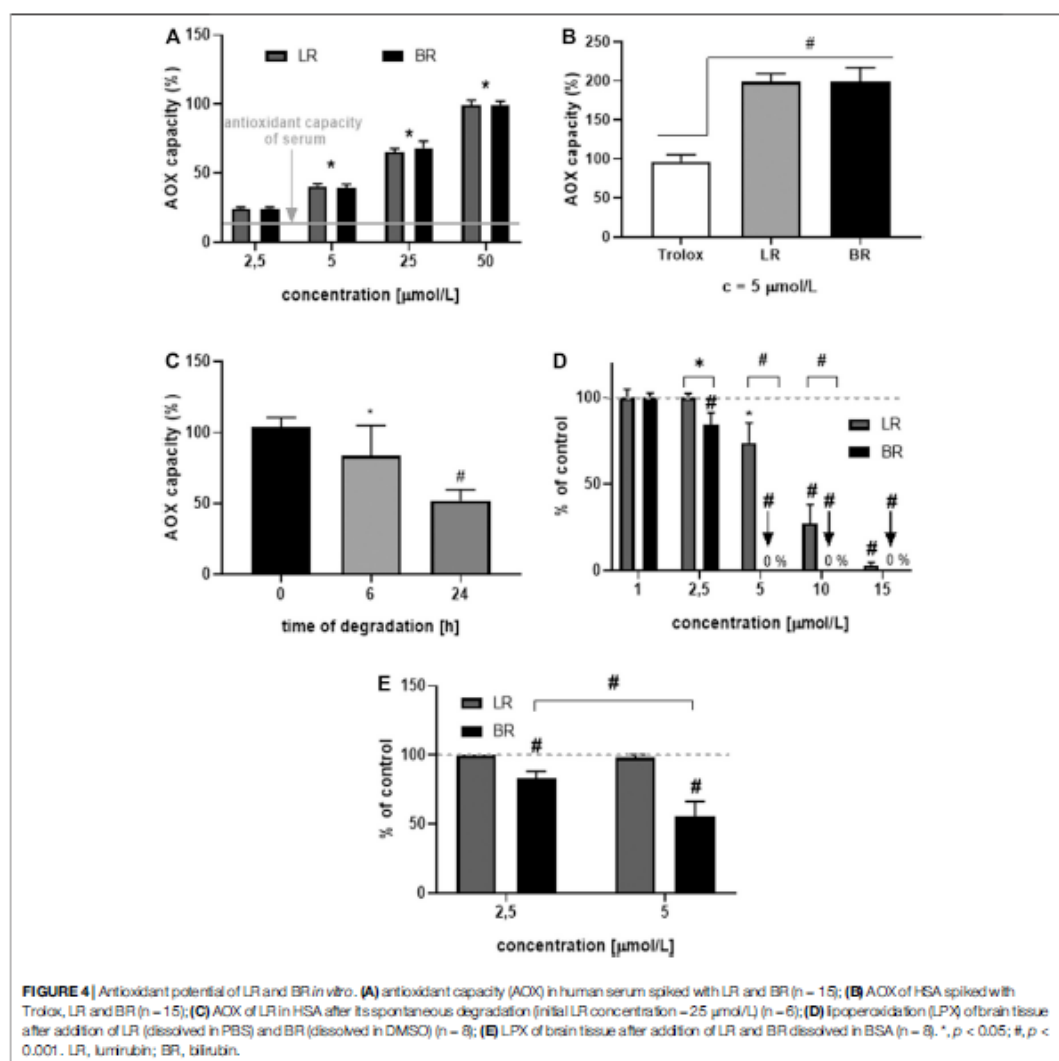
SH-SY5Y cells, only the higher concentrations of LR or BR caused a significant drop in superoxide production (Figures 5A,B); while in MRC5 cells, even the lower concentrations were significantly efficient (Figure 5C).

The Effect of LR and BR on Mitochondrial Respiration

Since both pigments inhibited mitochondrial superoxide production, and previous studies had demonstrated an inhibitory role of BR on mitochondrial respiration (Mustafa et al., 1969; Noir et al., 1972; Almeida and Rezende, 1981;

Rodrigues et al., 2002), we were thus interested in the effects of LR and BR on mitochondrial respiration in our cell models.

Cell respiration was measured in all cell lines after overnight incubation with BR and LR in two different concentrations (5 and 25 μmol/L) (Figures 6A–C). Practically no changes in respiration were observed in any of the studied cells, except for the higher BR concentration (25 μmol/L), which decreased both basal as well as maximal respiration in all cell lines (Figures 6A–C). Substantial inhibition of respiration was observed under serum-free conditions, in particular in the cells of hepatic and cerebral origin; BR/LR treatment did not affect respiration in these specific conditions (Figures 6A–C).

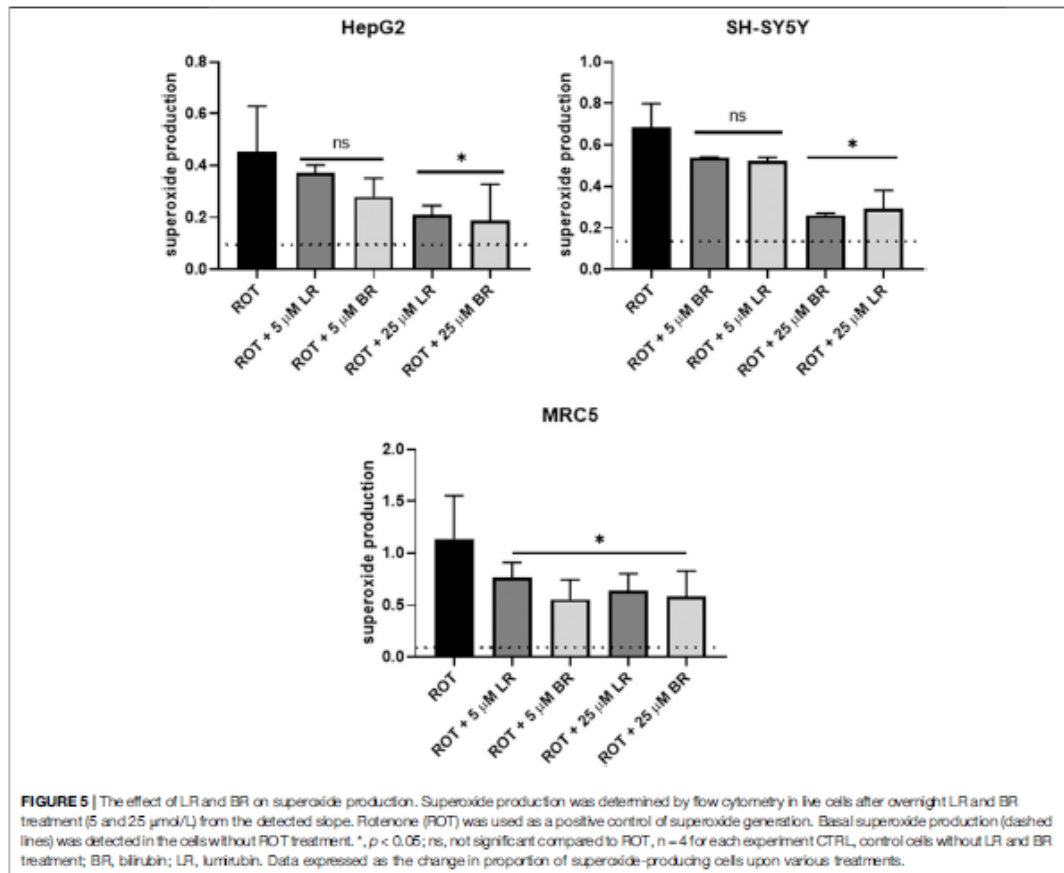


The ratio of maximal to endogenous (basal) respiration, corresponding to the respiratory capacity (Brand and Nicholls, 2011), was different for each cell line ± 4 for MRC5; ± 2.8 for HepG2; ± 1.8 for SH-SY5Y; with no significant changes between the controls and treated cells (Figure 6D). Serum-free conditions did not affect the ratio of maximal to basal respiration (Figure 6D).

The ATP-synthesis intensity was calculated as the ratio of basal (endogenous) respiration to respiration after inhibition of ATP-synthase with oligomycin. The values of the ATP-synthesis intensity under studied conditions did not differ (Figure 6E),

suggesting that ATP-synthesis (or ATP-synthase involvement) is proportional to the reduction of maximal and basal respiration. Insignificant changes of both ratios between the control and cells treated with BR and LR indicated an overall depression of mitochondrial respiration with higher concentrations of BR, but not with LR.

Finally, the glycolytic reserve of tested cell lines (without BR/LR treatment) was determined. The data demonstrate the highest glycolytic reserve in SH-SY5Y cells, whereas the lowest values were observed in HepG2 (Figure 6F). Interestingly, ATP production was not improved when glucose was exchanged for



galactose; instead, it was further substantially decreased in the galactose medium in HepG2 cells, while only mild or no effects were observed in SH-SY5Y and MRC5 cells (Figure 7).

These results negatively correlated with the viability data, where the highest vulnerability was observed in HepG2 cells; contrasting with the lowest values observed in SH-SY5Y cells (Figure 3).

The Effect of LR and BR on PPAR α and its Downstream Effector Gene Expressions, and FGF21 Production

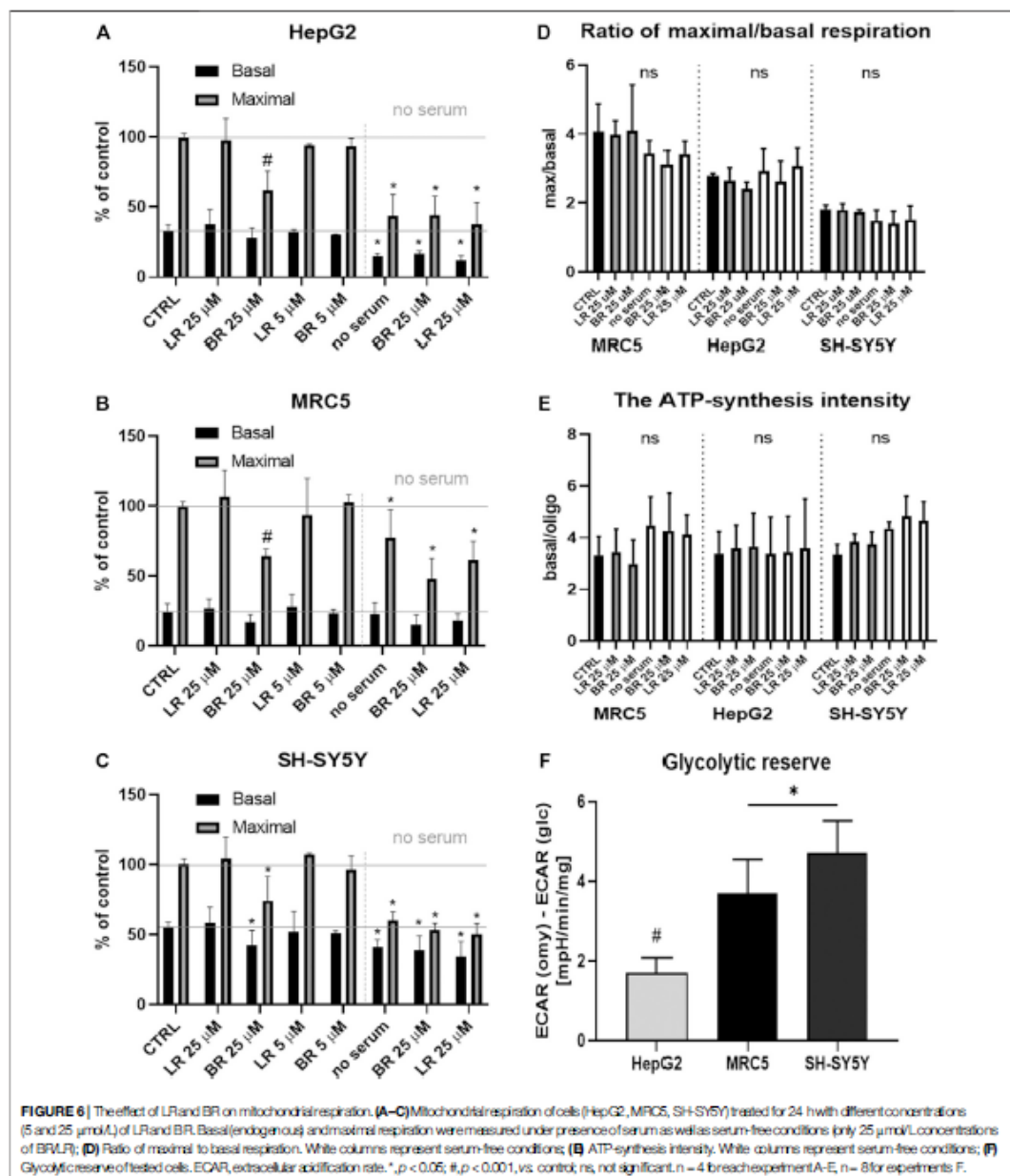
Since BR was recently demonstrated to improve metabolic functions in white adipose tissue via PPAR α -activated mitochondrial metabolism (Gordon et al., 2020), we analyzed the effect of LR and BR on PPAR α and its downstream effector gene expressions in HepG2 cells. While PPAR α gene expression was not affected by exposure to both pigments, its downstream effector genes FGF21 and ANGPTL4

were significantly, time-dependently upregulated by both BR and LR. Interestingly, LR, but not BR significantly upregulated also *CPT1A* and *PDK4* gene expressions (Figure 8). Increased gene expression of FGF21 upon exposure to BR and LR was reflected by increased FGF21 production as demonstrated by significantly increased FGF21 concentrations in culture media (Figure 9).

The Effect of LR and BR on Production of TCA Cycle Metabolites

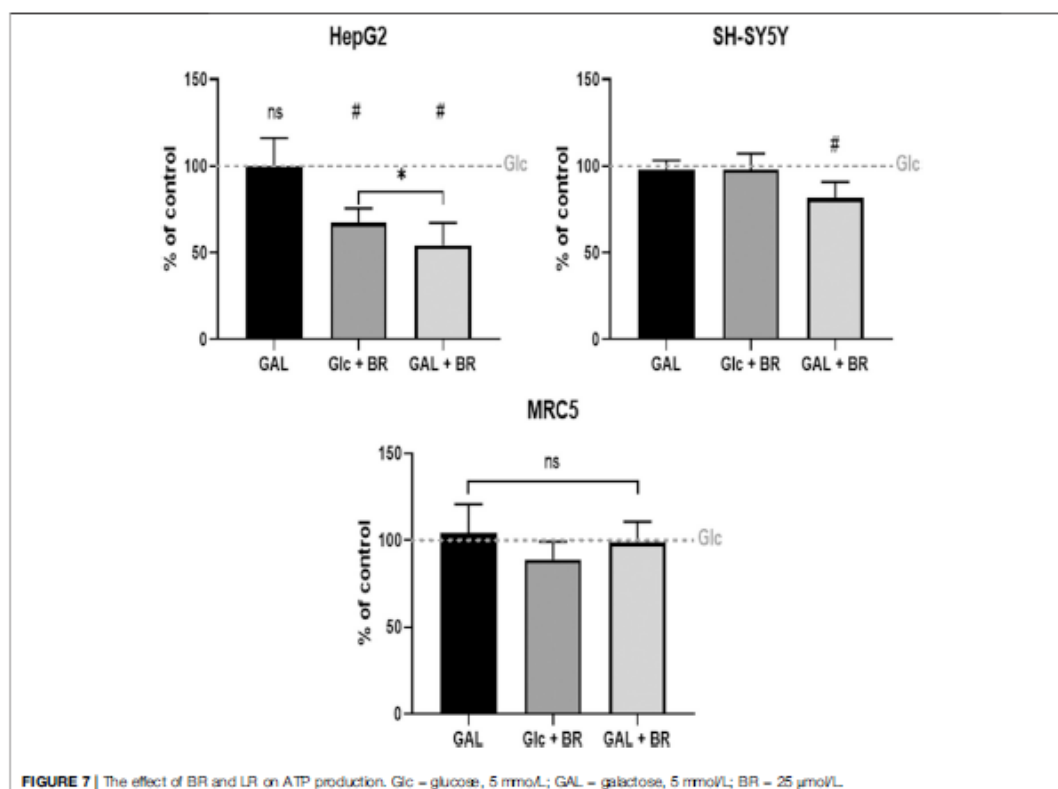
Due to the impact of BR on mitochondrial metabolism, we next investigated the possible effects of LR and BR on the production of intracellular metabolites of the TCA cycle, known to not only affect energy balance but also to modulate multiple cellular functions (Martinez-Reyes and Chandel, 2020).

Hence, the potential effects of LR and BR on the production of metabolic intermediates of the TCA cycle were measured in all investigated cell lines exposed to LR and BR. At lower concentrations



(5 $\mu\text{mol/L}$), both compounds did not have any marked effect in MRC5 and HepG2 cells; while in SH-SY5Y cells the concentrations of 2-hydroxyglutarate and 2-oxoglutarate significantly decreased ($p < 0.05$) in the presence of both compounds (Figure 10).

A different response was observed with a 5x greater concentration of BR, with most metabolites significantly reduced in all cell lines; whereas virtually no effect was observed in cells exposed to LR (Figure 10).



Anti-Inflammatory Effect of BR and LR

BR is a potent immunosuppressive compound (Jangi et al., 2013), but LR does not seem to act in the same manner (Jašprová et al., 2018). Thus, we were interested in the effects of BR and LR on *TNFα* expression as well as on NO production through inducible NO synthase (Xie et al., 1994).

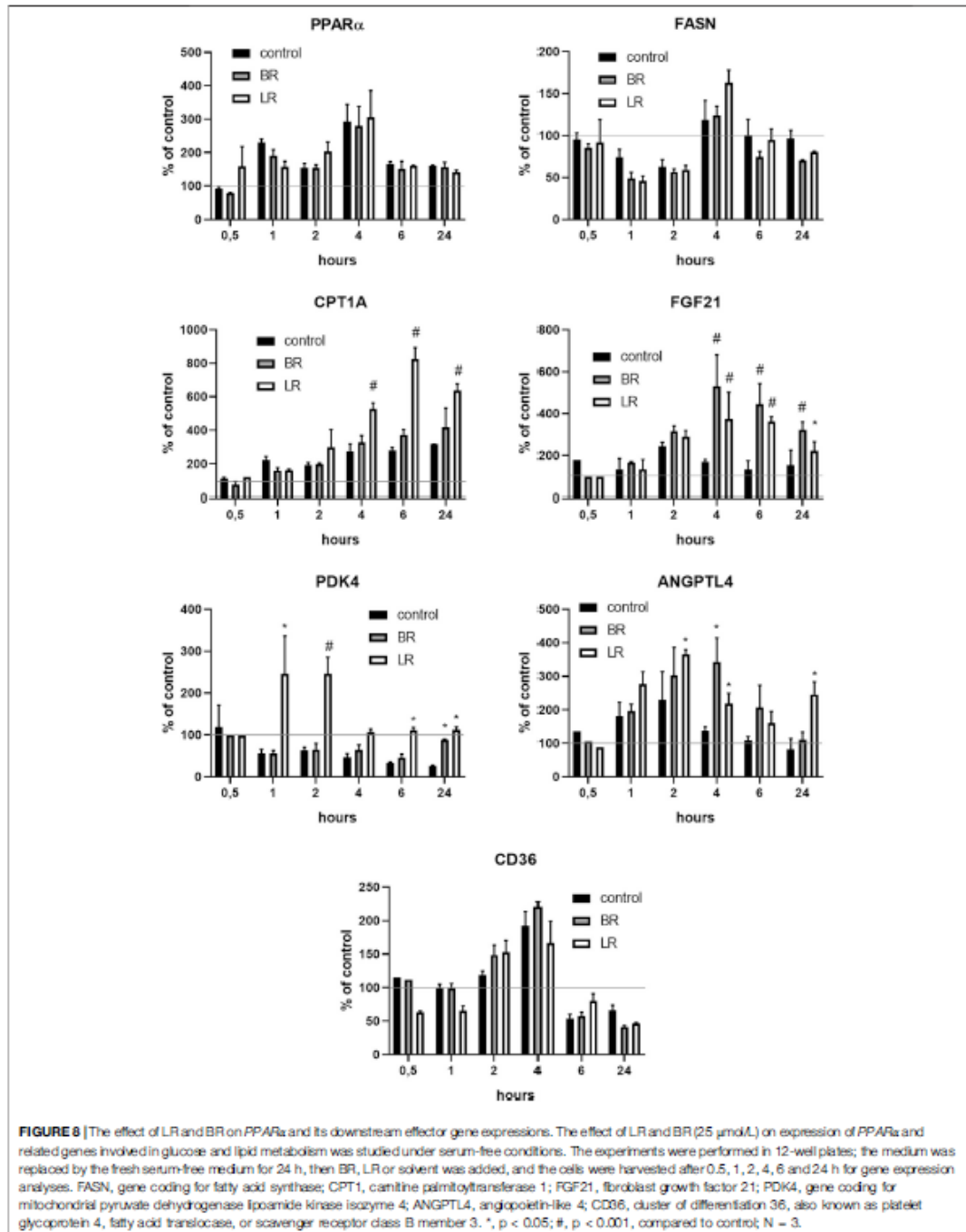
The anti-inflammatory effects of BR and LR were assessed in murine macrophage-like RAW 264.7 cells exposed to LPS. Basal *TNFα* expression was increased by both pigments (2-fold increase upon exposure to higher concentrations); with LR being effective in low concentrations (increase in *TNFα* expression by 40% at 5 μmol/L) (Figure 11A). When the cells were exposed to LPS, both pigments slightly, although significantly, modified *TNFα* expression (Figure 11A). More importantly, both pigments increased *TNFα* protein expression under unstimulated conditions (200- and 4-fold increase for BR and LR, respectively), and this effect persisted with almost 2-fold increase with 25 μmol/L concentration of BR ($p < 0.05$) (Figure 11B).

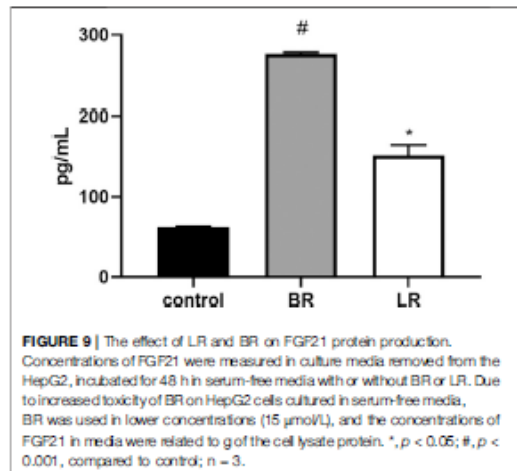
However, an increase in *TNFα* expression was not reflected by increased NO production (Figure 11C). On contrary, a decreased

TNFα expression by higher BR concentration led to a decreased NO production, and a slight decrease in NO production was also observed with LR treatment despite its increasing effect on *TNFα* expression (Figure 11C).

DISCUSSION

During the last several decades BR has been increasingly recognized as an important bioactive molecule, with substantial toxic effects when it reached high concentrations within the human body (such as during the neonatal period). The gold standard treatment for severe neonatal jaundice is PT with blue-green light, generating more water-soluble BR photoisomers. Although considered safe, the biological properties of BR photoisomers and their oxidation products have not properly been investigated. However, the still scarce data obtained until now suggests some biological activity of these products (Jašprová et al., 2018), which may account for the reported clinical observations (Raghavan et al., 2005; Xiong et al., 2011; Mcnamee et al., 2012; Arnold et al., 2014; Khan





et al., 2016; Auger et al., 2019; Safar and Elsayy, 2020). In addition, practically no mechanistic studies have been performed to address these issues.

In our current study, we tried to compare and correlate the data on BR and LR cell toxicity with the parameters of mitochondrial metabolism and oxidative stress. As expected, compared to BR, LR was found to be much less toxic in all cell lines used including hepatic, fibroblast as well as neuronal models (Figure 3). The cytotoxicity of BR was affected by the cellular glycolytic reserve, which was most compromised in human hepatoblastoma HepG2 cells (Figure 6F). This data was consistent with the inhibitory effects of BR on mitochondrial respiration, and more importantly on the TCA cycle. In fact, BR in contrast to LR exhibited profound inhibitory effects toward TCA cycle metabolites, being tightly linked to oxidative phosphorylation (Martinez-Reyes and Chandel, 2020). BR inhibited the mitochondrial respiration of all tested cell lines of different origins. This is consistent with previous reports of the impact of BR on mitochondrial morphology and metabolism (Mustafa et al., 1969; Noir et al., 1972; Almeida and Rezende, 1981; Rodrigues et al., 2002), while LR did not have any serious harmful effect. Importantly, these inhibitory effects were demonstrated mostly in brain cells (Mustafa et al., 1969; Almeida and Rezende, 1981; Rodrigues et al., 2002), whereas in other tissues, such as liver or heart, the effects on mitochondrial metabolism were opposite, i.e. beneficial, especially in lower concentrations (Mustafa et al., 1967; Mustafa et al., 1969; Stumpf et al., 1985). In addition, beneficial effects of BR on mitochondrial function were also reported recently in adipocytes (Gordon et al., 2020). Hence, it seems that the effects of BR and its derivatives are complex, being cell-specific and dependent on concentration as well as other conditions. We were also able to confirm, consistent with a previous recent report (Gordon et al., 2019), potential metabolic activities of both BR and LR, as demonstrated by increased expressions of PPAR α -dependent genes *FGF21* (reflected also by increased FGF21 protein production) and *ANGPTL1*, both involved in glucose and

lipid metabolism. Interestingly, LR, but not BR significantly upregulated also the other important metabolic genes *CPT1A* and *PDK4* gene expressions, pointing to the possible metabolic importance of this BR photoproduct. Up-regulations of these PPAR α -dependent genes became apparent under albumin-free conditions indicating that presence of albumin in the cell culture interfered with PPAR α signaling mechanisms.

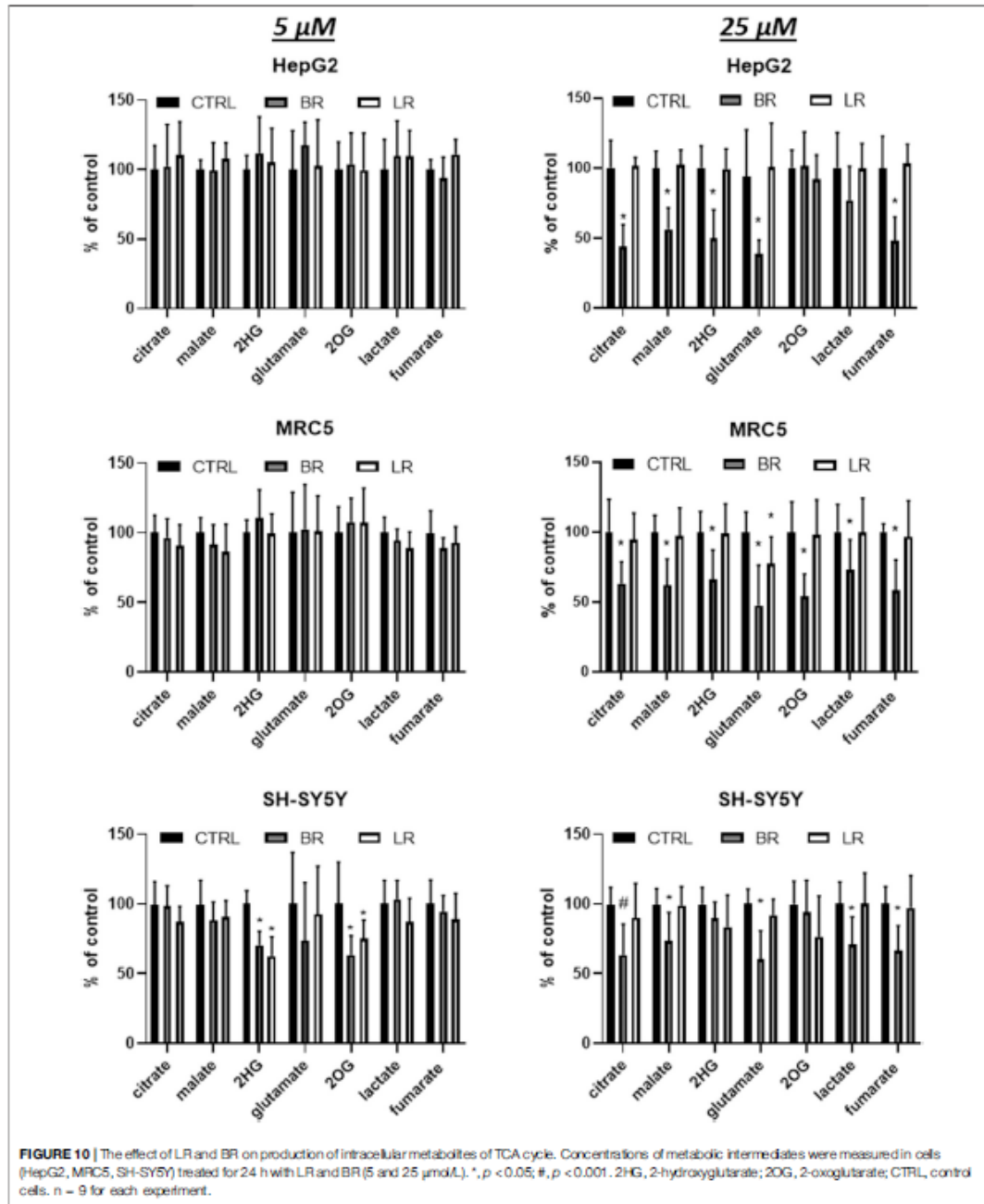
It is well known that deficiencies of respiratory complexes causes a drop in ATP production, with the appropriate metabolic consequences (Zielinski et al., 2016), including pseudo-hypoxic changes with hypoxia inducible factor (HIF)1 α activation and pyruvate dehydrogenase inhibition (Kim et al., 2006), followed by an impairment of metabolic substrate utilization (Crewe et al., 2013; Kappler et al., 2019). Based on our data, it seems that inhibition of respiration may result in subsequent inhibition of anaplerotic pathways, and also to compensate for the undesirable and excessive production of NADH. This step may be crucial to avoid Krebs cycle overload associated with overwhelming redox stress (Koves et al., 2008).

An important finding of our study is the effect of LR on oxidative stress. LR exerted serum antioxidant capacity as well as mitochondrial superoxide production suppressing activity comparable to BR, which is known to be one of the most potent endogenous antioxidants (Stocker et al., 1987). Interestingly, a substantial antioxidant effect of LR was observed in our cell models despite its marked degradation, suggesting a marked ROS-scavenging activity of LR degradation products. Nevertheless, LR was much less efficient in preventing lipoperoxidation, most likely due to its lower lipophilicity.

Additionally, BR was found to behave as a pro-inflammatory molecule in the macrophage-like RAW 264.7 cells, while only mild and insignificant effect was observed for LR. This is in contrast with our previous study performed on different cell models of CNS origin (Jašprová et al., 2018) indicating substantial cell variability of BR/LR-induced pro-inflammatory effects. This observation may be linked to the BR-induced TCA cycle dysregulation known to affect inflammatory status, NO production, as well as post-translational acetylation (Williams and O'Neill, 2018). Interestingly, both treatments lead to a decrease in NO availability. Although inducible NO synthase activity is up-regulated by TNF α , and positive associations between TNF α and NO were reported in clinical settings (Soufli et al., 2016); BR is known to scavenge NO by forming N-nitroso derivatives (Barone et al., 2009), and the same might also be true for LR. In addition, BR inhibits inducible NO synthase (Zucker et al., 2015), and LR may also act in a similar manner.

One of the limitations of our study is that metabolic changes were only analyzed for LR, and not for the other specific BR photo-oxidation products (such as biopyrins, propentdyopents, or monopyrrolic BOXes), which might have different biological impacts upon mitochondrial metabolism. In addition, the data from our *in vitro* experiments should be confirmed in *ex vivo*, animal and/or clinical studies.

Nevertheless, our data point to the biological effects of BR and its photo-oxidation products, which seem to have clinical relevance in phototherapy-treated hyperbilirubinemic neonates and adult patients.



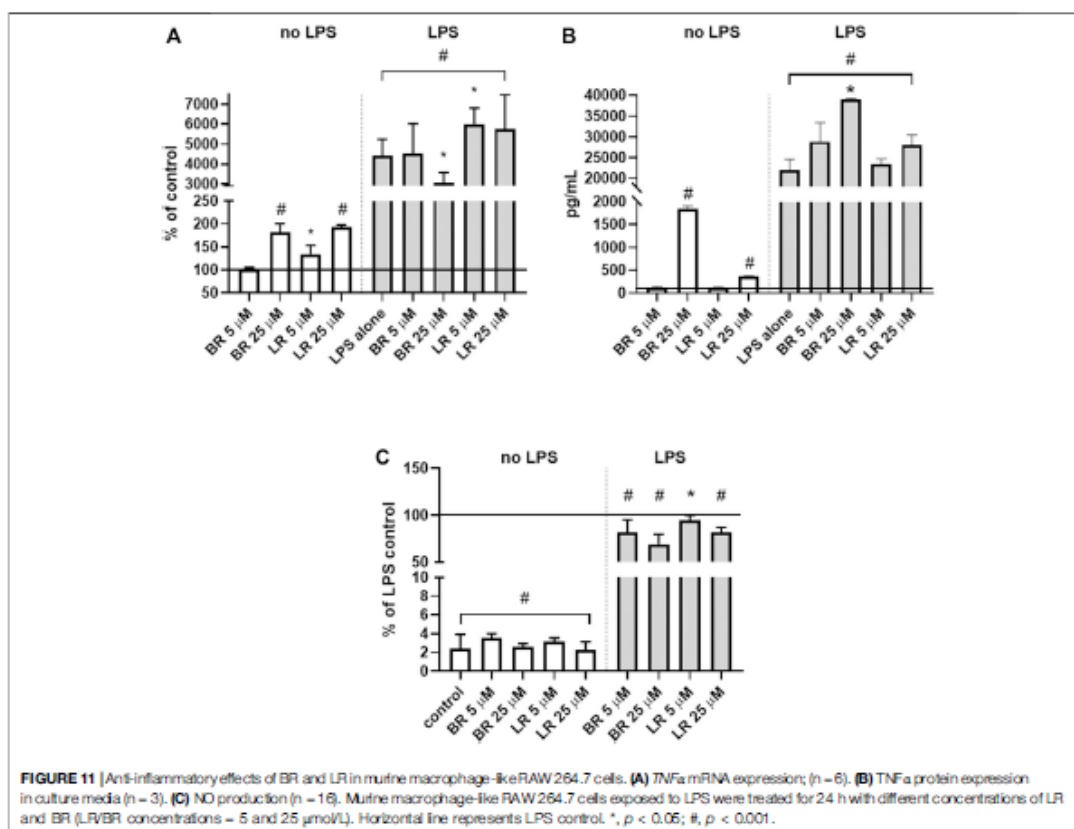


FIGURE 11 | Anti-inflammatory effects of BR and LR in murine macrophage-like RAW264.7 cells. **(A)** TNF α mRNA expression; (n = 6). **(B)** TNF α protein expression in culture media (n = 3). **(C)** NO production (n = 16). Murine macrophage-like RAW264.7 cells exposed to LPS were treated for 24 h with different concentrations of LR and BR (LR/BR concentrations = 5 and 25 μ M/L). Horizontal line represents LPS control. *, $p < 0.05$; #, $p < 0.001$.

DATA AVAILABILITY STATEMENT

The raw data supporting the conclusions of this article will be made available by the authors, without undue reservation.

AUTHOR CONTRIBUTIONS

AD proposed all the experiments, and performed cell viability tests and superoxide production experiments, KP and KZ performed most of the cell culture studies, NC prepared lumirubin for all experiments, LM performed lipoperoxidation

studies, MV performed LC-MS studies, NV and JZ performed peroxyl scavenging radical testing, JK performed Seahorse experiments, LV proposed the whole study, supervised all the experiments and wrote the Ms. All authors contributed to data analysis and Ms. preparation, all authors agreed with the final Ms.

FUNDING

The study was supported by grants NV18-07-00342 and RVO-VFN64165/2020 from the Czech Ministry of Health.

REFERENCES

- Almeida, M. A., and Rezende, L. (1981). The serum levels of unbound bilirubin that induce changes in some brain mitochondrial reactions in newborn guinea-pigs. *Experientia* 37, 807–809. doi:10.1007/BF01985651
- Arnold, C., Pedrosa, C., and Tyson, J. E. (2014). Phototherapy in ELBW newborns: does it work? Is it safe? The evidence from randomized clinical trials. *Semin. Perinatol.* 38, 452–464. doi:10.1053/j.semperi.2014.08.008
- Auger, N., Laverdiere, C., Ayoub, A., Lo, E., and Lum, T. M. (2019). Neonatal phototherapy and future risk of childhood cancer. *Int. J. Cancer* 145, 2061–2069. doi:10.1002/ijc.32158
- Barone, E., Trombino, S., Cassano, R., Sgambato, A., De Paola, B., Di Stasio, E., et al. (2009). Characterization of the S-nitrosylating activity of bilirubin. *J. Cell Mol. Med.* 13, 2365–2375. doi:10.1111/j.1582-4934.2009.00680.x
- Brand, M. D., and Nicholls, D. G. (2011). Assessing mitochondrial dysfunction in cells. *Biochem. J.* 435, 297–312. doi:10.1042/BJR20110162

- Crewe, C., Kinter, M., and Sweda, L. I. (2013). Rapid inhibition of pyruvate dehydrogenase: an initiating event in high dietary fat-induced loss of metabolic flexibility in the heart. *PLoS One* 8, e7280. doi:10.1371/journal.pone.0077280
- Dal Ben, M., Bottin, C., Zanconati, F., Tiribelli, C., and Gazzin, S. (2017). Evaluation of region selective bilirubin-induced brain damage as a basis for a pharmacological treatment. *Sci. Rep.* 7, 41032. doi:10.1038/srep41032
- Dvorak, A., Zelenka, J., Smolkova, K., Vittek, L., and Jezek, P. (2017). Background levels of neomorphic 2-hydroxyglutarate facilitate proliferation of primary fibroblasts. *Physiol. Res.* 66, 293–304. doi:10.33549/physiolres.933249
- Gordon, D. M., Blomquist, T. M., Mirzazi, S. A., Mccullumsmith, R., Stec, D. E., and Hinds, T. D., Jr. (2019). RNA sequencing in human HepG2 hepatocytes reveals PPAR- α mediates transcriptome responsiveness of bilirubin. *Physiol. Genomics* 51, 234–240. doi:10.1152/physiolgenomics.00028.2019
- Gordon, D. M., Neifer, K. L., Hamoud, A. A., Hawk, C. F., Nestor-Kalinoski, A. L., Mirzazi, S. A., et al. (2020). Bilirubin remodels murine white adipose tissue by reshaping mitochondrial activity and the coregulator profile of peroxisome proliferator-activated receptor α . *J. Biol. Chem.* 295, 9804–9822. doi:10.1074/jbc.RA120.013700
- Grojean, S., Korziel, V., Vert, P., and Daval, J. L. (2000). Bilirubin induces apoptosis via activation of NMDA receptors in developing rat brain neurons. *Exp. Neurol.* 166, 334–341. doi:10.1006/exnr.2000.7518
- Hansen, R., Gibson, S., De Paiva Alves, E., Goddard, M., Maclaren, A., Karcher, A. M., et al. (2018). Adaptive response of neonatal sepsis-derived Group B *Streptococcus* to bilirubin. *Sci. Rep.* 8, 6470. doi:10.1038/s41598-018-24811-3
- Heggy, T., Goldie, E., and Hiatt, M. (1994). The protective role of bilirubin in oxygen-radical diseases of the preterm infant. *J. Perinatol.* 14, 296–300.
- Hinds, T. D., Jr., and Stec, D. E. (2019). Bilirubin safeguards cardiometabolic and metabolic diseases: a protective role in health. *Curr. Hypertens. Rep.* 21, 87. doi:10.1007/s11906-019-0994-z
- Hinds, T. D., Jr., and Stec, D. E. (2018). Bilirubin, a cardiometabolic signaling molecule. *Hypertension* 72, 788–795. doi:10.1161/HYPERTENSIONAHA.118.11130
- Hyperbilirubinemia (2004). Management of hyperbilirubinemia in the newborn infant 35 or more weeks of gestation. *Pediatrics* 114, 297–316. doi:10.1542/peds.114.1.297
- Jangl, S., Oterheirn, L., and Robson, S. (2013). The molecular basis for the immunomodulatory activities of unconjugated bilirubin. *Int. J. Biochem. Cell Biol.* 45, 2843–2851. doi:10.1016/j.biocel.2013.09.014
- Jajprovič, J., Dal Ben, M., Ilumý, D., Hwang, S., Žižalová, K., Kotek, J., et al. (2018). Neuro-inflammatory effects of photo-degradative products of bilirubin. *Sci. Rep.* 8, 7444. doi:10.1038/s41598-018-25684-2
- Jasprova, J., Dal Ben, M., Vianello, E., Goncharova, I., Urbanova, M., Vyroubalova, K., et al. (2016). The biological effects of bilirubin photoisomers. *PLoS One* 11, e0148126. doi:10.1371/journal.pone.0148126
- Jasprova, J., Dvorak, A., Vecka, M., Lenick, M., Lacina, O., Valaskova, P., et al. (2020). A novel accurate LC-MS/MS method for quantitative determination of Z-luminubin. *Sci. Rep.* 10, 4411. doi:10.1038/s41598-020-61280-z
- Kappler, M., Pabst, U., Weirhaldt, C., Taubert, H., Rot, S., Kaune, T., et al. (2019). Causes and consequences of a glutamine induced normoxic HIF1 activity for the Tumor metabolism. *Int. J. Mol. Sci.* 20, 4742. doi:10.3390/ijms20194742
- Khan, M., Malik, K. A., and Bai, R. (2016). Hypocalcemia in jaundiced neonates receiving phototherapy. *Pak. J. Med. Sci.* 32, 1449–1452. doi:10.12669/pjms.326.10849
- Kim, J. W., Tchernyshyov, I., Semenza, G. L., and Dang, C. V. (2006). HIF-1-mediated expression of pyruvate dehydrogenase kinase: a metabolic switch required for cellular adaptation to hypoxia. *Cell Metab.* 3, 177–185. doi:10.1016/j.cmet.2006.02.002
- Koves, T. R., Ussher, J. R., Noland, R. C., Slenz, D., Mosedale, M., Ilkayeva, O., et al. (2008). Mitochondrial overload and incomplete fatty acid oxidation contribute to skeletal muscle insulin resistance. *Cell Metab.* 7, 45–56. doi:10.1016/j.cmet.2007.10.013
- Lightner, D. A., and Quistad, G. B. (1972). Hematinic acid and propenylolipens from bilirubin photo-oxidation *in vitro*. *FEBS Lett.* 25, 94–96. doi:10.1016/0014-5793(72)80462-9
- Lightner, D. A., Linrane, W. P., 3rd, and Ahlfors, C. E. (1984). Bilirubin photooxidation products in the urine of jaundiced neonates receiving phototherapy. *Pediatr. Res.* 18, 696–700. doi:10.1203/00006450-198408000-00003
- Maisels, M. J., and McDonagh, A. F. (2008). Phototherapy for neonatal jaundice. *N. Engl. J. Med.* 358, 920–928. doi:10.1056/NEJMc0708376
- Martinez-Reyes, L., and Chandel, N. S. (2020). Mitochondrial TCA cycle metabolites control physiology and disease. *Nat. Commun.* 11, 102. doi:10.1038/s41467-019-13668-3
- McDonagh, A. F., and Assisi, F. (1972). The ready isomerization of bilirubin IX in aqueous solution. *Biochem. J.* 129, 797–800. doi:10.1042/bj1290797
- McDonagh, A. F., and Palma, L. A. (1980). Hepatic excretion of circulating bilirubin photoproducts in the Gunn rat. *J. Clin. Invest.* 66, 1182–1185. doi:10.1172/JCI109951
- McNamee, M. B., Gardwell, C. R., and Patterson, C. C. (2012). Neonatal jaundice is associated with a small increase in the risk of childhood type 1 diabetes: a meta-analysis of observational studies. *Acta Diabetol.* 49, 83–87. doi:10.1007/s00592-011-0326-5
- Mustafa, M. G., Cowger, M. L., and King, T. E. (1969). Effects of bilirubin on mitochondrial reactions. *J. Biol. Chem.* 244, 6403–6414. doi:10.1016/s0021-9258(18)63479-9
- Mustafa, M. G., Cowger, M. L., and King, T. E. (1967). On the energy dependent bilirubin induced mitochondrial swelling. *Biochem. Biophys. Res Commun.* 29, 661–666. doi:10.1016/0006-291x(67)90267-7
- Noir, B. A., Boveris, A., Garaza Pereira, A. M., and Stoppani, A. O. (1972). Bilirubin: a multi-site inhibitor of mitochondrial respiration. *FEBS Lett.* 27, 270–274. doi:10.1016/0014-5793(72)80638-0
- Orishi, S., Kawade, N., Itoh, S., Isobe, K., Sugiyama, S., Hashimoto, T., et al. (1981). Kinetics of biliary excretion of the main two bilirubin photoproducts after injection into Gunn rats. *Biochem. J.* 198, 107–112. doi:10.1042/bj1980107
- Raghavan, K., Thomas, E., Patole, S., and Müller, R. (2005). Is phototherapy a risk factor for ileus in high-risk neonates? *J. Matern. Fetal Neonatal Med.* 18, 129–131. doi:10.1080/14767050500233076
- Rakshandehroo, M., Knoch, B., Müller, M., and Kersten, S. (2010). Peroxisome proliferator activated receptor alpha target genes. *PPAR Res.* 2010, 612089. doi:10.1155/2010/612089
- Roca, L., Calligaris, S., Wennberg, R. P., Ahlfors, C. E., Malik, S. G., Ostrow, J. D., et al. (2006). Factors affecting the binding of bilirubin to serum albumin: validation and application of the peroxidase method. *Pediatr. Res.* 60, 724–728. doi:10.1203/01.pdr.0000245992.89965.94
- Rodrigues, C. M., Sola, S., and Brites, D. (2002). Bilirubin induces apoptosis via the mitochondrial pathway in developing rat brain neurons. *Hepatology* 35, 1186–1195. doi:10.1053/jhep.2002.32967
- Safar, H., and El-Sary, A. Y. (2020). Neonatal jaundice: the other side of the coin in the development of allergy. *Am. J. Perinatol.* 37, 1357–1363. doi:10.1055/s-0039-1693697
- Seidel, R. A., Schowtka, B., Klopffleisch, M., Kuhl, T., Weiland, A., Koch, A., et al. (2014). Total synthesis and characterization of the bilirubin oxidation product (Z)-2-(4-ethenyl-3-methyl-5-oxo-1,5-dihydro-2H-pyrrol-2-ylidene)ethanamide (Z-BOX B). *Tetrahedron Lett.* 55, 6526–6529. doi:10.1016/j.tetlet.2014.09.108
- Shekesh, S. M., Kumar, P., Sharma, N., Narang, A., and Prasad, R. (2008). Evaluation of oxidant and antioxidant status in term neonates: a plausible protective role of bilirubin. *Mol. Cell Biochem.* 317, 51–59. doi:10.1007/s11010-008-9807-4
- Smolkova, K., Dvorak, A., Zelenka, J., Vittek, L., and Jezek, P. (2015). Reductive carboxylation and 2-hydroxyglutarate formation by wild-type IDH2 in breast carcinoma cells. *Int. J. Biochem. Cell Biol.* 65, 125–133. doi:10.1016/j.biocel.2015.05.012
- Soufli, L., Toumi, R., Rifa, H., and Touil-Boukoffa, C. (2016). Overview of cytokines and nitric oxide involvement in immuno-pathogenesis of inflammatory bowel diseases. *World J. Gastrointest. Pharmacol. Ther.* 7, 353–360. doi:10.4292/wjgpt.v7.i3.353
- Soutar, M. P. M., Kempthorne, L., Annunzio, E., Luft, C., Wray, S., Kettler, R., et al. (2019). FBS/BSA media concentration determines CCCP's ability to depolarize mitochondria and activate PINK1/Parkin mitophagy. *Autophagy* 15, 2002–2011. doi:10.1080/15548627.2019.1603549
- Stec, D. E., John, K., Trabbic, C. J., Lunival, A., Harkins, M. W., Baum, J., et al. (2016). Bilirubin binding to PPAR α inhibits lipid accumulation. *PLoS One* 11, e0153427. doi:10.1371/journal.pone.0153427
- Stocker, R., Yamamoto, Y., McDonagh, A. F., Glazer, A. N., and Ames, B. N. (1987). Bilirubin is an antioxidant of possible physiological importance. *Science* 235, 1043–1046. doi:10.1126/science.3029864
- Stumpf, D. A., Eiguren, I. A., and Parks, J. K. (1985). Bilirubin increases mitochondrial inner membrane conductance. *Biochem. Med.* 34, 226–229. doi:10.1016/0006-2944(85)90115-2

- Valaskova, P., Dvorak, A., Lemick, M., Zizalova, K., Kutinova-Ganova, N., Zelenka, J., et al. (2019). Hyperbilirubinemia in Gunn rats is associated with decreased inflammatory response in IPS-mediated systemic inflammation. *Ijms* 20, 2306. doi:10.3390/ijms20092306
- Vitek, I. (2020). Bilirubin as a signaling molecule. *Med. Res. Rev.* 40, 1335–1351. doi:10.1002/med.21660
- Vreman, H. J., Wong, R. J., Sanesi, C. A., Dennery, P. A., and Stevenson, D. K. (1998). Simultaneous production of carbon monoxide and thiobarbituric acid reactive substances in rat tissue preparations by an iron-ascorbate system. *Can. J. Physiol. Pharmacol.* 76, 1057–1065. doi:10.1139/cjpp-76-12-1057
- Wagner, K. H., Wallner, M., Molzer, C., Gazzin, S., Bulmer, A. C., Tiribelli, C., et al. (2015). Looking to the horizon: the role of bilirubin in the development and prevention of age-related chronic diseases. *Clin. Sci.* 129, 1–25. doi:10.1042/CS20140566
- Watchko, J. F., and Tiribelli, C. (2013). Bilirubin-induced neurologic damage—mechanisms and management approaches. *N. Engl. J. Med.* 369, 2021–2030. doi:10.1056/NEJMr1308124
- Williams, N. C., and O'Neill, L. A. J. (2018). A role for the Krebs cycle intermediate citrate in metabolic reprogramming in innate immunity and inflammation. *Front. Immunol.* 9, 141. doi:10.3389/fimmu.2018.00141
- Xie, Q. W., Kashiwabara, Y., and Nathan, C. (1994). Role of transcription factor NF-kappa B/Rel in induction of nitric oxide synthase. *J. Biol. Chem.* 269, 4705–4708. doi:10.1016/s0021-9258(17)37600-7
- Xiong, T., Qu, Y., Cambier, S., and Mu, D. (2011). The side effects of phototherapy for neonatal jaundice: what do we know? What should we do?. *Eur. J. Pediatr.* 170, 1247–1255. doi:10.1007/s00431-011-1454-1
- Yamaguchi, T., Shioji, I., Sugimoto, A., Komoda, Y., and Nakajima, H. (1994). Chemical structure of a new family of bile pigments from human urine. *J. Biochem.* 116, 298–303. doi:10.1093/oxfordjournals.jbchem.a124523
- Zelenka, J., Dvorak, A., Alan, L., Zadinova, M., Haluzik, M., and Vitek, I. (2016). Hyperbilirubinemia protects against aging-associated inflammation and metabolic deterioration. *Oxid. Med. Cell Longev.* 2016, 6190609. doi:10.1155/2016/6190609
- Zelenka, J., Muchova, L., Zelenkova, M., Vanova, K., Vreman, H. J., Wong, R. J., et al. (2012). Intracellular accumulation of bilirubin as a defense mechanism against increased oxidative stress. *Biochimie* 94, 1821–1827. doi:10.1016/j.biochi.2012.04.0210.1016/j.biochi.2012.04.026
- Zielinski, L. P., Smith, A. C., Smith, A. G., and Robinson, A. J. (2016). Metabolic flexibility of mitochondrial respiratory chain disorders predicted by computer modelling. *Mitochondrion* 31, 45–55. doi:10.1016/j.mito.2016.09.003
- Zucker, S. D., Vogel, M. E., Kindel, T. L., Smith, D. L., Idelman, G., Avissar, U., et al. (2015). Bilirubin prevents acute DSS-induced colitis by inhibiting leukocyte infiltration and suppressing upregulation of inducible nitric oxide synthase. *Am. J. Physiol. Gastrointest. Liver Physiol.* 309, G841–G854. doi:10.1152/ajpgi.00149.2014

Conflict of Interest: The authors declare that the research was conducted in the absence of any commercial or financial relationships that could be construed as a potential conflict of interest.

Copyright © 2021 Dvořák, Pospíšilová, Žizalová, Čapková, Muchová, Vecka, Vrzáčková, Křížová, Zelenka and Vitek. This is an open-access article distributed under the terms of the Creative Commons Attribution License (CC BY). The use, distribution or reproduction in other forums is permitted, provided the original author(s) and the copyright owner(s) are credited and that the original publication in this journal is cited, in accordance with accepted academic practice. No use, distribution or reproduction is permitted which does not comply with these terms.

Article

The Effects of Bilirubin and Lumirubin on the Differentiation of Human Pluripotent Cell-Derived Neural Stem Cells

Nikola Capková ^{1,†}, Veronika Pospíšilová ^{2,†}, Veronika Fedorová ², Jan Raška ², Kateřina Pospíšilová ¹, Matteo Dal Ben ¹, Aleš Dvořák ¹, Jitka Viktorová ³, Dáša Boháčiková ^{2,4} and Libor Vitek ^{1,5,*}

¹ Institute of Medical Biochemistry and Laboratory Diagnostics, Faculty General Hospital and 1st Faculty of Medicine, Charles University, 110 00 Prague, Czech Republic; nikola.capkova@lf1.cuni.cz (N.C.); katerina.pospisilova@lf1.cuni.cz (K.P.); dalben.matteo@yahoo.it (M.D.B.); ales.dvorak@lf1.cuni.cz (A.D.)

² Department of Histology and Embryology, Faculty of Medicine, Masaryk University, 601 77 Brno, Czech Republic; veronika.pospisilova@med.muni.cz (V.P.); 436702@mail.muni.cz (V.F.); raska@med.muni.cz (J.R.); bohacikova@med.muni.cz (D.B.)

³ Department of Biochemistry and Microbiology, University of Chemistry and Technology, 166 28 Prague, Czech Republic; jitka.prokesova@vscht.cz

⁴ International Clinical Research Center (ICRC), St. Anne's University Hospital, 656 91 Brno, Czech Republic

⁵ 4th Department of Internal Medicine, Faculty General Hospital and 1st Faculty of Medicine, Charles University, 110 00 Prague, Czech Republic

* Correspondence: vitek@cesnet.cz; tel: +420-224-964-203

† Both authors contributed equally.



Citation: Capková, N.; Pospíšilová, V.; Fedorová, V.; Raška, J.; Pospíšilová, K.; Dal Ben, M.; Dvořák, A.; Viktorová, J.; Boháčiková, D.; Vitek, L. The Effects of Bilirubin and Lumirubin on the Differentiation of Human Pluripotent Cell-Derived Neural Stem Cells. *Antioxidants* **2021**, *10*, 1532. <https://doi.org/10.3390/antiox10101532>

Academic Editor: Peter I. Oltver

Received: 27 August 2021

Accepted: 22 September 2021

Published: 27 September 2021

Publisher's Note: MDPI stays neutral with regard to jurisdictional claims in published maps and institutional affiliations.



Copyright © 2021 by the authors. Licensee MDPI, Basel, Switzerland. This article is an open access article distributed under the terms and conditions of the Creative Commons Attribution (CC BY) license (<https://creativecommons.org/licenses/by/4.0/>).

Abstract: The ‘gold standard’ treatment of severe neonatal jaundice is phototherapy with blue–green light, which produces more polar photo-oxidation products that are easily excreted via the bile or urine. The aim of this study was to compare the effects of bilirubin (BR) and its major photo-oxidation product lumirubin (LR) on the proliferation, differentiation, morphology, and specific gene and protein expressions of self-renewing human pluripotent stem cell-derived neural stem cells (NSC). Neither BR nor LR in biologically relevant concentrations (12.5 and 25 $\mu\text{mol/L}$) affected cell proliferation or the cell cycle phases of NSC. Although none of these pigments affected terminal differentiation to neurons and astrocytes, when compared to LR, BR exerted a dose-dependent cytotoxicity on self-renewing NSC. In contrast, LR had a substantial effect on the morphology of the NSC, inducing them to form highly polar rosette-like structures associated with the redistribution of specific cellular proteins (β -catenin/N-cadherin) responsible for membrane polarity. This observation was accompanied by lower expressions of NSC-specific proteins (such as SOX1, NR2F2, or PAX6) together with the upregulation of phospho-ERK. Collectively, the data indicated that both BR and LR affect early human neurodevelopment in vitro, which may have clinical relevance in phototherapy-treated hyperbilirubinemic neonates.

Keywords: bilirubin; neurodevelopment; phototherapy

1. Introduction

Bilirubin (BR) is the end product of the heme degradation pathway. While in the past BR was considered a potentially neurotoxic waste product of heme catabolism, numerous in vitro, in vivo, and clinical studies over recent decades have demonstrated that when it is only mildly elevated it is also an endogenous antioxidant with potent anti-inflammatory and cytoprotective effects, mediated via true endocrine mechanisms [1].

Elevated serum BR concentrations are present in most newborn infants [2]. The physiological neonatal jaundice spontaneously resolves within a few days after birth, and it is believed to even have a protective role against pathological conditions associated with increased oxidative stress [3,4]. However, severely jaundiced neonates (i.e., with hyperbilirubinemia above 340 $\mu\text{mol/L}$) are in danger of serious health risks, which may lead to

bilirubin encephalopathy or even death [5]. BR is capable of binding to myelin-rich membranes, making neurons the principal target cells, with multiple biological consequences including motor and intellectual disorders, chronic BR encephalopathy, hearing deficits, or paralysis of the oculomotor muscles [6].

Phototherapy (PT) with blue–green light (400–520 nm) is the worldwide gold standard for the treatment of severe neonatal jaundice. During this therapeutic approach, BR is transformed into more polar and easily excreted BR photoproducts [7], with *Z*-lumirubin (LR), *E,Z*-BR, and *Z,E*-BR being the principal compounds. Additional BR photoproducts include monopyrrolic (*Z*-BOX A–D), dipyrrolic (propentdyopents), and tripyrrolic (biopyrrin A/B) compounds [8,9]. Although PT is generally believed to be a safe therapeutic procedure, intensive PT of extremely low birth-weight (ELBW) newborn infants has recently been reported to be associated with an increased risk of allergies, diabetes, and even cancer and overall mortality (for reviews see [10,11]). These surprising recent observations might be due to the possible negative effects of BR photoproducts on the developing newborn brain. In fact, Kranc et al. showed in their *in vivo* and *in vitro* experimental models that monopyrrolic BOXes can have vasoconstrictive effects [12]. In one of our own studies, we demonstrated the striking upregulation of proinflammatory cytokines in organotypic rat hippocampal slices after short-term exposure to LR [13]. Nevertheless, in another of our recent *in vitro* studies, LR exerted beneficiary effects on metabolic and oxidative stress markers when compared to BR [14]. Based on these observations, BR photoproducts could possibly affect early human neurodevelopment, although no scientific data relevant to this assumption are currently available.

Hence, the aim of this study was to compare the effects of BR and its major photo-oxidation product (LR) on the proliferation, differentiation, morphology, and specific gene and protein expressions of self-renewing neural stem cells (NSC) derived from human pluripotent stem cells (hPSC) [15–18]. These NSC lines have the ability to self-renew and terminally differentiate into neurons and glia [15], and thus they represent a biologically and developmentally relevant surrogate human model to study the influence of the potentially biologically active compounds on these processes.

2. Materials and Methods

All chemicals and reagents were obtained from Sigma-Aldrich (St. Louis, MO, USA), unless otherwise specified.

2.1. Unconjugated BR and LR Preparation

Unconjugated BR was purified according to McDonagh and Assisi 1972 [19], and LR was prepared as previously described [20] with slight modifications. Briefly, unconjugated BR was dissolved in 2 mL of NaOH (0.1 mol/L), immediately neutralized with 1 mL of H₃PO₄ (0.1 mol/L) and gently mixed with 7 mL of human serum albumin in PBS (phosphate buffer saline) (660 μmol/L). The final concentration of unconjugated BR was 480 μmol/L. The mixture was irradiated for 120 min at 460 nm using a Lilly phototherapeutic device (TSE Medical, Czech Republic) at 70 μW/(cm²·nm). The irradiated solution was mixed with ammonium acetate in methanol (0.1 mol/L; 1:1 *v/v*) and then vortexed. Following the Folch extraction, the solution was mixed with chloroform and vortexed intensively for at least 30 s, followed by the addition of water; the mixture was then briefly vortexed and centrifuged at 3000 × *g* for 10 min at 4 °C. After the separation, the lower chloroform phase containing LR was transferred to the glass flask, and chloroform was evaporated by a vacuum rotary evaporator (RVO 200 A, INGOS, Czech Republic). The residue was dissolved in chloroform/methanol solution and separated by thin-layer chromatography (TLC) on silica gel plates (TLC silica gel 60 plates, 0.5 × 200 × 200 mm, Merck, Darmstadt, Germany); mobile phase = chloroform/methanol/water (40:9:1, *v/v/v*). The LR was isolated from scraped silica gel by methanol, dried under a stream of nitrogen, and its purity and identity verified by both HPLC and LC-MS/MS analyses (19). For all

experiments, the BR was dissolved in DMSO (dimethyl sulphoxide) (final concentration of DMSO = 0.1%), whereas the LR was dissolved in PBS.

2.2. Cell Cultivation and Differentiation to Neurons

An established NSC cell line (CoMo-NSC) was derived from human embryonic stem cells (cell line ESI-017, ESI BIO, Alameda, CA, USA) as described previously [15]. These self-renewing NSC were cultured at 37 °C in a 5% CO₂ atmosphere, on the cultivation plates coated with poly-L-ornithine and laminin (Thermo Fisher Scientific, Waltham, MA, USA) in the basic NSC (standard growth) medium consisting of DMEM/F12 (Dulbecco's Modified Eagle Medium), 1% Glutamax, 1% non-essential amino acids, 0.5% N₂ supplement, 0.5% B27 supplement without vitamin A, FGF2 (fibroblast growth factor 2) recombinant human protein (Thermo Fisher Scientific, Waltham, MA, USA), and 5 µL/mL of Zell shield cell culture contamination preventive solution (Minerva Biolabs, Berlin, Germany). The first step of the coating was the addition of 20 µg/mL poly-L-ornithine diluted in PBS. After 15 min of incubation at room temperature, the plates were washed three times with PBS, coated with 4.2 µg/mL laminin diluted in PBS, and incubated for 30 min at room temperature. For passage, the cells were detached from the surface by Accutase (Thermo Fisher Scientific, Waltham, MA, USA) and harvested with the basic NSC medium without FGF2. After centrifugation at 200 × g for 5 min, the cells were resuspended in NSC medium, counted in a hemocytometer, and immediately seeded in the appropriate density on plates coated with poly-L-ornithine and laminin for the experiments.

For terminal differentiation studies, the NSC on day 0 were seeded at the density of 25,000/cm² on a 24-well plate with cover glasses, and cultured at 37 °C in a 5% CO₂ atmosphere. From day 3, the cells were treated for 4 days with BR (12.5 µM) and LR (12.5 and 25 µM), PBS (1%), and DMSO (0.1%) in basic NSC medium without FGF2, with the addition of brain-derived neurotrophic factor (BDNF) and glial cell line-derived neurotrophic factor (GDNF) (20 ng/mL) (Peprotech, London, UK), cAMP (300 ng/mL) and Zell shield solution (5 µL/mL). The medium was changed every day. On day 7, the cells were cultured in basic NSC medium without FGF2 and with Zell shield solution (5 µL/mL) and DAPT γ-secretase inhibitor (2.5 µM; Selleckchem, Houston, TX, USA). NSC were cultured in this medium for the next 10 days and the medium was changed every second day. The experiment lasted for a total of 17 days.

2.3. Additional In Vitro Studies

Unless otherwise specified, in all of the other in vitro studies the NSC were seeded at the density of 12,000/cm² in five 96-well plates. One day after seeding, the NSC were treated for 96 h with fresh basic medium and the addition of BR (6.25, 12.5, 25, and 50 µM), LR (6.25, 12.5, 25, and 50 µM), with PBS (1%)/DMSO (0.1%) as the negative control. The medium was changed every day.

2.3.1. Growth Curve Analysis

Each day one of the 96-well plates was fixed with 4% paraformaldehyde, then washed two times with PBS, stained with 0.1% crystal violet for 60 min at room temperature, and washed three times with deionized water. Subsequently, 33% acetic acid was added for 20 min at room temperature while being shaken. Absorbance was measured at 570 nm with a Synergy HTX spectrophotometer (BioTek Instruments, Inc., Winooski, VT, USA).

2.3.2. Cytotoxicity Assay

A 96-well plate was fixed with 4% paraformaldehyde and washed three times with PBS. Nuclei were labeled with Hoechst 33342 solution (Thermo Fisher Scientific, Waltham, MA, USA), diluted to a final concentration of 5 µg/mL in PBS, incubated for 20 min, and washed three times with PBS.

Cell imaging was performed on an ImageXpress Micro XL automated epifluorescence microscope (Molecular Devices, San Jose, CA, USA) using a Plan Fluor ELWD

20 × /0.45 objective. The acquired images were analyzed as the combination of these two techniques by use of CellProfiler 4.2.0 open-source software (Boston, MA, USA; www.cellprofiler.org accessed on 15 July 2021) as well as manually by the use of FIJI software (Madison, WI, USA; www.fiji.sc accessed on 15 July 2021).

2.3.3. MTT Cell Viability/Metabolic Activity Test

Viability/mitochondrial metabolic activity was measured by an assay using 3-(4,5-dimethylthiazol-2-yl)-2,5-diphenyltetrazolium bromide (MTT). The cells were incubated with 1 mg/mL of MTT dissolved in NSC medium at 37 °C for 1 h. Then, the NSC medium was aspirated and cells were treated with 99.9% DMSO for 10 min while being shaken. Absorbance was detected at 570 nm and 690 nm, as a reference, using a Synergy HTX spectrophotometer (BioTek Instruments, Inc., Winooski, VT, USA).

2.3.4. Flow Cytometry Analyses

For the flow cytometry analyses, the cells at the end of the treatment were harvested into the medium using Accutase, centrifuged at 200 × g for 5 min at room temperature, washed with PBS, centrifuged again at 200 × g for 5 min, and then fixed by the addition of 1 mL of ice-cold 70% ethanol by individual drops with gentle vortexing, and stored at 4 °C for at least 30 min. Before the flow cytometry analyses, fixed cells were centrifuged (200 × g for 5 min), and the pellet was washed twice with FACS (Fluorescent Activated Cell Sorting) buffer (0.5 M EDTA, 2% FBS, 1 × PBS) and finally resuspended in 250 µL of FACS buffer with 50 µL of RNase A (0.1 mg/mL) for 30 min at 37 °C. The nuclei were stained by adding propidium iodide (Thermo Fisher Scientific, Waltham, MA, USA) to make a final concentration of 50 µg/mL. Samples were incubated in the dark for 30 min at room temperature and subjected to FACS analysis. Data were collected for a minimum of 6000 events per sample. Flow cytometry was performed by use of a BD FACS Canto II cytometer (Becton Dickinson, Franklin Lakes, NJ, USA) with excitation at 535 nm and emission at 617 nm. The analyses were performed with FlowJo 7.2.2 software (Tree Star, Ashland, OR, USA).

2.4. Western Blot Analysis

Samples of self-renewing NSC were harvested after 96 h of treatment with BR (12.5 µM) or LR (12.5 and 25 µM) and analyzed according to Fedorová et al. [21]. In brief, the NSC were washed once with PBS, lysed by 250 µL of lysis buffer (50 mM TRIS-HCl pH 6.8, 1% SDS, 10% glycerol), and stored at −20 °C. The protein concentration was measured by a DC Protein Assay Kit (BioRad, Prague, Czech Republic). Ten µg of total protein per well was separated using 8 to 10% SDS-polyacrylamide gel electrophoresis. The proteins were transferred to the PVDF (polyvinylidene fluoride) membrane (Merck, Millipore, MA, USA), blocked with 5% milk in Tris-buffered saline, and incubated overnight at 4 °C with the appropriate primary antibody. The membranes were incubated with secondary antibodies, and the proteins were visualized on AGFA film using Amersham ECL Prime Western blotting detection reagent (GE Healthcare Life Sciences, Marlborough, MA, USA). β-actin was used as a loading control. The list of antibodies is described in Table S1. The densitometry was performed using FIJI software, and the data were visualized using GraphPad Prism version 8.0.0 for Windows (GraphPad Software, San Diego, CA, USA; www.graphpad.com accessed on 15 July 2021).

2.5. DNA Damage Analysis (Comet Assay)

For these analyses, the NSC that were treated with H₂O₂ (3.7 ppm) for 10 min before harvesting were used as a positive control. The cells were detached from the surface by Accutase and harvested in the basic NSC medium without FGF2. After centrifugation at 200 × g for 5 min, the supernatant was aspirated and cells were stored in the freezing medium (60% basic NSC medium, 30% FBS, 10% DMSO) in liquid nitrogen. To measure the genotoxicity, the cell suspension was centrifuged at 1000 × g for 1 min, and the pellet was

re-suspended in 0.5 mL of PBS. Fifty μ L of the suspension was mixed with 150 μ L of low melting point agarose (0.01 g/mL), and 80 μ L of the resulting agarose-cell suspension was seeded on a pre-coated slide with 1% agarose. Cell lysis, gel electrophoresis, and staining were performed as previously described [22]. The slides were analyzed for the tail length and intensity using an ImageJ 1.51s (National Institutes of Health, Bethesda, MA, USA) connected to a fluorescence microscope (AX70 Provis, Olympus, Japan).

2.6. Immunofluorescence and Cell Imaging

For the cell imaging experiments, NSC cells were seeded at a density of either 12,000/cm² or 25,000/cm² (for differentiation to neurons) as previously described. After fixation with 4% paraformaldehyde, the cells were washed three times with PBS and permeabilized with buffer (0.2% Triton X100 with 1 \times PBS) for 15 min, and the primary antibodies were incubated overnight at 4 °C. Next, the slides were washed three times with PBS. Secondary antibodies and Hoechst were added with the permeabilization buffer and incubated for 1 h at room temperature (the antibodies' dilutions are described in Table S2A,B). After incubation, the slides were washed three times with PBS, dried, and mounted onto microscopic slides with Mowiol 4-88 Reagent (Merck, Darmstadt, Germany). Cell imaging was performed with a Zeiss LSM 800 Laser scanning confocal microscope using an ORCA-Flash 4.0LT digital sCMOS monochromatic camera and Plan-Neofluar 20 \times /0.50 AIR objective (Zeiss, Jena, Germany).

2.7. RNA Isolation and Quantitative Real-Time RT-PCR

Samples for analyses were harvested 12 and 17 days after the seeding of the NSC for terminal differentiation. Total RNA was isolated using RNA Blue reagent (Top-Bio, Prague, Czech Republic) according to the manufacturer's instructions. The total amount of RNA was measured by a NanoDrop[®] ND 1000 UV-Vis spectrophotometer (Thermo Fisher Scientific, Waltham, MA, USA). For quantitative real-time RT-PCR, cDNA was synthesized by a Transcriptor first-strand cDNA synthesis kit (Roche, Basel, Switzerland), and the analyses were performed in triplicates using SYBR Green I Master (Roche, Basel, Switzerland) according to the manufacturer's instructions. The designed PCR primers by PrimerBank and OriGene are described in Table S3. DNA amplification was detected with 2^{- Δ Ct} analysis using a LightCycler 480 II (Roche, Mannheim, Germany). The relative mRNA levels were normalized to GAPDH. The data were visualized using GraphPad Prism version 8.0.0 for Windows.

2.8. Statistical Analyses

All data are expressed as the mean \pm standard deviation. Depending on their distribution, the data were assessed either by *t*-test or Mann-Whitney test using Prism 8.0.1 software (GraphPad, San Diego, CA, USA). Differences were considered statistically significant at a *p*-value \leq 0.05.

3. Results

3.1. The Effect of BR and LR on the Viability of NSC

In the initial phase of our studies on self-renewing NSC derived from hPSC, we intended to assess the possible cytotoxic effects of both BR and its major photoisomer LR. After 96 h of continuous exposure to BR or LR, a decreased number of the cells treated with higher concentrations of both pigments were clearly detectable; this effect was most pronounced with the 50 μ M concentration of BR (Figure 1A—Brightfield panels).

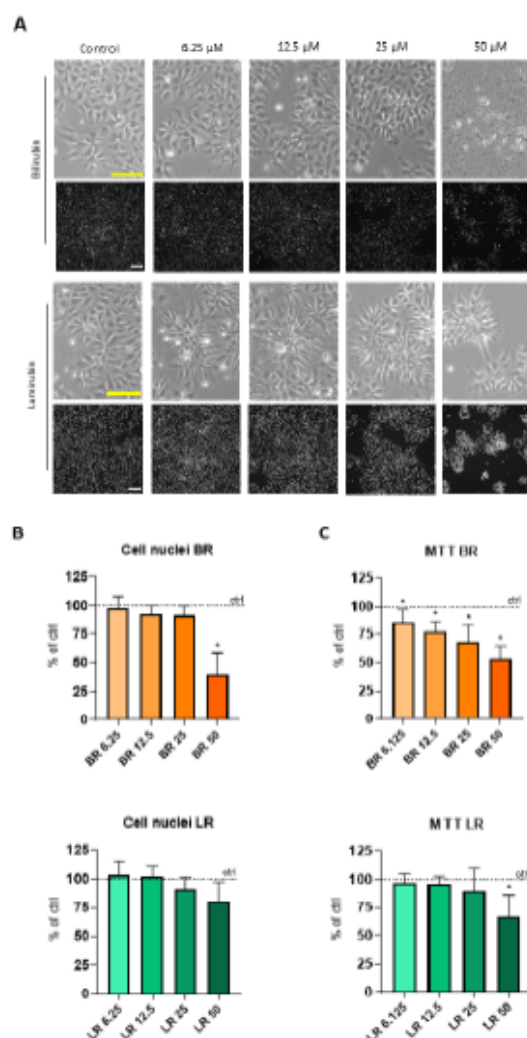


Figure 1. The effect of BR and LR on the viability of NSC. (A) Morphology of NSC exposed to BR and LR (brightfield images, scale bar = 250 μ m) and Visualization of the cell nuclei (bottom black panels; scale bar = 150 μ m, stained with Hoechst). (B) Cell nuclei quantification of NSC exposed to BR and LR. Stained by Hoechst and analyzed by CellProfiler and ImageJ. Controls expressed as 100%. $n = 4$. (C) Viability/metabolic activity of NSC exposed to BR and LR. Analyzed by MTT test. Controls expressed as 100%. $n = 4$, * $p < 0.05$, exposure time = 96 h.

To quantify this phenomenon, the number of cell nuclei was evaluated using image analysis and the MTT assay was also performed. A significantly decreased number of nuclei was observed in the cells after exposure to the 50 μ M BR concentration ($p < 0.05$) (Figure 1A—upper black panel, and Figure 1B), which was also confirmed in the viability assay (MTT test). In this test, a gradual and significant decrease in the viability/metabolic activity of the cells exposed to BR was observed within the whole range of tested concentrations (6.25–50 μ M) (Figure 1C). Compared to BR, the effect of LR on the viability/metabolic activity of the treated cells was much lower, and only visible at the highest concentration

(50 μ M) (Figure 1C), indicating the much higher toxicity of BR on NSC compared to LR, its photo-oxidation product.

3.2. The Effect of BR and LR on the Proliferation and Cell Cycle of NSC

Based on the morphology and data on the counting of nuclei shown in Figure 1, 12.5 μ M concentrations of BR and LR were selected for all of the experiments that followed. For both BR and LR, the cells exposed to these concentrations retained a healthy morphology and the numbers of cell nuclei were comparable to those in the solvent controls. As the MTT assay is a measure of metabolic activity [14,23], we assumed that adverse effects detected after treatment with BR might have been affected by its impact on cellular metabolism rather than viability. In addition, it should be noted that the selected LR concentration is biologically relevant for hyperbilirubinemic neonates treated with PT, as proven in our previous clinical observation [8].

The growth curves constructed to analyze the effect of both pigments on the NSC proliferation rate did not demonstrate anything adverse during 96 h of exposure (Figure 2A); although a slight but a non-significant trend toward slower proliferation of BR-treated cells was detectable. Subsequent measurements of the cell cycle profile and distribution of cells in the cell cycle phases confirmed that NSC treated with BR or LR do not accumulate in any of the phases of the cell cycle (Figure 2B,C).

To further explore the possible effects of BR and LR on the NSC, the protein expressions of the following apoptotic or DNA damage-related markers were analyzed in NSC exposed to both pigments for 96 h: tumor suppressor protein p53, cleaved nuclear poly (ADP-ribose) polymerase (c-PARP), and the phosphorylated form of H2A histone family member X (γ -H2AX). Although no significant changes in the expression of p53 were detectable in the cells, a significantly increased c-PARP ($p < 0.05$) and γ -H2AX ($p < 0.05$) protein expression was observed in NSC exposed to BR. Conversely, a significant and completely opposite trend of the expression of c-PARP in NSC exposed to LR was detected ($p < 0.05$, Figure 2D). Lastly, in this set of experiments the extent of DNA damage/single- and double-strand breaks in the cells exposed to BR and LR was quantified by Comet assay. Nevertheless, no significant changes in these parameters of NSC exposed to both pigments were observed (Figure 2E). Overall, our results demonstrated that the proliferation and cell cycle of NSC were not significantly altered after exposure to BR or LR. However, substantial changes were detectable on a molecular level where BR exposure induced apoptotic (c-PARP) and DNA damage (γ -H2AX) markers, while LR-exposure in clinically relevant concentrations exerted protective effects against these changes.

3.3. LR Induces Morphological Changes and Rosette Formation in Self-Renewing NSC

While testing the toxicity of various concentrations of LR on NSC (as shown in Figure 1A), we noticed that with increasing concentrations of LR, the NSC significantly changed their undifferentiated arrangement and acquired a different phenotype.

In order to explore this phenomenon in greater detail, immunofluorescent staining of those markers typical for the rosette structures was performed to confirm this observation. Specifically, we detected substantial changes in the N-cadherin, zonula occludens-1 (ZO-1), and β -catenin distribution within the NSC, all markers of the formation of neural rosettes (Figure 3A) [24,25]. As visualized by immunostaining, the cells retained the expression of SOX1 and SOX2, the crucial transcription factors (Figure 3A) [25,26]. These changes were clearly visible in LR at a concentration of 12.5 μ M and were even more pronounced when using 2-fold higher concentration. Our data indicated that NSC treated with LR showed a significantly polarized phenotype, typical for immature neural rosettes, being even more apparent with higher concentrations of LR. Importantly, this phenomenon was unique to LR; it was not detected in NSC exposed to BR.

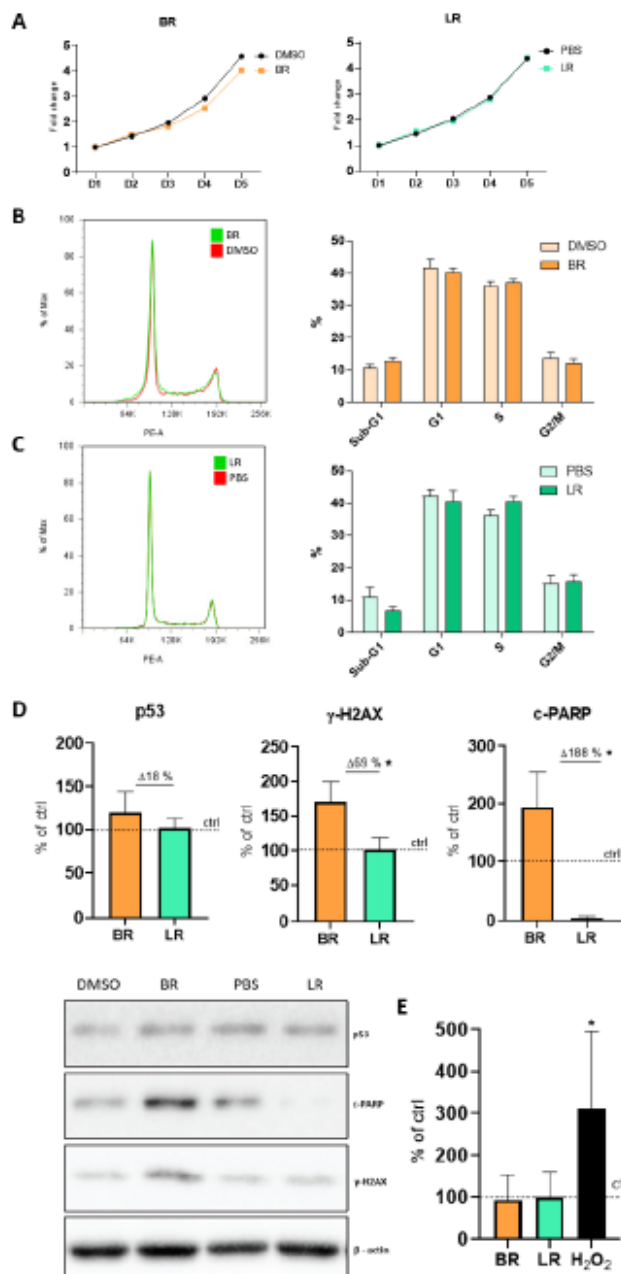


Figure 2. The effect of BR and LR exposure on behavior of NSC. (A) Growth curve of the NSC exposed BR. BR and LR concentration = 12.5 μM, 0.1% DMSO and 1% PBS used as respective controls. Exposure time = 96 h, n = 4. (B,C) Cell cycle analysis of NSC exposed to BR and LR. (B) 12.5 μM BR (BR 12.5) and 0.1% DMSO (BR control). n = 4; (C) 12.5 μM LR (LR 12.5) with 1% PBS (LR control). n = 4; charts represent the quantification of at least four independent measurements. BR and LR concentrations = 12.5 μM, 0.1% DMSO and 1% PBS used as respective controls. Exposure time = 96 h,

$n = 4$. (D) Expression of p53, c-PARP, and γ -H2AX proteins in NSC exposed to BR and LR. BR and LR concentrations = 12.5 μ M, 0.1% DMSO and 1% PBS used as the respective controls. β -actin was used as a loading control. Quantification of Western blots was performed using ImageJ. Exposure time = 96 h, $n = 3$, * $p < 0.05$. (E) The extent of DNA damage/single- and double-strand breaks of NSC exposed to BR and LR. Analyses performed by the Comet assay. BR and LR concentrations = 12.5 μ M, 0.1% DMSO and 1% PBS used as respective controls, H_2O_2 was used as a positive control. Exposure time = 96 h, $n = 3$.

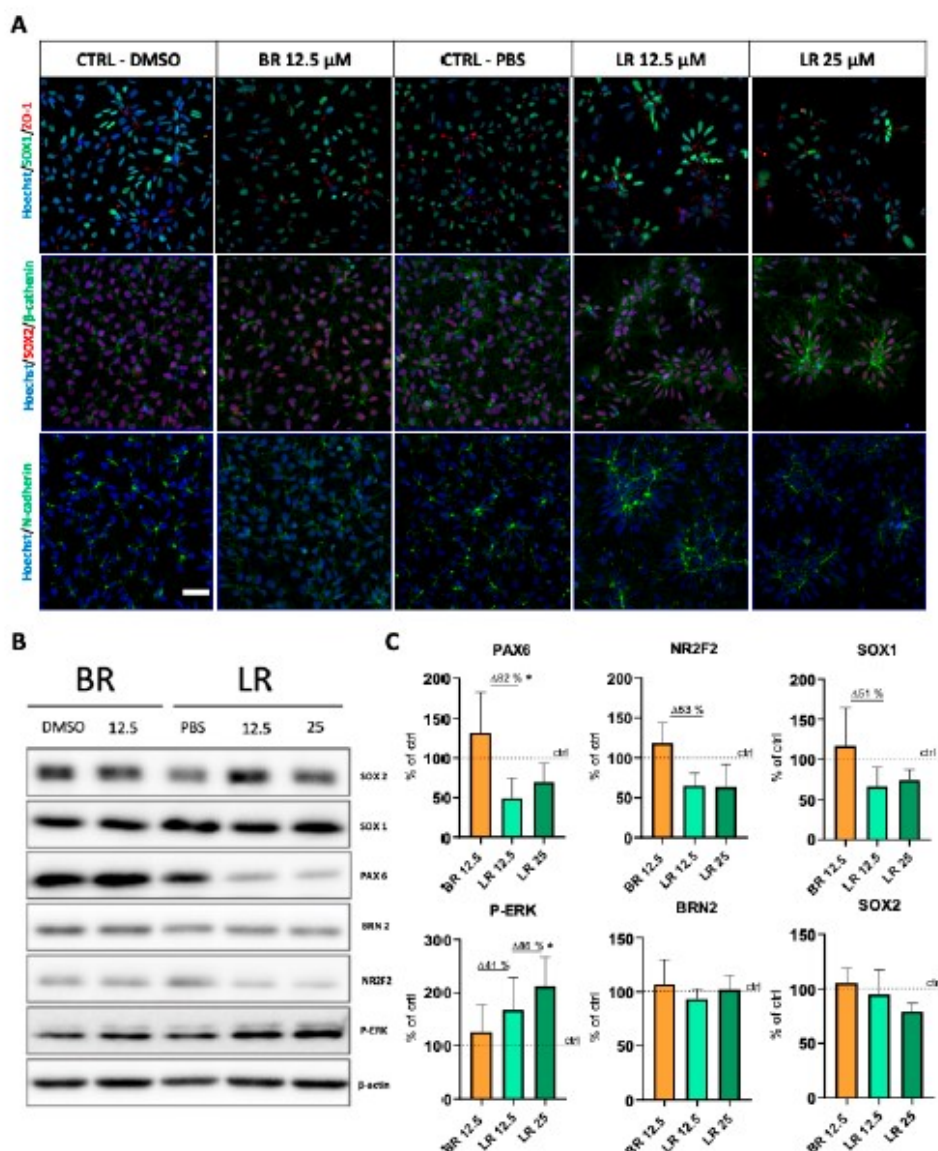


Figure 3. The effect of BR and LR on the NSC differentiation markers. (A) Immunostaining of apically localized cell polarity proteins of NSC exposed to BR and LR. Staining and visualization was performed after 96 h exposure of the NSC to 12.5 μ M

BR (BR 12.5) with 0.1% DMSO (BR control), 12.5/25 μ M LR (LR 12.5/25) with 1% PBS (LR control). Cells were labeled by three combinations (1) SOX1 (green) and ZO-1 (red), (2) SOX2 (red) and β -catenin (green), and (3) N-cadherin (green). Nuclei were counterstained with Hoechst (blue) and visualized with a Zeiss LSM 800. Scale bar = 50 μ m. (B) Western Blot analysis of NSC-specific transcription factors. Data were normalized first to β -actin (used here as a loading control), and then visualized as percentage of respective control. (C) Quantification of protein expressions of NSC-specific transcription factors. Quantification of Western blot signals performed using ImageJ. $n = 3$. * $p < 0.05$.

Based on these results, Western blot analysis of NSC-specific transcription factors was performed. These included those expressed upon differentiation of hPSC towards neuroectoderm, such as PAX6, SOX1, SOX2, BRN2, and NR2F2 [21]. Interestingly, compared to BR treatment, expressions of NSC-specific markers upon exposure to LR showed no change (BRN2, SOX2), a minor decrease (SOX1, NR2F2), or a significant drop (PAX6; $p < 0.05$) (Figure 3B,C). In addition, we also analyzed ERK activation (ERK/P-ERK), a signaling pathway important for neural cell differentiation from NSC [27]. Interestingly, a significant and dose-dependent upregulation of P-ERK expression was clearly present upon exposure of the NSC to LR.

The data strongly suggested that LR-treated self-renewing NSC acquire a significantly different morphology reminiscent of immature rosettes, with apically localized cell polarity proteins; a phenomenon accompanied by changes in various transcription factors and activation of an ERK signaling pathway.

3.4. The Effect of BR and LR Exposure on Terminal Differentiation of NSC

Lastly, in order to determine if BR or LR affected the ability of the NSC to terminally differentiate into neurons, the NSC were exposed to both pigments and the extent of their terminal differentiation was subsequently assessed. NSC were seeded in a standard conditioned growth medium on Day 0, and the treatment was started three days after plating (for details of the experimental design see Figure 4A).

First, the general morphology of the neurons was evaluated using immunofluorescence staining at the end of our differentiation protocol. As shown in Figure 4B, differentiating NSC formed a homogeneously distributed network of tubulin (TUJ)-positive neuronal filaments. However, no significant morphological differences between BR- or LR-treated cells (and their respective solvent controls) were detectable in these experiments. The gene expression of selected differentiation-associated markers was then analyzed. The results showed that the NSC had gradually increased the expression of selected neuronal markers (such as DCX, TUJ, MAP2, NFL, and NFM) as well as glial markers (S100 β and GFAP), while there were no changes in the expression of the neural stem cell markers (SOX2, SOX1, and PAX6). However, no significant changes in the expression of any of these analyzed markers were observed after treatment with BR or LR. This is certainly a notable observation, since just a short-term exposure led to significant changes in these markers (Figure 3C), suggesting these pigments played a role in the earlier phases of differentiation of the NSC, an influence which, however, was later lost. Altogether, our data suggest that despite visible changes in the morphology of NSC, no major changes can be detected at the level of the terminal differentiation of NSC towards neuronal and glial cell types.

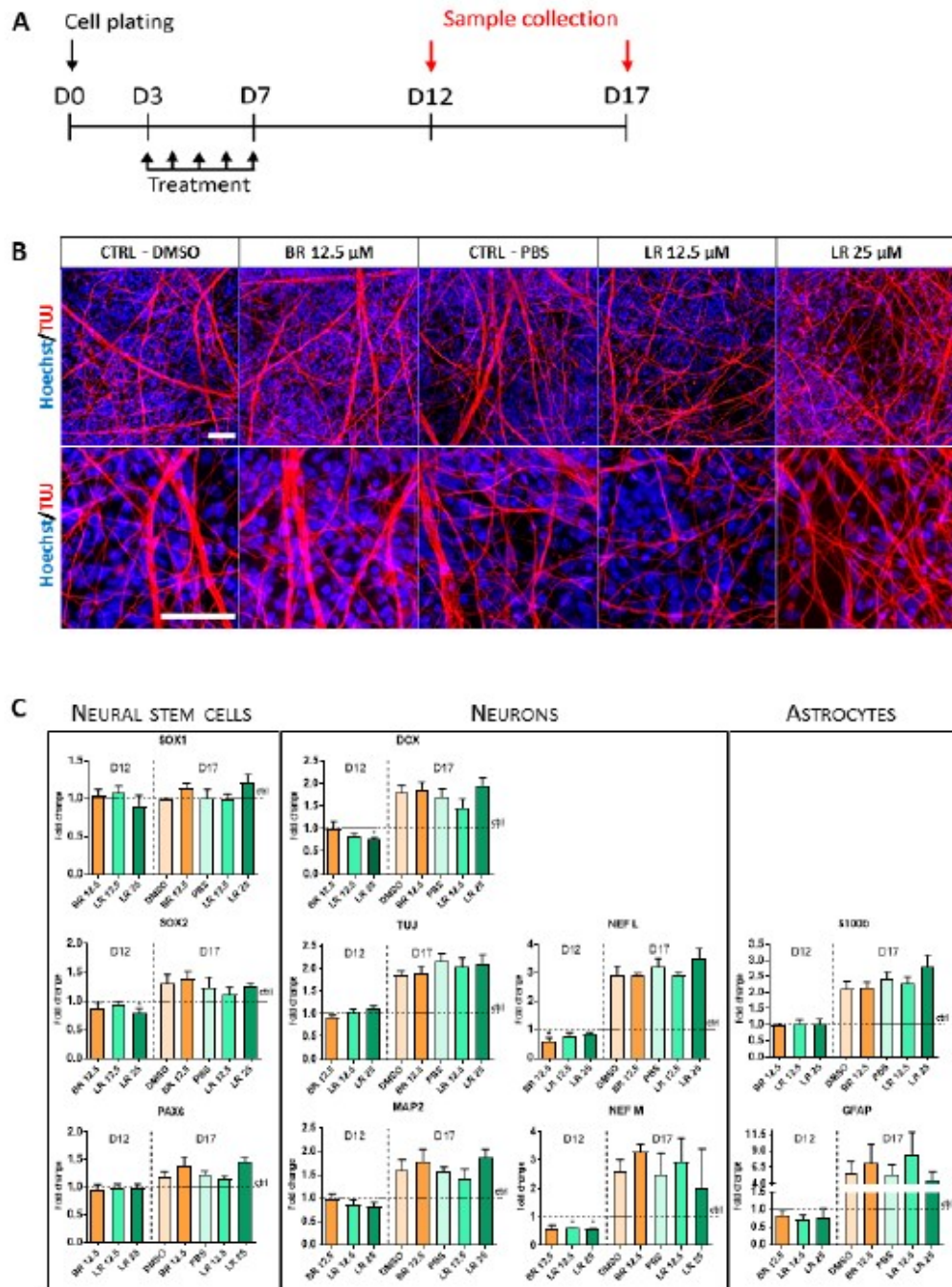


Figure 4. The effect of BR and LR on terminal differentiation of NSC. (A) Experimental layout. (B) Tubulin-positive neuronal filament formation upon exposure to BR and LR. Visualization was performed after 17 days of terminal differentiation, when the NSC were treated with 12.5 μ M BR (BR 12.5) and 0.1% DMSO as a control, and 12.5 μ M LR (LR 12.5) and 25 μ M

LR (LR 25) with 1% PBS as a control. Cells were stained by Hoechst (blue) and TUJ (red) and visualized with a Zeiss LSM 800. Scale bars = 50 μm . (C) The effect of BR and LR exposure on the expression of selected markers specific for NSC, neurons, and astrocytes. Samples were harvested on Day 12 and 17 of terminal differentiation. * $p < 0.05$. Two different time points were chosen to evaluate possible changes in the onset/timing of the differentiation process. Genes were detected using a LightCycler 480 II. Relative mRNA levels were normalized to GAPDH with $2^{-\Delta\text{Ct}}$ analysis. $n = 3$.

4. Discussion

Severe neonatal hyperbilirubinemia represents a serious health threat for newborn infants with global health and socioeconomic burdens [2,28]. Although PT is considered the gold standard treatment for severely jaundiced neonates, there is a surprising lack of scientific data on the biological effects of bilirubin photo-oxidation products generated during PT. Importantly, PT does not seem to be entirely safe, particularly in ELBW preterm neonates [10,11].

As was demonstrated in our recent study, a short-term 4-h exposure to BR and its photoisomer LR, as well as monopyrrolic BOX-A and BOX-B of human neuroblastoma (SH-SY5Y), glioblastoma (U-87), and microglial cells (HMC3) (representing major brain cerebral cell populations), did not affect cell viability at all, even at the biologically relevant concentrations (25 μM) [13]. However, prolongation of exposure of the neuronal cells up to 24–48 h revealed clear BR toxicity, while LR did not have this toxic effect [14]. One of the reasons for these observations lies in the profound inhibitory effects of BR on mitochondrial respiration and the tricarboxylic acid cycle metabolism [14]. BR neurotoxicity has also been confirmed in more complex studies, such as those on organotypic brain slices derived from hyperbilirubinemic Gunn rat pups [29], plus other experimental studies (for review of the mechanisms see [5]), as well as in numerous clinical observations [2,28]. These findings are consistent with the early studies by Silberberg et al., who did not detect any toxic effects of photo-irradiated bilirubin on myelinating cerebellum cultures—in contrast to bilirubin [30]. However, LR (and also the other BR photo-oxidation products) do not appear to be harmless. In another of our recent studies, the potential neuroinflammatory effects of LR as evidenced by overexpression of proinflammatory cytokines in brain cells were clearly documented [13]. It is important to note that numerous studies confirmed proinflammatory cytokines exerting harmful effects on neurogenesis [31]; these results are in agreement with the clinical data on hyperbilirubinemic newborn infants treated with PT, which demonstrate an increase in systemic concentrations of circulating proinflammatory cytokines [32].

Based on these findings, and since NSC have never been studied for their susceptibility to the potentially harmful effects of BR, we focused on the possible cytotoxic effects of BR and LR on these cells. We observed a significantly decreased viability and metabolic activity in those cells treated with gradually increasing concentrations of BR, while LR only had a significant effect only at the highest concentration.

As discussed above, BR in high concentrations clearly exerts cytotoxicity, in particular on cells of the central nervous system (CNS). However, the pathogenesis of the whole process is not fully understood, with significant differences in susceptibility to BR toxicity across various brain regions and cell populations [29,33]. Previous studies have also shown that exposure to increasing concentrations of unconjugated BR are cytotoxic to rat oligodendrocytes and increase its apoptosis *in vitro* [34]. Several additional studies have shown the cytotoxic and pro-apoptotic effects of BR on astrocytes' neuronal cultures [35–39]. Although under our study conditions no significant changes in DNA damage were observed using the Comet assay, and the flow cytometry analysis demonstrated only a negligible modulation of the cell cycle of treated NSC exposed to BR, an increase in c-PARP (apoptotic), $\gamma\text{-H2AX}$ (DNA damage), and p53 (apoptosis activator) protein expression was clearly demonstrable, consistent with previous reports mapping BR-induced apoptosis and DNA fragmentation in rat brain neurons [40]. Importantly, these changes in NSC were prevented by the biologically relevant concentration of LR (12.5 μM), suggesting the neuroprotective effects of LR. Hence, changes at the molecular level may not be apparent when using non-

specific methods, such as the Comet assay (used in our study), where the negative result could be explained by its decreased sensitivity during the analysis of small pro-apoptotic changes [41]. On the other hand, the data are in contrast with observations on DNA damage in peripheral blood lymphocytes [42–45] and increased serum apoptotic markers [46] in phototherapy-treated newborn infants suggesting cell-specific responsiveness to BR and LR.

Interestingly, while performing these studies on the cytotoxicity of BR and LR, we noticed that LR induced major morphological changes in our self-renewing NSC, while no such changes were noticed after exposure to BR. This observation may be of clinical importance, since cellular polarity plays a significant role during the development of the CNS [47]. During the onset of neural differentiation *in vivo*, the neuroepithelium forming the neural tube represents the first polarized single cell layer with a central lumen and cells displaying apicobasal polarity [48]. Under *in vitro* conditions, this phenomenon is mimicked by the formation of neural rosettes—radially organized neuroepithelial cells differentiated from hPSC [21,48–50]. Such polarity also ensures a different distribution of junction proteins (such as N-cadherin, ZO-1, and β -catenin) as well as of signaling molecules including Notch, Sonic Hedgehog, or FGF2/ERK [24,49,50]. Importantly, the rosette structures also represent the niche from which NSC are isolated. Surprisingly, our study demonstrated for the first time that LR induces NSC to repolarize, and that this induction is dose-dependent. Additionally, these repolarized NSC cultures, possibly as a positive feedback mechanism, expressed higher amounts of phosphorylated ERK, important for the process of neurogenesis [27], as well as showing an altered expression of NSC-specific markers including PAX6, NR2F2, and SOX1. Thus, our data suggested that LR has the potential to affect the polarity and identity of NSC during early human neural development. These results may be of clinical relevance, since aggressive PT is used on preterm ELBW neonates, often accompanied by serious adverse effects [10,11]. It is also well known that the processes of neurogenesis and neurodevelopment are impaired in these neonates [51], which may even be exacerbated by BR photo-oxidation products generated during PT, based on our current data.

Finally, we also assessed the capacity of BR or LR to affect the terminal differentiation of NSC. Previously, it has been shown that moderate to severe hyperbilirubinemia could induce neurological dysfunction and potentially impair brain myelination with long-term sequelae, particularly in preterm infants [6]. However, studies addressing the possible effects of LR and/or other BR photo-oxidation products so far have not been reported. Here, we found that despite significant changes in the expression of pro-apoptotic markers in BR-exposed NSC, or altered cell polarity and morphology in LR-exposed NSC, no major changes were detected in differentiating neurons or in their gene expressions.

5. Conclusions

Our study has assessed the possible impact of BR as well as its major photoisomer LR on human neurodevelopment using an *in vitro* model of hPSC-derived NSC. Our data demonstrate that neither of these compounds significantly affected the extent of terminal differentiation of neurons and astrocytes. However, compared to LR, BR exerted a higher cytotoxicity on self-renewing NSC, and this effect was dose-dependent and accompanied by mildly elevated pro-apoptotic markers. On the other hand, LR had a dose-dependent effect on the morphology of self-renewing NSC, inducing them to form highly polarized structures with lower expressions of some NSC-specific markers, but with activation of ERK signaling. Considering the tightly orchestrated processes during the formation of the CNS, this effect of changed cell polarity and identity could potentially have a detrimental effect on the developing brain. Although complex mechanisms behind these phenomena remain to be addressed, both BR and LR clearly affect early human neurodevelopment *in vitro*.

Supplementary Materials: The following are available online at <https://www.mdpi.com/article/10.3390/antiox10101532/s1>, Table S1: List of antibodies used for Western blot analyses, Table S2: List of primary and secondary antibodies used for the studies, Table S3: List of genes used for gene expression analyses.

Author Contributions: Conceptualization, D.B. and L.V.; methodology, N.C., V.P., V.E., J.R., K.P., A.D., J.V. and M.D.B.; validation, N.C., A.D. and L.V.; investigation, N.C., V.P. and A.D.; resources, L.V. and D.B.; writing original draft preparation, N.C.; writing, review and editing, A.D., D.B. and L.V.; visualization, L.V.; supervision, A.D., D.B. and L.V.; project administration; funding acquisition, L.V. and D.B. All authors have read and agreed to the published version of the manuscript.

Funding: This research was funded by the grants RVO-VFN64165/2021 from the Czech Ministry of Health, NV18-07-00342 from the Czech Health Research Council, and 21-01799S and 18-25429Y from the Czech Science Foundation. Further support was provided by the following institutional projects: the European Regional Development Fund—Project INBIO (No. CZ.02.1.01/0.0/0.0/16_026/0008451), the National Program of Sustainability II (by the Ministry of Education, Youth, and Sports of the Czech Republic (Project no. LQ1605)). We also acknowledge the core facility CELLIM supported by MEYS CR (LM2018129 Czech-BioImaging).

Institutional Review Board Statement: Not applicable.

Informed Consent Statement: Not applicable.

Data Availability Statement: All research data are available on request from the Corresponding Author. We do not have webpages created for such purpose, but as clearly stated the data are available on request and can be sent to anyone interested in our research.

Acknowledgments: The authors would like to acknowledge Stjepan Uldrijan and Natalia Vadicova, from the Department of Biology, Masaryk University Brno, for their help with measurements and for the sharing of equipment; Borivoj Vojtesek (MOU, Brno) for providing us with Do-1 antibody; and Ales Hampl, from the Department of Histology and Embryology, Masaryk University Brno, for his support.

Conflicts of Interest: The authors all declare no conflict of interest. The funders had no role in the design of the study, nor in the collection, analyses, and interpretation of data, in the writing of the manuscript, or in the decision to publish the results.

References

- Vitek, L.; Tiribelli, C. Bilirubin: The yellow hormone? *J. Hepatol.* **2021**. [CrossRef] [PubMed]
- Stevenson, D.K.M.M.J.; Watchko, J.F. (Eds.) *Care of the Jaundiced Neonate*; McGraw-Hill: New York, NY, USA, 2012.
- Hegyí, T.; Goldie, E.; Hiatt, M. The protective role of bilirubin in oxygen-radical diseases of the pre-term infant. *J. Perinatol.* **1994**, *14*, 296–300. [PubMed]
- Shekeeb, S.M.; Kumar, P.; Sharma, N.; Narang, A.; Prasad, R. Evaluation of oxidant and antioxidant status in term neonates: A plausible protective role of bilirubin. *Mol. Cell. Biochem.* **2008**, *317*, 51–59. [CrossRef] [PubMed]
- Watchko, J.F.; Tiribelli, C. Bilirubin-induced neurologic damage-mechanisms and management approaches. *N. Engl. J. Med.* **2013**, *369*, 2021–2030. [CrossRef] [PubMed]
- Brites, D.; Fernandes, A. Bilirubin-induced neural impairment: A special focus on myelination, age-related windows of susceptibility and associated co-morbidities. *Sem. Fetal Neonatal Med.* **2015**, *20*, 14–19. [CrossRef] [PubMed]
- Maisels, M.J.; McDonagh, A.E. Phototherapy for neonatal jaundice. *N. Engl. J. Med.* **2008**, *358*, 920–928. [CrossRef] [PubMed]
- Jasprova, J.; Dvorak, A.; Vecka, M.; Lenicek, M.; Lacina, O.; Valaskova, P.; Zapadlo, M.; Plavka, R.; Klan, P.; Vitek, L. A novel accurate LC-MS/MS method for quantitative determination of Z-lumirubin. *Sci. Rep.* **2020**, *10*, 4411. [CrossRef]
- Lightner, D.A.; Linnane, W.P., III; Ahlfors, C.E. Bilirubin photooxidation products in the urine of jaundiced neonates receiving phototherapy. *Pediatr. Res.* **1984**, *18*, 696–700. [CrossRef]
- Wang, J.; Guo, G.; Li, A.; Cai, W.Q.; Wang, X. Challenges of phototherapy for neonatal hyperbilirubinemia (Review). *Exp. Ther. Med.* **2021**, *21*, 231. [CrossRef]
- Faulhaber, F.R.S.; Procianny, R.S.; Silveira, R.C. Side effects of phototherapy on neonates. *Am. J. Perinatol.* **2019**, *36*, 252–257. [CrossRef]
- Clark, J.F.; Reilly, M.; Sharp, F.R. Oxidation of bilirubin produces compounds that cause prolonged vasospasm of rat cerebral vessels: A contributor to subarachnoid hemorrhage-induced vasospasm. *J. Cereb. Blood Flow Metab.* **2002**, *22*, 472–478. [CrossRef]
- Jašprová, J.; Dal Ben, M.; Humý, D.; Hwang, S.; Žižalová, K.; Koček, J.; Wong, R.J.; Stevenson, D.K.; Gazzin, S.; Tiribelli, C.; et al. Neuro-inflammatory effects of photodegradative products of bilirubin. *Sci. Rep.* **2018**, *8*, 7444. [CrossRef]

14. Dvorak, A.; Pospisilova, K.; Zizalova, K.; Capkova, N.; Muchova, L.; Vecka, M.; Vrzackova, N.; Krizova, J.; Zelenka, J.; Vitek, L. The effects of bilirubin and lumirubin on metabolic and oxidative stress markers. *Front. Pharmacol.* **2021**, *12*, 567001. [\[CrossRef\]](#)
15. Bohaciakova, D.; Hruska-Plochan, M.; Tsunemoto, R.; Gifford, W.D.; Driscoll, S.P.; Glenn, T.D.; Wu, S.; Marsala, S.; Navarro, M.; Tadokoro, T.; et al. A scalable solution for isolating human multipotent clinical-grade neural stem cells from ES precursors. *Stem Cell Res. Ther.* **2019**, *10*, 83. [\[CrossRef\]](#) [\[PubMed\]](#)
16. Falk, A.; Koch, P.; Kesavan, J.; Takashima, Y.; Ladewig, J.; Alexander, M.; Wiskow, O.; Taylor, J.; Trotter, M.; Pollard, S.; et al. Capture of neuroepithelial-like stem cells from pluripotent stem cells provides a versatile system for in vitro production of human neurons. *PLoS ONE* **2012**, *7*, e29597. [\[CrossRef\]](#) [\[PubMed\]](#)
17. Koch, P.; Opitz, T.; Steinbeck, J.A.; Ladewig, J.; Brustle, O. A rosette-type, self-renewing human ES cell-derived neural stem cell with potential for in vitro instruction and synaptic integration. *Proc. Natl. Acad. Sci. USA* **2009**, *106*, 3225–3230. [\[CrossRef\]](#) [\[PubMed\]](#)
18. Yuan, S.H.; Martin, J.; Elia, J.; Flippin, J.; Paramban, R.I.; Hefferan, M.P.; Vidal, J.G.; Mu, Y.; Killian, R.L.; Israel, M.A.; et al. Cell-surface marker signatures for the isolation of neural stem cells, glia and neurons derived from human pluripotent stem cells. *PLoS ONE* **2011**, *6*, e17540. [\[CrossRef\]](#)
19. McDonagh, A.E.; Assisi, F. The ready isomerization of bilirubin IX-a in aqueous solution. *Biochem. J.* **1972**, *129*, 797–800. [\[CrossRef\]](#) [\[PubMed\]](#)
20. Jaspova, J.; Dal Ben, M.; Vianello, E.; Goncharova, I.; Urbanova, M.; Vyroubalova, K.; Gazzin, S.; Tiribelli, C.; Sticha, M.; Cerna, M.; et al. The biological effects of bilirubin photoisomers. *PLoS ONE* **2016**, *11*, e0148126. [\[CrossRef\]](#)
21. Fedorova, V.; Vanova, T.; Elnefae, L.; Pospisil, J.; Petrasova, M.; Kolajova, V.; Hudacova, Z.; Baniarova, J.; Barak, M.; Peskova, L.; et al. Differentiation of neural rosettes from human pluripotent stem cells in vitro is sequentially regulated on a molecular level and accomplished by the mechanism reminiscent of secondary neurulation. *Stem Cell Res.* **2019**, *40*, 101563. [\[CrossRef\]](#) [\[PubMed\]](#)
22. McKelvey-Martin, V.J.; Green, M.H.; Schmezer, P.; Pool-Zobel, B.L.; De Meo, M.P.; Collins, A. The single cell gel electrophoresis assay (comet assay): A European review. *Mutat. Res.* **1993**, *288*, 47–63. [\[CrossRef\]](#)
23. Chacon, E.; Acosta, D.; Lemasters, J.J. Primary cultures of cardiac myocytes as in vitro models for pharmacological and toxicological assessments. In *In Vitro Methods in Pharmaceutical Research*; Castell, J.V., Gomez-Lechon, M.J., Eds.; Academic Press: New York, NY, USA, 1997; pp. 209–223. [\[CrossRef\]](#)
24. Miyamoto, Y.; Sakane, F.; Hashimoto, K. N-cadherin-based adherens junction regulates the maintenance, proliferation, and differentiation of neural progenitor cells during development. *Cell Adhes. Migr.* **2015**, *9*, 183–192. [\[CrossRef\]](#)
25. Efthymiou, A.G.; Chen, G.; Rao, M.; Chen, G.; Boehm, M. Self-renewal and cell lineage differentiation strategies in human embryonic stem cells and induced pluripotent stem cells. *Expert Opin. Biol. Ther.* **2014**, *14*, 1333–1344. [\[CrossRef\]](#)
26. Kamachi, Y.; Cheah, K.S.; Kondoh, H. Mechanism of regulatory target selection by the SOX high-mobility-group domain proteins as revealed by comparison of SOX1/2/3 and SOX9. *Mol. Cell Biol.* **1999**, *19*, 107–120. [\[CrossRef\]](#)
27. Kunath, T.; Saba-El-Leil, M.K.; Almousaillekh, M.; Wray, J.; Meloche, S.; Smith, A. FGF stimulation of the Erk1/2 signalling cascade triggers transition of pluripotent embryonic stem cells from self-renewal to lineage commitment. *Development* **2007**, *134*, 2895–2902. [\[CrossRef\]](#) [\[PubMed\]](#)
28. Slusher, T.M.; Zamora, T.G.; Appiah, D.; Stanke, J.U.; Strand, M.A.; Lee, B.W.; Richardson, S.B.; Keating, E.M.; Siddappa, A.M.; Olusanya, B.O. Burden of severe neonatal jaundice: A systematic review and meta-analysis. *BMJ Paediatr. Open* **2017**, *1*, e000105. [\[CrossRef\]](#)
29. Dal Ben, M.; Bottin, C.; Zanconati, F.; Tiribelli, C.; Gazzin, S. Evaluation of region selective bilirubin-induced brain damage as a basis for a pharmacological treatment. *Sci. Rep.* **2017**, *7*, 41032. [\[CrossRef\]](#) [\[PubMed\]](#)
30. Silberberg, D.H.; Johnson, L.; Schutta, H.; Ritter, I. Effects of photodegradation products of bilirubin on myelinating cerebellum cultures. *J. Pediatr.* **1970**, *77*, 613–618. [\[CrossRef\]](#)
31. Kim, Y.K.; Na, K.S.; Myint, A.M.; Leonard, B.E. The role of pro-inflammatory cytokines in neuroinflammation, neurogenesis and the neuroendocrine system in major depression. *Prog. Neuropsychopharmacol. Biol. Psychiatry* **2016**, *64*, 277–284. [\[CrossRef\]](#)
32. Kurt, A.; Aygun, A.D.; Kurt, A.N.; Godekmerdan, A.; Akarsu, S.; Yilmaz, E. Use of phototherapy for neonatal hyperbilirubinemia affects cytokine production and lymphocyte subsets. *Neonatology* **2009**, *95*, 262–266. [\[CrossRef\]](#)
33. Gazzin, S.; Zelenka, J.; Zdrahalova, L.; Konickova, R.; Zabetta, C.C.; Giraudi, P.J.; Berengeno, A.L.; Raseni, A.; Robert, M.C.; Vitek, L.; et al. Bilirubin accumulation and Cyp mRNA expression in selected brain regions of jaundiced Gunn rat pups. *Pediatr. Res.* **2012**, *71*, 653–660. [\[CrossRef\]](#)
34. Genc, S.; Genc, K.; Kumral, A.; Baskin, H.; Ozkan, H. Bilirubin is cytotoxic to rat oligodendrocytes in vitro. *Brain Res.* **2003**, *985*, 135–141. [\[CrossRef\]](#)
35. Silva, R.F.; Rodrigues, C.M.; Brites, D. Rat cultured neuronal and glial cells respond differently to toxicity of unconjugated bilirubin. *Pediatr. Res.* **2002**, *51*, 535–541. [\[CrossRef\]](#)
36. Rodrigues, C.M.P.; Sola, S.; Silva, R.F.M.; Brites, D. Aging confers different sensitivity to the neurotoxic properties of unconjugated bilirubin. *Pediatr. Res.* **2002**, *51*, 112–118. [\[CrossRef\]](#) [\[PubMed\]](#)
37. Rhine, W.D.; Schmitter, S.P.; Yu, A.C.; Eng, L.F.; Stevenson, D.K. Bilirubin toxicity and differentiation of cultured astrocytes. *J. Perinatol.* **1999**, *19*, 206–211. [\[CrossRef\]](#) [\[PubMed\]](#)
38. Kumral, A.; Genc, S.; Genc, K.; Duman, N.; Tatli, M.; Sakizli, M.; Ozkan, H. Hyperbilirubinemic serum is cytotoxic and induces apoptosis in murine astrocytes. *Biol. Neonate* **2005**, *87*, 99–104. [\[CrossRef\]](#)

39. Rodrigues, C.M.; Sola, S.; Brites, D. Bilirubin induces apoptosis via the mitochondrial pathway in developing rat brain neurons. *Hepatology* **2002**, *35*, 1186–1195. [[CrossRef](#)] [[PubMed](#)]
40. Grojean, S.; Koziel, V.; Vert, P.; Daval, J.L. Bilirubin induces apoptosis via activation of NMDA receptors in developing rat brain neurons. *Exp. Neurol.* **2000**, *166*, 334–341. [[CrossRef](#)] [[PubMed](#)]
41. Yu, Y.; Zhu, W.; Diao, H.; Zhou, C.; Chen, F.F.; Yang, J. A comparative study of using comet assay and gammaH2AX foci formation in the detection of N-methyl-N'-nitro-N-nitrosoguanidine-induced DNA damage. *Toxicol. In Vitro* **2006**, *20*, 959–965. [[CrossRef](#)]
42. El-Abdin, M.Y.Z.; El-Salam, M.A.; Ibrahim, M.Y.; Koraa, S.S.M.; Mahmoud, E. Phototherapy and DNA changes in full term neonates with hyperbilirubinemia. *Egypt. J. Med. Hum. Genet.* **2012**, *13*, 29–35. [[CrossRef](#)]
43. Mesbah-Namin, S.A.; Shahidi, M.; Nakhshab, M. An increased genotoxic risk in lymphocytes from phototherapy-treated hyperbilirubinemic neonates. *Iran. Biomed. J.* **2017**, *21*, 182–189. [[CrossRef](#)]
44. Ramy, N.; Ghany, E.A.; Alsharany, W.; Nada, A.; Darwish, R.K.; Rabie, W.A.; Aly, H. Jaundice, phototherapy and DNA damage in full-term neonates. *J. Perinatol.* **2016**, *36*, 132–136. [[CrossRef](#)] [[PubMed](#)]
45. Yahia, S.; Shabaan, A.E.; Gouida, M.; El-Ghanam, D.; Eldegl, H.; El-Bakary, A.; Abdel-Hady, H. Influence of hyperbilirubinemia and phototherapy on markers of genotoxicity and apoptosis in full-term infants. *Eur. J. Pediatr.* **2015**, *174*, 459–464. [[CrossRef](#)] [[PubMed](#)]
46. Afifi, M.F.; Abdel Mohsen, A.H.; Abdel Naeem, E.; Abdel Razic, M.I. Role of phototherapy, BAX gene expression in hyperbilirubinemia development in full-term neonates. *Egypt. J. Med. Hum. Genet.* **2020**, *21*, 1–6. [[CrossRef](#)]
47. Solecki, D.J.; Govek, E.E.; Tomoda, T.; Hatten, M.E. Neuronal polarity in CNS development. *Genes Dev.* **2006**, *20*, 2639–2647. [[CrossRef](#)] [[PubMed](#)]
48. Wilson, P.G.; Stice, S.S. Development and differentiation of neural rosettes derived from human embryonic stem cells. *Stem Cell Rev.* **2006**, *2*, 67–77. [[CrossRef](#)] [[PubMed](#)]
49. Grabiec, M.; Hribkova, H.; Varecha, M.; Stritecka, D.; Hampf, A.; Dvorak, P.; Sun, Y.M. Stage-specific roles of FGF2 signaling in human neural development. *Stem Cell Res.* **2016**, *17*, 330–341. [[CrossRef](#)]
50. Banda, E.; McKinsey, A.; Germain, N.; Carter, J.; Anderson, N.C.; Grabel, L. Cell polarity and neurogenesis in embryonic stem cell-derived neural rosettes. *Stem Cell Dev.* **2015**, *24*, 1022–1033. [[CrossRef](#)]
51. Rice, D.; Barone, S., Jr. Critical periods of vulnerability for the developing nervous system: Evidence from humans and animal models. *Environ. Health Perspect.* **2000**, *108* (Suppl. S3), 511–533.